

Fluid Geochemistry of Shear Zone-Hosted  
Gold and Copper Deposits  
in the Kautokeino Greenstone Belt,  
Norway

by David C. Ettner  
Submitted Dissertation for degree doctor scientiarum  
Department of Geology, University of Oslo

*...and I argue that there is no necessary connection  
between the size of an object and the value of a fact,  
and that, though the objects I have described are minute,  
the conclusions to be derived are great.*

H.C. Sorby, 1858, founder of modern fluid inclusion analysis

# Contents

**-Introduction** 1

**-Paper I:**

Ettner, D.C., Bjørlykke, A., Andersen., T., A fluid inclusion and stable isotope study of the Proterozoic Bidjovagge mesothermal gold-copper deposit, Finnmark, northern Norway. (*Mineralium Deposita*, submitted).

**-Paper II:**

Ettner, D.C., Bjørlykke, A., Andersen., T., Fluid evolution and Au-Cu genesis along a shear zone: A regional fluid inclusion study of shear zone-hosted alteration and gold and copper mineralization in the Kautokeino greenstone belt, Finnmark, Norway. (*Journal of Geochemical Exploration*, submitted).

**-Paper III:**

III.) Ettner, D.C., Lindblom, S., and Karlsen, D., Identification and implications of light hydrocarbon fluid inclusions from the Bidjovagge Au-Cu deposit, Finnmark, Norway. (to be submitted to *NGT* or *GFF*)

**-Paper IV:**

Ettner, D.C., Bjørlykke, A., Andersen., T., Fluid geochemistry of the Bidjovagge gold-copper deposit, Norway: An example of a Proterozoic greenstone belt-hosted mesothermal gold -base metal deposit. (to be submitted to *Economic Geology*)

## Acknowledgements

Foremost, I need to thank my advisor, Professor Arne Bjørlykke for his support and supervision which kept me straight during the past 3 years of collecting data and interpreting results. Working with Arne has been both enjoyable and rewarding. My co-adviser, Tom Andersen has also been an invaluable resource especially regarding fluid inclusion analysis and the understanding of phase behaviour. Through Tom's supervision and patience I have become confident in the technique of fluid inclusion analysis, which only 3 years prior I was oblivious.

I am very grateful to the generous financial support provided for me by NTNF, the Royal Norwegian Research Council for Scientific and Industrial Research, grant number BF-25469. Outokumpu Oy and Bidjovagge Gruber A/S have also provided financial support and excellent field support during my past 3 summer field seasons on Finnmarksvidda.

There are so many other numerous people that have helped with motivation, valuable discussion, and technical help throughout this Dr. Scient. study. First, I want to thank my wife Elisabeth Sanne who helped to keep me sane and full of energy after crazy weeks, usually through large dosages of Nordmarka fresh air. I am also indebted to my family in the U.S. for their numerous letters and telephone phone calls of support. Friends such as Christian Zwach at the KFA in Jülich, Germany, and Rhonda and Scott Simmons have been greatly encouraging during this period, and their E-mail messages made sitting at the Macintosh bearable on otherwise rough days. I am thankful to Kjell Nilsen, Dr. Nie Fenjuin, Harald Åsen, Morten Rostad and Stein Lønne for their helpful discussions about Bidjovagge and Finnmark geology, and their generous access to their samples. Dag Karlsen and Kristen Backer-Owe are thanked for the impromptu instruction in hydrocarbon and gas chromatography. Access and help by Sten Lindblom and Curt Broman, with the Raman laser microprobe at the Institute for Geology, Univ. of Stockholm, is gratefully acknowledged. Excellent technical support and the preparation of uncountable samples has been provided by Malcolm Lynn and Harald Åsen in the thin section lab at the Institute. Further, the university's Photography Department has provided valuable help with photos for publications and presentations. I must also thank Terje Bjerkgård, Kåre Kullerud and Scott Simmons for technical help with the use of the Mac.

Finally, I thank the faculty, staff and students at the Institute of Geology and the Geological-Mineralogical Museum for providing a rewarding and exciting scientific environment in which to study and conduct research.

## Introduction

Several hydrothermal copper-gold deposits occur within the Kautokeino greenstone belt in Finnmark County, northern Norway. The largest and most notable among these is the Bidjovagge Au-Cu deposit. This dissertation study describes the fluids and fluid evolution involved in the formation of the gold and copper ore in the Kautokeino greenstone belt including the Bidjovagge deposit, and proposes methods for continued exploration for Bidjovagge-type deposits in the Kautokeino region. As implied in the name "hydrothermal ore deposit", heated aqueous solutions are essential for the formation of most types of ore. The economic importance of ore deposits through the few decades has resulted in the development of geochemical techniques to study ore-forming fluids in an attempt to determine the nature of the fluids and ultimately to successfully explore for other hydrothermal ore deposits.

Fluid inclusion analysis is the most direct method to study the geochemistry of the fluids related to ore formation. Fluid inclusions are pockets of trapped fluid within crystals that are seldom larger than 1 mm, but usually 1 to 10 $\mu$ m in size (Roedder, 1984). As first realized by Sorby (1858), detailed analysis of these minute pockets of trapped fluids may provide valuable information on the fluid composition, molar volume and possibly the temperature and pressure of fluid trapping. Within the discipline of ore deposits geology, the study of fluid inclusions is usually aimed at determining the composition of the ore-forming fluids and the conditions of the metal transport and precipitation (e.g. Spooner, 1981; Kerkhof, 1987; Walsh et al., 1989; Shaw and Morton, 1990). The concept of primary fluid inclusions within an ore deposit representing "ore-forming fluids" (e.g. Roedder, 1977) may be an incorrect oversimplification, especially when we consider that most hydrothermal ore deposits are complex zones of alteration and mineralization. If one regards a hydrothermal ore deposit as a result of chemical (e.g. reactions, pH,  $fO_2$ ) and/or physical changes (e.g. temperature or pressure), then it may be realized that ore-forming fluids must be changing chemically and/or physically to result in the metal precipitation. Therefore,

fluid inclusions observed within a hydrothermal ore deposit may be either a true sample of the "ore forming fluid" or probably more likely, the product of chemical or physical changes during mineralization. It becomes obvious that fluid inclusion studies of hydrothermal ore deposits should attempt to identify both the original ore-forming fluids and the evolved fluid products in order to determine the chemical and/or physical changes and its bearing on the ore precipitation.

Fluid inclusions may be analyzed by two general methods, nondestructive and destructive (Roedder, 1984). Nondestructive fluid inclusion methods, such as microthermometry and Raman laser microprobe analysis allow the determination of composition and molar volume without the removal the fluid from the inclusion. Destructive fluid inclusion analysis requires the removal of fluid from the inclusion by crushing or thermal means, followed by analysis of the extracted fluid, for example by gas chromatography or mass spectrometry. Detailed microscopic observations of fluid inclusions in combination with analysis using these methods may be used as a powerful tool to determine the fluid evolution resulting in metal precipitation in a hydrothermal ore deposit, such as at the Bidjovagge deposit. As Sorby (1858) noted concerning fluid inclusions,

*...though the objects that I have described are minute, the conclusions to be derived from the facts are great.*

### **Geology of the Kautokeino greenstone belt**

A series of Proterozoic greenstone belts occur within the northern Fennoscandinavian Shield (Fig. 1), and include the Kautokeino greenstone belt on the western edge of Finnmarksvidda and the Karasjok greenstone belt in the eastern region of Finnmarksvidda in Norway. The Kautokeino greenstone belt, which hosts the Au-Cu mineralization of interest, is bordered by two gneissic domes, the Jer'gul gneiss complex on the east and the Rai'sædno gneiss on the west (Fig. 2).

The Kautokeino greenstone belt formed during the rifting of the Archean Karelian Continent (Pharaoh and Brewer, 1990), or Inari microcontinent of Marker (1985), between 2.45 to 2.0 Ga (Bjørlykke et al., 1993) (Fig. 3a). Rifting of the Kautokeino greenstone belt resulted in the extrusion of some komatiite magmas (Olsen and Nilsen, 1985), tholeiitic basalts and intrusions, and the sedimentation of sandstone, shallow water carbonate, black shale, volcanoclastics, and conglomerate (Siedlecka et al., 1985). During the Svecokarelian orogeny at approximately 1,900-1850 Ma (Bjørlykke et al., 1987; Skiöld, 1988) two major events are recognized which resulted in metamorphism and deformation in the Kautokeino greenstone belt. The closure of the Kola ocean basin to the *east*, as the Kola continent collided with the Karelian continent, resulted in the emplacement of the Karasjok greenstone belt, a back arc and island arc sequence, (Pharaoh and Brewer, 1990; Marker, 1985) (Fig. 3c). During this collisional event, Bjørlykke et al. (1993) suggest that the Kautokeino greenstone belt was metamorphosed. The second event which affected the Kautokeino greenstone belt was the collision of the Svecofennian Skjellefte arc with the *western* border of the Karelian Continent at approximately 1.88 Ga (Pharaoh and Brewer, 1990) (Fig. 3d). Oblique compression during this collision resulted in sinistral movement along shear zones in the Kautokeino greenstone belt, such as along the north-south trending Baltic-Bothnian megashear zone (Berthelsen and Marker, 1986) and the NE-SW trending Mierujav'ri-Sværholt fault zone (Olesen et al., 1991). These shear zones are suggested to be reactivated older rift structures in the Kautokeino rift (Nilsen and Bjørlykke, 1990; Bjørlykke et al., 1993).

Fluids moving upwards along the shear zones in the Kautokeino greenstone belt resulted in areas of alteration and Au-Cu mineralization. Alteration of the country rocks along the shear zones, such as at Bidjovagge or along the Masi River (Fig. 2), is dominated by albitization, carbonatization, and scapolitization. Shear zone-hosted gold and/or copper deposits include the Bidjovagge deposit, Uccavuovdas and Object 43 (Fig. 2), among others. Radiometric dating of minerals related to the gold at Bidjovagge indicate that mineralization occurred during or

slightly after the peak of the Svecokarelian orogeny (Bjørlykke et al., 1990; Cumming et al., in prep.).

Mineralized areas within the Kautokeino greenstone belt clearly show that the fluids that moved along the shear zones were capable of transporting both Au and Cu in solution. Of the deposits discovered, the only economically important area of gold mineralization is the Bidjovagge Au-Cu deposit, and areas such as Ucca-vuovdas and Object 43 contain significant copper but very little gold (Fig. 2). The different gold/copper ratios between these shear zone-hosted deposits may be primary metal zonation caused by physical and/or chemical changes in the "ore-forming fluids". An understanding of the fluids responsible for gold-copper mineralization and zonation has obvious implications for the further exploration of "Bidjovagge-type" deposits in the Kautokeino greenstone belt.

### **Present Contribution**

The four papers introduced in this dissertation all present fluid inclusion data related to gold and copper mineralization in the Kautokeino greenstone belt. The importance of the evolution between the parent "ore-forming fluid" and its product of chemical and physical changes and its affect on Au and Cu transport and precipitation is discussed at different scales in the following papers. Paper I presents the evolution of fluids at the Bidjovagge deposit and their role in the transport and precipitation of Au and Cu at the Bidjovagge deposit. Paper II discusses the evolution of the fluids related to Au and Cu mineralization and zonation on a regional scale. Paper III focuses on the fluid products from the fluid-rock reaction which resulted in Au and Cu precipitation at Bidjovagge. Finally, paper IV sums up the fluid inclusion and stable isotope data from the Bidjovagge deposit and attempts to explain the formation of similar gold-base metal deposits occurring in Proterozoic greenstone belts.

**Paper I:** A fluid inclusion and stable isotope study of the Proterozoic Bidjovagge mesothermal gold-copper deposit, Finnmark, northern Norway.

This first paper focuses on fluid inclusion and stable isotope data related to the first gold-rich phase of mineralization at Bidjovagge and presents a model for mineralization. Fluid inclusions observed at Bidjovagge are composed of varying amounts of highly saline H<sub>2</sub>O + CO<sub>2</sub> + CH<sub>4</sub> + salt solutions. A general zonation is observed with H<sub>2</sub>O + CO<sub>2</sub> + salt fluid inclusions within the footwall of the deposit and a domination CH<sub>4</sub> towards the ore zone, which occurs within an alteration and oxidation zone to graphitic schists. This fluid inclusion zonation, together with a range carbonate δ<sup>13</sup>C values from -0.66‰ in the footwall veins to -4.64‰ in ore zone veins, is suggested to be the result of fluid rock interaction. The highly saline H<sub>2</sub>O + CO<sub>2</sub> solution observed in the footwall fluid inclusions is interpreted to represent the "ore-bearing fluid" which transported both Au and Cu as chloride complexes upwards along shear zones. This fluid appears to have experienced phase separation as it moved into more highly deformed albite felsites at Bidjovagge. Red-ox reactions between the fluid and the graphitic schist resulted in the oxidation zone and production of CH<sub>4</sub>. The precipitation of Au and Cu is suggested to occur at temperatures between 300 to 375°C and pressures between 2 to 4 kbars as a result of decreased *f*O<sub>2</sub> by red-ox reactions with the graphitic schist in combination with increased pH, because of phase separation of the fluid.

**Paper II:** Fluid evolution and Au-Cu genesis along a shear zone: A regional fluid inclusion study of shear zone-hosted alteration and gold and copper mineralization in the Kautokeino greenstone belt, Finnmark, Norway.

In this paper, fluid inclusion data is presented from several areas of shear zone-hosted alteration and mineralization in the Kautokeino greenstone belt and a

model for the fluid evolution and resulting gold-copper zonation is discussed. The occurrence of alteration and mineralization within different metamorphic facies and structural regimes allows an unique opportunity to study fluids at different crustal levels. Fluid inclusions observed within these areas are comprise saline  $H_2O \pm CO_2 \pm CH_4 \pm N_2$ . A  $H_2O + CO_2 +$  salt fluid appeared to evolved as it moved upward along the shear zone becoming more saline by either hydration reactions with the wall rocks or addition of salts from metasedimentary rocks. The fluids were at temperatures between 250 and 400°C and carried Au and Cu as chloride complexes. As the fluids moved upwards along shear zones and encountered the ductile-brittle transition phase separation of  $CO_2$  from the saline aqueous solution, due to the drop in pressure, resulted in increase pH in the fluid. Copper-rich mineralization, occurs at each crustal levels examined and is not affected by crustal depth. Gold-rich mineralization is restricted to the ductile-brittle transition, such as at the Bidjovagge deposit, and is interpreted to be a result of the phase separation due to a pressure drop, in combination with red-ox reactions with the graphitic schist.

**Paper III:** Identification and implications of light hydrocarbon fluid inclusions from the Bidjovagge Au-Cu deposit, Finnmark, Norway.

The unique occurrence of light hydrocarbon fluid inclusions observed within the ore zone at Bidjovagge are discussed in further detail in this paper. Data from a combination of fluid inclusion analytical methods, including nondestructive microthermometry and Raman microspectrometry and destructive gas chromatography is presented in this paper. Primary hydrocarbon-bearing inclusions from the Bidjovagge deposit are found to comprise methane, ethane, propane and butanes. The presence of hydrocarbons within mineralized alteration and oxidation zone to the graphitic schists, and absence in the footwall, indicates that the light hydrocarbons were formed during reaction between the hydrothermal fluids and the

schists. At the high temperatures and pressures estimated for the Bidjovagge deposit, light hydrocarbons may have been formed either by reaction with organic material within the graphitic schists or by abiotic synthesis.

**Paper IV:** Fluid geochemistry of the Bidjovagge gold-copper deposit, Norway: An example of a Proterozoic greenstone belt-hosted mesothermal gold-base metal deposit.

Proterozoic mesothermal gold-base metal deposits, such as Bidjovagge, occur within similar structural setting as Archean mesothermal gold dominated deposits, but have substantial differences in gold-base metal ratios than the Archean deposits. This paper contains comprehensive fluid inclusion and stable isotope data for both the Au-rich and Cu-rich mineralization phases at the Bidjovagge deposit and presents an explanation for the occurrence of Proterozoic mesothermal gold-base metal deposits. Fluid inclusions observed at Bidjovagge related to gold-rich mineralization contain varying amounts of highly saline  $H_2O + CO_2 + CH_4 +$  light hydrocarbons solutions. Gas chromatography of whole rock samples show that a zonation of light hydrocarbons exists around the ore zone. Also, a pronounced zonation of magnetite + pyrite, to pyrite, to pyrite + pyrrhotite exists between the footwall and the ore zone. Fluid inclusions related to copper-rich mineralization comprise lower salinity  $H_2O \pm CH_4$  solutions and appear to be similar to fluid inclusions within syenodiorite dikes which crosscut shear structures which host gold mineralization. Transport of both gold and copper as chloride complexes, favored by high temperature ( $>300^\circ C$ ), high chlorinity, lower pH, and high  $fO_2$  of the fluids, is interpreted to have occurred at the Bidjovagge deposit. Mineralization is interpreted to have formed in two phases, an earlier Au-rich phase that occurred during ductile to brittle deformation, followed by Cu-rich phase which occurred within brittle structures and was possibly related to the intrusion of syenodiorite dikes. The fluids which are interpreted to have resulted in

mineralization at Bidjovagge are similar to fluids described for other Proterozoic mesothermal gold-base metal deposits. The restriction of Proterozoic mesothermal gold-base metal deposits only occurring within intracratonic rifts having felsic basements may be linked to the high salinity fluids which transported both gold and base metals.

### References Cited

- Berthelsen, A. and Marker, M. (1986) 1.9-1.8 Ga old strike-slip megashears in the Baltic Shield, and their plate tectonic implications. *Tectonophysics* 128: 163-181
- Bjørlykke A., Cumming, G.L. and Krstic, D. (1990) New isotopic data from davidites and sulfides in the Bidjovagge gold-copper deposit, Finnmark, northern Norway. *Mineralogy Petrology* 43: 1-12
- Bjørlykke, A., Hagen, R. and Søderholm, K. (1987) Bidjovagge Copper-Gold Deposit in Finnmark, Northern Norway. *Economic Geology* 82: 2059-2075
- Bjørlykke, A., Nilsen, K.S., Anttonen, R. and Ekberg, M. (1993) Geological setting of the Bidjovagge deposit and related gold-copper deposits in the northern part of the Baltic Shield. In: Y.T. Maurice (ed.) *Proceedings 8th Quadrenn. IAGOD Symposium*, Ottawa, Can. 1990, Schweizerbart'sche, Stuttgart, pp. 667-680
- Cumming, G.L., Krstic, D., Bjørlykke, A. and Åsen, H. (in prep.) Further analysis of radiogenic minerals from the Bidjovagge gold-copper deposit, Finnmark, northern Norway.
- Kerkhof, A.M. VAN DEN (1987) The fluid evolution of the Harmsarvet ore deposit, central Sweden. *Geologiska Föreningens i Stockholm Förhandlingar* 109: 1-12
- Krill, A.G., Kesola, R., Sjöstrand, T. and Stephens, M.B. (1988) Metamorphic, structural and isotopic age map, northern Fennoscandia 1:1,000,000. *Geological Surveys of Finland, Norway and Sweden*

- Marker, M. (1985) Early Proterozoic (c. 2000-1900 Ma) crustal structure of the northeastern Baltic Shield: tectonic division and tectogenesis. *Norges geologiske undersøkelse* 403: 55-74
- Olesen, O., Henkel, H. and Lile, O.B. (1991) Major fault zones within the Precambrian Kautokeino Greenstone Belt, Finnmark, Norway: combined interpretation of geophysical data. *Norges geologiske undersøkelse unpublished report* 90.161, 26 pp.
- Olsen, K. I. and Nilsen, K.S. (1985) Geology of the southern part of the Kautokeino Greenstone Belt: Rb-Sr geochronology and geochemistry of associated gneisses and late intrusions. *Norges geologiske undersøkelse* 403: 131-160
- Pharaoh, T.C. and Brewer, T.S. (1990) Spatial and temporal diversity of early Proterozoic volcanic sequences - comparisons between the Baltic and Laurentian shields. *Precambrian Research* 47: 169-189
- Roedder, E. (1977) Fluid inclusions as tools in mineral exploration. *Economic Geology* 72: 503-525
- Roedder, E. (1984) Fluid Inclusions. In: Ribbe, P.H. (ed.) *Reviews in Mineralogy: Vol. 12*, 646 pp.
- Sandstad, J.S. (1992) Kautokeinogrønnsteinsbeltet - Berggrunnskart 1:100,000. *Norges geologiske undersøkelse*
- Shaw, R.P. and Morton, R.D. (1990) A fluid inclusion study of quartzite-hosted lode gold mineralization at Athabasca Pass, central Rocky Mountains, Canada. *Economic Geology* 85: 1881-1893
- Siedlecka, A., Iversen, I., Krill, A.G., Lieungh, B., Often, M., Sandstad, J.S. and Solli, A. (1985) Lithostratigraphy and correlation of the Archean and Early Proterozoic rocks of Finnmarksvidda and the Sørvaranger district. *Norges geologiske undersøkelse* 403: 7-36
- Skiöld, T. (1988) Implications of new U-Pb zircon chronology to early Proterozoic crustal accretion in northern Sweden. *Precambrian Research* 38: 147-164

Sorby, H.C. (1858) On the microscopic structure of crystals, indicating the origin of minerals and rocks. *Geological Society London Quarterly Journal* 14: 453-500

Spooner, E.T.C. (1981) Fluid inclusions studies of hydrothermal ore deposits. In: Hollister L.S. and Crawford, M.L. (eds.) *Mineralogical Association of Canada short Course Handbook* 6: 209-240

Walsh, J.F., Kesler, S.E., Duff, D. and Cloke, P.L (1988) Fluid inclusion geochemistry of high-grade, vein-hosted gold ore at the Pamour mine, Porcupine camp, Ontario. *Economic Geology* 83: 1347-1367

### Figure Captions

**Figure 1:** General geologic map of the northern portion of the Fennoscandic Shield including areas of northern Norway, Sweden and Finland with the locations of the Bidjovagge, Pahtohavare, and Saattopora deposits. After Krill et al. (1988) and Bjørlykke et al., (1993).

**Figure 2:** Generalized geologic map of Finnmarks plateau, with the Kautokeino Greenstone belt, emphasizing metamorphic grade after Sandstad (1992) and Krill et al. (1988). Mineralized and altered areas are marked with boxes. Shear zones are marked "BBMZ" for Baltic-Bothnian megashear zone (Berthelsen and Marker, 1986) and "MSFZ" for Mierujav'ri-Sværholt Fault Zone (Olesen et al., 1991).

**Figure 3:** Simplified tectonic model for the Early Proterozoic development of the Fennoscandinavian Shield, from Bjørlykke (1993) modified from Pharaoh and Brewer (1990). BBZ: Bothnian-Baltic zone; BF: Bergslagen Field; JC: Jorma ophiolitic complexes; KB: Karasjok Belt; LGC: Lapland Granulite Complex; PG: Petchenga Group; SD: Svecofennian domain; SF: Skjellefte Field.

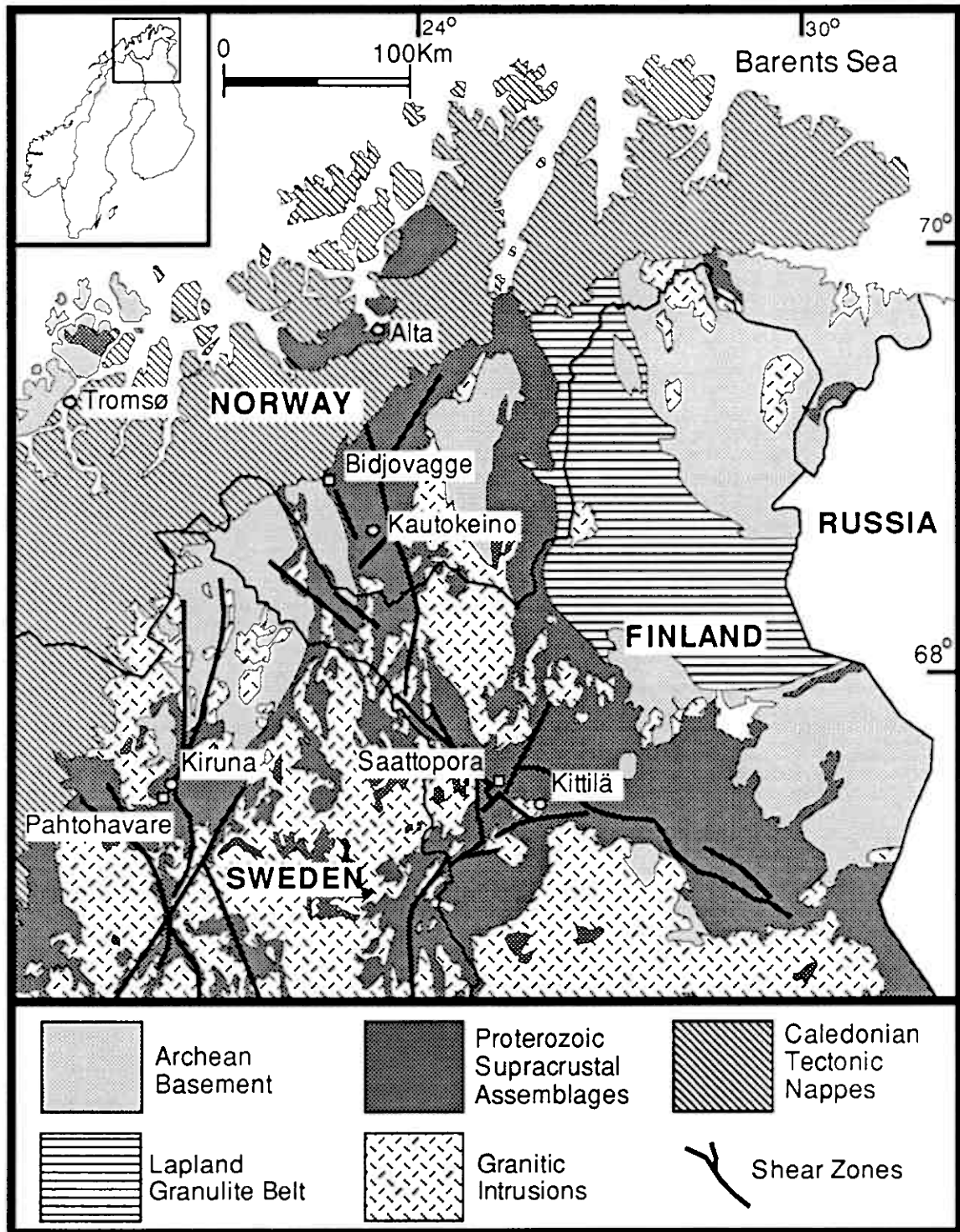


Figure 1

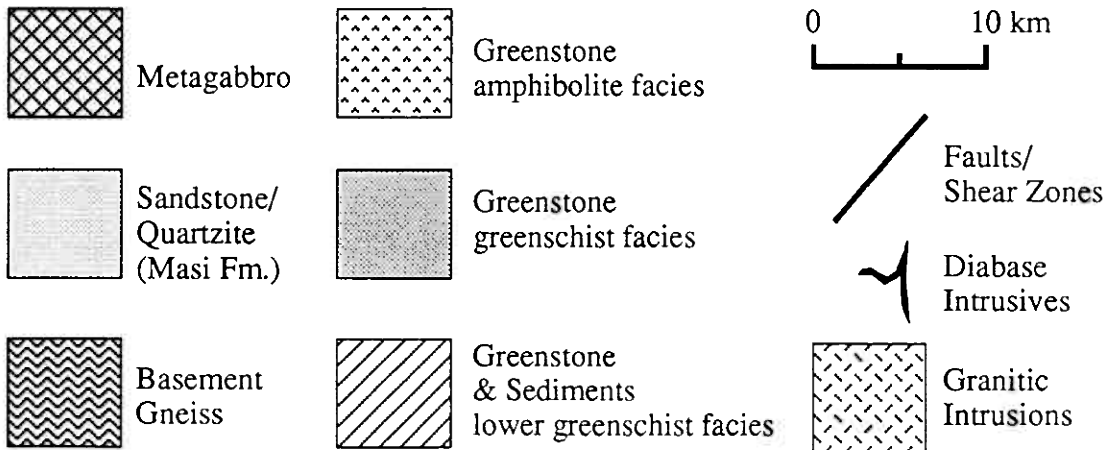
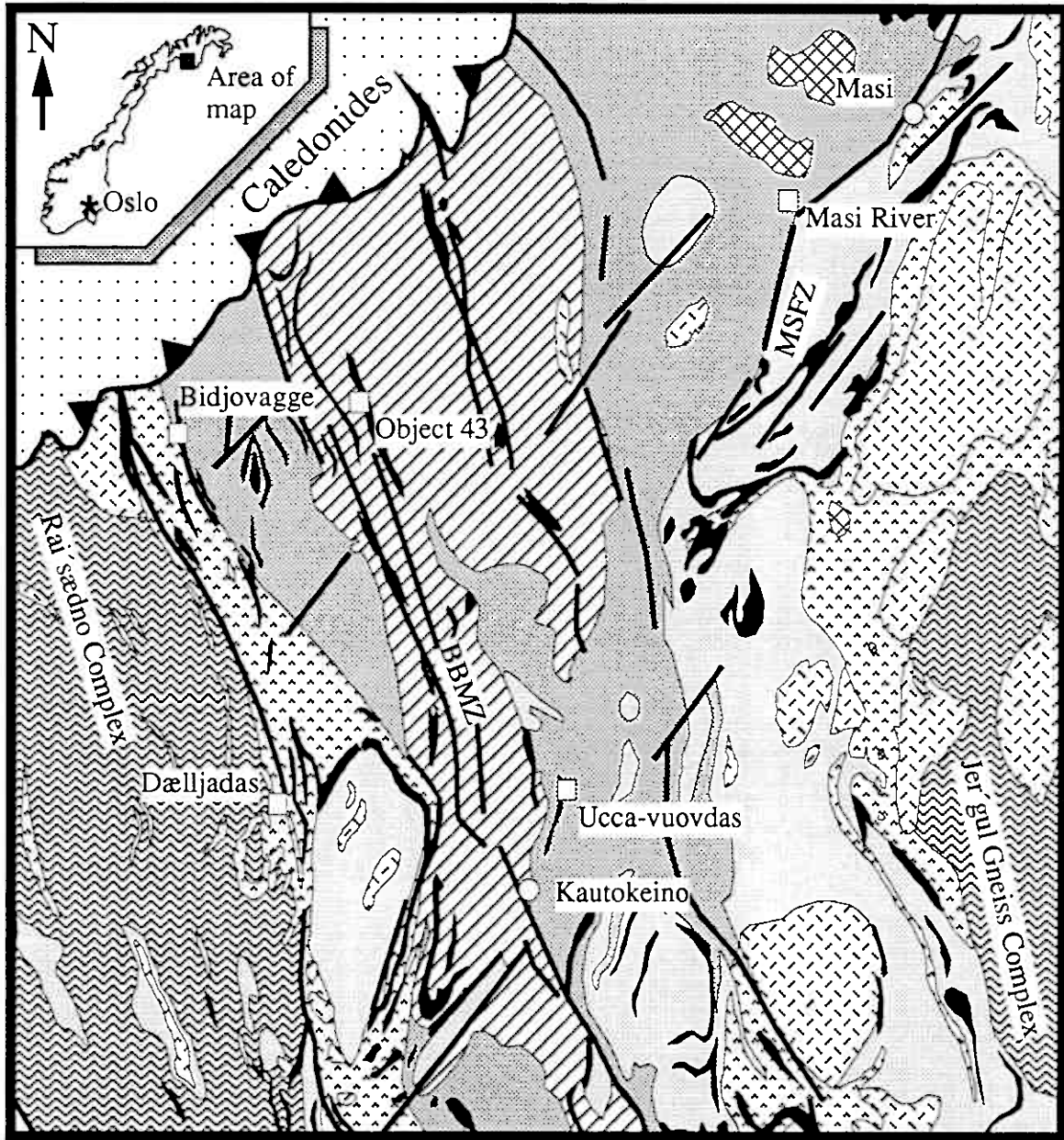
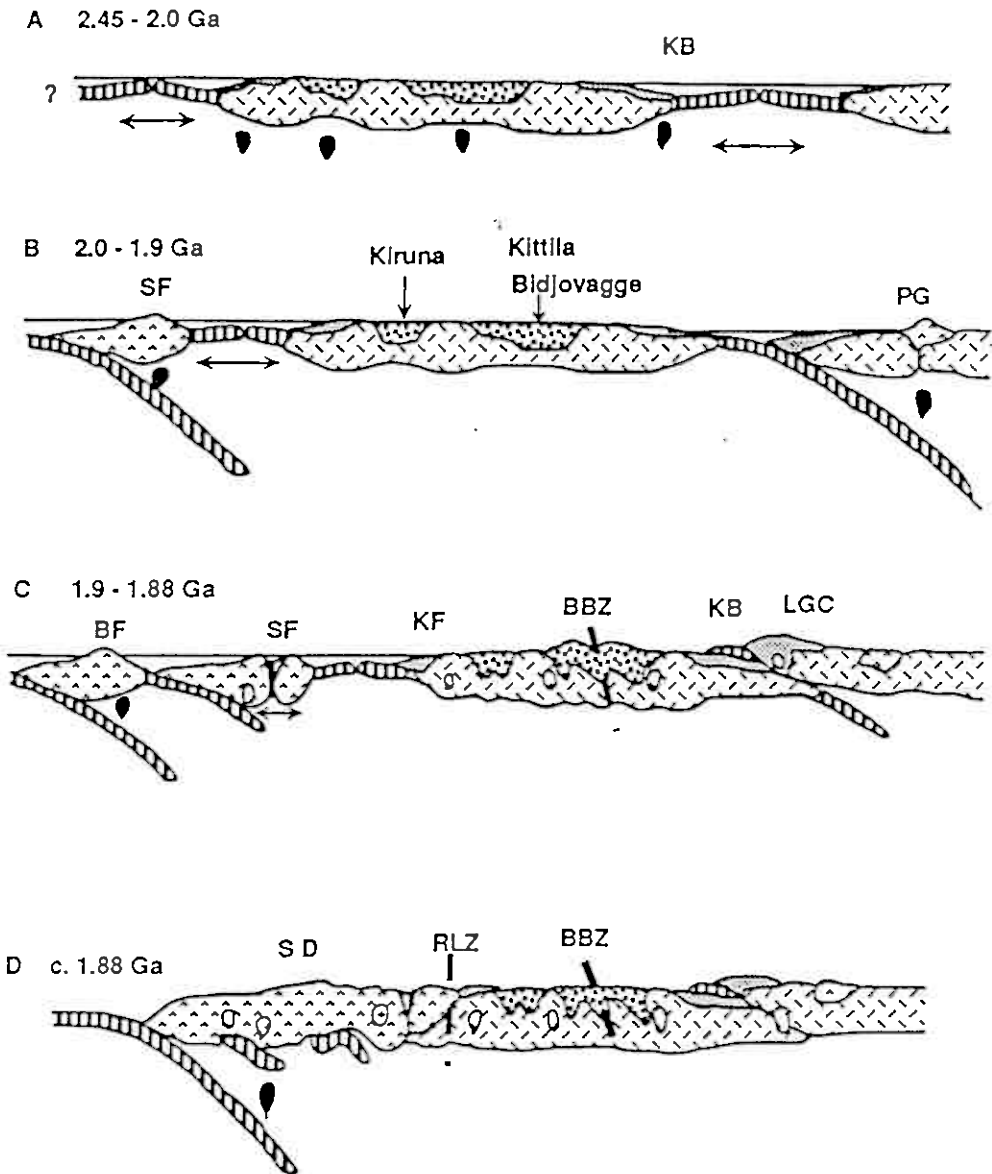


Figure 2



Legend

- |   |                     |   |  |
|---|---------------------|---|--|
|  | Granitic intrusions |  | Platform and continental margin environments |
|  | Arc environment     |  | Rift environment                             |
|  | Oceanic crust       |  | Archean basement                             |

Figure 3

# PAPER I

Version of 18.6.93

## A fluid inclusion and stable isotope study of the Proterozoic Bidjovagge Au-Cu Deposit, Finnmark, Northern Norway

**DAVID C. ETTNER, ARNE BJØRLYKKE**

Institute for Geology, University of Oslo,  
P.O. Box 1047, Blindern,  
N-0316 Oslo, Norway

and

**TOM ANDERSEN**

Mineralogical-Geological Museum,  
University of Oslo, Sarsgate 1,  
N-0562 Oslo, Norway

## Abstract

The Bidjovagge Au-Cu deposit, northern Norway, hosted within a shear zone in the Early Proterozoic Kautokeino greenstone belt, is more base metal-rich than Archean mesothermal gold deposits. The Bidjovagge deposit was therefore chosen to study the fluid composition by means of fluid inclusion microthermometry, Raman microprobe spectrometry, and stable isotope geochemistry to study the fluids responsible for both gold and copper mineralization. An early phase of gold and copper mineralization is hosted by sheared albitic felsites, within an oxidation front to graphitic schists, along with a series of syenodiorite dikes. Fluid inclusions related to gold mineralization comprise varying amounts of H<sub>2</sub>O, CO<sub>2</sub>, CH<sub>4</sub>, and salt, with salinities between 30 to 45 wt. % NaCl equivalent. Microthermometric data indicate that fluid trapping occurred between 300 to 375°C and 2 to 4 kbars. Carbon isotope data display a trend from -0.66‰ in the footwall to -4.64‰ within the ore zone. Fluid inclusion and carbon isotope data suggest that a combination of phase separation and redox reactions between the fluid and the graphitic schists resulted in gold precipitation from chloride complexes.

## Introduction

On the Fennoscandinavian Shield several mesothermal gold-copper deposits occur within Proterozoic greenstone belts (Gaál and Sundblad, 1990; Bjørlykke et al., 1992). These deposits include the Bidjovagge deposit in Norway (Bjørlykke et al., 1985 & 1987), Saattopora near Kittilä in Finland (Nurmi et al., 1991), and the Pahtohavare deposit near Kiruna in Sweden (Martinsson, 1991). These deposits along with other Proterozoic greenstone belt-hosted gold deposits, such as the Telfer deposit (Goellnicht et al., 1989) and the Tennant Creek field (Nguyen et al., 1989; Wedekind et al., 1989), tend to be base metal-rich. In contrast, Archean lode gold deposits generally have a much lower base metal ratio (i.e. Groves and Foster, 1991; Hodgson and MacGeehan, 1982).

The Bidjovagge Au-Cu deposit was chosen for a fluid inclusion and stable isotope study in order to model the fluid evolution involved in the formation of the gold-base metal deposit. This paper presents new fluid inclusion and isotopic data for the Bidjovagge deposit, and a genetic model for the formation of gold and copper mineralization at the deposit, which may be applicable to other Proterozoic mesothermal gold-base metal deposits.

## **General Geology and Structure**

The Bidjovagge Au-Cu deposit is located on the plateau of Finnmarksvidda, in Finnmark county, northern Norway, approximately 40 km north-west of the village of Kautokeino (Fig. 1). The deposit is hosted in the early Proterozoic north-south-trending Kautokeino greenstone belt which occurs in the Fennoscandinavian Shield. The Kautokeino greenstone belt is comprised of a series of basic volcanics and sediments considered to be Early Proterozoic in age by Krill et al. (1985). The greenstone belt is bordered by Archean gneiss domes, the Jer'gul gneiss complex on the east, and to the west, the Rai'sædno gneiss complex. Stratigraphy in the Bidjovagge area is comprised of metavolcanics and metasediments of the lowermost Cas'kejas Formation, metasediments of the Bik'kac'akka Formation and the overlying sandstones and conglomerates of the Caravari Formation as described by Siedlecka et al. (1985) and Bjørlykke et al. (1987) and mapped by Sandstad (1985). The Bidjovagge deposit is exposed at the northern edge of the greenstone belt where it is bordered by overlying sediments of the Cambrian Dividal Group, and the Caledonian thrust nappes. Aeromagnetic maps of Finnmark by Olesen et al. (1990) suggest that the Kautokeino greenstone belt continues north, under the Caledonian nappes, and is exposed in the Alta-Kvenangen, Altenes, and Repparfjord-Komagfjord tectonic windows (Fig. 1).

The Cas'kejas Formation hosts gold and copper mineralization at Bidjovagge, and is predominantly composed of amphibolites and mafic metavolcanics but is interbedded with minor thin beds of carbonate, graphitic schist, albitic felsite, and metatuffites. Mafic

metavolcanics and metasediments of the Cas'kejas Formation are thought to have deposited as lava flows, ash deposits, black shales, limestones and shales in a shallow early rift basin (Bjørlykke et al., 1987). The overlying sediments of the Bik'kac'akka Formation consist of feldspathic sandstones, argillites, shales and siltstones (Siedlecka et al., 1985). The uppermost formation in northern Kautokeino greenstone belt is the Caravarri Formation which is mainly composed of conglomerates and feldspathic sandstones (Siedlecka et al., 1985).

A series of thick diabase sills are intruded into the metasediments and related metavolcanic rocks, of the Cas'kejas Formation, and are considered by Bjørlykke et al. (1992) to be a result of an early rift stage of the greenstone belt. Between the contact of the diabase sills and graphitic schists, in the Bidjovagge area, a zone of albitic felsite has developed. Originally, the albitic felsite was suggested to be a volcanic ash exhalative (Hollander, 1979), but is now considered to be a result sodic metasomatism of the black shales by the intrusion of the diabase sills and circulation of hot saline brines (Bjørlykke et al., 1987; Bjørlykke et al., 1992; Nilsen and Bjørlykke, 1991). The albitic felsite is composed of very fine-crystalline albite with impurities of rutile and carbonate.

A later phase of syenodiorite intrusions related coarse-crystalline albite-carbonate veins crosscut the shear fabric, metasediments, albitic felsites and metadiabases at Bidjovagge. Previous workers have earlier named these intrusions as leucodiabase (Gjelsvik, 1957a and 1957b, Holmsen et al., 1957), albite-carbonate dikes (Holmsen et al., 1957), and albitite dikes (Bjørlykke, et al., 1987). These intrusions may be related to mineralization and is further discussed below.

In the Bidjovagge area the rocks of the Cas'kejas Formation are sheared, isoclinally folded and metamorphosed. Metamorphic grades, near the Bidjovagge deposit, gradually ranges from lower amphibolite facies west of the Bidjovagge anticline, towards the basement gneiss, to upper greenschist facies to the east of Bidjovagge (Sandstad, 1983). The dominant structure at the Bidjovagge deposit is a tight antiformal structure which plunges

gently to the north, with an exposed axial length of 8.5 km, and folds the diabase sills, tuffites, carbonates, graphitic schists and albitic felsites (Fig. 3). A discontinuous and sinuous shear zone runs parallel to the antiform's limbs, predominantly on the eastern limb and displays multiple events of both sinistral and dextral displacement (Nilsen and Bjørlykke, 1991). Shear deformation styles differ between more brittle shearing and microbrecciation in the competent albitic felsites and albitized metadiabases, to ductile folding in the incompetent graphitic schist. This shear zone is probably part of the northern extension of the Baltic-Bothnian megashear zone described by Berthelsen and Marker (1986). Both the structural deformation and the metamorphism appear to have occurred during the Svecokarelian orogeny at approximately 1,900-1,850 Ma (Bjørlykke et al., 1992; Pharaoh and Brewer, 1990; Skiöld, 1988).

## **Mineralization and Alteration**

### *Gold vs. Copper mineralization*

The shear zone at Bidjovagge has been mineralized within lenses along a length of about 2.5 km. Gold and copper ore is described by Hagen (1977) and divided into two general ore-types, the gold-rich ore and the copper-rich ore, by Bjørlykke et al., (1987). The gold-rich ore can be hosted within ductile to brittle structures, whereas the copper-rich ore occurs within brittle structures that crosscut the ductile fabric.

The gold-rich type has grades of 5-20 ppm Au and 0.1-0.5 % Cu. The gold-rich mineralization occurs along shear zones and is hosted within oxidation zones in sheared and microbrecciated albite metasomatized graphitic schists (Fig. 3 & 4). Mineralization typically occurs as finely disseminated native gold and gold telluride (calaverite) within sheared and microbrecciated albitic felsite. Veins related to gold mineralization extend from the footwall metadiabases upwards along the shear zone to the ore zone, and comprise carbonate, quartz,

actinolite (Fe-amphibole), magnetite, pyrite, pyrrhotite, chalcopyrite and minor amounts of apatite, green Cr-rich muscovite, tellurides (altaite, melonite, and tellurobismuthite) and davidite. Generally, a zonation of magnetite + pyrite, to pyrite, to pyrite + pyrrhotite occurs within the veins from the footwall towards the ore zone in the oxidized albitized graphitic schists. Highest grades of gold occur disseminated throughout the oxidation zone together with calaverite (Nilsen and Bjørlykke, 1991; Bjørlykke et al., 1992), and davidite, a member of the crichtonite mineral series (Mathiesen; 1970; Gatehouse et al., 1978; Bjørlykke, 1987). Mineralized shear texture displays a ductile fabric and veins are locally folded and boudinaged (Bjørlykke et al., 1987). Veins related to gold mineralization also occur in more brittle structures and angular wall rock clasts are occasionally observed within veins. Gold-rich mineralization within both ductile and brittle structures suggest that the gold-rich mineralization formed during the structural transition from ductile to brittle conditions.

The copper-rich ore grades are 2-5 % Cu and less than 1-2 ppm Au. Copper mineralization occurs as chalcopyrite and minor bornite within large vein systems that are predominantly composed of coarse grained carbonate (ankerite and calcite), but also albite, actinolite, quartz, pyrite, and minor amounts of telluride and native gold. The copper mineralization characteristically occurs within brittle structures which are subparallel to shear structure. Veins range in size up to about 1.5 meters. The copper-rich mineralization probably represents a second phase of mineralization at Bidjovagge within a more brittle deformation regime.

#### *Alteration of Wallrocks*

The predominant alteration at the Bidjovagge deposit includes albitization, carbonatization and scapolitization. Mica and hematite alteration all occur to lesser extents as described by Bjørlykke et al. (1987) and Nilsen and Bjørlykke (1991). Although there may be an early albite metasomatic event due to the intrusion of the diabase sills into the

sedimentary sequence, as previously described, a second albitization event related to mineralization has been recognized. Within the deposits, albitization has been intensive, altering the metadiabases, graphitic schists, carbonates and the mixed tuffite series. Typically, the albitic felsite is microcrystalline, but also is coarsely crystalline, especially where it replaces the plagioclase in the metadiabase (Bjørlykke et al., 1987). Rutile is ubiquitous in the albitic felsite, and minor amounts of quartz, carbonate, mica and amphibole also occur within the albitic felsite (Bjørlykke et al., 1987; Nilsen and Bjørlykke, 1991). Carbonatization is in association with the albitization, usually as carbonate mainly replacing the amphiboles within the metadiabases (Bjørlykke et al., 1987). Scapolitization occurs extensively in the central metadiabase as poikiloblasts replacing plagioclase, and within tuffites located in the hanging wall of the deposit (Bjørlykke et al., 1987; Nilsen and Bjørlykke, 1991).

Mica alteration is controlled by wallrock lithology, and includes the addition of biotite in the metadiabases, and sericite and fuchsite in the metasediments (Nilsen and Bjørlykke, 1991). The hematite and chlorite alteration, associated with coarse crystalline carbonate, probably postdates the earlier gold mineralization and may be related to Cambrian supergene alteration (Bjørlykke et al., 1987).

#### *Syenodiorite intrusions*

A series of dikes of syenodioritic composition and associated albite-carbonate veins, as previously mentioned, crosscut the shear texture in the albitic felsites, and are also crosscut by quartz-carbonate-chalcopyrite veins. Locally, these dikes have been experienced pervasive carbonate alteration. Based on crosscutting relationships and alteration, the syenodiorite dikes are interpreted to have been intruded at some period during or between gold-rich to copper-rich mineralization.

### *Age of Mineralization*

The age of mineralization at Bidjovagge has been constrained by isotopic age dating of the davidite (Bjørlykke et al., 1990). Ages of davidites, found in association with the gold ore, have been estimated by U/Pb to be  $1885 \pm 18$  Ma and supported by a Sm/Nd date of  $1886 \pm 88$  Ma. Based on these ages, the gold-ore mineralization is considered to have formed during the peak, or slight after the peak, of the Svecokarelian orogeny. Gold-rich mineralization may then have occurred during or slightly after peak metamorphic conditions. Copper-rich mineralization crosscuts the gold-rich mineralization indicating later phase of mineralization.

## **Fluid Inclusion Study**

### *Analytical Methods*

Approximately 25 samples from eight of the main ore bodies along the Bidjovagge anticline were selected for fluid inclusions analysis. Fluid inclusions analyzed are hosted within quartz in veins and veinlets from the high grade gold zone, proximal ore zone and the barren footwall vein systems.

Doubly polished sections, 100 to 150  $\mu\text{m}$  thick, of the Bidjovagge samples were made, and microthermometric measurements were conducted at the fluid inclusion laboratory at the Mineralogical-Geological Museum, Oslo, Norway. All measurements were made during heating of the sample, generally at a rate of  $5^\circ$  per minute. Measurements were mostly made using a LINKAM THM 600 heating-freezing stage, but because of temperature fluctuations, high precision low temperature measurements were made on a gas-cooled CHAIXMECA stage. Calibration of the LINKAM THM 600 stage was conducted with a series of natural and MERCK synthetic standards. Between  $-142^\circ\text{C}$  (melting point of

methylcyclopentane) to +200°C precision is approximately  $\pm 5^\circ\text{C}$ , and in the range of +200 to +400°C the instrument showed a +10 to 15°C deviation above true temperatures. High quality low temperature measurements were made on the gas-cooled CHAIXMECA stage that displayed a consistent accuracy and precision of  $\pm 1.0^\circ\text{C}$  between  $-142^\circ\text{C}$  and  $+30^\circ\text{C}$ , as described for the same instrument by Andersen et al. (1991).

Symbols used for presentation of microthermometric data are presented in Table 1 and microthermometric and Raman microprobe data for selected fluid inclusions are presented in Tables 2 and 3.

#### *Fluid Inclusion Description and Relationship to gold mineralization*

Fluid inclusions, related to the gold mineralization, were classified into three different groups using a modification of Shepherd et al. (1985) classification scheme based upon fluid and solid phases present at room temperature. The three fluid inclusion groups also appear to have a spatial zonation within the deposits, ranging from Group I inclusions within the footwall vein system, Group II in the low grade ore zone, to Group III in the high grade gold zone.

**Group I.** These fluid inclusions predominantly consist of liquid-rich two-phase fluid inclusions with multiple solids, and also single-phase liquid inclusions (Fig. 5). The liquid-rich two- or three-phase fluid inclusions, with multiphase solids, are composed of an aqueous brine with one to two salt crystals, and a  $\text{H}_2\text{O}$  vapor or pure  $\text{CO}_2$  bubble, and daughter crystals. The liquid-rich two-phase fluid inclusions contain  $\text{CO}_2$  bubbles that are single-phase liquid, while the three-phase fluid inclusions contain  $\text{CO}_2$  bubbles that are liquid-rich, two-phase. Solid daughter crystals within these inclusions are common, and although not positively identified probably include carbonate, actinolitic amphibole and minor small opaque crystals. The second inclusion type of Group I are single-phase pure  $\text{CO}_2$

liquid inclusions. Although the CO<sub>2</sub> rich inclusions tend to occur in separate clusters, both types of fluid inclusions can be found within any same quartz crystal, which also contains abundant carbonate solid inclusions. Fluid inclusions of Group I are found within the footwall gold barren veins, composed of quartz, carbonate, and actinolite.

**Group II.** Multiphase solid + liquid inclusions and minor single-phase liquid inclusions are found together in Group II. The multiphase solid + liquid inclusions consist of an aqueous brine and one or two salt crystals, similar to Group I, and may contain a H<sub>2</sub>O vapor or CO<sub>2</sub>-CH<sub>4</sub> bubble (Fig. 5). These inclusions also contain daughter crystals of possibly actinolitic amphibole and carbonate. Minor single-phase CO<sub>2</sub>-CH<sub>4</sub> inclusions are found scattered as small clusters among the multiphase solid + liquid inclusions. Quartz-carbonate veins hosting Group II inclusions are located within the oxidized albitic felsites of the proximal or low grade gold ore zone. Minor quartz-chalcopyrite veins crosscutting syenodiorite intrusions also host Group II fluid inclusions.

**Group III.** This group of inclusion is composed primarily of single-phase liquid inclusions (Fig. 5). The CO<sub>2</sub>-CH<sub>4</sub> fluids range between samples from CO<sub>2</sub> dominated to CH<sub>4</sub> dominated. Also, minor amounts of ethane-rich inclusions (determined by Raman microprobe, see below) occur in some samples containing CH<sub>4</sub> dominated fluid inclusions. Group III inclusions are found within quartz-carbonate veinlets within the high grade ore zones occurring in the sheared albitic felsites and follow either the shear planes or crosscut the shear fabric.

#### *Microthermometric analysis*

Group I fluid inclusions dominated by CO<sub>2</sub> freeze to solid CO<sub>2</sub> and vapor upon cooling to below -80°C. During heating, the majority melt (T<sub>mCO<sub>2</sub></sub>) at the CO<sub>2</sub> eutectic of

-56.6°C. Occasional samples, from veins displaying similar mineralogy as of veins hosting pure CO<sub>2</sub> inclusions, have CO<sub>2</sub> rich inclusions with depressed melting temperatures between -57 and -63.5°C. These depressed melting temperatures suggest a slight contamination of CH<sub>4</sub> (Burruss, 1981). Heating of the pure CO<sub>2</sub> inclusions results in the homogenization (T<sub>hCO<sub>2</sub></sub>) to liquid at temperatures between -53 and 0°C, but with 75% of the inclusions homogenizing between -53 and -25°C (Fig.6). Homogenization temperatures of the CO<sub>2</sub> inclusions contaminated with CH<sub>4</sub> are similar to pure CO<sub>2</sub>, ranging from -55 to -28°C (Fig. 8).

Saline brines from Group I fluid inclusions freeze to ice plus salt, hydrates, and vapor below -100°C. During heating the ice begins to melt (T<sub>m initial ice</sub>) in the range of -90 to -30°C. Final ice melting temperatures (T<sub>m final ice</sub>) are between -25 and -19°C. Hydrohalite melting was difficult to observe because of the high wt. % of salt in the inclusions. The low T<sub>m initial ice</sub> melting behaviour of the saline brine indicates that both NaCl and CaCl<sub>2</sub> are present in the inclusions (Crawford, 1981). The unusual initial melt temperatures observed below -50°C may be due to metastable melting of the saline brine (Roedder, 1984).

Continued heating of the inclusions first resulted in the partial homogenization of the water and vapor (T<sub>hH<sub>2</sub>O</sub>) typically between 100 to 200°C, usually followed by salt dissolution (T<sub>d salt</sub>) in a wide range between 150 to 370°C (Fig. 7). Salt contents are calculated from Haas (1976) and Tanger and Pitzer (1989), based on the salt dissolution temperatures (T<sub>d salt</sub>), to be between 30 to 43 wt. %, equivalent NaCl. Decrepitation of fluid inclusion before the final melting of the salt (T<sub>m salt</sub>) is common, occurring in up to 50% of the inclusions measured in a sample, with average decrepitation temperatures between 200 and 250°C.

Group II saline brine inclusions demonstrate very similar microthermometric characteristics as Group I. The ice has similar low temperature first initial melts (T<sub>m initial ice</sub>) ranging between -90 and -35°C and final ice melting (T<sub>m final ice</sub>) generally occurring between -33 and -20°C. Also, with these inclusions hydrohalite melting was difficult to observe

because of the high salt contents. By continued heating of Group II saline brines the homogenization of the brine and gas ( $T_{H_2O}$ ) usually occurred before salt dissolution although the temperatures of homogenization of the  $H_2O$  and the gas are not consistent. Temperatures of homogenization to liquid ( $T_{H_2O}$ ) range between 90 to 365°C (Fig. 7), which is probably due to varying composition of gases including  $H_2O$  vapor and  $CH_4$ - $CO_2$  mixtures. Generally, salt dissolution ( $T_{d_{salt}}$ ) in Group II inclusions occurs between 170 to 370°C (Fig. 7). Salinities of these inclusions are between 30 to 43 wt. %, equivalent NaCl (Haas, 1976; Tanger and Pitzer, 1989). Decrepitation of about 50% of the studied fluid inclusions usually occurs during heating with average temperatures between 150 to 250°C.

A minor number of gas-rich fluid inclusions found among the saline brines of Group II show variable microthermometric measurements. Fluids dominated by  $CO_2$  display melting temperatures ( $T_{m_{CO_2}}$ ) ranging from -72 to -56.6°C, and temperatures of homogenization to liquid ( $T_{H_{CO_2}}$ ) from -6 to -60°C. Variable amounts of saline brine in the inclusions result in clathrates that melt ( $T_{m_{clathrate}}$ ) between -11.4 to -6.8°C. Other inclusions dominated by  $CH_4$  homogenized at temperatures ( $T_{H_{CH_4}}$ ) between -102 and -75°C, and have clathrate melting temperatures ( $T_{m_{clathrate}}$ ) of -4.7 to -2.4°C.

Group III inclusions, dominated by  $CH_4$  rich inclusions, display varied behaviour during freezing including both homogenization type inclusions (H-type) and sublimation type inclusions (S-type) as defined by Van Den Kerkhof (1990) for  $CO_2$ - $CH_4$  fluid mixtures (Fig. 8). The majority of the Group III inclusions did not freeze during cooling to temperatures of around -180°C, and during heating the inclusions homogenized to liquid at temperatures ( $T_{H_{CH_4}}$ ) between -125 and -65°C. These inclusions, therefore, classify as homogenization type (H1-type). The lower temperatures of homogenization ( $T_{H_{CH_4}}$ ), below -105°C, are in agreement with a very  $CH_4$ -rich fluid (Van Den Kerkhof, 1990). The higher temperatures of homogenization to liquid ( $T_{H_{CH_4}}$ ), for H1-type, between -105 and -65°C indicate a component present in the fluid other than  $CH_4$ . Minor occurrences of H-type inclusions, have been found, that did not freeze, but homogenized to liquid in the range of -50 to -25°C.

The microthermometric behaviour of these inclusions may indicate that ethane ( $T_{\text{critical}}=+32.2$ ; Weast et al., 1988) is present, or possibly other higher hydrocarbons.

Less commonly, sublimation type (S2-type) inclusions were found. These inclusions experienced partial freezing during cooling to about  $-180^{\circ}\text{C}$  and during heating, homogenization to liquid occurred before final melting of the solid phase. Homogenization in the presence of solid  $\text{CO}_2$  ( $T_{\text{hsCH}_4+\text{CO}_2}$ ) usually was measured between  $-105$  to  $-65^{\circ}\text{C}$ , and sublimation ( $T_{\text{sCO}_2+\text{CH}_4}$ ), the final melting in a S2-type inclusion, occurred between  $-95$  and  $-60^{\circ}\text{C}$ . This behaviour is found in  $\text{CH}_4$  fluids with 4 to 35%  $\text{CO}_2$  content (Van Den Kerkhof, 1990).

#### *Raman Microprobe analysis*

Laser-excited Raman microprobe analysis were conducted in the laboratory of the Geological Institute at Stockholm University, Sweden, with the help of Sten Lindblom. The instrument used for analysis was a multichannel DILOR-XY, which is a successor to the MICRODIL-28 (Burke and Lustenhouwer, 1987). Measured line positions of  $\text{CO}_2$ ,  $\text{CH}_4$ , and  $\text{C}_2\text{H}_6$  were identified by comparison of listed values by Dubessy et al. (1989) and Van Den Kerkhof (1991). Raman data for selected fluid inclusions are presented, along with microthermometric data, in Table 3

Raman microprobe analysis were conducted on a series of gas-rich inclusions from the  $\text{CO}_2$ -rich inclusions of Group I, and the  $\text{CH}_4$ -rich inclusions of Group III. Analysis of the  $\text{CO}_2$  inclusions in Group I confirmed that the fluids were pure  $\text{CO}_2$ , as no other appreciable species were found. Raman spectra for  $\text{CO}_2$  showed two peaks, the strongest peak at  $\Delta\nu=1385\text{ cm}^{-1}$ , and the second peak at  $\Delta\nu=1279\text{ cm}^{-1}$  (Fig. 10a).

Methane-rich fluids analysed with the Raman microprobe from Group III provided varied results. Generally, H2-type  $\text{CH}_4$ -rich inclusions which homogenized below  $-105^{\circ}\text{C}$  showed a strong  $\text{CH}_4$  peak at  $\Delta\nu=2911\text{ cm}^{-1}$  (Fig. 10b) and sometimes a characteristic

carbon spectra. The carbon spectra was identified on the basis of two peaks, the strongest peak at about  $\Delta\nu=1605$  to  $1608\text{ cm}^{-1}$  is usually narrower and more angular, whereas the second peak found between  $\Delta\nu=1327$  to  $1340\text{ cm}^{-1}$  is wider with a rounded top (Fig. 10e). Carbon is probably present as a thin coating on the walls of the inclusions, as crystals were not noted in the inclusions. The H-type  $\text{CH}_4$ -rich inclusions which homogenized between  $-125$  and  $-65^\circ\text{C}$  also displayed the same characteristic  $\text{CH}_4$  peak, but the high surrounding background suggested the presence of ethane or other hydrocarbons (Fig. 10c). The presence of  $\text{CO}_2$  was not detected in these inclusions so the simple model of  $\text{CH}_4 + \text{CO}_2$  mixing could not be applied to account for the higher homogenization temperatures ( $T_{\text{HCH}_4}$ ) measured during microthermometric studies. Characteristic carbon peaks, as previously described, were found in all the inclusions of this type which were measured. Inclusions that displayed unusual homogenization temperatures in the range of  $-50$  to  $-25^\circ\text{C}$  indicating ethane were confirmed to be composed of a mixture of  $\text{CH}_4$  and  $\text{C}_2\text{H}_6$ , and possibly other hydrocarbons. An ethane peak was found between  $\Delta\nu=2940$  to  $2951\text{ cm}^{-1}$ . In all fluid inclusions measured of this type, carbon spectra was measured, probably indicating the presence of carbon as a wall coating.

The  $\text{CH}_4$ -rich fluid inclusions exhibiting S2-type characteristics were also analysed with the Raman microprobe. These inclusions revealed the presence of both  $\text{CH}_4$  and  $\text{CO}_2$ . The  $\text{CO}_2$  spectra, in these inclusions measured, had the strongest  $\text{CO}_2$  peak at  $\Delta\nu=1294\text{ cm}^{-1}$ , and the second peak was at  $\Delta\nu=1383\text{ cm}^{-1}$  (Fig. 10d). No other higher hydrocarbons or carbon coating were found.

After Raman microprobe analysis, temperatures of homogenization remained unchanged indicating that graphite was present in the inclusions before the analysis and did not form during laser excitement.

### *Pressure-temperature estimation*

No independent potential geothermometric or geobarometric mineral assemblages have been found at Bidjovagge, although temperatures and depths of burial during metamorphism have been estimated. The metamorphic grade is approximately upper greenschist facies (chlorite + biotite + actinolite + hornblende + plagioclase) grading to amphibolite facies (garnet + hornblende + cummingtonite + plagioclase) towards the basement gneisses to the west (Sandstad, 1983). The tectonostratigraphic depth of burial is estimated as 10 to 15 km.

An attempt has been made to calculate isochores from the fluid inclusion data from Bidjovagge. Isochores for different compositions of fluid inclusions have been calculated by ISOCHOR (Holloway, 1981) and FORTRAN programs by Nicholls and Crawford (1985). Molar volumes of CO<sub>2</sub> + CH<sub>4</sub> inclusions were estimated from application of Raman Probe data, described below, and microthermometric data to TX diagrams of the system CO<sub>2</sub> + CH<sub>4</sub> by Van Den Kerkhof (1990). Calculated isochores and T<sub>m,salt</sub> are plotted on figure 9. Fluid inclusions composed of C<sub>2</sub>H<sub>6</sub>, CH<sub>4</sub> + C<sub>2</sub>H<sub>6</sub> mixes (Group III), or CH<sub>4</sub> (±CO<sub>2</sub>) + H<sub>2</sub>O + salt were not used for calculation of isochores.

Isochores plotted for water + salt + CO<sub>2</sub> from Group I, and CH<sub>4</sub> along with CH<sub>4</sub> + CO<sub>2</sub> from Group III inclusions cluster as a roughly parallel group (Fig. 9). Calculated isochores for pure CO<sub>2</sub> inclusions of Group I plot at higher pressures, for corresponding temperatures. Combined data for Group I and II for average T<sub>m,salt</sub> and highest T<sub>m,salt</sub> have been calculated and plotted as 245°C and 370°C, respectively.

Considering that mineralization occurred contemporaneously with deformation and metamorphism we may loosely constrain the PT conditions of mineralization to be around 2 to 4 kbars, lithostatic, and less than 450°C. Generally, most isochores lie cross the 2 to 4 kbar range between 300 to 375°C (Fig. 9). Some CO<sub>2</sub>-rich inclusions isochores cross above this "box" and some CH<sub>4</sub>-rich inclusion and H<sub>2</sub>O inclusions cross below, resulting in

a larger "polygon" of possible trapping conditions (Fig. 9). By correlating the isochores and the regional geology we interpret mineralization to have occurred under lithostatic pressure of 2 to 4 kbars and at temperatures of 300 to 375°C.

### **Carbon and oxygen isotope geochemistry**

Fluid-rock interaction, between the ore-forming fluids and the graphitic schists, appears to be involved in the ore forming processes at Bidjovagge, therefore an attempt has been made to determine the sources of carbon using carbon isotopes. Carbonate from veins from a profile across the H deposit (Fig. 3) were selected for analysis of both carbon and oxygen isotopic values. Carbonates were systematically selected from veins associated with the Group I CO<sub>2</sub> and saline brine in the footwall, the Group II saline brine, CH<sub>4</sub> and CO<sub>2</sub> in the low grade ore zone, the Group III CH<sub>4</sub> in the ore zones, and also carbonate altered syenodiorite intrusions and mineralized carbonate veinlets in the graphitic schists. Samples for carbon isotope analysis were also selected from sedimentary carbonates, skarn altered carbonates, and graphitic schist from the Bidjovagge area.

A total of 19 carbonate samples have been analyzed for both carbon and oxygen isotopes by the GMS laboratory at the University of Bergen, Norway. Four graphite samples from the graphitic schist were analyzed at Global Geochemistry. Carbon isotopes are standardized to PDB, and oxygen is standardized relative to SMOW.

#### *Results*

Results of  $\delta^{13}\text{C}$  analysis from vein carbonates show variable values (Fig. 11). Analysis of 6 carbonate samples from the footwall veins and low grade ore zone veinlets show  $\delta^{13}\text{C}$  values of -0.66 to -1.9‰. Six carbonate samples separated from veinlets within the higher grade gold zones have  $\delta^{13}\text{C}$  values ranging from -1.72 and -4.64‰. Carbonate

separated from mineralized veinlets found within the graphitic schists, proximal to the ore zones, demonstrate  $\delta^{13}\text{C}$  values of -7.04 and -7.25‰. Carbon analysis from two carbonate altered syenodiorite dikes have  $\delta^{13}\text{C}$  values of -1.22 to -1.55‰.

Carbon isotope values around 0‰ PDB are displayed by both the sedimentary carbonate and the skarn altered sedimentary carbonate, with  $\delta^{13}\text{C}$  values of +0.36 and -0.05‰, respectively. Graphite from 4 graphitic schist samples have  $\delta^{13}\text{C}$  values which group around -20‰.

Analysis of  $\delta^{18}\text{O}$ , from the carbonates, typically have values between +10.92 and +13.43‰, relative to SMOW (Fig. 11). The sedimentary carbonate and the skarn altered sedimentary carbonate display higher  $\delta^{18}\text{O}$  values of +16.11 and +19.42‰, respectively.

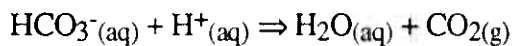
## Discussion

Fluids related to gold and copper mineralization at Bidjovagge, represented by fluid inclusions and stable isotope data, are similar to those described at other Proterozoic deposits in Fennoscandia and Australia (Goellnicht et al., 1989; Nguyen, 1989; Lindblom, 1993), show a distinctive difference compared to the low salinity  $\text{H}_2\text{O} + \text{CO}_2$  fluids described for Archean gold deposits (e.g. Wood et al., 1986; Robert and Kelly, 1987; Walsh et al., 1988; Burrows and Spooner, 1990). A model presented here provides an explanation for both the transport and precipitation of gold and copper at the Bidjovagge deposit, and may be applicable for other Proterozoic mesothermal gold-base metal deposits.

### *Fluid source*

Fluid inclusion and stable isotope data from Bidjovagge suggest that a primary fluid was introduced and interacted with the rocks during the alteration and ore-forming processes. The primary fluid may be represented by Group I high-salinity  $\text{CO}_2 + \text{H}_2\text{O}$  dominated fluid

inclusions located within quartz-carbonate-actinolite veins in the footwall metadiabase. The occurrence of these inclusions in the footwall metadiabase suggest that the fluids were transported upwards along conduits within the shear zone. Fluid inclusions within the highly sheared albite felsites, above the metadiabase, which comprise coeval groups of H<sub>2</sub>O + salt and pure CO<sub>2</sub> inclusions, indicate that phase separation of the CO<sub>2</sub> + H<sub>2</sub>O + salt fluid occurred. The phase separation of CO<sub>2</sub> from H<sub>2</sub>O-rich fluids results in an increase in pH of the fluid (Reed and Spycher, 1985) because of the reaction:



The structural changes between the slightly deformed metadiabases and the highly deformed albite felsites indicate that phase separation occurred because of pressure reduction.

Carbon isotopes from carbonate separated from the footwall veins display  $\delta^{13}\text{C}$  values of  $-0.66$  to  $-1.9\text{‰}$ , relative to PDB, indicating that fluids had dissolved CO<sub>2</sub> with  $\delta^{13}\text{C}$  values of approximately  $+1.0$  to  $+4\text{‰}$ , as calculated at a temperature of 350°C (Ohmoto and Rye, 1979). Amphibolitization of the sedimentary carbonates within the footwall and core of the Bidjovagge anticline indicates that fluid-rock interaction occurred which would have resulted in the production of CO<sub>2</sub> during actinolite-forming reactions between H<sub>2</sub>O and the carbonate. The carbonates may have been a source of the CO<sub>2</sub> found in the Group I inclusions as reflected by the  $\delta^{13}\text{C}$  values.

Oxygen isotopes from the carbonate samples with  $\delta^{18}\text{O}$  values generally between  $+10.92$  and  $+13.43 \text{‰}$  indicate that the fluid had  $\delta^{18}\text{O}$  values of approximately  $+6.7$  to  $+9.2 \text{‰}$  at 350°C, relative to SMOW (Friedman and O'Neil, 1977). With  $\delta^{18}\text{O}$  values such as these, sources of water could either be primary magmatic or metamorphic (Taylor, 1979). The salts which occur in high concentrations within the aqueous solutions may have been derived from an igneous source or the surrounding metamorphosed sedimentary and volcanic assemblage, and focused along the shear zone structures.

### *Transport of metals*

The highly saline  $H_2O + CO_2$  solutions found in the footwall most likely represent the fluids which carried metals in solution before gold mineralization. Transport of gold as chloride complexes is dependent on temperature, pH, and  $fO_2$  (Henley, 1973; Hayashi and Ohmoto, 1991), therefore, high temperatures, high salinity, and the high  $fO_2$  of the fluid at Bidjovagge support gold transport as a chloride complexes (Fig. 12). The salinity of the transporting fluid is estimated by salt dissolution temperatures in fluid inclusions to have been between 30 to 45 wt. % NaCl. The  $fO_2$  of the solution, based on the presence of pure  $CO_2$  and the magnetite-pyrite and pyrite-pyrrhotite assemblages appears to have been about -30 to -34 at 350° (Fig. 12).

Similarly, other metals found at Bidjovagge such as copper and uranium may have been transported by the same highly saline oxidizing fluid. Transport of copper by high salinity brines as chloride complexing is likely. Uranium, found in davidites in association with gold, would easily be transported in the oxidized uranyl state of  $U^{6+}$  possibly complexed with  $CO_2$  as uranyl dicarbonate complexes (Kimberley, 1978; Rich et al., 1977).

### *Fluid-rock interaction*

Although  $CH_4$ -rich fluids can be produced during low grade metamorphism of organic-rich sediment (Mullis, 1979; 1987) and at high grade metamorphic conditions (Hollister and Burruss, 1976), we suggest that  $CH_4$  at Bidjovagge was produced in situ during fluid-rock interaction. The presence of  $CO_2$  dominated fluids (Group I) in the footwall, versus  $CH_4$  dominated fluids (Group III) in the oxidized ore zone surrounding the graphitic schist shows two end-member fluids, with the latter presumably forming during an equilibrium fluid-rock reaction.

Oxidation fronts along the boundaries of the graphitic schists appear to have been caused by the introduction of CO<sub>2</sub> + saline H<sub>2</sub>O fluids which moved up along the shear zones in the footwall. Reaction of these fluids with carbon in the graphitic schists could have produced CH<sub>4</sub>-rich fluids, seen in both Group II and Group III fluid inclusions, by a reaction such as



Group II fluid inclusions with highly saline H<sub>2</sub>O with minor amounts of CH<sub>4</sub> and CO<sub>2</sub> may represent a partial reaction, involving the reaction (1), with the wall rocks.

Lowering of  $fO_2$  along the narrow oxidation zone produced a steep  $fO_2$  gradient. The  $fO_2$  gradient is exemplified by oxidation fronts seen in outcrop (Fig. 4), and the zonation of magnetite + pyrite in the footwall veins to pyrite + pyrrhotite in the oxidation zone.

Carbon isotope data from vein carbonate supports a fluid-rock interaction model. Two end member sources for carbon include the graphitic schists ( $\delta^{13}C \cong -20\text{‰}$ ) and the sedimentary carbonates ( $\delta^{13}C \cong 0\text{‰}$ ). Deeper crustal sources may have contributed carbon but mixing with enriched <sup>13</sup>C during skarn alteration of the sedimentary carbonates may have obscured the presence of this source. Isotope analysis of footwall vein carbonates, as discussed above, suggest that fluids had  $\delta^{13}C$  values of approximately +1.3 to +.7‰ reflecting sedimentary carbonates as the carbon source. The progressively more depleted  $\delta^{13}C$  values from the ore zone vein carbonates ( $\delta^{13}C = -1.2$  to  $-4.64\text{‰}$ ) to the graphitic schist-hosted vein carbonates ( $\delta^{13}C \cong -7\text{‰}$ ) appear to be the result of a complex equilibrium fractionation between a fluctuating CO<sub>2</sub> and CH<sub>4</sub> fluid formed during fluid-rock interaction.

#### *Deposition of metals*

Fluid inclusion and carbon isotope data indicate that phase separation together with fluid-rock red-ox reactions were controlling factors in the deposition of gold and copper

within ductile to brittle shear structures, followed by copper mineralization. Gold, minor uranium, and some copper mineralization occurring in zones within the intersection of the shear structures and the oxidation front to the graphitic schists led Bjørlykke et al. (1987) to suggest that changes in oxygen fugacity or pH resulted in gold precipitation at Bidjovagge.

The solubilities of gold as chloride complexes, as discussed previously, is dependent on temperature, pH, and  $fO_2$  (Henley, 1973; Hayashi and Ohmoto, 1991). Phase separation of  $CO_2$  from the  $H_2O$  + salt solution as fluids moved up into the highly sheared albite felsites would have resulted in an increase in pH, buffered by the assemblage magnetite + pyrite, and resulting in reduced solubility of gold as chloride complexes (Fig. 12). Reducing the  $fO_2$  of the fluid by the red-ox reaction with graphitic schist would result in further reduced solubility of gold (Fig. 12). The combination of increased pH and decrease  $fO_2$  therefore resulted in the precipitation of gold together with pyrite + pyrrhotite. Similar mechanisms of a reduction in  $fO_2$  for precipitation of gold in quartz veins has been proposed by Bottrell et al. (1988), Cox et al. (1991), Goellnicht et al. (1989) and Nguyen et al. (1989). Uranium transport as uranyl dicarbonate complex would similarly become unstable by lowering  $fO_2$  (Kimberley, 1978; Rich et al., 1977) therefore resulting in uranium precipitation. Chalcopyrite found in the quartz + carbonate  $\pm$  actinolite vein system, related to gold mineralization, may have precipitated from the same fluids. Copper precipitation from chloride complexes is dependent on temperature, pH, oxygen and sulfur fugacity (Barnes, 1979; Helgeson, 1969). Similar to the proposed mechanism of gold precipitation at Bidjovagge, an increase in pH together with a decrease in  $fO_2$  would result in chalcopyrite precipitation (Fig. 12).

Chalcopyrite-carbonate veins, and minor bornite, within brittle structures that crosscut earlier gold-copper mineralization may have occurred during a later event of an evolving hydrothermal system. This evolved system, which is the subject of continuing research, will be described in detail (in preparation). Considering that mineralization occurred in open brittle veins and is spatially associated with the graphitic schists a few mechanisms of copper precipitation is possible. If transport in this evolved fluid occurred as chloride complexes

precipitation mechanisms may include the influx of meteoric water reducing chloride concentration, decreased temperature, and a increase of H<sub>2</sub>S concentration by redox reaction with the graphitic schists (Barnes, 1979). Alternatively, deposition from sulfide complexes may occur as a result of pH increase, or phase separation by pressure decrease (Barnes, 1979) during brittle deformation, or by phase separation by CH<sub>4</sub> mixing (Bowers, 1986) during fluid reaction with the graphitic schists, similar to the gold precipitation mechanism described by Walsh et al. (1988).

### **Preferred model**

Both ductile and brittle structural textures at Bidjovagge indicate that shear deformation, correlated to the Baltic Bothnian megashear zone, occurred near the brittle-ductile transition. The correlation of the ductile-brittle shear structures and the metamorphic transition from upper greenschist to amphibolite metamorphism (Colvine, 1989; Sibson, 1977) as found at Bidjovagge, agrees with the proposed geologic evolution of the Fennoscandinavian Shield in that metamorphism and shear deformation were roughly synorogenic (Berthelsen and Marker, 1986; Bjørlykke et al.; 1992; Pharaoh and Brewer, 1990). Age dating of  $1885 \pm 18$  Ma of the gold mineralization at Bidjovagge (Bjørlykke et al., 1990) indicates that fluid migration up through the shear zone and mineralization, may therefore have at the peak, or slightly after the peak, of the Svecokarelian orogeny. Deformation of the ore body and supports this proposal.

Similar to structural models proposed for many other quartz vein hosted gold lode deposits (Colvine, 1989; Vearncombe, et al., 1989), the fluids at Bidjovagge appear to have been focused along shear zones. Cameron (1989a, 1989b, 1989c) proposes that relatively oxidizing CO<sub>2</sub> and H<sub>2</sub>O fluids derived from the lower crust during metamorphism would transport both sulfides and gold up through shear zones. Within the Bamble Belt, of southern Norway, Cameron (1989b, 1989c) showed that zones of granulite to upper

amphibolite metamorphosed and deformed rocks are strongly depleted in Au, Sb and As, and depleted in Rb, S and Cu. Cameron (1989a) therefore suggests that fluids rich in CO<sub>2</sub> could transport Au, Sb, As, Rb, S, and Cu from the lower crust up along shear zones, depleting the lower crust in these elements, and precipitate gold in the brittle-ductile transition. Fluid inclusion studies of the Bamble Zone indeed show a pervasive dominance of CO<sub>2</sub> + H<sub>2</sub>O fluids (Touret, 1981).

Within deep fluid-rich shear zones Newton (1990) has shown that high CO<sub>2</sub> pressures may result in the formation of alkaline partial melts. The presence of syenodiorite intrusions at Bidjovagge occurring as lenses within the fluid-rich shear zone may have been formed similar to the model proposed by Newton (1990). These lens-shaped intrusions, crosscutting shear texture, albitized and carbonatized locally, and occasionally crosscut by quartz-chalcopyrite veins hosting fluid inclusions with a saline H<sub>2</sub>O and CH<sub>4</sub>+CO<sub>2</sub> composition (Group II) appear to be roughly syngenetic to mineralization.

In the case of Bidjovagge, where it appears that, together with syenodiorite intrusions, highly saline H<sub>2</sub>O + CO<sub>2</sub> fluids have transported gold and copper along a shear zone and deposited the metals in the brittle-ductile zone, the model of Cameron (1989a) is applicable. Relatively oxidizing fluids rich in high salinity H<sub>2</sub>O+CO<sub>2</sub> could have transported gold and copper as chloride complexes, both derived from the lower crust, and was focused along the shear zone exposed in the Bidjovagge area (Fig. 13). Amphibolite-forming reactions with the sedimentary carbonates within the Bidjovagge anticline may have resulted in a mixing of carbon isotopes and, therefore reflecting fluids with lower  $\delta^{13}\text{C}$  values seen in the footwall of the Bidjovagge deposit. As the CO<sub>2</sub> + H<sub>2</sub>O + salt fluids moved upwards into the highly sheared albite feldspar phase separation of the CO<sub>2</sub> from the H<sub>2</sub>O + salt solution occurred resulting in an increase in pH of the fluid which was buffered by the magnetite + pyrite assemblage (Fig. 12 & 13). Redox reactions between the fluids and the graphitic schist resulted in the oxidation of the schist, production of CH<sub>4</sub>, zonation of magnetite + pyrite to pyrite to pyrite + pyrrhotite, and lowered  $f\text{O}_2$  of the fluids (Fig. 12). The

combination of increased pH and lowered  $fO_2$  of the fluids resulted in reduced solubility of the gold and copper as chloride complexes and precipitation occurred (Fig. 12). Copper precipitation appears to have occurred throughout the pH and  $fO_2$  changes, but gold precipitation is restricted to the stability boundary of pyrite + pyrrhotite within the oxidation front to the graphitic schist (Fig. 13). Pressure and temperature estimates for mineralization, based on fluid inclusions and geologic constraints, are between 2 to 4 kbars and around 300 to 375°C. Although the syenodiorite dikes appear to have been intruded during the phases of mineralization, their participation in mineralization by is unclear, yet the high temperature aqueous fluids and corresponding high salinities indicate that the intrusions may have influenced the temperature of the fluid and/or was a source of saline aqueous fluids and metals.

As the hydrothermal system matured, copper-rich mineralization occurred in more brittle structures crosscutting structures hosting gold-rich mineralization. Generally, the mineralization style and vein mineralogy indicate that conditions were different than during the earlier gold mineralization. Precipitation of dominantly chalcopyrite and carbonate possibly occurred as a result of phase separation by pressure decrease during brittle deformation, influx of meteoric water, an increase of  $H_2S$  concentration by redox reaction with the graphitic schists, pH increase, or by phase separation by  $CH_4$  mixing during fluid reaction with the graphitic schists.

The model of ore paragenesis for Archean mesothermal gold deposits does not easily fit the Bidjovagge gold-copper deposit. Models for Archean deposits suggest that gold was transported as  $Au(HS)_2^-$  complexes by low salinity  $H_2O + CO_2$  solutions (Groves et al., 1987; Neall and Phillips, 1987; Robert and Kelly, 1987; Walsh et al., 1988) and deposition occurred as a result of either fluid unmixing (Robert and Kelly, 1987; Walsh et al., 1988) or sulfidization (Groves et al., 1987; Neall and Phillips, 1987). Transport of gold and base metals, such as copper at Bidjovagge, in a high temperature, high  $fO_2$ , and highly saline aqueous solution is most easily accomplished by chloride complexing. At Bidjovagge

precipitation of gold and copper from chloride complexes appears to have occurred by a combination of increasing pH during phase separation and decreasing  $fO_2$  during red-ox reaction between the fluid and the graphitic schists. Similar mechanisms for gold precipitation, including temperature reduction, has been proposed by Bottrell et al. (1988), Cox et al. (1991), Goellnicht et al. (1989) and Nguyen et al. (1989).

The co-mineralization of copper and gold mineralization in the Bidjovagge deposit is, therefore, explained by the ability to transport both metals as chloride complexes. The low base metal contents of Archean gold deposits, in contrast to the Bidjovagge gold-copper deposit may simply be explained by the absence of high salinity solutions to transport base metals.

### **Acknowledgements**

We wish to thank Bidjovagge Gruber A/S and Outokumpu Oy for partial support of this research and permission to publish these results. We also gratefully acknowledge financial support from NTNF (Royal Norwegian Research Council for Scientific and Industrial Research), project number BF-25469. We are grateful to Sten Lindblom and Kurt Broman from the Institute of Geology, University of Stockholm, for Raman microprobe analysis. The first author would like to thank A.M. Van Den Kerkhof and J.L.R. Touret for helpful discussions of fluid phase behaviour, and Per Aagaard and Kurt Bucher for help in constructing thermodynamic diagrams, although the author accepts any errors in this publication. Important discussion and some samples were kindly supplied by Nie Fengjun, Kjell Nilsen, Harald Aasen, and Morten Rostad. Metamorphic expertise and technical computer help was kindly provided by Kåre Kullerud. Also, superb preparation of hundreds of doubly polished fluid inclusion sections by Malcolm Lynn and Harald Aasen at the Institute of Geology thin section lab, University of Oslo, is gratefully acknowledged.

## References

- Andersen, T., Austrheim, H., and Burke, E.A.J. (1991) Mineral-fluid-melt interactions in high-pressure shear zones in the Bergen Arcs nappe complex, Caledonides of W. Norway: Implications for the fluid regime in Caledonian eclogite-facies metamorphism. *Lithos* 27: 187-204
- Barnes, H.L. (1979) Solubilities of ore minerals. In: Barnes, H.L., ed., *Geochemistry of Hydrothermal Ore Deposits*. Wiley, New York, pp. 404-460.
- Berg, H.J. (1992) Geokjemi av gull i hydrothermale systemer, anvendt på tre Norske forekomster. Unpub. Cand. Scient. Thesis, University of Oslo, 199 pp.
- Berthelsen, A., and Marker, M. (1986) 1.9-1.8 Ga old strike-slip megashears in the Baltic Shield, and their plate tectonic implications. *Tectonophysics* 128: 163-181
- Bjørlykke A., Cummings, G.L., and Krstic, D. (1990) New isotopic data from davidites and sulfides in the Bidjovagge gold-copper deposit, Finnmark, northern Norway. *Mineral. Petrol.* 43: 1-12
- Bjørlykke, A., Hagen, R., and Söderholm, K. (1987) Bidjovagge Copper-Gold Deposit in Finnmark, Northern Norway. *Econ. Geol.* 82: 2059-2075
- Bjørlykke, A., Nilsen, K.S., Anttonen, R., and Ekberg, M. (1992) Geological Setting of the Bidjovagge deposit and related gold-copper deposits in the northern part of the Baltic Shield.
- Bjørlykke, A., Olerud, S., and Sandstad, J.S. (1985) Metallogeny of Finnmark, north Norway. *Norges Geol. Unders.* 403: 183-196
- Bottrell, S.H., Shepherd, T.J., Yardley, B.W.D., and Dubessy, J. (1988) A fluid inclusion model for the genesis of the ores of the Dolgellau Gold Belt, North Wales. *J. Geol. Society London* 145: 139-145
- Bowers, T.S., (1986) The geochemical consequences of H<sub>2</sub>O-CO<sub>2</sub> fluid immiscibility on ore deposition: A reaction path approach. (abs) *Geol. Soc. Amer. Abstracts with Programs* 18: 548
- Burke, E.A.J. and Lustenhouwer, W.J. (1987) The application of a multichannel laser Raman microprobe (Microdil-28) to the analysis of fluid inclusions. *Chem. Geol.* 61: 11-17
- Burrows, D.R., and Spooner, E.T.C. (1990) Archaean intrusion-hosted, stockwork Au-quartz vein mineralization, Lamaque mine, Val d'Or, Quebec: Part I. Geological and fluid characteristics. In: Robert, F., Sheahan, P.A., and Green, S.B., eds., *Greenstone Gold and Crustal Evolution: NUNA Conference Vol.*, Geol. Assoc. Canada, pp. 139-141.
- Burruss, R.C. (1981) Analysis of phase equilibria in C-O-H-S fluid inclusions. *Mineral. Assoc. Canada Short Course Handbook* 6: 39-74

Cameron, E.M. (1989a) Derivation of gold by oxidative metamorphism of a deep ductile shear zone: Part 1. Conceptual model. *J. Geochem. Expl.* 31: 135-147

Cameron, E.M. (1989b) Derivation of gold by oxidative metamorphism of a deep ductile shear zone: Part 2. Evidence from the Bamble Belt, south Norway. *J. Geochem. Expl.* 31: 149-169

Cameron, E.M. (1989) Scouring of gold from the lower crust. *Geology* 17: 26-29

Card, K.D., Poulsen, K.H., and Robert, F. (1989) The Archean Superior province of the Canadian Shield and its lode gold deposits. *Econ. Geol. Mon.* 6: 19-36

Colvine, A.C. (1989) An empirical model for the formation of Archean gold deposits: Products of final cratonization of the Superior Province, Canada. *Econ. Geol. Mon.* 6: 37-53

Cox, S.F., Wall, V.J., Etheridge, M.A., and Potter, T.F. (1991) Deformation and metamorphism processes in the formation of mesothermal vein-hosted gold deposits - examples from the Lachlan Fold Belt in central Victoria, Australia. *Ore Geol. Reviews* 6: 391-423

Crawford, M.L. (1981) Phase equilibria in aqueous fluid inclusions. *Mineralog. Assoc. Canada Short Course Handbook*, V. 6, pp. 75-100.

Crerar, D.A., and Barnes, H.L. (1976) Ore solution chemistry V. Solubilities of chalcopyrite and chalcocite assemblages in hydrothermal solution at 200° to 350°C. *Econ. Geol.* 71: 772-794

Drummond, S.E. Jr. (1981) Boiling and mixing of hydrothermal fluids; chemical effects on mineral precipitation. Unpubl. doctor dissertation, Pennsylvania State Univ., 380 pp.

Dubessy, J., Poty, B., and Ramboz, C. (1989) Advances in C-O-H-N-S fluid geochemistry based on micro-Raman spectrometric analysis of fluid inclusions. *European Jour. Mineral.* 1: 517-534

Friedman, I., and O'Neil, J.R. (1977) Compilation of stable isotope fractionation factors of geochemical interest. In: Fleischer, M., ed., *Data of Geochemistry*, sixth eds., U.S. Geol. Surv. Prof. Paper 440-KK, 12 pp.

Gaál, G., and Sundblad, K. (1990) Metallogeny of gold in the Fennoscandian Shield. *Mineral. Dep.* 25: 104-114

Gatehouse, B.M., Greay, I.E., Campbell, I.H., and Kelly, P. (1978) The crystal structure of loweringite-a new member of the crichtonite group. *Amer. Mineral.* 63: 28-36

Gjelsvik, T. (1957a) Albittrike bergarter i den karelske fjellkjede på Finnmarksvidda, Nord-Norge. *Norges Geol. Unders.* 203: 60-72

Gjelsvik, T. (1957b) Epigenetisk koppermineralisering på Finnmarksvidda. *Norges Geol. Unders.* 203: 49-59

Goellnicht, N.M., Groves, D.I., McNaughton, N.J., and Dimo, G. (1989) An epigenetic origin for the Telfer gold deposit, Western Australia. *Econ. Geol. Mon.* 6: 151-167

- Groves, D.I., and Foster, R.P. (1991) Archaean lode gold deposits. In: Foster, R.P. (ed.) Gold metallogeny and exploration. London, Blackie, pp. 63-103.
- Groves, D.I., Phillips, N., Ho, S.E., Houston S.M., and Standing, C.A. (1987) Craton-scale distribution of Archean greenstone gold deposits. Predictive capacity of the metamorphic model: *Econ. Geol.* 82: 2045-2058
- Haas, J.L. (1976) Physical properties of the coexisting phases and thermochemical properties of the H<sub>2</sub>O component in boiling NaCl solutions. *U.S. Geol. Survey Bull.* 1421-A, 73 p.
- Hagen, R. (1977) En malmgeologisk undersøkelse av Bidjovagge forekomstene med henblikk på å kartlegge oppkomsten av gull i malm og sidebergart. Unpub. Cand. Scient. Thesis, Trondheim, Norges Tekniske Høyskole, 90 pp.
- Hayashi, K. and Ohmoto, H. (1991) Solubility of gold in NaCl- and H<sub>2</sub>S-bearing aqueous solutions at 250-350°C. *Geochem. Cosmoch.* 55: 2111-2126.
- Helgeson, H.C. (1969) Thermodynamics of hydrothermal systems at elevated temperatures and pressures. *Amer. J. Sci.* 267: 729-804
- Henley, R.W. (1973) Solubility of gold in hydrothermal chloride solutions. *Chem. Geol.* 11: 73-87
- Hees, E.H.P. Van, and Kesler, S.E. (1990) Geochemistry of fluid inclusions in gold, Porcupine camp, Ontario. In: Robert, F., Sheahan, P.A., and Green, S.B. (eds.) *Greenstone Gold and Crustal Evolution: NUNA Conference Vol.*, Geol. Assoc. Canada, pp. 222.
- Hodgson, C.J., and MacGeehan, P.J. (1982) A review of the geological characteristics of "gold-only" deposits in the Superior Province of the Canadian Shield. In: Hodder R.W., and Petruk, W. (eds.) *Geology of Canadian gold deposits: Can. Inst. of Mining and Metallurgy, Spec. Vol.* 24: 211-229
- Hollander, N.B. (1979) The geology of the Bidjovagge mining field, western Finnmark, Norway. *Norsk Geol. Tidsskr.* 59: 327-336
- Hollister, L.S., and Burruss, R.C. (1976) Phase equilibria in fluid inclusions from the Khtada metamorphic complex. *Geochim. Cosmochim. Acta* 40: 163-175
- Holloway, J.R. (1981) Compositions and volumes of supercritical fluids in the earth's crust. *Mineralog. Assoc. Canada Short Course Handbook*, V. 6, pp. 13-38.
- Holmsen, P., Padget, P., and Pehkonen, E. (1957) The Precambrian geology of Vest-Finnmark, northern Norway: *Norges Geol. Unders.* 210, 107 pp.
- Johnson, J.W., Oelkers, E.H., and Helgeson, H.C. (1991) SUPCRT92: A software package for calculating the standard molal thermodynamic properties of minerals, gases, aqueous species, and reactions from 1 to 5000 bars and 0° to 1000°C. Univ. of California, Berkeley, 101 pp.

Kerkhof, A.M. Van Den (1990) Isochoric phase diagrams in the systems CO<sub>2</sub>-CH<sub>4</sub> and CO<sub>2</sub>-N<sub>2</sub>: Application to fluid inclusions. *Geochim. Cosmochim. Acta* 54: 621-629

Kerkhof, A.M. Van Den (1991) Heterogeneous fluids in high-grade siliceous marbles of Pusula (SW Finland). *Geologische Rundschau* 80: 249-258

Kerrick, R. (1989) Archean gold: Relation to granulite formation or felsic intrusions? *Geology* 17: 1011-1015

Kimberley, M.M. (1978) High-temperature uranium geochemistry, *Mineralog. Assoc. Canada Short Course Handbook*, V. 3, pp. 101-104.

Krill, A.G., Bergh, S., Lindahl, I., Mearns, E.W., Often, M., Olerud, S., Olesen, O., Sandstad, J.S., Siedlecka, A., and Solli, A. (1985) Rb-Sr, U-Pb and Sm-Nd isotopic dates from Precambrian rocks of Finnmark. *Norges Geol. Unders.* 403: 37-54

Krill, A.G., Kesola, R., Sjöstrand, T., and Stephens, M.B. (1988) Metamorphic, structural and isotopic age map, northern Fennoscandia. *Geol. Surveys of Finland, Norway and Sweden*, 1:1,000,000

Martinsson, O. (1992) Greenstone hosted Au-Cu ores: The Viscaria and Pahtohavare sulfide deposits and the stratigraphy of the Kiruna greenstones. M.S. thesis, Luleå Univ. Tech., Sweden, 79 p.

Mathiesen, C.O. (1970) An occurrence of unusual minerals at Bidjovagge, northern Norway. *Norges Geol. Unders.* 266: 86-104

Mullis, J. (1979) The system methane-water as a geologic thermometer and barometer from the external part of the Central Alps. *Bull. Minéral.* 102: 526-536

Mullis, J. (1987) Fluid inclusion studies during very low-grade metamorphism. In: Frey, M. (ed.) *Low temperature metamorphism*: Glasgow, Blackie, pp. 162-199.

Neall, F.B., and Phillips, G.N. (1987) Fluid-wall rock interaction in an Archean hydrothermal gold deposit: A thermodynamic model for the Hunt mine, Kambalda. *Econ. Geol.* 82: 1679-1694

Newton, R.C. (1990) Fluids and shear zones in the deep crust. *Tectonophysics* 182: 21-37

Nguyen, P.T., Booth, S.A., Both, R.A., and James, P.R. (1989) The White Devil gold deposit, Tennant Creek, Northern Territory, Australia. *Econ. Geol. Mon.* 6: 180-192

Nicholls, J., and Crawford, M.L., (1985) FORTRAN programs for calculation of fluid properties from microthermometric data on fluid inclusions. *Computers Geosci.* 11: 619-645

Nilsen, K.S., and Bjørlykke, A. (1991) Geological setting of the Bidjovagge gold-copper deposit, Finnmark, northern Norway. *Geol. Foreningens i Stockholm Forhandlingar* 113: 60-61

Nurmi, P.A., Lestinen, P., and Niskavaara, H. (1991) Geochemical characteristics of mesothermal gold deposits in the Fennoscandian Shield, and a comparison with selected Canadian and Australian deposits. *Geol. Survey of Finland* 351, 83 pp.

- Olesen, O., Roberts, D., Henkel, H., Lile, O.B., and Torsvik, T.H. (1990) Aeromagnetic and gravimetric interpretation of regional structural features in the Caledonides of West Finnmark and North Troms, northern Norway. *Norges Geol. Unders.* 419: 1-24
- Ohmoto, H., and Rye, R.O. (1979) Isotopes of sulfur and carbon. In: Barnes, H.L. (ed.) *Geochemistry of Hydrothermal Ore Deposits*. New York, Wiley, pp. 509-567.
- Pharaoh, T.C., and Brewer, T.S. (1990) Spatial and temporal diversity of early Proterozoic volcanic sequences - comparisons between the Baltic and Laurentian shields. *Precambrian Research* 47: 169-189
- Phillips, G.N. (1990) Nature of Archean gold-bearing fluids in Australian greenstone terrains. In: Robert, F., Sheahan, P.A., and Green, S.B. (eds.) *Greenstone Gold and Crustal Evolution: NUNA Conference Vol.*, Geol. Assoc. Canada, p. 192a.
- Reed, M.H. and Spycher, N. (1985) Boiling, cooling, and oxidation in epithermal systems: A numerical modeling approach. In: Berger, B.R. & Bethke, P.M. (eds.) *Geology and geochemistry of epithermal systems, Reviews in Economic Geology Vol. 2*: 249-272
- Rich, R.A., Holland, H.D., and Petersen, U. (1977) *Hydrothermal uranium deposits*. Amsterdam, Elsevier, 264 pp.
- Robert, F., and Kelly, W.C. (1987) Ore-forming fluids in Archean gold-bearing quartz veins at the Sigma mine, Abitibi greenstone belt, Quebec, Canada. *Econ. Geol.* 82: 1464-1482
- Roedder, E. (1984) Fluid Inclusions. In: Ribbe, P.H. (ed.) *Reviews in Mineralogy: Vol. 12*, 646 pp.
- Sandstad, J.S. (1983) *Berggrunnsgeologisk kartlegging av prekambrisk grunnfjell innen kartbladet Målljus, Kvænangen/Kautokeino, Troms/Finnmark: Norges Geol. Unders. Unpub. report. 84.095: 73-76*
- Sandstad, J.S. (1985) *Geologisk berggrunnskart Mållejus 1833 4, 1:50000*. Norges Geol. Unders.
- Shepherd, T.J., Rankin, A.H., and Alderton, D.H.M. (1985) *A practical guide to fluid inclusion studies*. Glasgow, Blackie, 239 pp.
- Skiöld, T. (1988) Implications of new U-Pb zircon chronology to early Proterozoic crustal accretion in northern Sweden. *Precambrian Research* 8: 147-164
- Sibson, R.H. (1977) Fault rocks and fault mechanisms. *J. Geol. Soc. London* 1: 191-213
- Siedlecka, A., Iversen, I., Krill, A.G., Lieungh, B., Often, M., Sandstad, J.S., and Solli, A. (1985) Lithostratigraphy and correlation of the Archean and Early Proterozoic rocks of Finnmarksvidda and the Sørvaranger district. *Norges Geol. Unders.* 403: 7-36
- Stacey, J.S., and Kramers, J.D. (1975) Approximation of terrestrial lead isotope evolution by a two-stage model. *Earth Plan. Sci. Letters* 26: 207-221
- Tanger, J.C. IV, and Pitzer, K.S. (1989) Thermodynamics of NaCl-H<sub>2</sub>O: A new equation of state for the near-critical region and comparison with other equations for adjoining regions. *Geochim. Cosmochim. Acta* 53: 973-987

Taylor, H.P. Jr. (1979) Oxygen and hydrogen isotope relationships in hydrothermal mineral deposits. In: Barnes, H.L. (ed.) *Geochemistry of Hydrothermal Ore Deposits*. New York, Wiley, pp. 236-277.

Touret, J.L.R. (1981) Fluid inclusions in high-grade metamorphic rock. *Mineralog. Assoc. Canada Short Course Handbook*, V. 6, pp. 182-208.

Vearncombe, J.R., Barley, M.E., Eisenlohr, B.N., Groves, D.I., Houstoun, S.M., Skwarnecki, M.S., Grigson, M.W., and Partington, G.A. (1989) Structural controls on mesothermal gold mineralization: Examples from the Archean terranes of southern Africa and Western Australia. *Econ. Geol. Mon.* 6: 124-134

Vik, E. (1985) En geologisk undersøkelse av kobbermineraliseringene i Alta-Kvænangenvinduet, Troms og Finnmark. Unpub. Cand. Scient. Thesis, Trondheim, Norges Tekniske Høyskole, 295 pp.

Walsh, J.F., Kesler, S.E., Duff, D., and Cloke, P.L. (1988) Fluid Inclusion geochemistry of high-grade, vein-hosted gold ore at the Pamour mine, Porcupine camp, Ontario. *Econ. Geol.* 83: 1347-1367

Weast, R.C., Astle, M.J., and Beyer, W.H. (eds.) (1988) *Handbook of chemistry and physics*, 6th ed. CRC Press, Boca Raton, Florida.

Wedekind, M.R., Large, R.R., and Williams, B.T. (1989) Controls on high-grade mineralization at Tennant Creek, Northern Territory, Australia. *Econ. Geol. Mon.* 6: 168-179

Wood, P.C., Burrows, D.R., Thomas, A.V., and Spooner, E.T.C. (1986) The Hollinger-McIntyre Au-quartz vein system, Timmons, Ontario, Canada; Geological characteristics, fluid properties and light stable isotope geochemistry. In: Macdonald, A.J. (ed.) *Proceedings of Gold '86, an International Symposium on the Geology of Gold*: Toronto, 1986, pp. 56-80.

## Figure Captions

**Figure 1:** Generalized geologic map of the northwest portion of the Baltic Shield including areas of northern Norway, Sweden and Finland. After Krill et al. (1988) and Bjørlykke et al. (1992). Small boxes labelled "S" and "P" locate the Saattopora and Pahtohavare deposits. Tectonic windows in the Caledonides exposing the northern extension of the Kautokeino greenstone belt are labelled as "AK": Alta-Kvænangen, "A": Altenes, and "R": Repparfjord-Komagfjord.

**Figure 2:** Generalized tectono-stratigraphic section of the northwestern Kautokeino greenstone belt (after Siedlecka et al., 1985; Vik, 1985). Circled asterisk schematically shows location of the Bidjovagge Au-Cu deposit.

**Figure 3:** Geologic map of the Bidjovagge antiform with location of individual ore lenses along shear zones on the antiform's eastern limb. Modified from Nilsen and Bjørlykke (1991).

**Figure 4:** Oxidation front in graphitic schists at outcrop scale. Hammer for scale.

**Figure 5:** Composite photos of the three main fluid inclusion groups found at Bidjovagge, photographed at room temperature and different focal levels. Scale bars: 0.05 mm. a.) Group I saline aqueous solution with salt crystal, liquid CO<sub>2</sub> bubble and minor daughter crystals. b.) Group I liquid CO<sub>2</sub> inclusions. c.) Group II saline aqueous solutions with salt crystal and additional daughter crystal. d.) Group III liquid CH<sub>4</sub> ± liquid CO<sub>2</sub> inclusions.

**Figure 6:** Microthermometric data for homogenization of Group I pure CO<sub>2</sub> inclusions contained within footwall quartz-carbonate-actinolite veins.

**Figure 7:** Microthermometric data of homogenization and salt dissolution for Groups I and II.

**Figure 8:** Microthermometric data of GROUP III gas-rich inclusions, with homogenization temperatures above the baseline and gas melting, or sublimation for "S" type inclusions, below the baseline.

**Figure 9:** Isochores for Group I and III fluid inclusions, along with average and maximum salt dissolution temperatures. A "polygon" of possible fluid trapping conditions is drawn between 275 and 375°C. Interpreted trapping conditions based on geological evidence (see text) is between 2 to 4 kbars and 275 and 375°C.

**Figure 10:** Typical Raman probe spectra obtained from Bidjovagge samples including a.) CO<sub>2</sub> spectra, b.) H-type CH<sub>4</sub> spectra, c.) carbon spectra, d.) H-type CH<sub>4</sub> spectra with hydrocarbons, and e.) S-type CO<sub>2</sub> spectra.

**Figure 11:** Carbon and oxygen isotope compositions of carbonates from different lithologies, ore zones and veins at Bidjovagge. Carbon isotopes are standardized to PDB and oxygen isotopes are standardized to SMOW.

**Figure 12:** Log f<sub>O<sub>2</sub></sub> vs. pH diagram for the Fe-S-O system, showing phase relationships calculated for 350°C and 3 kbar with SUPCRT92 (Johnson et al., 1991). CH<sub>4</sub>-CO<sub>2</sub>-HCO<sub>3</sub><sup>-</sup> equilibrium shown as short dashed lines. Solubilities of AuCl<sub>2</sub><sup>-</sup> are shown as solid lines in ppm, calculated at 350°C with a log K of -2.5 (Hayashi and Ohmoto, 1991). CuCl

solubilities, in ppm, shown as long dashed lines (Data from Crerar and Barnes, 1976). Fluid composition used in diagram include  $\Sigma S=0.01m$ , and 25 wt % NaCl ( $Cl^-=5.7m$ ). Arrows shows possible fluid path during gold and copper mineralization; A.) Fluids decrease in pH and  $fO_2$  during phase separation and buffering by the pyrite-magnetite-hematite assemblage, B.) A dramatic drop in  $fO_2$  during red-ox reaction with graphitic schist results in gold precipitation together with a pyrite-pyrrhotite assemblage.

**Figure 13:** Schematic block diagram of a Bidjovagge deposit showing the fluid evolution and mineralization. An  $H_2O + CO_2 +$  salt fluid carrying Au and Cu as chloride complexes moves up along shear zone. See text for discussion.

TABLE 1: Explanation for abbreviations of microthermometric measurements

$T_{\text{dsalt}}$	Dissolution of Salt Temperature
$T_{\text{hCO}_2}$	Homogenization of $\text{CO}_2$ Temperature
$T_{\text{hCH}_4}$	Homogenization of $\text{CH}_4$ Temperature
$T_{\text{hH}_2\text{O}}$	Homogenization of $\text{H}_2\text{O}$ +vapor/gas Temperature $\text{H}_2\text{O}$
$T_{\text{hsCH}_4+\text{CO}_2}$	Homogenization Temperature of $\text{CH}_4+\text{CO}_2$ in presence of solid $\text{CO}_2$ (Van Den Kerkhof, 1991)
$T_{\text{mclathrate}}$	Clathrate melting Temperature
$T_{\text{mCO}_2}$	Melting of $\text{CO}_2$ Temperature
$T_{\text{mfinal ice}}$	Final Melting of Ice Temperature
$T_{\text{minitial ice}}$	Initial Melting of Ice Temperature
$T_{\text{sCO}_2+\text{CH}_4}$	Sublimation of $\text{CO}_2+\text{CH}_4$ solid Temperature (Van Den Kerkhof, 1991)

TABLE 2: Microthermometric data for selected saline aqueous inclusions, Groups I and II.

GROUP	Inclusion No.	T <sub>m</sub> initial ice	T <sub>m</sub> final ice	T <sub>m</sub> hydrate	T <sub>m</sub> CO <sub>2</sub>	T <sub>h</sub> CO <sub>2</sub> /CH <sub>4</sub>	T <sub>m</sub> clathrate	T <sub>h</sub> H <sub>2</sub> O+gas	T <sub>d</sub> salt
Group I	BG90-1-1	-39.9	-22.4			25.3	-2.3	150	
	BG90-1-28	-39.6	-22.1					116	222
	BG90-1-49	-35.0	-22.9	9.1	-56.6	-1.8	-12.3		
	BG90-1-52	-34.1	-21.4					150	227
	BG90-17-A10							186	274
	BG90-8-A1	-79.9	-34.9	4.8					
Group II	BG90-8-A11	-80.3	-35.2	1.6					
	BC90-156-A8	-82.9	-28.5	3.5				150	269
	BC90-156-A11	-88.4	-24.8					159	178
	BC90-156-A13	-86.1	-28.2	3.8				126	212
	BC90-156-A21	-71.6	-24.7			-102	-3.0		112
	BC90-156-A22	-57.6	-23.5	8.3		-91	-2.4		289
	BC90-114-B11	-54.8	-21.5	6.2	-72		-11.4	157	236

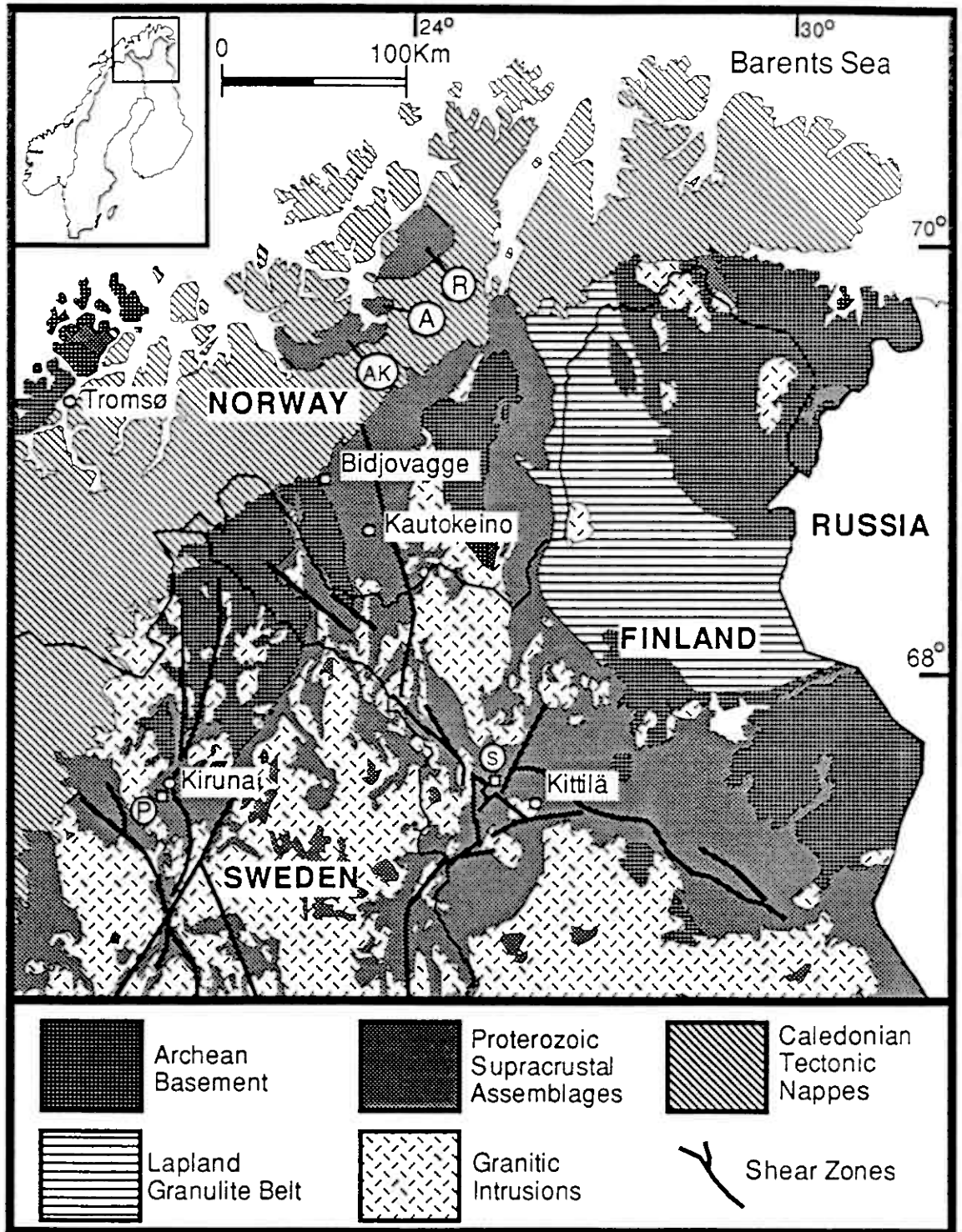
Table 2

TABLE 3: Microthermometric and Raman data on selected gas-rich inclusions of Groups I, II, and III

GROUP	Inclusion No.	T <sub>m</sub> CO <sub>2</sub>	T <sub>h</sub> CO <sub>2</sub>	T <sub>s</sub> CO <sub>2</sub> +CH <sub>4</sub>	T <sub>hs</sub> CH <sub>4</sub> +CO <sub>2</sub>	T <sub>h</sub> CH <sub>4</sub>	T <sub>h</sub> CH <sub>4</sub> +C <sub>2</sub> H <sub>6</sub>	CO <sub>2</sub> peak (cm <sup>-1</sup> )	CH <sub>4</sub> peak (cm <sup>-1</sup> )	CO <sub>2</sub> mole%
Group I	BG90-17-C1	-56.6	-37.7							
	BG90-17-C5	-56.6	-30.4							
	BG90-17-C10	-56.6	-15.0					1385.1		
	BG90-42-A2	-56.6	-39.6					1385.1		
	BG90-42-A3	-56.6	-49.3					1385.1		
	BG90-42-A5	-56.6	-47.1					1385.1		
Group II	BG90-42-B24	-56.6	-52.0							
	BC90-114-B9	-64.2	-38.4							
	BC90-114-B10	-64.3	-60.7							
	BC90-114-B12	-65	-59.5							
	BC90-156-A30					-86.4				
Group III	BC90-156-A32					-79.7				
	BC90-137-A10	-76.7	-76.0							
	BG91-72-A1	-63.3	-28.0					1385.1	2911.5	
	BG91-72-A2	-63.7	-50.9					1385.1	2912.8	
	BG91-72-A3	-62.7	-41.8					1385.1	2911.5	
	BG91-72-A4	-63.5	-47.6					1385.1	2912.8	0.85
	BG91-72-A5	-63.9	-43.2					1385.1	2910.7	0.78
	BG91-72-A18	-60.1	-37.3					1385.1	2911.5	0.92
	BC90-137-A4					-70			2911.5	
	H250-A4					-111.4			2910.7	
	H250-A21					-78.7			2911.5	
	BC90-137-A8			-73.0	-78			1299.4*	2911.5	
	H250-B35			-68.9	-88.6					
	H250-B37			-87.2	-96.6			1294.3*	2911.5	0.15
	H250-B45			-71.1	-108.9					
	BC91-249-A2							-52.9	2911.5	
	BC91-249-A8							-39.6		

\* Strongest CO<sub>2</sub> peak in "S-type" inclusions

Table 3



(Fig. 1)

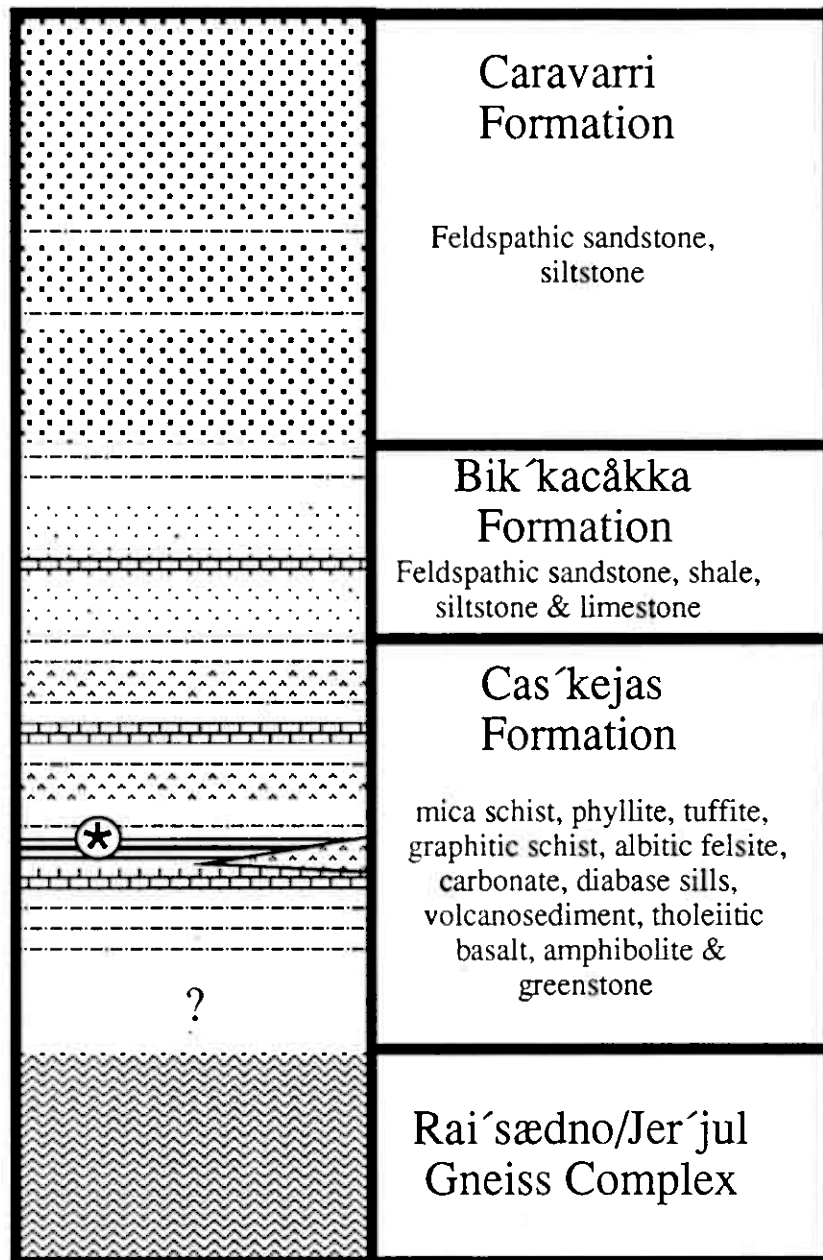


Fig. 2

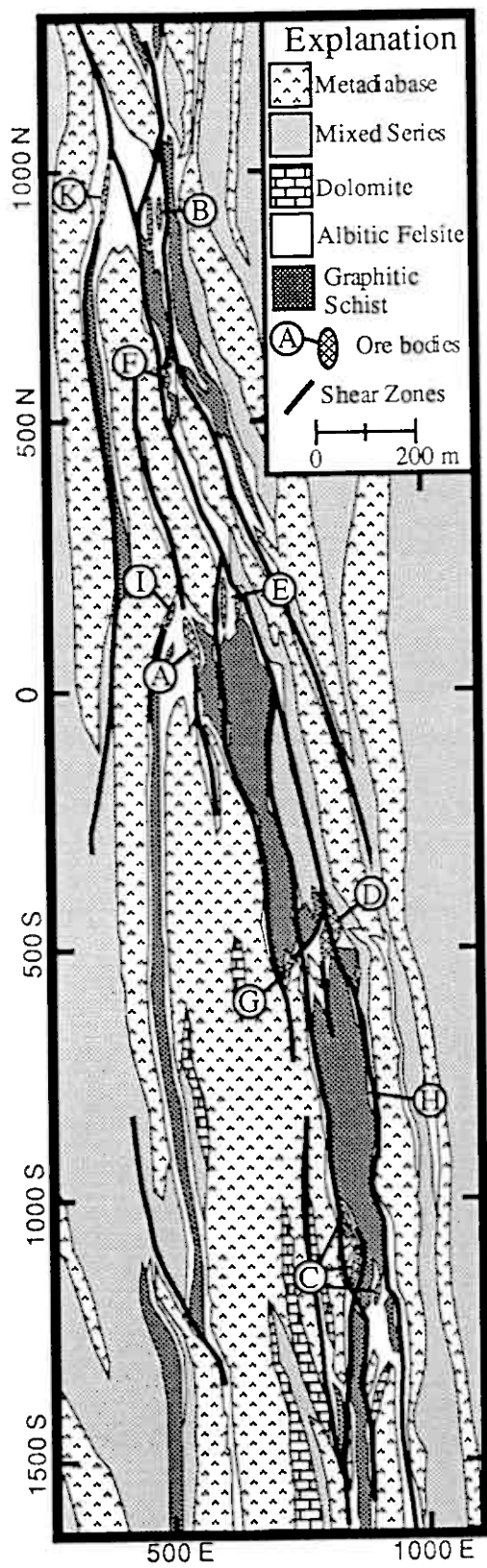


Fig. 3



Fig. 4

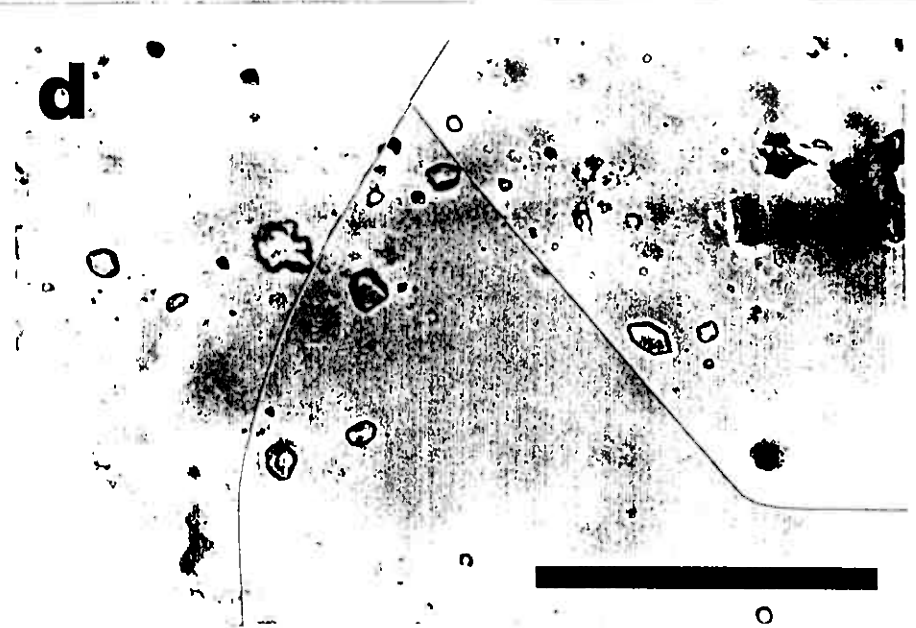
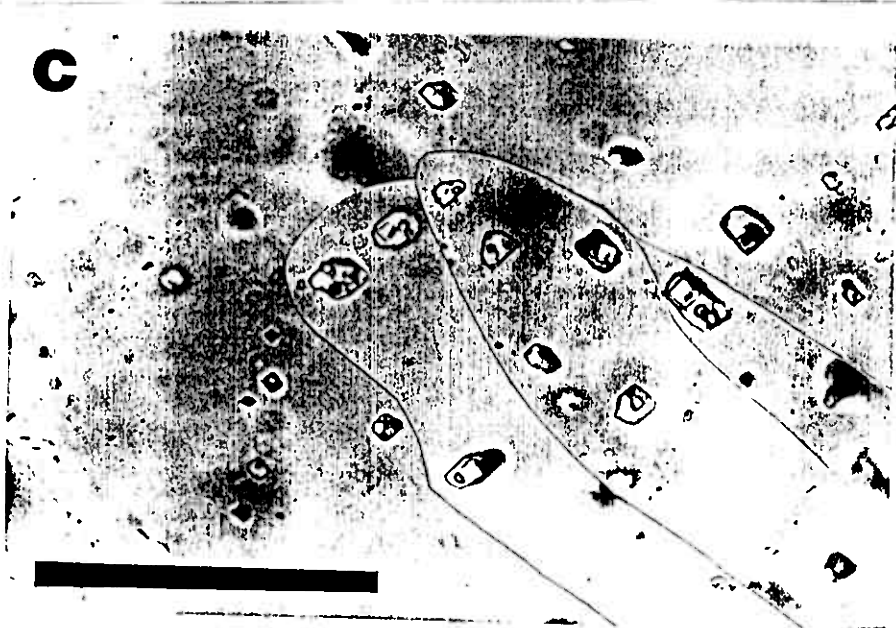
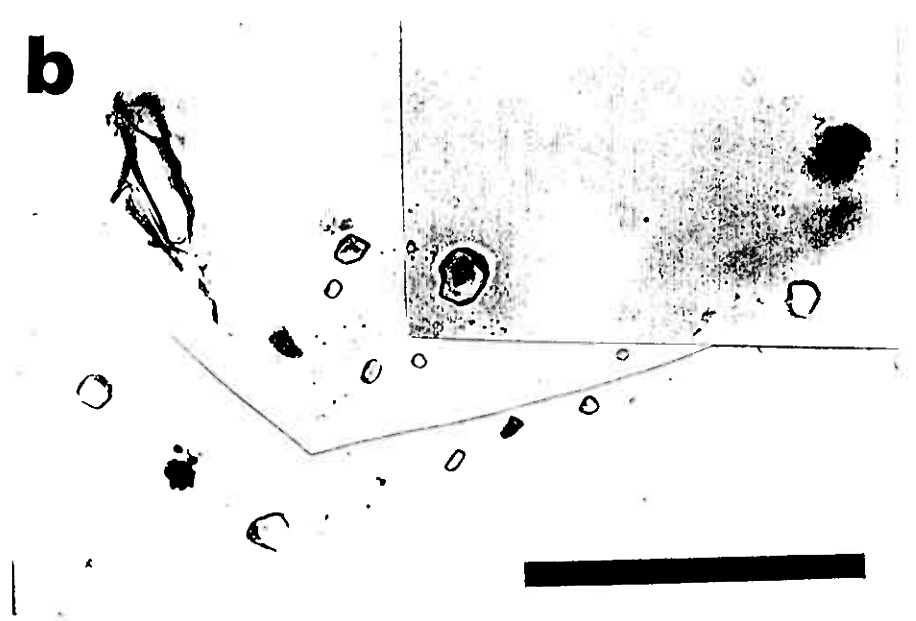
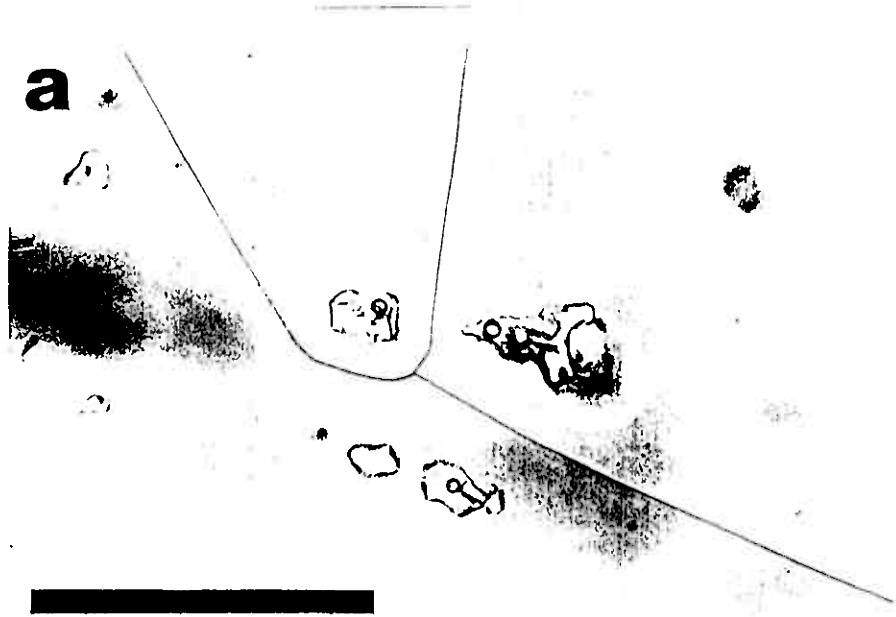


Fig. 5

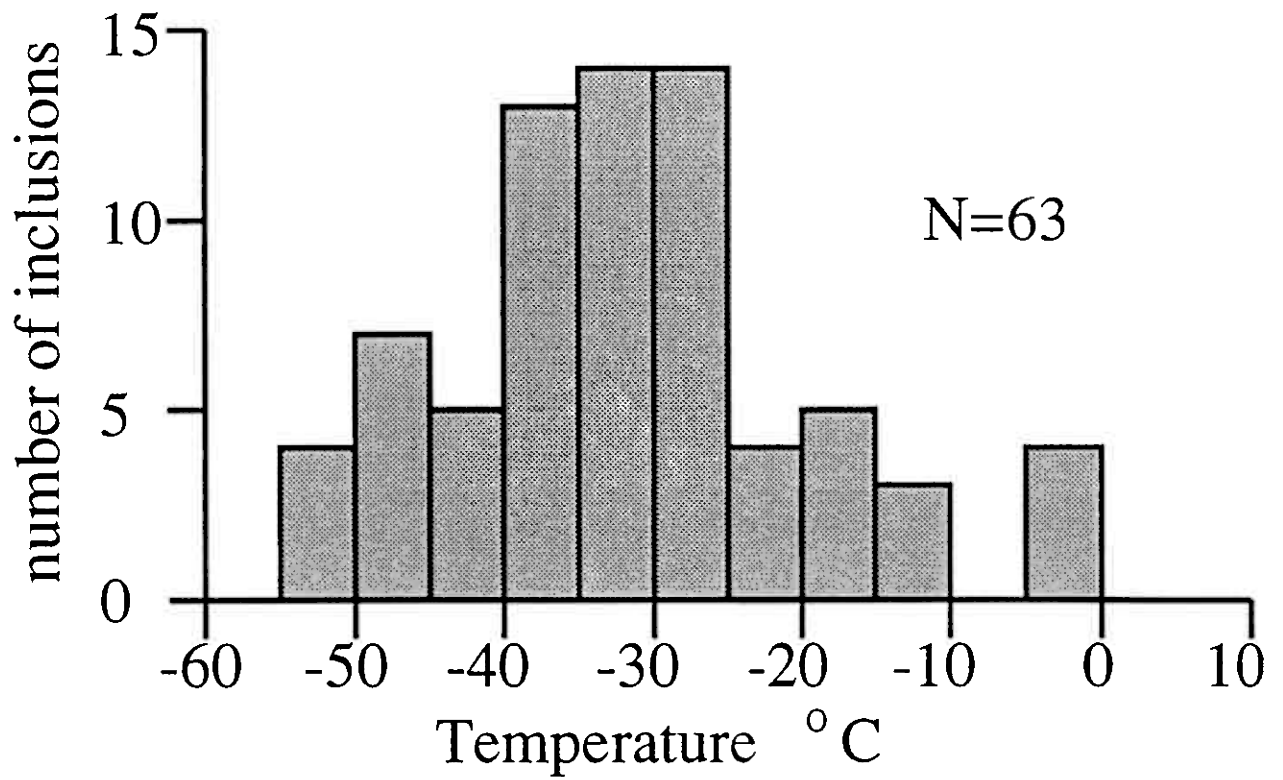
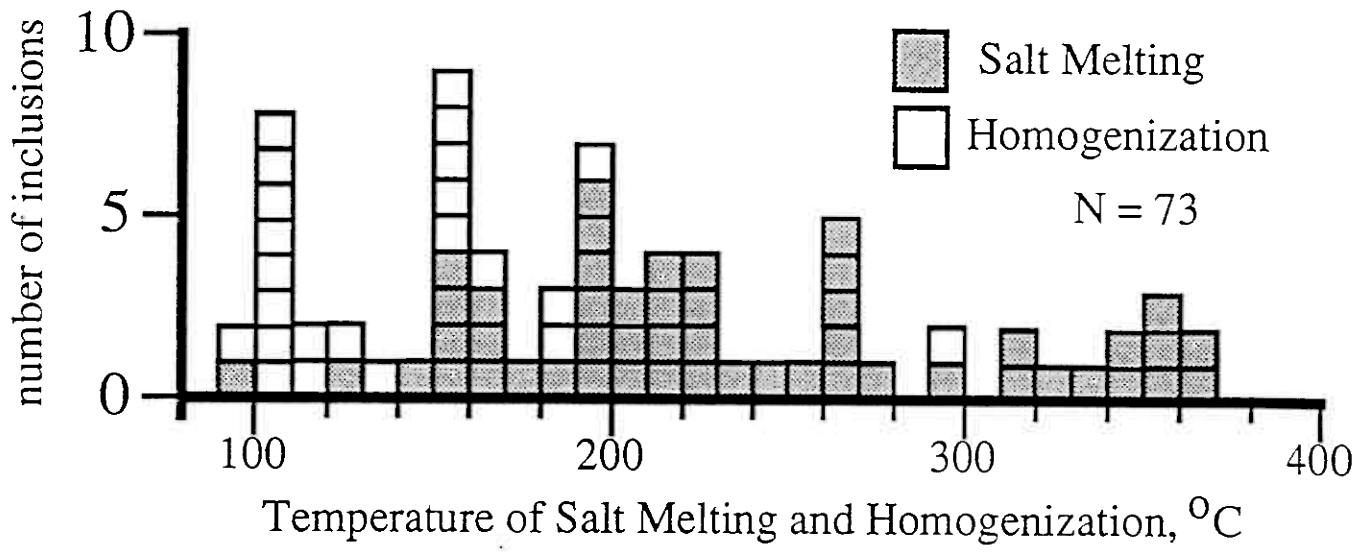


Fig. 6

### GROUP I



### GROUP II

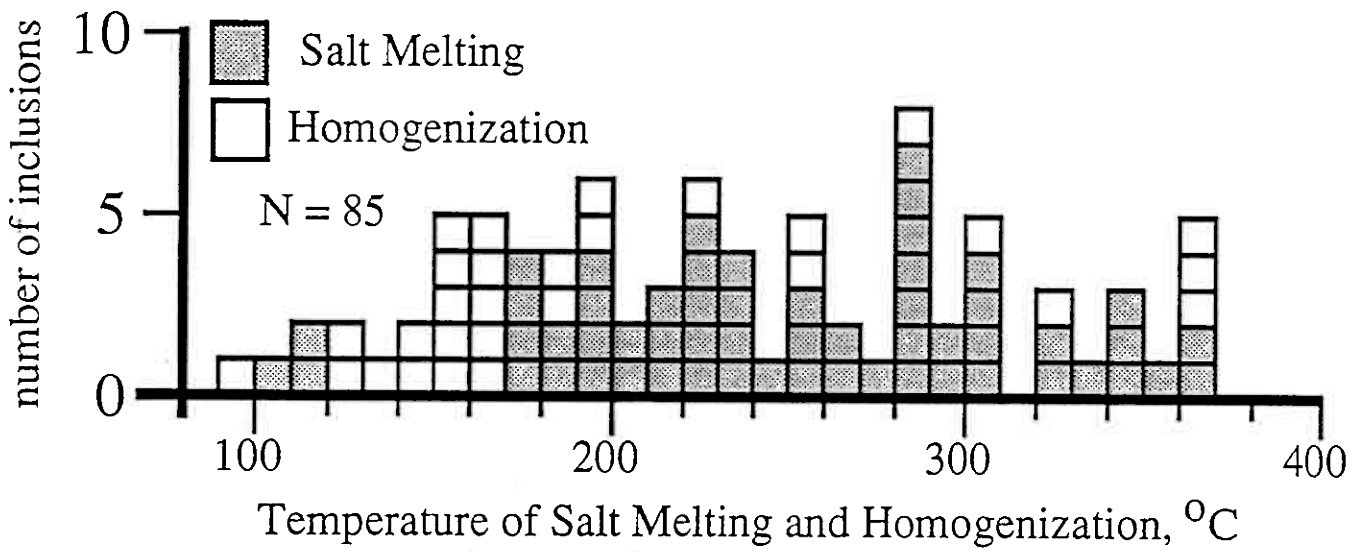


Fig. 7

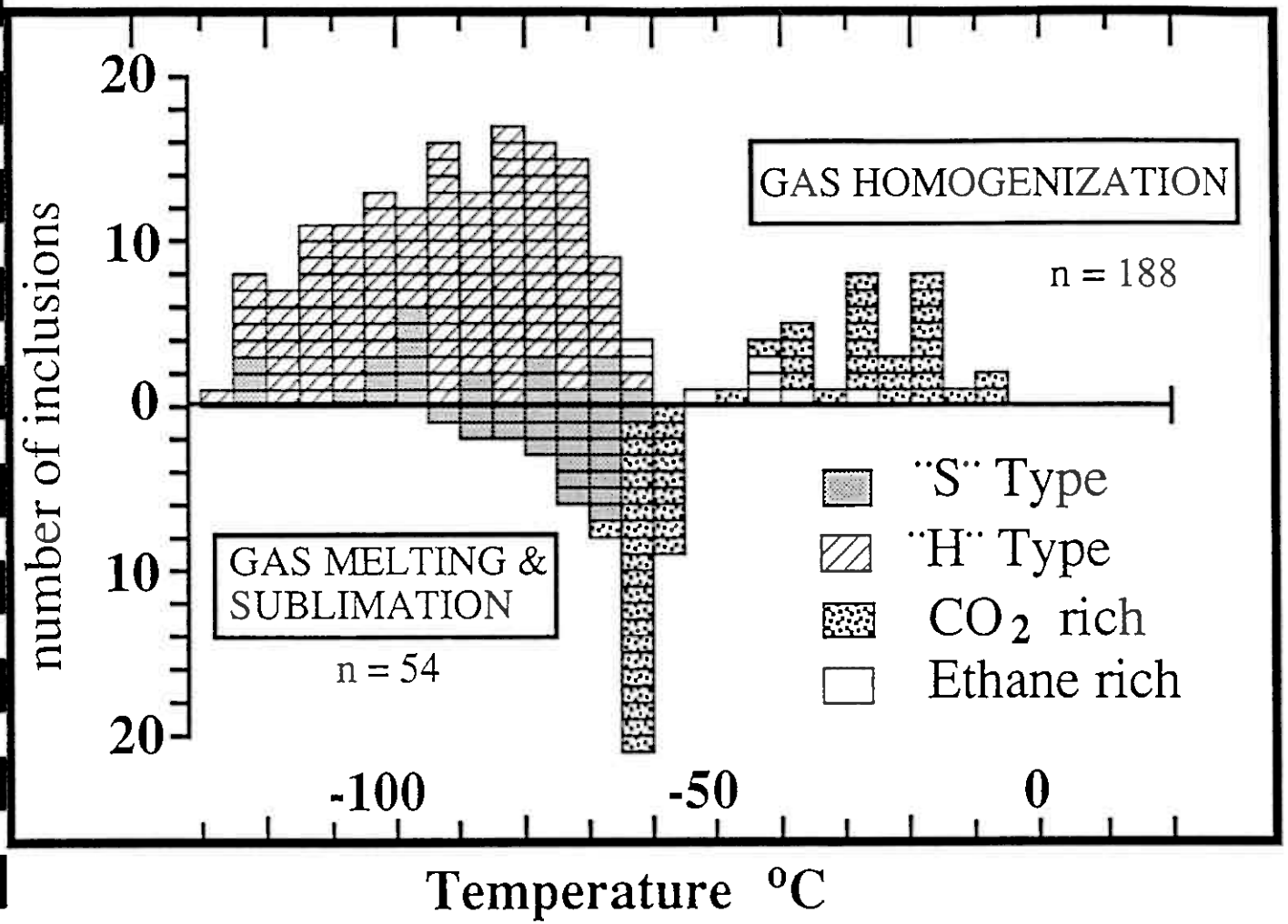


Fig. 8

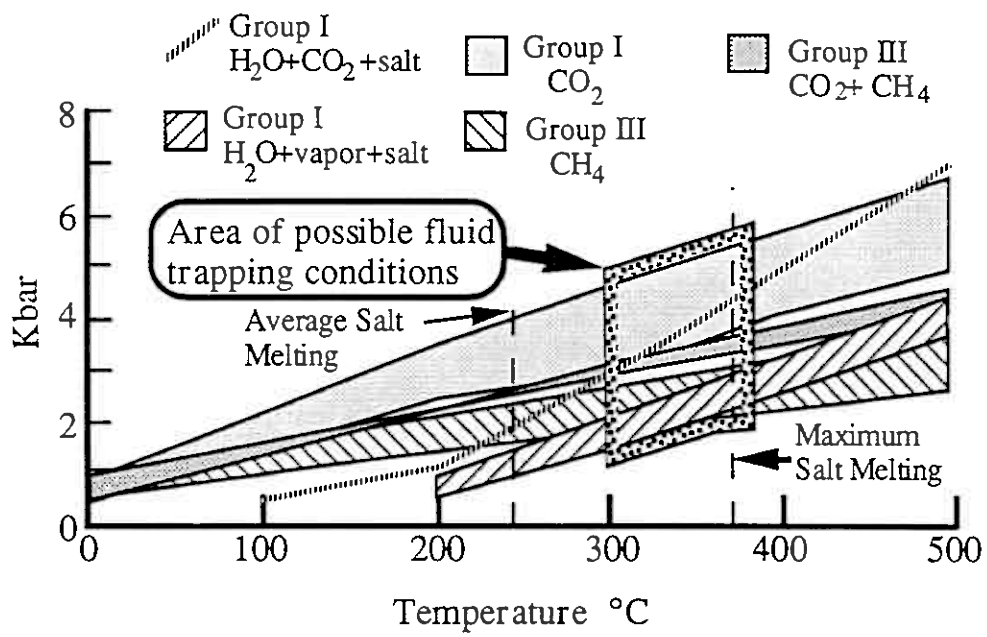


Fig. 9

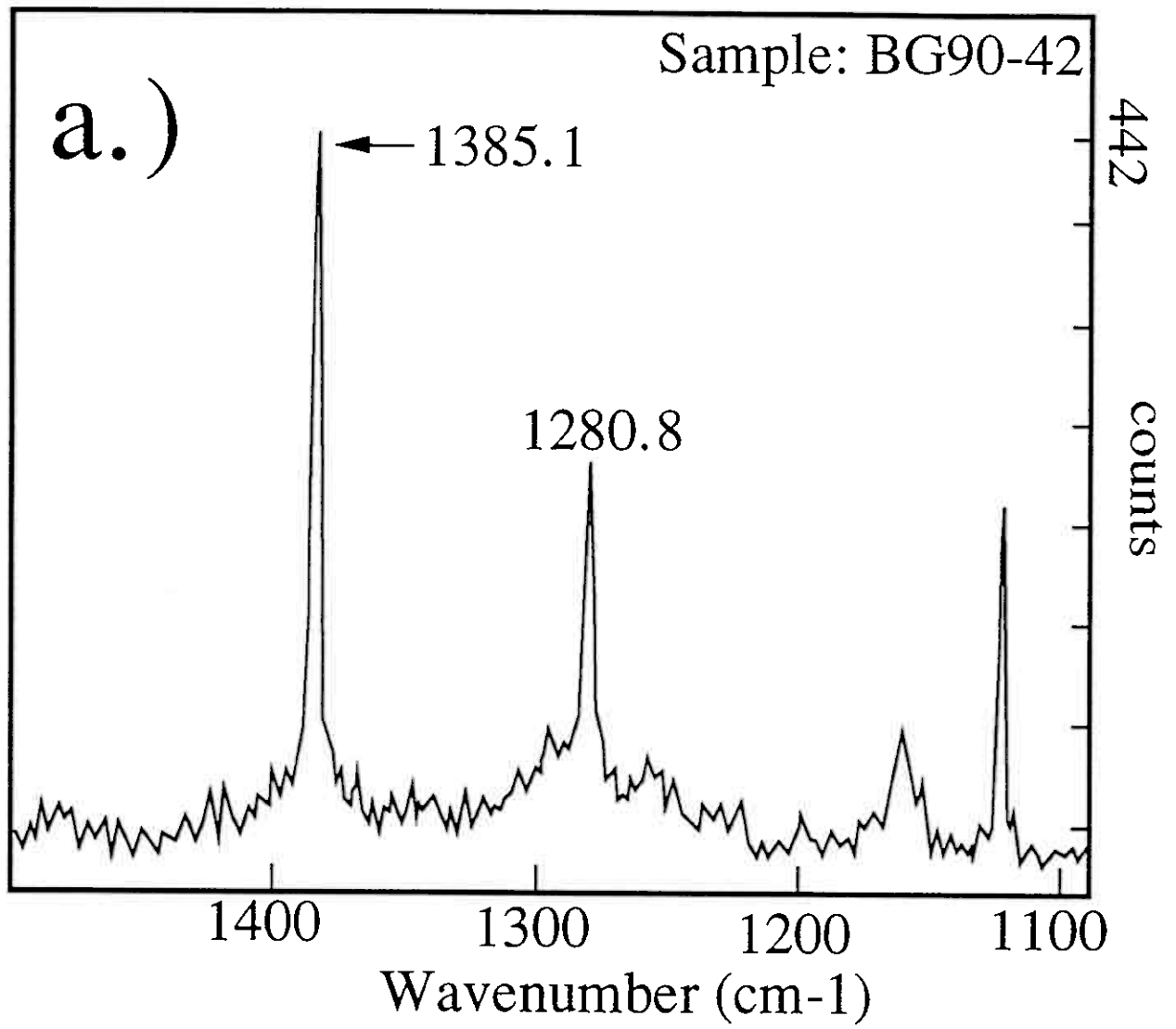


Fig. 10a

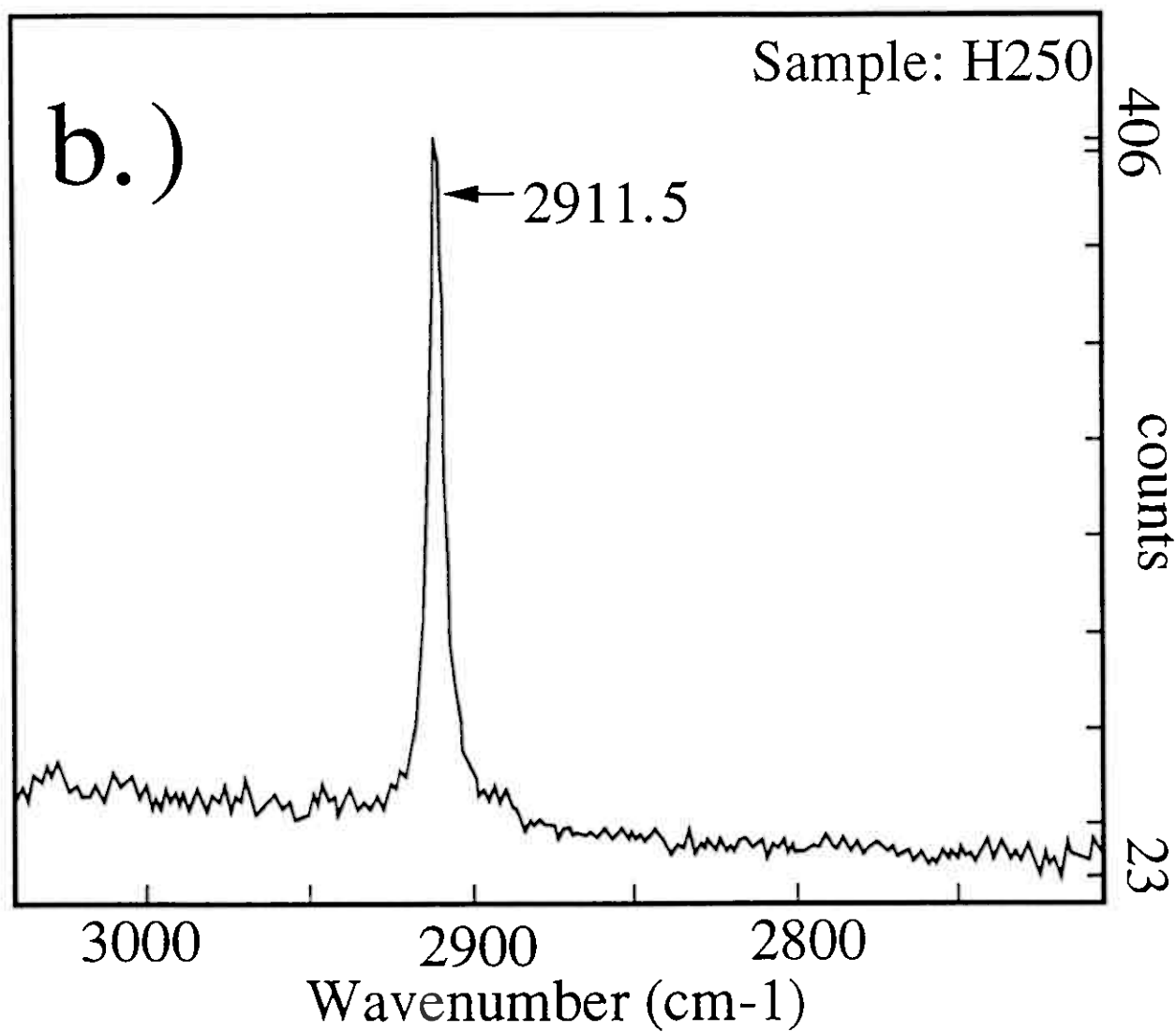


Fig. 10b

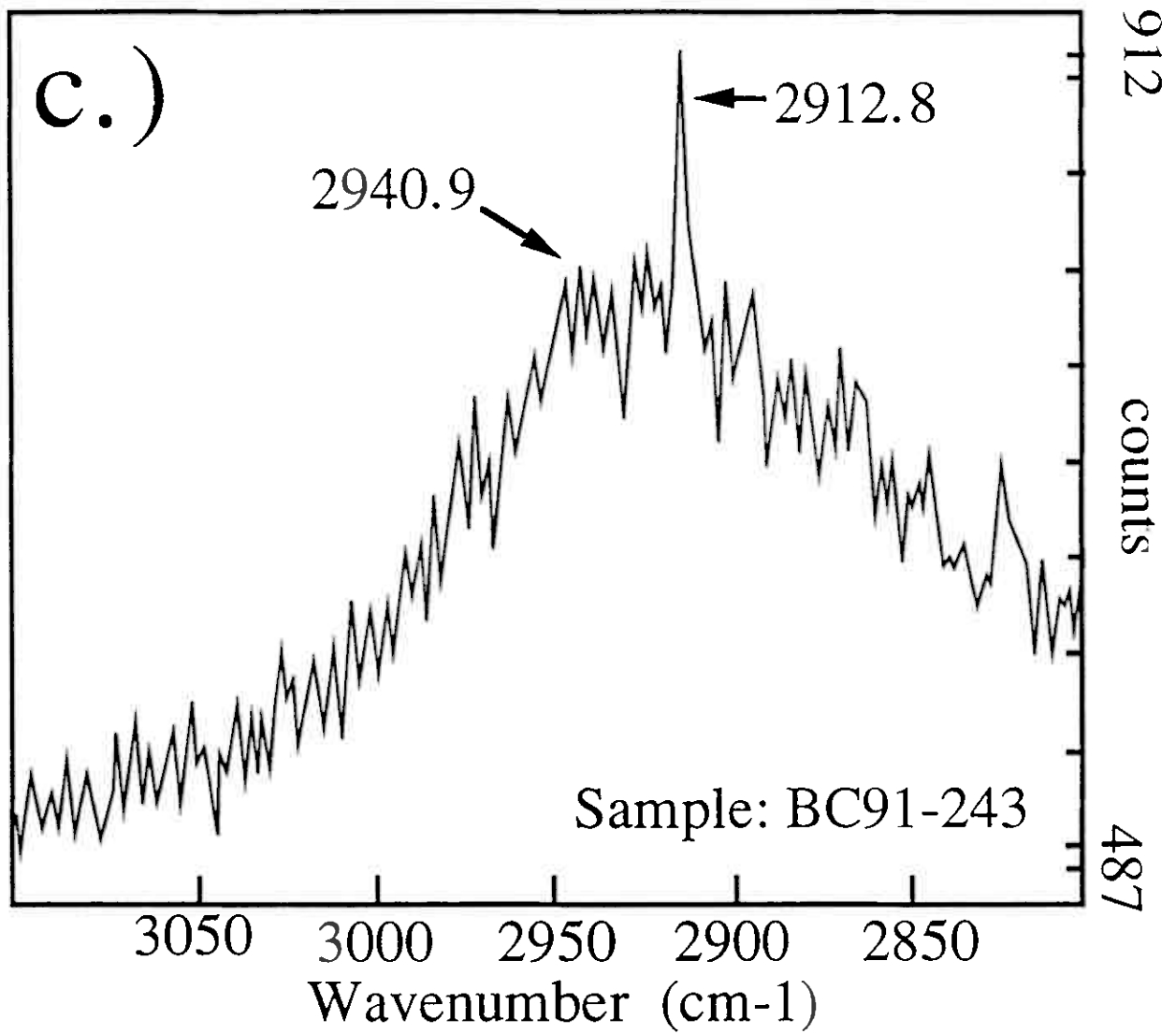


Fig. 10c

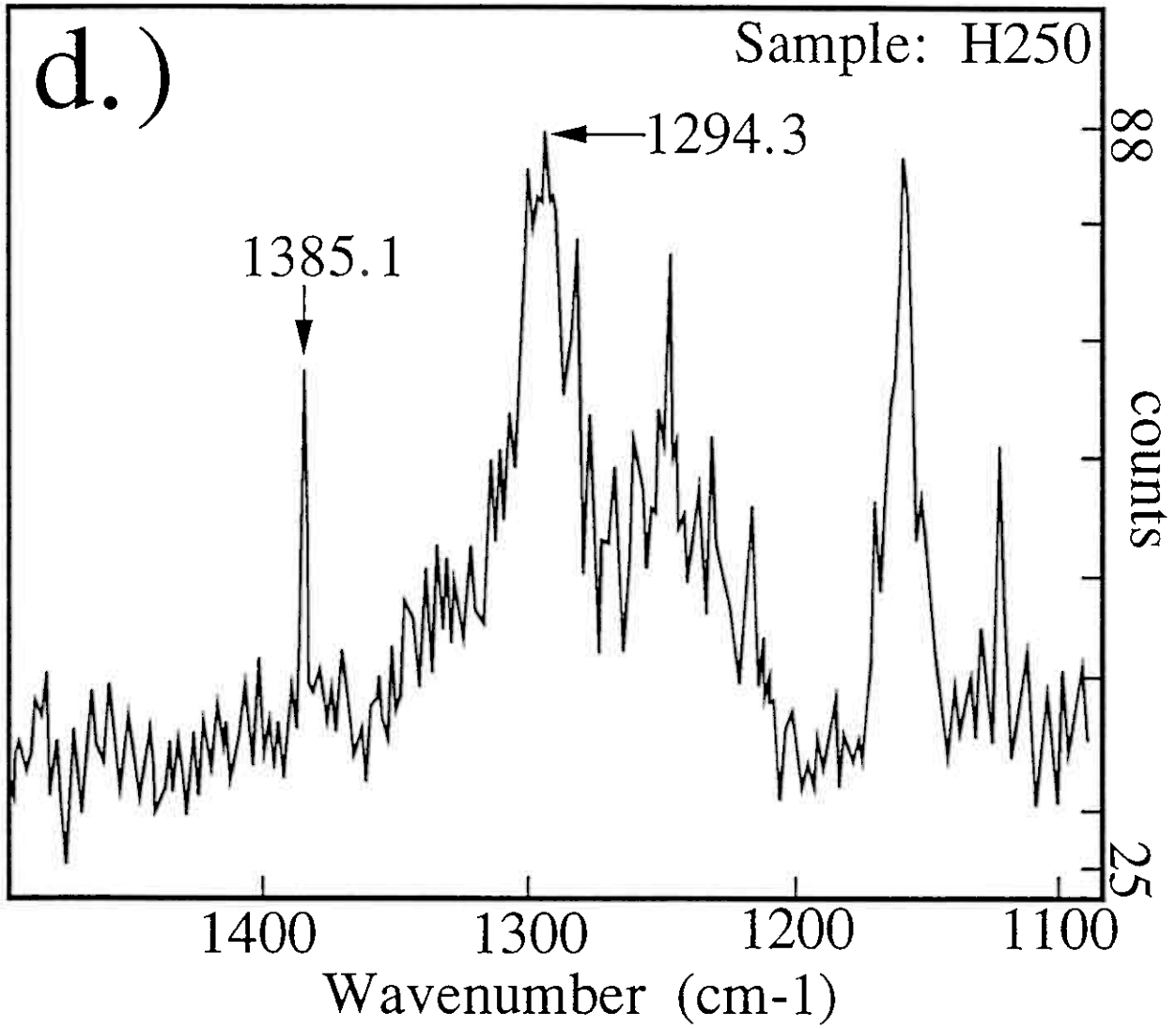


Fig. 10d

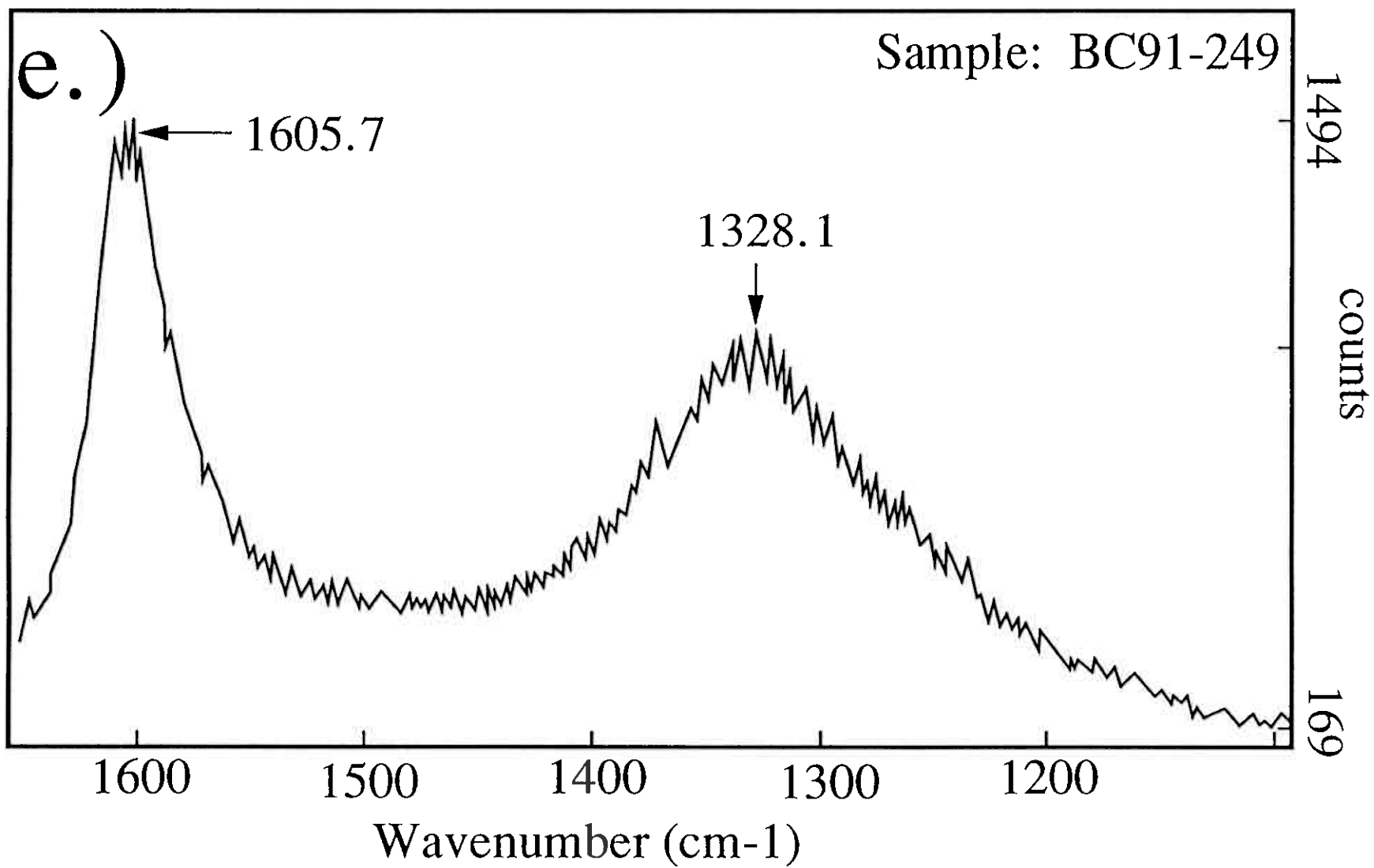


Fig. 10e

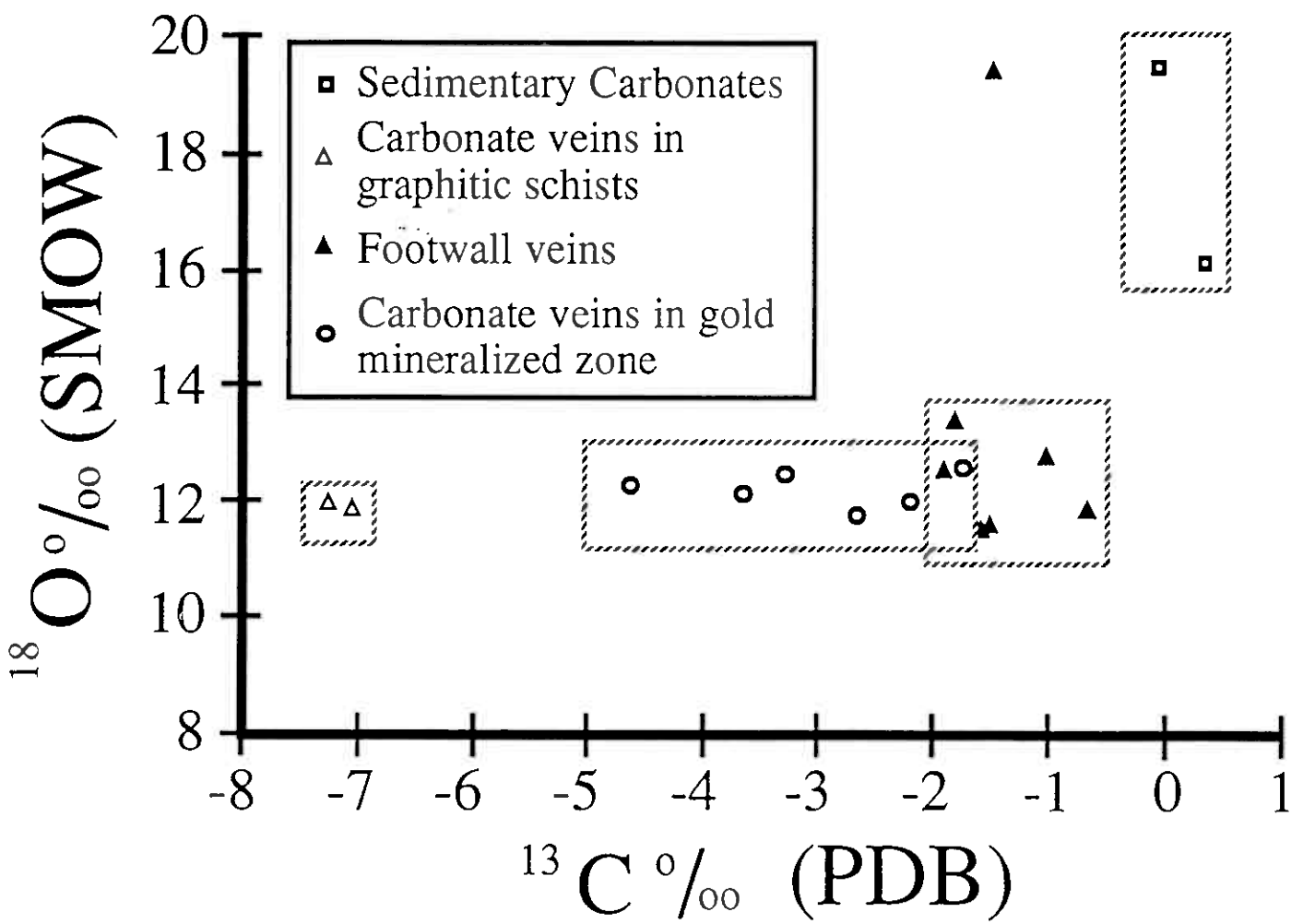


Fig 11

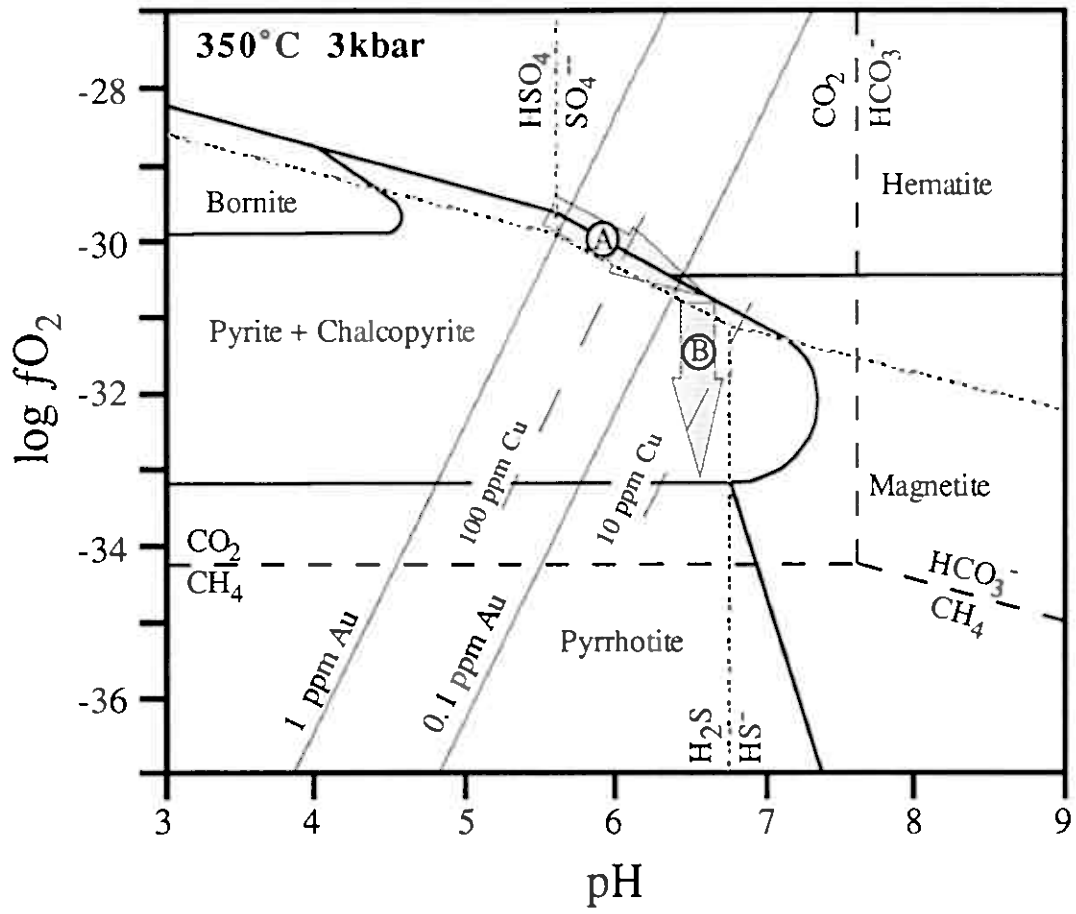


Fig . 12

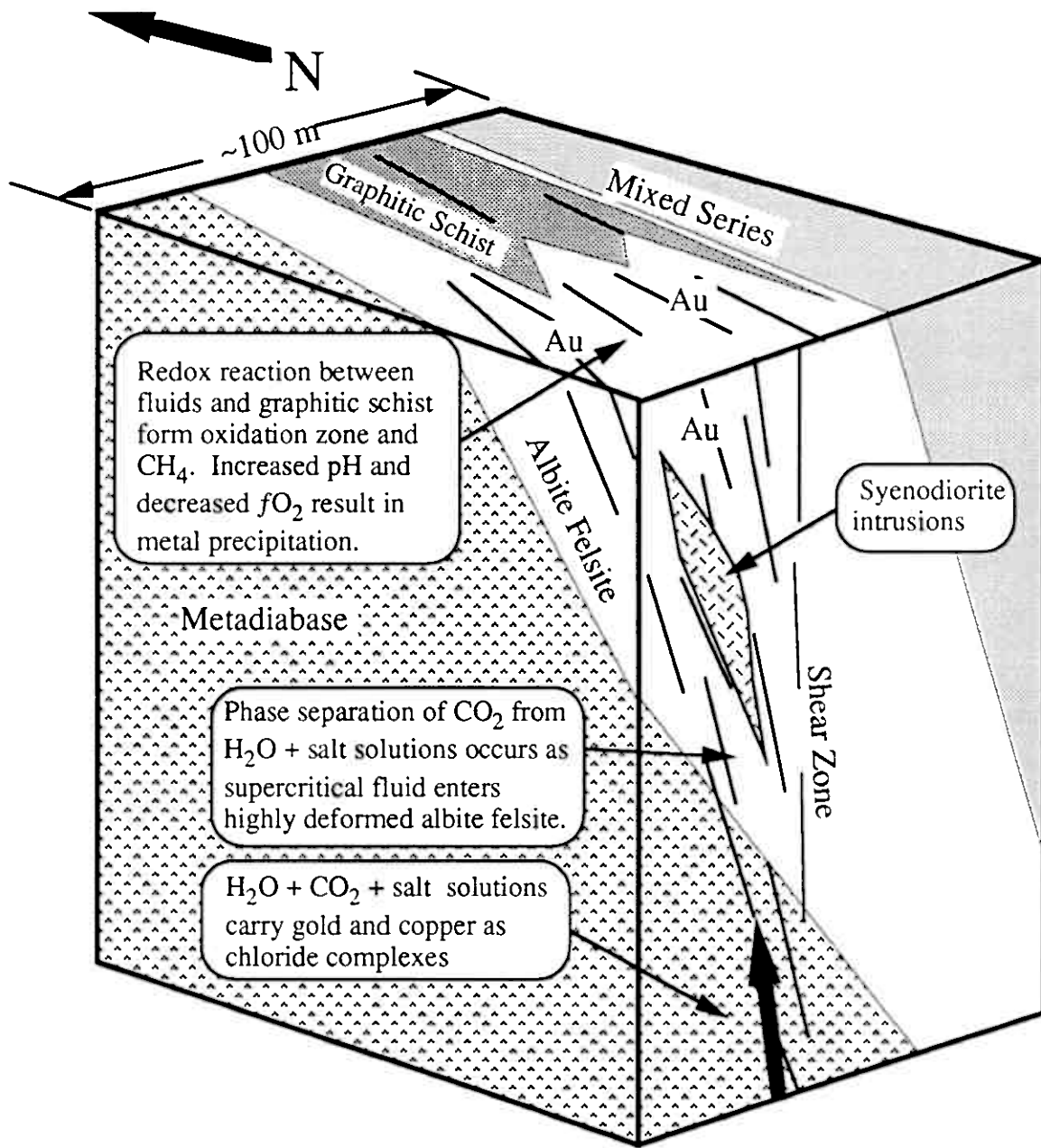


Fig. 13

# PAPER II

Version of 15.6.1993

Fluid evolution and Au-Cu genesis along a shear zone:  
A regional fluid inclusion study of shear zone-hosted  
alteration and gold and copper mineralization in the  
Kautokeino greenstone belt, Finnmark, Norway

David C. Ettner<sup>a</sup>, Arne Bjørlykke<sup>a</sup>, Tom Andersen<sup>b</sup>

*<sup>a</sup>Institute for Geology, University of Oslo, P.O. Box 1047, Blindern, N-0316 Oslo,  
Norway*

*<sup>b</sup>Mineralogical-Geological Museum, University of Oslo, Sarsgate 1, N-0562 Oslo,  
Norway*

ABSTRACT

Gold and copper mineralization of Early Proterozoic age occur along shear zones cutting metamorphosed sedimentary and volcanic rocks, within the Kautokeino greenstone belt, Finnmark, northern Norway. A fluid inclusion study of quartz veins at the Bidjovagge Au-Cu mine, Ucca-vuovdas, Masi River and Object 43, and of pegmatitic quartz at Dælljadas, has been conducted in order to model fluid evolution along the shear zone at different crustal levels. Fluid inclusions associated with the pegmatitic intrusions in amphibolite facies metamorphic rocks are composed of a low to moderately saline H<sub>2</sub>O + CO<sub>2</sub> solution. Within the upper to middle greenschist facies, fluid inclusions contain immiscible highly saline H<sub>2</sub>O and CO<sub>2</sub>. At low greenschist facies, fluid inclusions contain immiscible highly saline H<sub>2</sub>O and N<sub>2</sub>. The highly saline H<sub>2</sub>O + CO<sub>2</sub> fluids were at temperatures between 250 and 400°C and resulted in the albitization, carbonatization and scapolitization of the wall rocks along the shear zones. High temperatures, high salinities, and high *f*O<sub>2</sub> of the fluid resulted in transport of gold and base metals as chloride complexes. Mineralization, such as at the Bidjovagge Au-Cu mine, formed within the ductile to brittle transition in the shear zone as a result of phase separation and reaction of the mineralizing fluids with graphitic schist. Reduced solubility of metal chloride complexes resulted from the phase separation of CO<sub>2</sub> from H<sub>2</sub>O-rich fluids which increased pH, and from interaction with graphitic schist that drastically reduced the oxygen fugacity of the fluid. Reaction with the graphitic schist also resulted in oxidation of the schist, and addition of CH<sub>4</sub> and higher hydrocarbons to the fluid. A metal zonation exists, with copper occurring at each crustal level examined and gold restricted to the brittle-ductile transition. The tendency of gold to be precipitated predominantly in the brittle-ductile transition may reflect the dependence of gold transport on temperature and pressure. Methane in fluid inclusions may serve as a guide to areas where fluid reaction with graphitic schist occurred, such as in the Bidjovagge Au-Cu deposit.

## INTRODUCTION

Metamorphic and magmatic fluids are thought to migrate and evolve along shear zones, on a regional scale, within metamorphic and tectonic belts (Crawford and Hollister, 1986; Newton, 1990). Studies of fluid inclusions have profoundly contributed to the understanding of fluid migration and evolution within shear zones (i.e. Craw, 1988 and 1990; Nwe and Grundmann, 1990; Andersen et al., 1991). The transport of metals and formation of some hydrothermal mineral deposits has been attributed to the evolution of such fluids along shear zones (Cameron, 1989b; Colvine, 1989; Kerrich and Feng, 1992).

The Kautokeino greenstone belt of Proterozoic age, in Finnmark county, Norway, contains several areas of shear zone-hosted gold and copper mineralization, and of albite-carbonate alteration within a cross-section of medium to low grade metamorphic facies. Similarities in hydrothermal alteration and mineralization between different areas suggest that the fluids had related chemical and physical characteristics. This cross-section of mineralized and altered areas in the Kautokeino greenstone belt allows an unique opportunity to study shear zone-hosted mineralization at different metamorphic grades (i.e. crustal levels).

The best known area of mineralization and alteration in the Kautokeino greenstone belt is the Bidjovagge gold and copper mine. The Bidjovagge deposit was exploited for copper between 1970 to 1975 by A/S Bleikvassli Mining Company and A/S Sydvaranger (Hollander, 1979), and between 1985 to 1991 both gold and copper were mined by Outokumpu Oy. During the first mining period approximately 400,000 ton of copper ore, with grades of about 1.8% Cu, were mined (Ekberg and Sotka, 1991). By the end of 1990 1,700,000 tons of ore grading 4.1 g/t gold and 1.19% Cu had been mined by Outokumpu Oy (Ekberg and Sotka, 1991).

A fluid inclusion investigation of the Bidjovagge deposit and other selected mineralized and altered areas has been undertaken to compare fluid chemistry and physical conditions (temperature and pressure) of related fluids along the shear zones. Knowledge of the PT conditions (i.e. crustal depth) for formation of Au-dominated

vs. Cu-dominated mineralized areas in the Kautokeino greenstone belt may benefit exploration for Bidjovagge-type deposits. Results of this investigation together with a model of fluid evolution and Au and Cu mineralization at different crustal levels along shear zones in the Kautokeino greenstone belt are presented in this paper.

## REGIONAL GEOLOGY

Within the northern Fennoscandian shield of Norway, Sweden and Finland, a series of Proterozoic greenstone belts, hosting mesothermal gold deposits, occur within Archean basement complexes (Fig 1). Deposits similar to the Bidjovagge deposit include the Saattopora deposit near Kittilä in Finland, and the Pahtohavare deposit near Kiruna in Sweden (Bjørlykke et al., 1993) (Fig. 1).

The Kautokeino greenstone belt, which hosts the Bidjovagge deposit, trends north-south through the western portion of the Finnmark plateau. This greenstone belt is bordered by two Archean gneissic domes; the Jer'gul gneiss complex on the east and the Rai'sædno gneiss complex on the west (Fig. 2). Along the northern edge of the Kautokeino greenstone belt, the rocks are unconformably overlain by Late Precambrian sandstones of the Dividal Group, which is overlain by Caledonian thrust nappes (Ramsay et al., 1985). Aeromagnetic maps of Finnmark (Olesen et al., 1990) indicate that the Kautokeino greenstone belt continues northward, under the Dividal Group and Caledonian nappes, and is exposed in tectonic windows near the town of Alta (Fig. 1).

### *Lithology*

The Kautokeino greenstone belt is composed of mafic volcanic and sedimentary rocks (Holmsen et al., 1957; Olsen and Nilsen, 1985; Siedlecka et al., 1985), inferred to be early Proterozoic in age (Krill et al., 1985) and to have been deposited during the rifting and subsequent filling of an intracratonic or back arc rift (Siedlecka et al., 1985; Bjørlykke et al., 1987). Three tectono-stratigraphic sections have been

compiled for parts of the Kautokeino greenstone belt; the southern and central areas (Olsen and Nilsen, 1985), the north-western Bidjovagge area and the eastern Masi-Carajav'ri area (Siedlecka et al., 1985) (Fig. 3).

The oldest unit of the Kautokeino greenstone belt are the amphibolites of the Gál'denvarri Formation are inferred to be Archean or Early Proterozoic in age (Siedlecka et al., 1985). The Gál'denvarri Formation is unconformably overlain by the basal portion of the Proterozoic greenstone belt section, which is dominantly composed of quartzite of the Masi Formation. Locally, komatiites of the Baharav'dujav'ri Formation, having a Sm-Nd age of  $1980 \pm 25$  Ma, are found at the base of the section (Olsen and Nilsen, 1985; Olsen and Nilsen, 1989). In the north-western Bidjovagge area the section is truncated by faults and granitic intrusions (Sandstad, 1985, 1992) and the basal section is not exposed (Fig. 2 & 3).

The middle portion of the tectono-stratigraphic section of the greenstone belt is represented by the Cas'kejas, Suoluvuobmi, Lik'ca, Av'zi, and Stuurajav'ri formations (Fig. 3). These formations comprise metamorphosed sedimentary rocks, volcano-sedimentary rocks, mafic volcanic rocks, and diabasic rocks (Olsen and Nilsen, 1985; Siedlecka et al., 1985). A minor occurrence of ultramafic rocks in the Suoluvuobmi Formation are interpreted as komatiites (Siedlecka et al., 1985). Metasedimentary rocks of the middle portion of the tectono-stratigraphic section consist of carbonates, black graphitic schists, and meta pelites (Siedlecka et al., 1985).

The upper part of the tectono-stratigraphic section of the Kautokeino greenstone belt, represented by the Caravarri and Bik'kacâkka formations (Fig. 3), is dominantly comprised of siltstones and feldspathic sandstones (Olsen and Nilsen, 1985; Siedlecka et al., 1985).

#### *Metamorphism and Structure*

The rocks of the Kautokeino greenstone belt have been regionally metamorphosed and also deformed along shear zones of regional extent during the Early Proterozoic Svecokarelian orogeny. The highest metamorphic grade is upper amphibolite facies

(garnet zone or biotite zone + lower garnet zone) and occurs along the margins to the gneissic terrains (Holmsen et al., 1957). The higher metamorphic facies gradually grade to lower greenschist facies (chlorite and lower chlorite zones) towards the middle of the greenstone belt (Holmsen et al., 1957; Siedlecka et al., 1985; Krill et al., 1988; Sandstad, 1992) (Fig. 2). Metamorphic grades can be roughly correlated with the stratigraphic units described above. For example, the lower parts of the tectono-stratigraphic section are amphibolite to upper greenschist facies, the middle portions of the section are upper to middle greenschist facies, while the upper parts of the section are lower greenschist facies. Therefore, we can consider the metamorphic grades to roughly reflect crustal depths.

Field mapping (i.e. Holmsen et al., 1957; Sandstad, 1992) combined with detailed geophysical studies Olesen et al. (1991) of the Kautokeino greenstone belt have revealed intense shear deformation and folding. Two main regional shear zones, described by Olesen et al. (1991), include the NE-SW trending Mierujav'ri-Sværholt Fault Zone (MSFZ) which cut the northeastern section of the Kautokeino greenstone belt, and the NNW-SSE trending shear zones in the western area of the greenstone belt (BBMZ) (Fig. 2). These NNW-SSE trending shear structures have been interpreted by Nilsen and Bjørlykke (1991), Olesen et al. (1991), and Bjørlykke et al. (1993) to be northern extensions of the Baltic-Bothnian megashear zone (BBMZ) of Berthelsen and Marker (1986). Large scale fold structures within the Kautokeino greenstone belt generally trending parallel to shear structures, NNW to NE (Holmsen et al., 1957; Olesen and Solli, 1985; Sandstad, 1985).

Both the structural deformation and the metamorphism appear to be a result from two separate continent-continent and arc-continent collisions during the Svecokarelian orogeny at approximately 1.9 to 1.88 Ga (Skiöld, 1988; Pharaoh and Brewer, 1990; Bjørlykke et al., 1993). Two intrusive periods occurred related to the Svecokarelian orogeny, resulting in foliated "old" granites between 1900 and 1880 Ma and monzonitic intrusions between 1870 and 1860 Ma (Skiöld, 1988; Bjørlykke et al., 1993). Fluvial sedimentation occurred in the Baltic Shield shortly after the main

orogenic event, and before intrusion of post-orogenic monzonites, reflecting rapid crustal uplift (Bjørlykke et al., 1993).

## REGIONAL MINERALIZATION AND ALTERATION

Several areas of Cu, Au, and U-REE mineralization or albite-carbonate alteration, including the Bidjovagge Au-Cu mine, occur in the Kautokeino greenstone belt and have been the focus of prospecting and study (i.e. Holmsen et al., 1957; Bjørlykke et al., 1985; Bjørlykke et al., 1987).

Metasomatic alteration includes albitization, carbonatization and scapolitization. Albitization has been described from several mineralized and unmineralized areas by Gjelsvik (1957), Holmsen et al. (1957), Bjørlykke et al. (1985) and Jensen (1988). Albitization ranges from incomplete albitization of wall rocks to pervasive coarsely crystalline albite and microcrystalline albite felsite. Two periods of albitization are apparent, an early metasomatic period producing albite felsite at the contacts between diabase sills and metasedimentary rocks, and later discordant albite felsite along shear zones. At the Bidjovagge mine, the earlier albite felsite occurs at the contact between graphitic schist and diabase sills. Bjørlykke et al. (1987) suggested that this albite felsite formed when diabase sills intruded wet sediments, and albitization resulted from the circulation of hot sea water. Discordant albite felsite are associated with carbonatization along faults and appears to be related to fluids that migrated through the shear zones.

Scapolitization occurs extensively in the Kautokeino greenstone belt and has been described by Holmsen et al. (1957) and Bjørlykke et al. (1987). In places at Bidjovagge, host rocks consist of scapolite poikiloblasts forming up to 50 volume percent of the rock (Bjørlykke et al., 1987). Similar regional scapolitization has been described in Finnish Proterozoic greenstone belts by Tuisku (1983).

Of the many areas of mineralization and alteration in the Kautokeino greenstone belt, five localities have been chosen in this study to represent mineralization at

different metamorphic grades. These areas include the U-Cu anomaly at Dælljadas in amphibolite facies rocks, the Bidjovagge Au-Cu mine which is located at the boundary between amphibolite to greenschist facies, the Masi River carbonate-albite alteration area in greenschist facies rocks, copper with minor gold mineralization at Ucca-vuovdas which is in greenschist facies, and copper with minor gold mineralization at Object 43 in lower greenschist facies rocks (Fig. 2).

#### *Dælljadas*

The Dælljadas area has been a focus of prospecting by Outokumpu Oy because of a Cu anomaly. Dælljadas is located west-northwest of Kautokeino, along the western edge of the Kautokeino greenstone belt (Fig. 2). The area is composed of amphibolite facies metavolcanic and metasedimentary rocks of the Caskejas Formation which are intruded by granodioritic to granitic pegmatites (Fig. 3). Chalcopyrite occurs as structurally controlled disseminations together with uranium. Minor albitization of the greenstones occurs at Dælljadas.

#### *Bidjovagge Au-Cu deposit*

The Bidjovagge Au-Cu deposit is hosted within shear zones that cut upright isoclinally folded metavolcanic and metasedimentary rocks of the Caskejas Formation at the metamorphic boundary between the amphibolite and the greenschist facies rock (Fig. 2, 3). Host rocks for mineralization are commonly tectonized albitic felsites, produced from metasomatism of black shale and tuffaceous sediment. Syenodiorite dikes, located close to mineralization, are crosscutting shear fabric and may be related to mineralization.

Mineralization at Bidjovagge has been divided into two types, gold-ore type and copper-ore type (Bjørlykke et al., 1987). The gold-ore type has grades of 5-20 ppm Au and 0.1-0.5 % Cu. The copper-ore type grades are 2-5 % Cu and less than 1-2 ppm Au. Generally, the gold and copper ore types can also be distinguished by the nature of the structural setting in which mineralization is hosted; generally gold is

within ductile to brittle structures, whereas copper mineralization is within brittle structures.

Mineralization of the gold-ore type is located within the shear zones where the structures intersect graphitic schists and oxidation and albitic alteration of the graphitic schists is developed. On a small scale, gold mineralization occurs within shear planes and microbrecciation zones in the albitic felsite. Mineralization typically occurs as finely disseminated native gold and gold telluride (calaverite) within sheared and microbrecciated albitic felsite. Veins also contain quartz, carbonate, actinolite (Fe-amphibole), magnetite, pyrite, pyrrhotite, chalcopyrite and minor amounts of apatite, green Cr-rich muscovite, tellurides (altaite, melonite, and tellurobismuthite) and davidite. Davidite, a radioactive mineral which is a member of the crichtonite mineral series (Gatehouse et al., 1978), only occurs within the gold-ore zones (Mathiesen, 1970; Bjørlykke et al., 1987). A zonation of magnetite + pyrite (with some magnetite pseudomorphs after hematite), to pyrite, to pyrite + pyrrhotite occurs from the footwall towards the ore zone. Gangue minerals with some gold mineralization occur as small shear lenses or sets of parallel veinlets, which are locally folded and boudinaged (Bjørlykke et al., 1987), within the sheared albitic felsite. This vein system includes pervasive footwall veins, up to 1 meter thick, extending along the shear zone through the footwall metadiabases and the albitic felsites. In places footwall veins appear in more brittle structures and exhibit discordant contacts with the wall rocks, and occasionally angular clasts of wall rock are found incorporated into the vein.

The copper-ore type mineralization characteristically occurs as chalcopyrite and minor bornite within large vein systems, within more brittle structures, which are predominantly composed of coarse grained carbonate (ankerite and calcite), with albite, actinolite, quartz, pyrite, and minor amounts of telluride and native gold. The large veins are usually subparallel to the shear structure, ranging in thickness up to about 1.5 meters. This vein system probably represents a second or later stage of

mineralization, following the gold-rich mineralization, within a more brittle deformation regime.

Age determinations of the Bidjovagge Au-Cu deposit has been constrained by isotopic dating of the davidite and uraninite by Bjørlykke et al. (1990) and Cumming et al. (in prep.). Davidites found in association with gold gave a U/Pb date of  $1885 \pm 18$  Ma and a Sm/Nd date of  $1886 \pm 88$  Ma (Bjørlykke et al., 1990). Bjørlykke et al. (1990) suggest that these dates indicate that Bidjovagge mineralization occurred during the early phases of the Svecokarelian orogeny. Cumming et al., (in prep) argues that a U/Pb date of  $1837 \pm 8$  Ma, from uraninite containing gold inclusions from Bidjovagge, may be a result of a closure temperature about  $150^\circ\text{C}$  lower than for davidite, consistent with slow cooling after a metamorphic event.

#### *Masi River*

Albite-carbonate alteration occurs in several locations along shear and breccia zones in the Kautokeino greenstone belt (Gjelsvik, 1957; Holmsen et al., 1957) including along the Mierujav'ri-Sværholt Fault Zone (MSFZ) (Olesen et al., 1991) at Masi River where it was described in detail by Holmsen et al. (1957) and Solli (1988) (Fig. 2). The albite-carbonate alteration occurs predominantly within amphiboles and mica schists of the Suoluvuobmi Formation, and quartzite of the Masi Formation (Solli, 1988) along the northward dipping roof of a large duplex structure within the Mierujav'ri-Sværholt Fault Zone (MSFZ) (Olesen et al., 1991). The metamorphic grade in this area is middle to upper greenschist facies (Fig. 2) and brecciation along the shear zone is noted by Holmsen et al. (1957).

Analysis of the albite-carbonate altered rock from the Masi River area by Holmsen et al. (1957), show an enrichment in Na, Si, and  $\text{CO}_2$  and a depletion of Ca, Fe and Mg, as compared to unaltered amphibolite and mica schists. Holmsen et al. (1957) also report occurrences of epidote, actinolite, hematite and scapolite, and minor amounts magnetite, pyrite, chalcopyrite, ilmenite, and molybdenite.

### *Ucca-vuovdas*

Copper and minor gold mineralization occurs at the Ucca-vuovdas area, located approximately 6 km northeast of Kautokeino (Fig. 2). Lithologies in the mineralized area include magnetite-rich metadiabase, biotite schist, albitic felsite, and graphitic schist (Hagen, 1985) of the Cas'kejas Formation or Av'zi Formation which are metamorphosed to the greenschist facies. Both albite-carbonate and biotite alteration are present. Chalcopyrite mineralization occur as breccia filling in albitic felsites, together with quartz, carbonate, pyrite and magnetite. Mineralization at Ucca-vuovdas tends to occur near graphitic schists, but oxidation of the schist is much less pervasive than at the Bidjovagge deposit.

### *Object 43*

Chalcopyrite and minor gold mineralization associated with graphitic schist and albitic felsite has been found 11 km to the east of Bidjovagge at Object 43 (Fig. 2). The area is composed of graphitic schist, albitic felsite, carbonate, metatuffite, argillite and metadiabase intrusions (Hagen, 1986) of the upper Cas'kejas Formation (Sandstad, 1985). Metamorphic grades are lower than at Bidjovagge. Metadiabases display a mineral assemblage of albite, calcite, chlorite, epidote, clinozoisite, titanite, magnetite, ilmenite, and biotite (Stein Lønne, pers. comm., 1993), indicating lower greenschist facies. Mineralization dominantly occur as veinlets and disseminations in brecciated albitic felsites, albite-carbonate altered rock, and graphitic felsites (Hagen, 1986) and gangue minerals include quartz and carbonate. Although a pervasive oxidation zone is not developed in the altered graphitic schists as compared to Bidjovagge, mineralization at Object 43 is spatially related to the schists (Hagen, 1986).

## FLUID INCLUSION STUDY

### *Analytical methods*

Seventeen samples from Dælljadas, Bidjovagge, Masi River, Ucca-vuovdas, and Object 43 were selected for fluid inclusions analysis. Fluid inclusions analyzed from Dælljadas are in large quartz crystals from the pegmatite intrusions. Fluid inclusions analyzed from Bidjovagge, Masi River, Ucca-vuovdas, and Object 43, are in quartz from veins and veinlets.

Doubly polished sections, 100 to 150  $\mu\text{m}$  thick, of the fluid inclusion samples were prepared, and microthermometric measurements were conducted at the fluid inclusion laboratory at the Mineralogical-Geological Museum, Oslo, Norway. All measurements were taken during heating of the sample, generally at a rate of  $5^\circ$  per minute. Measurements were mostly made using a LINKAM THM 600 heating-freezing stage, but because of temperature fluctuations, high precision low temperature measurements were made with a gas-cooled CHAIXMECA stage. Calibration of the LINKAM THM 600 stage was conducted with a series of natural and MERCK synthetic standards. Between  $-142^\circ\text{C}$  (melting point of methylcyclopentane) to  $+200^\circ\text{C}$  precision is approximately  $\pm 5^\circ\text{C}$ , and in the range of  $+200$  to  $+400^\circ\text{C}$  the instrument showed a  $+10$  to  $15^\circ\text{C}$  deviation above true temperatures. High quality low temperature measurements were made on the gas-cooled CHAIXMECA stage that has a precision of  $\pm 1.0^\circ\text{C}$  between  $-142^\circ\text{C}$  and  $+30^\circ\text{C}$ , and a deviation of  $1.0^\circ\text{C}$  which is compensated for after measurement, as described by Andersen et al. (1991).

#### *Fluid inclusions description and relationship to mineralization*

Fluid inclusions described include those interpreted to be primary or pseudosecondary, based on criteria presented by Roedder (1984). Secondary inclusions are omitted from this discussion. The fluid inclusions analyzed during this study contained a range of fluid types, which were composed of  $\text{H}_2\text{O}$ ,  $\text{CO}_2$ ,  $\text{CH}_4$ , and  $\text{N}_2$  (Fig. 4), with dissolved salts, salt crystals, and other daughter crystals (Fig. 5). A systematic division of fluid inclusion types, based on the main fluid phases present at room temperature, is presented in Table 1, together with localities of occurrence.

Fluid inclusions related to gold mineralization at the Bidjovagge deposit, described by Ettner et al. (1992 and in prep.), are included in Table 1.

The first type of fluid inclusion is characterized by either a dominant non-aqueous fluid (CO<sub>2</sub>, CH<sub>4</sub>, or N<sub>2</sub>) or H<sub>2</sub>O. (Table 1). Non-aqueous fluid-rich inclusions are subdivided on the basis of gas impurities, and then further subdivided by the absence or presence of H<sub>2</sub>O. H<sub>2</sub>O-rich inclusions are divided on the basis of salt content; pure H<sub>2</sub>O, salt undersaturated H<sub>2</sub>O, and salt saturated H<sub>2</sub>O. H<sub>2</sub>O-rich inclusions are further subdivided on the presence or absence of gas bubbles (CO<sub>2</sub>, CH<sub>4</sub>, or N<sub>2</sub>). Characteristic microthermometric measurements of selected fluid inclusions are presented in tables 2 and 3.

#### *Microthermometric data*

*CO<sub>2</sub>-rich inclusions.* - CO<sub>2</sub>-rich fluid inclusions, characterized by >50 vol. % CO<sub>2</sub> at room temperature, are observed in samples from Bidjovagge (Ettner et al., in prep.), Masi River, and Ucca-vuovdas together with salt saturated H<sub>2</sub>O inclusions. Fluid inclusions from Masi River and Ucca-vuovdas are single-phase CO<sub>2</sub>-rich inclusions and no water is observed (Fig. 4b,c). At Dælljadas samples contained both single-phase CO<sub>2</sub> and two phase CO<sub>2</sub> + H<sub>2</sub>O fluid inclusions (Fig. 4a).

The single-phase liquid CO<sub>2</sub> inclusions freeze to solid CO<sub>2</sub> + vapor CO<sub>2</sub> upon cooling below around -80°C. During heating, slight CO<sub>2</sub> melting intervals of up to 2.5° were observed, with temperatures of final melting, to liquid plus vapor, ranging from -58.1 to -57.9°C at Ucca-vuovdas, -62.1 to -58.0°C at Masi River, and -57.4 to -56.6 at Dælljadas. Melting behaviour of this type (S+V⇒S+L+V⇒L+V) is classified as "H3 type" by Van Den Kerkhof (1990). These depressed temperatures of CO<sub>2</sub> final melting suggest a slight contamination by CH<sub>4</sub> or N<sub>2</sub> (Burruss, 1981). Some inclusions from Dælljadas melt at the eutectic temperature of CO<sub>2</sub> (-56.6), and therefore, are pure CO<sub>2</sub>.

Homogenization of CO<sub>2</sub> liquid + CO<sub>2</sub> vapor to liquid CO<sub>2</sub> occur over a wide range of temperature for each area (Fig. 6). At Dælljadas, homogenization occurs between

-50 and +25°C with a mode near -20°C. CO<sub>2</sub> homogenization at Masi River ranges between -50 to +10°C with no clear mode, but the majority homogenized at temperatures below -10°C. Measurements from Ucca-vuovdas show generally higher temperatures of homogenization with a range of -30 to +10°C.

Two phase CO<sub>2</sub> + H<sub>2</sub>O inclusions from Dælljadas comprise H<sub>2</sub>O with 10 to 40 volume % fill. Carbonate daughter crystals are sometimes present. Similar two phase inclusions from Dælljadas with >50 volume % H<sub>2</sub>O are described as H<sub>2</sub>O-rich inclusions. Upon cooling below -90°C these inclusion freeze to ice + solid CO<sub>2</sub> + CO<sub>2</sub> vapor. A slight CO<sub>2</sub> melting interval of about 2° is rarely observed, and CO<sub>2</sub> final melting temperature range between -57.6 to -56.6°C. Similar to single-phase CO<sub>2</sub> inclusions, the depressed final melting temperature indicates the presence of small amount of CH<sub>4</sub> or N<sub>2</sub> (Burruss, 1981). Measured temperatures of homogenization of the carbonic liquid + CO<sub>2</sub>-rich vapor to carbonic liquid range between -25 to +10°C. Clathrate melting occurs between +9 and +12.5°C, below and above the invariant point of a pure CO<sub>2</sub> clathrate (Hollister and Burruss, 1976). Clathrate melting between the invariant point of pure CO<sub>2</sub> clathrate (+10°C) and +12.5°C suggests the presence of CH<sub>4</sub> (Unruh and Katz, 1949; Hollister and Burruss, 1976). Clathrate melting in the presence of pure CO<sub>2</sub> liquid and CO<sub>2</sub> vapor, may be used to estimate the salinity of the water (Collins, 1979), but the presence of CH<sub>4</sub> complicates this estimation of salinity (Hollister and Burruss, 1976). Generally, it may be said that the clathrate melting temperatures in Dælljadas samples are compatible with very low salinity.

*Nitrogen-rich inclusions.* - Rare nitrogen-rich inclusions have been observed in one sample from Object 43 (Fig. 4d). Fluid inclusions are found in quartz which, along with carbonate, albite, and chalcopyrite, occur as breccia filling within a tectonized metadiabase. From textural observations neither the single-phase liquid nitrogen inclusions or the salt saturated H<sub>2</sub>O inclusions align themselves along healed secondary fractures, and appear to be coeval. These inclusions do not freeze when

supercooled to  $-189^{\circ}\text{C}$ . Homogenization of liquid + vapor to liquid occurs around  $-149^{\circ}\text{C}$ . This low temperature suggests that the inclusion is dominated by nitrogen (Swanenberg, 1980).

*Salt undersaturated H<sub>2</sub>O inclusions.* - Primary inclusions of this type were observed at both Dælljadas and in quartz gangue related to the copper mineralization at the Bidjovagge deposit.

H<sub>2</sub>O-rich fluid inclusions from Dælljadas freeze to ice upon cooling below  $-70^{\circ}\text{C}$ . During heating, first melting was observed between  $-30$  and  $-50^{\circ}\text{C}$ , and final melting between  $-1$  to  $-9^{\circ}\text{C}$ . First melting temperatures indicate that NaCl + CaCl<sub>2</sub> may be present as dissolved salts in the inclusion (Crawford, 1981). Final melting temperatures indicate low weight percents of dissolved salts, ranging from 1.5 to 12.5 wt. % NaCl equivalent (Potter et al., 1978). At room temperature inclusions contain a single-phase, although in some inclusions a vapor bubble forming less than 5 volume % of the inclusion, was observed.

Rare salt undersaturated H<sub>2</sub>O inclusions which contain liquid CO<sub>2</sub> bubbles have been observed at Dælljadas. A few of these inclusions also contain carbonate daughter crystals. Temperatures of both CO<sub>2</sub> and clathrate melting are similar to measurements of CO<sub>2</sub>-rich inclusions from Dælljadas

Fluid inclusions related to the copper-ore type at Bidjovagge are generally of the salt undersaturated H<sub>2</sub>O type (Fig. 5a). At room temperature the vapor bubble form less than 5 volume % of the inclusion. During cooling these fluid inclusions freeze to ice. First melting is observed between  $-90$  and  $-60^{\circ}\text{C}$  and final melting generally occurs between  $-30$  and  $-20^{\circ}\text{C}$ . Salt hydrates were observed in some inclusions, melting between  $-15$  and  $0^{\circ}\text{C}$ . The very low first melting temperatures are similar to those observed in salt saturated inclusions related to the gold-ore type at Bidjovagge (Ettner et al., in prep.), and may be due to metastability (Roedder, 1971) of a H<sub>2</sub>O + NaCl + CaCl<sub>2</sub> solution, or to the presence of an additional salt such as LiCl (Borisenko, 1977). The final ice melting temperatures and observed salt hydrate

melting temperatures correspond to a solution dominated by approximately a 25 wt. % salt mixture of NaCl + CaCl<sub>2</sub> (Crawford, 1981). The NaCl + CaCl<sub>2</sub> salt undersaturated H<sub>2</sub>O inclusions at Bidjovagge homogenize to liquid between 100 to 200°C, and display a mode between 105 to 120°C (Fig. 7).

*Salt saturated H<sub>2</sub>O inclusions.* - Inclusions of this type commonly occur at Bidjovagge, Masi River, Ucca-vuovdas and Object 43. At Bidjovagge, these inclusions are predominantly related to gold-ore (Ettner et al., in prep.), but a few inclusions of this type have also been observed related to the copper-ore.

Fluid inclusions from Masi River contained one salt crystal, at room temperature, and often a carbonate daughter crystal (Fig. 5b). First melting of ice in these inclusions occurs between -75 and -69°C and final melting of ice between -30 and -25°C. Salt hydrate melting was observed between -15 and -2°C. First melting temperatures of ice indicate that either metastability (Roedder, 1971) or complex salt mixtures are involved. The temperatures of final melting of ice suggest that NaCl and CaCl<sub>2</sub> salts are present (Crawford, 1981). Homogenization to liquid H<sub>2</sub>O occurs between 110 to 190°C followed by salt dissolution at from 140 to 350°C, thus indicating salinities between 29 to 42 wt. % NaCl equivalent (Haas, 1976; Tanger and Pitzer; 1989).

At Ucca-vuovdas, salt saturated H<sub>2</sub>O inclusions commonly contain up to 4 daughter crystals. These always comprise a NaCl crystal, but may also comprise a carbonate crystal or other unidentified daughter crystals (Fig. 5c). First melt of the ice occurs between -85 to -75°C and final melt around -45°C. Salt hydrate melting could be observed in a few inclusions at rough temperatures between -12 to -1, but could generally not be measured. Homogenization of the vapor + liquid H<sub>2</sub>O to liquid H<sub>2</sub>O occurs from 95 to 135°C. These inclusions commonly decrepitate above 230°C and before salt dissolution. Few measured temperatures of salt dissolution show a wide range between 170 and 450°C. Salt crystals do not display uniform volume ratios between fluid inclusions, with visual estimates of salinities ranging from 30 to

over 70% (Roedder, 1984). This range of volume ratios of the salt crystals suggests that the fluid may have been saturated in salt and that salt crystals were accidentally trapped (Roedder, 1984).

Salt saturated H<sub>2</sub>O inclusions at Object 43 typically contain a NaCl crystal, and 1 or 2 other daughter crystals comprising carbonate and unidentified phases (Fig. 5d). Vapor bubbles fill less than 5 volume % of the inclusion. The observed first melting of ice is usually between -85 and -70°C, the and final melting of ice between -50 to -30. Salt hydrate melting was difficult to observe but in a few inclusions hydrate melting occurred around -1°C. Similarly to Masi River, the first melting temperatures of ice indicate that either metastability (Roedder, 1971) or complex salt mixtures are involved. Also, the final melting temperatures of ice suggest that NaCl and CaCl<sub>2</sub> salts are present (Crawford, 1981). Homogenization of liquid H<sub>2</sub>O + vapor to liquid H<sub>2</sub>O generally occurs in the range of 80 to 210°C (Fig. 7). Salt dissolution typically occurs after homogenization over a wide range from 130 to 380°C, but most dissolution occur between 230 and 320°C (Fig. 7). Salinity estimations from final salt dissolution temperatures (Haas, 1976) indicate that most inclusions contain between 33 to 40 wt. % NaCl equivalent .

#### *Raman microprobe analysis*

Laser-excited Raman microprobe analysis were conducted at the Geological Institute, University of Stockholm, with the help of Sten Lindblom. The instrument used is a multichannel DILOR-XY, a successor to the MICRODIL-28 (Burke and Lustenhouwer, 1987). Measured line positions of CO<sub>2</sub>, CH<sub>4</sub> and N<sub>2</sub> were identified by comparison with listed values by Dubessy et al. (1989), Van Den Kerkhof (1991) and E.A.J. Burke (pers. comm.).

Non-aqueous liquid-rich fluid inclusions were analyzed to determine their chemical composition. The presence of liquid CO<sub>2</sub> was confirmed in samples from Dælljadas, Masi River, and Ucca-vuovdas. Raman spectra for the CO<sub>2</sub> inclusions show two peaks, the strongest peak at  $\Delta\nu=1386\text{ cm}^{-1}$ , and the second peak at  $\Delta\nu=1280.8$  to

1282.5  $\text{cm}^{-1}$ . The presence of a second gas, as indicated by microthermometric analysis, was confirmed by Raman analysis. In  $\text{CO}_2$ -rich inclusions from Dælljadas, minor nitrogen was identified by a peak at  $\Delta\nu=2326.9 \text{ cm}^{-1}$ . Masi River  $\text{CO}_2$ -rich inclusions contain minor  $\text{CH}_4$ , identified by a peak at  $\Delta\nu=2910.8$  to  $2912.2 \text{ cm}^{-1}$ , and possibly trace  $\text{N}_2$  was observed at  $\Delta\nu=2326.9 \text{ cm}^{-1}$ . Raman spectra from Ucca-vuovdas show that the  $\text{CO}_2$  contains minor  $\text{N}_2$ , indicated by a peak at  $\Delta\nu=2326.9 \text{ cm}^{-1}$ .

Raman microprobe analysis of non-aqueous liquid inclusions from Object 43, interpreted by microthermometric analysis to contain  $\text{N}_2$ , display a  $\text{N}_2$  peak at  $\Delta\nu=2327.7 \text{ cm}^{-1}$ , but also appear to contain trace  $\text{CH}_4$  as determined by a minor peak at  $\Delta\nu=2915.6 \text{ cm}^{-1}$ .

#### *Pressure-Temperature Estimation*

Microthermometric and Raman microprobe data have been used to construct isochores for non-aqueous liquid-rich inclusions from Dælljadas, Masi River, Ucca-vuovdas, and Object 43, and for  $\text{H}_2\text{O}$  inclusions, undersaturated with salt, from Bidjovagge. Molar volumes of non-aqueous liquid-rich inclusions were estimated with composition-molar volume projections of the  $\text{CO}_2$ - $\text{CH}_4$  and  $\text{CO}_2$ - $\text{N}_2$  systems (Van Den Kerkhof, 1990). Isochores for different the compositions and molar volumes of fluid inclusions have been calculated using the computer software, ISOCHOR (Holloway, 1981) and FORTRAN programs by Nicholls and Crawford (1985) (Fig. 8a).

Aside from general metamorphic grades, no independent pressure and temperature indicators are found to constrain isochore calculations. Final salt melting temperatures may be used to estimate the temperature of trapping, if salt saturation is assumed. Salt saturation is assumed for each area, except for both Ucca-vuovdas where fluids appear to have been oversaturated with salt, and also fluids related to copper mineralization at Bidjovagge where  $\text{H}_2\text{O}$  appears to have been undersaturated in salt.

Interpretation of isochores (Fig. 8b) indicates that trapping of fluid inclusions within the pegmatitic quartz at Dælljadas occurred at magmatic temperatures between 500 to 800°C, with corresponding pressures of 3 to 8 kbars. Generally, isochores from non-aqueous fluid-rich inclusions show decreasing pressures from Masi River to Ucca-vuovdas and to Object 43, at constant temperature.

It was estimated by Ettner et al. (in prep.) that fluid inclusions related to gold mineralization at Bidjovagge were trapped between 300 to 375°C at 2 to 4 kbars (Fig. 8b). Compared to estimated temperatures and pressures of trapping of fluid inclusions, related to copper mineralization at Bidjovagge, gold mineralization appears to have occurred at higher pressures, and possibly temperatures.

## DISCUSSION OF RESULTS

Previous fluid inclusion studies of other shear zone-hosted veins, within other tectonic belts have shown that fluids evolved during their upward migration (Crawford and Hollister, 1986; Craw, 1990; Nwe and Grundmann, 1990). Such changes in fluids may include phase separation (Crawford and Hollister, 1986) or the addition or the subtraction of components during fluid-rock interaction, such as increasing or decreasing salinity (Cloke and Kesler, 1979). Evolution of the fluids may be the cause, or result, of mineralization or metasomatism of the wall rocks (Trommsdorff and Skippen, 1987; Newton, 1990). Therefore, using the results of this study of fluids related to mineralization and alteration we will model the regional evolution of fluids in shear zones of the Kautokeino greenstone belt. Similarities between fluids observed at Dælljadas, Bidjovagge, Masi River, Ucca-vuovdas and Object 43 appear to exist. Most areas have fluid inclusion populations consisting of both salt saturated H<sub>2</sub>O and CO<sub>2</sub>-rich inclusions (Table 1). The presence of CH<sub>4</sub>, N<sub>2</sub>, and salt undersaturated H<sub>2</sub>O seems to occur in unique areas.

### *Saline H<sub>2</sub>O fluids*

Salt saturated H<sub>2</sub>O fluids occur in most of the areas discussed, including fluid inclusions related to the Bidjovagge gold mineralization (Ettner et al., in prep.), except for at Dælljadas and inclusions related to Bidjovagge copper mineralization where salt undersaturated H<sub>2</sub>O is present. Based on microthermometric data, these salts most likely comprise both NaCl and CaCl<sub>2</sub>, and possibly LiCl. Minor biotite alteration at Bidjovagge and Ucca-vuovdas suggest that KCl may have been present in the fluids, but low eutectic melting temperatures may be masking its presence in the fluid inclusions. Generally, calculated salinities of salt-saturated inclusions range between 30 to 45 wt % (NaCl equiv.), but Ucca-vuovdas inclusions have extremely high salinities (Fig. 9). Lower salinities are calculated for fluids related to Bidjovagge copper mineralization (around 25 wt %, NaCl equiv.) and at Dælljadas (1.5 to 12 wt %, NaCl equiv.) (Fig. 9).

The origin of highly saline fluids, such as found in the Kautokeino greenstone belt, may be due to boiling (Wilson et al., 1980), leaching of evaporites or sedimentary rocks (Rich, 1979), and from degassing of silicic intrusions (Andersen, 1990; Webster, 1992). The salinity of an initially moderately saline fluid may be increased by hydration reactions in the wall rocks absorbing water from the fluid (Trommsdorff and Skippen, 1987 and 1988). There is no fluid inclusion or alteration evidence for boiling in the mineralized and altered areas in the Kautokeino greenstone belt, and will be further dismissed from this discussion. Although the existence of evaporites in the Kautokeino greenstone belt is plausible, and has been suggested by Sollid and Torske (1993), no occurrences have yet been described. Because of the presence of granitic intrusions within metasomatized shear zones in the Kautokeino greenstone belt, saline fluids partitioned from melts and hydration of the rocks within the shear zones are the most likely explanations for the highly saline H<sub>2</sub>O inclusions.

Synorogenic granitic and diabase intrusions occur along the shear zones in the Kautokeino greenstone belt. One such intrusion, the pegmatites at Dælljadas, have salinities ranging from 1.5 to 12 wt. % NaCl equivalent, and obviously could not

alone produce the highly saline fluids found in the shear zones. The salinities observed at Dælljadas may not be typical for other intrusions in the Kautokeino greenstone belt, because the salinity (Cl content) of fluid exsolved from granitic melts is dependent on factors such as melt composition (i.e. Cl, F, K/Na, SiO<sub>2</sub> and CO<sub>2</sub> content), pressure, and temperature (Webster, 1992). Therefore, other granitic intrusions within the shear zones may have been a source for the highly saline waters, and the pegmatite at Dælljadas may represent a granitic melt which did not allow for extensive exsolution of Cl.

If intrusions such as the Dælljadas pegmatites were the source of fluids in the other areas studied, the salinity of the fluid may have increased during ascent along the shear zones. A possible reason for an increase in salinity during ascent of the fluid along shear zones may be due to hydration of wall rocks (Trommsdorff and Skippen, 1987 and 1988). During metasomatic hydration reactions, such as biotite- and amphibole-forming reactions, H<sub>2</sub>O would be preferentially removed from the fluid, driving the remaining fluid towards higher salinities.

The salt undersaturated H<sub>2</sub>O fluids, with an average 25 wt. % NaCl equivalent, that are related to copper mineralization at Bidjovagge have a much lower salinity than the saline fluids related to gold mineralization at Bidjovagge (Eitner et al., in prep.), Object 43, Ucca-vuovdas, and Masi River. This indicates that the fluids became less saline as the system evolved.

The saline aqueous solutions observed in the Kautokeino greenstone belt carried both gold and copper in solution. Transport of gold and copper as chloride complexes is favored by high salinities, high temperatures and high  $fO_2$ , as opposed to transport by sulfide complexes (Fig. 10) (Henley, 1973; Crerar and Barnes, 1976; Barnes, 1979; Hayashi and Ohmoto, 1991; Steward, 1991). Fluids from the shear zones in the Kautokeino greenstone belt are highly saline, were trapped at high temperatures between 250 to 400°C, and sulfide stabilities and fluid-rock interaction suggest that the  $fO_2$  of the fluid was high. It is therefore obvious that metal transport within the

shear zones in the Kautokeino greenstone belt occurred as chloride complexes, and may be compared to systems described by Large et al. (1989).

### *CO<sub>2</sub>-rich fluids*

Fluid inclusions rich in CO<sub>2</sub> have been found in abundance associated with gold mineralization at Bidjovagge (Ettner et al., in prep.), Ucca-vuovdas, Masi River, and Dælljadas. The presence of minor carbonate daughter crystals in inclusions at Object 43 indicate that a minor amount of CO<sub>2</sub> is present. Similarly, large chalcopyrite-carbonate veins of the Bidjovagge copper-ore type indicate that CO<sub>2</sub> was present in the fluids, although it is not observed in the fluid inclusions.

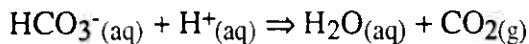
Both metamorphic and magmatic sources may have provided CO<sub>2</sub> for the fluids observed in the Kautokeino greenstone belt. At Bidjovagge,  $\delta^{13}\text{C}$  values indicate that the source for carbon was probably sedimentary carbonate (Ettner et al., in prep.). Decarbonatization reactions between the footwall carbonates and the saline H<sub>2</sub>O would have resulted in the release of CO<sub>2</sub>, such as described by Mercolli et al. (1987). Abundant CO<sub>2</sub> observed in the pegmatites at Dælljadas suggest that such magmatic rocks were also sources for carbonic fluids.

Fluid inclusions composed of CO<sub>2</sub> + H<sub>2</sub>O + salt, indicating phase miscibility, occur at Bidjovagge, related to gold mineralization (Ettner et al., in prep.), and at Dælljadas. Single-phase CO<sub>2</sub> inclusions, which appear to be coeval with H<sub>2</sub>O + salt inclusions, are observed at Bidjovagge, Masi River, Ucca-vuovdas, and more rarely at Dælljadas. The coeval nature of the single-phase CO<sub>2</sub> inclusions together with the H<sub>2</sub>O + salt inclusions in the same samples, may suggest immiscibility (Ramboz et al., 1982).

During the evolution of a miscible CO<sub>2</sub> + H<sub>2</sub>O + salt fluid, fluid unmixing could have resulted in the two immiscible fluids of single-phase CO<sub>2</sub>, and the H<sub>2</sub>O + salt. Fluid inclusion zonation at Bidjovagge, with CO<sub>2</sub> + H<sub>2</sub>O + salt occurring in the footwall, and CO<sub>2</sub> and H<sub>2</sub>O + salt inclusions occurring in the highly sheared albite felsite near the ore zone (Ettner et al., in prep.) indicate that a drop in pressure may have been responsible for the fluid unmixing. Fluid immiscibility at Bidjovagge

appears to have occurred prior to the fluid-rock interaction and the addition of CH<sub>4</sub>. Similarly, evidence suggests that phase separation of the supercritical CO<sub>2</sub> + H<sub>2</sub>O + salt fluid occurred on a regional scale as the fluid moved upwards along the shear zone.

The phase separation of CO<sub>2</sub> from H<sub>2</sub>O-rich fluids results in an increase in pH of the fluid (Reed and Spycher, 1985) because of the reaction:



Phase separation is considered to be an important mechanism for precipitation of precious metals from sulfide complexes (i.e. Bowers, 1986; Robert and Kelly, 1987; Walsh et al., 1988) but the increase in pH may also be important for the precipitation of metals from chloride complexes (Fig. 10) (Henley, 1973; Barnes, 1979).

#### *CH<sub>4</sub>-rich fluids*

Methane, and minor ethane in fluid inclusions related to gold mineralization occur within the oxidation zones within graphitic schists at Bidjovagge (Ettner et al., in prep.). Ettner et al. (in prep.) suggest that a CO<sub>2</sub> + H<sub>2</sub>O + salt fluid of high *f*O<sub>2</sub>, which was externally buffered, reacted with the graphitic schist to produce CH<sub>4</sub>. Methane has been identified in fluid inclusions at Masi River and Object 43 which indicate that fluid reaction with graphitic schist may have occurred, similar to that at Bidjovagge. A spatial relationship between mineralization and graphitic schist at Object 43, has been previously noted (Hagen, 1986).

The occurrence of gold and copper mineralization within the oxidation zone at Bidjovagge, together with the presence CH<sub>4</sub> inclusions, indicates that the fluid-rock reaction was important for mineralization. The interaction between the H<sub>2</sub>O + salt ± CO<sub>2</sub> carrying Au and Cu as chloride complexes, would clearly result in a lowered *f*O<sub>2</sub> of the fluid. Both gold and copper chloride complexes are dependent on the

oxygen fugacity, and a reduction  $fO_2$  would result in lower solubilities (Fig. 10) (Henley, 1973; Crerar and Barnes, 1976).

#### *N<sub>2</sub>-rich fluids*

Nitrogen-bearing inclusion are been observed both in higher crustal areas such as Object 43 and Ucca-vuovdas, and at deeper crustal levels at Dælljadas. The absence of N<sub>2</sub> at Bidjovagge and Masi River suggest that limited sources for N<sub>2</sub> existed in both the higher and deeper crustal levels, and that N<sub>2</sub> was a negligible component in the fluid which migrated upwards through the shear zones. Nitrogen in low metamorphic rocks in shallow crustal conditions are suggested to form as a result of breakdown of organic matter, or of NH<sub>4</sub><sup>+</sup>-bearing minerals such as biotite, muscovite or potassium feldspar (Stevenson, 1962; Kreulen and Schuiling, 1982; Duit et al., 1986; Bottrell et al., 1988). Within granulite facies metamorphic rocks in deeper crustal conditions, N<sub>2</sub> is suggested to be liberated during the breakdown of biotite and feldspar (Andersen et al., in press). Generally, N<sub>2</sub> does not appear to be important during the regional evolution of the fluid in the Kautokeino greenstone belt.

#### *Preferred model*

During the Svecokarelian orogeny, rocks of the Kautokeino greenstone belt were metamorphosed and highly sheared. The age of gold mineralization at Bidjovagge,  $1885 \pm 18$  Ma Bjørlykke et al. (1990) is in good correlation with the age of the Svecokarelian Orogeny between 1.9 to 1.88 Ga (Skiöld, 1988; Pharaoh and Brewer, 1990) indicating that mineralization along the shear zone occur during or slightly after peak metamorphism. Two shear zones, the Mierujav'ri-Sværholt Fault Zone (Olesen et al., 1991) and the Baltic-Bothnian megashear zone (Berthelsen and Marker, 1986), focused the upward migration of fluid through the crust during the orogen. Data suggest that the fluid evolved as it ascended along the shear zones from higher to lower pressure and temperature conditions, and reacted with wall rocks resulting in both alteration and mineralization (Fig. 11).

The parent fluid is interpreted to be a miscible mixture of  $\text{H}_2\text{O} + \text{CO}_2 + \text{NaCl}$  (<12 wt. % NaCl equiv.) dominated by NaCl and  $\text{CaCl}_2$  and minor  $\text{N}_2$ . Estimated temperatures of this fluid are between 350 to 600 °C (Fig. 12). As this high temperature  $\text{H}_2\text{O} + \text{CO}_2 + \text{salt}$  fluid moved upwards, hydration reactions with rocks within the shear zones (Trommsdorff and Skippen, 1987), or leaching of salts from evaporites within the metasedimentary sequence, resulted in increased salinities to values of 30 to 45 wt. %, NaCl equivalent. Decarbonatization of sedimentary carbonates resulted in the addition of  $\text{CO}_2$  to the fluids, such as at Bidjovagge (Ettner et al., in prep.). There are two apparent sources for  $\text{N}_2$ , a deeper crustal source and a shallow crustal source, but  $\text{N}_2$  does not appear to be an important component during the evolution of the fluid.

Albitization, carbonatization and scapolitization along the shear zones resulted from the reaction of the  $\text{H}_2\text{O} + \text{CO}_2 + \text{salt}$  fluids with the wall rocks. Although mineralization along shear zones in the Kautokeino greenstone belt is always accompanied by metasomatism, the reverse is not necessarily true. The metasomatized shear zones, such as Masi River, may represent a segment of shear zone where metals were transported in solution, but were not trapped. Comparison of other Archean and Phanerozoic mesothermal gold systems (i.e. Knopf, 1929; Kerrich, 1983; Card et al., 1989; Nesbitt, 1991) with the Bidjovagge deposit, shows that the Bidjovagge generally contains less quartz than other systems. This is one indication that a drop in temperature, which would promote silica precipitation, was not an important factor at Bidjovagge. The origin of the fluids is presently being studied by using initial ratios of Nd and Sr (Nie and Bjørlykke, in prep.).

The high temperature and high salinity fluids, with high  $f\text{O}_2$ , apparently transported base metals and gold as chloride complexes (Fig. 10). Metals sources may be interpreted to be from magmatic intrusions during fluid exhalation or by oxidation leaching (Cameron, 1989a) of metasedimentary rocks, metavolcanic rocks or intrusions.

Fluid unmixing of CO<sub>2</sub> appears to have occurred at higher levels in the shear zone, such as at Bidjovagge, Masi River, and Ucca-vuovdas (Fig. 11). Phase separation of the gas-rich from the H<sub>2</sub>O-rich phases could have occurred due to contamination of the fluid by salt, or the drop of pressure and temperature, or a combination of these factors. Phase separation due to CH<sub>4</sub> contamination does not appear to be the cause at Bidjovagge, but can not be ruled out at Masi River and Dælljadas.

At the Bidjovagge mine, a drop in pressure at the ductile to brittle boundary (Fig. 12) resulted in phase separation of CO<sub>2</sub> from the highly saline H<sub>2</sub>O fluid, thus increasing the pH of the fluid. Buffered by the assemblage pyrite-hematite and pyrite-magnetite assemblages, the pH of the fluid was increased and the *f*O<sub>2</sub> decreased (Fig. 10). Red-ox reactions between the fluid and graphitic schist resulted in the oxidation of the graphitic schist, the production of hydrocarbons in the fluid, and the lower of oxygen fugacity of the fluid (Fig. 10). Chloride metal complexes are dependent on both pH and oxygen fugacity (Henley, 1973; Barnes, 1979) and therefore, the combined effect of phase separation and fluid-rock interaction resulted in precipitation at the oxidation front with the graphitic schist at Bidjovagge. Because of the relationship of graphitic schist and copper mineralization at Ucca-vuovdas and Object 43, the same redox trapping mechanism may have occurred.

The presence of sulfur in the fluids is shown by the abundant sulfides found in the mineralized areas. At Bidjovagge, gold mineralization does not occur within the intense pyrite zones, rather gold is found in association with pyrrhotite + pyrite assemblages in the oxidation zone to the graphitic schist. This relationship shows that sulfur was not an important component for the transport and precipitation of gold.

Within the Kautokeino greenstone belt, the gold mineralization is restricted within the ductile-brittle transition in shear zones and the copper mineralization is not restricted by crustal depth. This metal zonation is interpreted to be a result of both a structural effect on fluid pressure conditions, and geochemical reactions with wall rocks. Gold mineralization in the brittle-ductile transition zone at Bidjovagge resulted from phase separation due to pressure drop, accompanied by fluid reaction

with graphitic schist. It is significant to note the correlation between ages of the Svecokarelian orogeny and gold mineralization at Bidjovagge (Skiöld, 1988; Bjørlykke et al., 1990; Pharaoh and Brewer, 1990) and between estimated PT conditions of fluid inclusion trapping and metamorphic grade at Bidjovagge. This evidence indicates that gold mineralization occurred at or slightly after peak metamorphic conditions within upper greenschist facies conditions.

As Bjørlykke et al. (1993) noted, the Bidjovagge, Saattopora, and Pahtohavare gold-copper deposits within the Fennoscandinavian Shield (Fig. 1) occur at the boundary between low and medium metamorphic facies. Restriction of gold mineralization at this metamorphic boundary during the Svecokarelian orogeny provides criteria for the exploration of mesothermal Au-Cu deposits. Additionally, the occurrence of CH<sub>4</sub> together with gold mineralization within oxidation zones to graphitic schists may allow CH<sub>4</sub> to be used as a geochemical tracer to gold mineralization.

#### ACKNOWLEDGEMENTS

We wish to thank Bidjovagge Gruver A/S and Outokumpu Oy for partial support of this research, and permission to publish these results. We also gratefully acknowledge financial support from NTNF (Royal Norwegian Research Council for Scientific and Industrial Research), project number BF-25469. Two anonymous reviewers are thanked for greatly improving this manuscript. We are grateful to Sten Lindblom from the Institute of Geology, University of Stockholm, for his generous help with Raman microprobe analysis. The first author is thankful to Jan Sverre Sandstad, from Norges Geologiske Undersøkelse, and Kjell Nilsen for help collecting samples during the summer field seasons on Finnmarksvidda. Stein Lønne provided fluid inclusion samples and helpful discussions of Object 43. Also, superb preparation of countless fluid inclusion sections by Malcolm Lynn and Harald Aasen

at the Department of Geology thin section lab, University of Oslo, is gratefully acknowledged.

## REFERENCES

- Andersen, T., 1990. Melt-interaction in peralkaline silicic intrusions in the Oslo Rift, Southeast Norway. IV: Fluid inclusions in the Sande nordmarkite. *Nor. Geol. Unders.* 417: 41-54.
- Andersen, T., Austrheim, H. and Burke, E.A.J., 1991. Mineral-fluid-melt interactions in high-pressure shear zones in the Bergen Arcs nappe complex, Caledonides of W. Norway: Implications for the fluid regime in Caledonian eclogite-facies metamorphism. *Lithos*, 27: 187-204.
- Andersen, T., Austrheim, H. and Burke, E.A.J., and Synnøve, E., (in press) Nitrogen and carbon dioxide in deep crustal fluids: Evidence from the Caledonides of Norway. *Chem. Geol.*
- Barnes, H.L., 1979. Solubilities of ore minerals. In: H.L. Barnes (Editor), *Geochemistry of Hydrothermal Ore Deposits*. Wiley, New York, pp. 404-460.
- Berthelsen, A. and Marker, M., 1986. 1.9-1.8 Ga old strike-slip megashears in the Baltic Shield, and their plate tectonic implications. *Tectonophysics*, 128: 163-181.
- Bjørlykke A., Cummings, G.L., and Krstic, D., 1990. New isotopic data from davidites and sulfides in the Bidjovagge gold-copper deposit, Finnmark, northern Norway. *Mineral. Petrol.* 43: 1-12.
- Bjørlykke, A., Hagen, R. and Söderholm, K., 1987. Bidjovagge copper-gold deposit in Finnmark, Northern Norway. *Econ. Geol.*, 82: 2059-2075.
- Bjørlykke, A., Nilsen, K.S., Anttonen, R. and Ekberg, M., 1993. Geological setting of the Bidjovagge deposit and related gold-copper deposits in the northern part of the Baltic Shield. In: Y.T. Maurice (Editor), *Proc. 8th Quadrenn. IAGOD Symp.*, Ottawa, Can. 1990, Schweizerbart'sche, Stuttgart, pp. 667-680.
- Bjørlykke, A., Olerud, S. and Sandstad, J.S., 1985. Metallogeny of Finnmark, north Norway. *Nor. Geol. Unders.* 403, 183-196.
- Borisenko, A.S., 1977. Study of the salt composition of solutions of gas-liquid inclusions in minerals by the cryometric method. *Geol. Geofiz.*, 18: 16-27. (English translation)
- Bottrell, S.H., Carr, L.P. and Dubessy, J., 1988. A nitrogen-rich metamorphic fluid and coexisting minerals in slates from North Wales. *Mineral. Mag.*, 52, 451-457.
- Bowers, T.S., 1986. The geochemical consequences of H<sub>2</sub>O-CO<sub>2</sub> fluid immiscibility on ore deposition: A reaction path approach. *Geol. Soc. Am. Abstr.*, 18: 548.
- Burke, E.A.J. and Lustenhouwer, W.J., 1987. The application of a multichannel laser Raman microprobe Microdil-28: to the analysis of fluid inclusions. *Chem. Geol.*, 61: 11-17.

- Burruss, R.C., 1981. Analysis of phase equilibria in C-O-H-S fluid inclusions. In: L.S. Hollister and M.L. Crawford (Editors), Mineralogical Association of Canada Short Course Handbook 6, pp. 39-74.
- Cameron, E.M., 1989a. Derivation of gold by oxidative metamorphism of a deep ductile shear zone: Part 1. Conceptual model. *J. Geochem. Explor.*, 31: 135-147.
- Cameron, E.M., 1989b. Scouring of gold from the lower crust. *Geology*, 17: 26-29.
- Card, K.D., Poulsen, K.H. and Robert, F., 1989. The Archean Superior province of the Canadian Shield and its lode gold deposits. *Econ. Geol. Mon.* 6: 19-36.
- Cloke, P.L. and Kesler, S.E., 1979. The halite trend in hydrothermal solutions. *Econ. Geol.*, 74: 1823-1831.
- Collins, P.L.F., 1979. Gas hydrates in CO<sub>2</sub>-bearing fluid inclusions and the use of freezing data for estimation of salinity. *Econ. Geol.*, 74: 1435-1444.
- Colvine, A.C., 1989. An empirical model for the formation of Archean gold deposits: Products of final cratonization of the Superior Province, Canada. *Econ. Geol. Mon.* 6: 37-53.
- Craw, D., 1988. Shallow level metamorphic fluids in a high uplift rate metamorphic belt; Alpine Schist, New Zealand. *J. Metamorph. Geol.*, 6: 1-6.
- Craw, D., 1990. Regional fluid and metal mobility in the Dalradian metamorphic belt, Southern Grampian Highlands, Scotland. *Mineral. Deposita*, 25: 281-288.
- Crawford, M.L., 1981. Phase equilibria in aqueous fluid inclusions. In: L.S. Hollister and M.L. Crawford (Editors), Mineralogical Association of Canada Short Course Handbook 6, pp. 75-100.
- Crawford, M.L. and Hollister, L.S., 1986. Metamorphic fluids: The evidence from fluid inclusions. In: J.V. Walther and B.J. Wood (Editors), *Fluid-rock interactions during metamorphism*, Springer-Verlag, New York, pp. 1-35.
- Crerar, D.A. and Barnes, H.L., 1976. Ore solution chemistry V. Solubilities of chalcopyrite and chalcocite assemblages in hydrothermal solution at 200° to 350°C. *Econ. Geol.*, 71: 772-794.
- Cumming, G.L., Krstic, D., Bjørlykke, A. and Åsen, H., (in prep.). Further analysis of radiogenic minerals from the Bidjovagge gold-copper deposit, Finnmark, northern Norway.
- Dubessy, J., Poty, B. and Ramboz, C., 1989. Advances in C-O-H-N-S fluid geochemistry based on micro-Raman spectrometric analysis of fluid inclusions. *Eur. J. Mineral.*, 1: 517-534.
- Duit, W., Jansen, B.H., Breemen, A. Van and Bos, A., 1986. Ammonium micas in metamorphic rocks as exemplified by Dome de l'Agout (France). *Am. J. Sci.*, 286: 702-732.
- Ekberg, M. and Sotka, P., 1991. Production mineralogy and selective mining at Bidjovagge mine, northern Norway. *Int. Con. Appl. Mineral.*, Pretoria, Aust.
- Ettner, D.C., Bjørlykke, A. and Andersen, T., 1992. Fluid inclusion study and model of gold transport and deposition from the Bidjovagge Au-Cu mine in Finnmark, Norway, 20th Nordic Geol. Winter Meet., Reykjavik, Iceland Abstr., p. 38.

Ettner, D.C., Bjørlykke, A. and Andersen, T., (in prep.). Fluid composition of Proterozoic gold and copper deposits: An example from the Bidjovagge gold-copper deposit, Finnmark, northern Norway.

Gatehouse, B.M., Greay, I.E., Campbell, I.H. and Kelly, P., 1978. The crystal structure of loveringite-a new member of the crichtonite group. *Amer. Mineral*, 63: 28-36.

Gjelsvik, T., 1957. Albittrike bergarter i den karelske fjellkjede på Finnmarksvidda, Nord-Norge. *Nor. Geol. Unders.* 203: 60-72.

Haas, J.L., 1976. Physical properties of the coexisting phases and thermochemical properties of the H<sub>2</sub>O component in boiling NaCl solutions. *U.S. Geol. Surv., Bull.* 1421-A, 73 pp.

Hagen, R., 1985. Oppfølging av helikoptermålinger i Kautokeino-området, innenfor avtaleområdet Kautokeino/Masi. ASPRO Prospecting internal report 1619, 15 pp.

Hagen, R., 1986. Area no 43, a new occurrence of Bidjovagge-type copper-gold mineralization in the Gulf/Sydvaranger joint venture area, Kautokeino, Finnmark. ASPRO Prospecting internal report 1672, 15 pp.

Hayashi, K. and Ohmoto, H., 1991. Solubility of gold in NaCl- and H<sub>2</sub>S-bearing aqueous solutions at 250-350°C. *Geochim. Cosmochim. Acta*, 55: 2111-2126.

Henley, R.W., 1973. Solubility of gold in hydrothermal chloride solutions. *Chem. Geol.*, 11: 73-87.

Hollander, N.B., 1979. The geology of the Bidjovagge mining field, western Finnmark, Norway. *Norsk Geol. Tidsskr.*, 59: 327-336.

Holloway, J.R., 1981. Compositions and volumes of supercritical fluids in the earth's crust. In: L.S. Hollister and M.L. Crawford (Editors), *Mineralogical Association of Canada Short Course Handbook 6*, pp. 13-38.

Hollister, L.S. and Burruss, R.C., 1976. Phase equilibria in fluid inclusions from the Khtada metamorphic complex. *Geochim. Cosmochim. Acta*, 40: 163-175.

Holmsen, P., Padget, P. and Pehkonen, E., 1957. The Precambrian geology of Vest-Finnmark, northern Norway. *Nor. Geol. Unders.* 210, 107 pp.

Jensen, I.E., 1988. En mineralogisk og geokjemisk undersøkelse av albittbergarter i Bidjovagge omraadet, Kautokeino, Finnmark. Unpub. Can. Scient. thesis, Univ. of Oslo, 151 pp.

Johnson, J.W., Oelkers, E.H. and Helgeson, H.C., 1991. SUPCRT92: A software package for calculating the standard molal thermodynamic properties of minerals, gases, aqueous species, and reactions from 1 to 5000 bars and 0° to 1000°C. *Univ. of California, Berkeley*, 101 pp.

Kerkhof, A.M. Van Den, 1990. Isochoric phase diagrams in the systems CO<sub>2</sub>-CH<sub>4</sub> and CO<sub>2</sub>-CH<sub>4</sub> : Application to fluid inclusions. *Geochim. Cosmochim. Acta*, 54: 621-629.

Kerkhof, A.M. Van Den, 1991. Heterogeneous fluids in high-grade siliceous marbles of Pusula (SW Finland). *Geol. Rdsch.* 80: 249-258.

- Kerrich, R., 1983. Geochemistry of gold deposits in the Abitibi greenstone belt. *Can. Inst. Mining Metallurgy, Spec. Vol. 27*, 75 p.
- Kerrich, R. and Feng, R., 1992. Archean geodynamics and the Abitibi-Pontiac collision: implications for advection of fluids at transpressive collisional boundaries and the origin of giant quartz vein systems. *Earth Sci. Rev.*, 32: 33-60.
- Knopf, A., 1929. The Mother Lode system of California. *U.S. Geol. Surv., Prof. Pap.* 157, 88 p.
- Kreulen, R. and Schuiling, R.D., 1982. N<sub>2</sub>-CH<sub>4</sub>-CO<sub>2</sub> fluids during formation of the Dôme de l'Agout, France. *Geochim. Cosmochim. Acta*, 46: 193-203.
- Krill, A.G., Bergh, S., Lindahl, I., Mearns, E.W., Often, M., Olerud, S., Olesen, O., Sandstad, J.S., Siedlecka, A. and Solli, A., 1985. Rb-Sr, U-Pb and Sm-Nd isotopic dates from Precambrian rocks of Finnmark. *Nor. Geol. Unders.* 403: 37-54.
- Krill, A.G., Kesola, R., Sjöstrand, T. and Stephens, M.B., 1988. Metamorphic, structural and isotopic age map, northern Fennoscandia 1:1,000,000. *Geol. Surv. Finland, Norway and Sweden.*
- Large, R.R., Huston, D.L., McGoldrick, P.J., Ruxton, P.A. and McArthur, G., 1988. Gold distribution and genesis in Australian volcanogenic massive sulfide deposits and their significance for gold transport models. *Econ. Geol. Mon.* 6: 520-536.
- Mathiesen, C.O., 1970. An occurrence of unusual minerals at Bidjovagge, northern Norway. *Norges Geol. Unders.* 266: 86-104.
- Mercogli, I., Skippen, G. and Trommsdorff, V., 1987. The tremolite veins of Campolungo and their genesis. *Schweiz. Mineral. Petrogr. Mitt.*, 6: 75-84.
- Nie, F. and Bjørlykke, A., (in prep.) The origin of Proterozoic gold-copper deposits in the Bidjovagge district, Finnmark, northern Norway, as deduced from rare earth element and Nd-Sr isotopic evidences on calcite.
- Nesbitt, B.E., 1991. Phanerozoic gold deposits in tectonically active continental margins. In : R.P. Foster (Editor), *Gold Metallogeny and Exploration*. Blackie, Glasgow, pp. 104-132.
- Newton, R.C., 1990. Fluids and shear zones in the deep crust. *Tectonophysics*, 182: 21-37.
- Nicholls, J. and Crawford, M.L., 1985. FORTRAN programs for calculation of fluid properties from microthermometric data on fluid inclusions. *Computers Geosci.*, 11: 619-645.
- Nilsen, K.S. and Bjørlykke, A., 1991. Geological setting of the Bidjovagge gold-copper deposit, Finnmark, northern Norway. *Geol. Fören. Stockholm Förh.*, 113: 60-61.
- Nwe, Y.Y. and Grundmann, G., 1990. Evolution of metamorphic fluids in shear zones: The record from the emeralds of Habachtal, Tauern Window, Austria. *Lithos*, 25: 281-304.
- Olesen, O., Henkel, H. and Lile, O.B., 1991. Major fault zones within the Precambrian Kautokeino Greenstone Belt, Finnmark, Norway: combined interpretation of geophysical data. *Nor. Geol. Unders. Unpubl. Rep.* 90.161, 26 pp.

- Olesen, O., Roberts, D., Henkel, H., Lile, O.B. and Torsvik, T.H., 1990. Aeromagnetic and gravimetric interpretation of regional structural features in the Caledonides of West Finnmark and North Troms, northern Norway. *Nor. Geol. Unders.* 419: 1-24.
- Olesen, O. and Solli, A., 1985. Geophysical and geological interpretation of regional structures within the Precambrian Kautokeino greenstone belt, Finnmark, north Norway. *Nor. Geol. Unders.* 403: 119-129.
- Olsen, K. I. and Nilsen, K.S., 1985. Geology of the southern part of the Kautokeino Greenstone Belt: Rb-Sr geochronology and geochemistry of associated gneisses and late intrusions. *Nor. Geol. Unders.* 403: 131-160.
- Olsen, K. I. and Nilsen, K.S., 1989. Greenstone formation and ore deposition related to possible rift tectonics in Kautokeino Greenstone Belt, north Norway. *EUG V, Strasbourg, 1989. Terra Abstr.*, 1, p. 3.
- Pharaoh, T.C. and Brewer, T.S., 1990. Spatial and temporal diversity of early Proterozoic volcanic sequences - comparisons between the Baltic and Laurentian shields. *Precambrian Res.*, 47: 169-189.
- Potter, R.W. II, Clyne, M.A. and Brown, D.L., 1978. Freezing point depression of aqueous sodium chloride solutions. *Econ. Geol.*, 73: 284-285.
- Ramboz, C., Pichavant, M. and Weisbrod, A., 1982. Fluid immiscibility in natural processes: Use and misuse of fluid inclusion data, II. Interpretation of fluid inclusion data in terms of immiscibility. *Chem. Geol.*, 37: 29-48.
- Ramsay, D.M., Sturt, B.A., Zwann, K.B. and Roberts, D., 1985. Caledonides of northern Norway. In: D.G. Gee and B.A. Sturt (Editors), *The Caledonide Orogen - Scandinavia and related areas*. John Wiley and Sons, Chichester, pp. 163-184.
- Reed, M.H. and Spycher, N., 1985. Boiling, cooling, and oxidation in epithermal systems: A numerical modeling approach. In: B.R. Berger and P.M. Bethke (Editors), *Geology and geochemistry of epithermal systems*. *Rev. Econ. Geol.*, 2: 249-272.
- Rich, R.A., 1979. Fluid inclusion evidence of Silurian evaporites in southeastern Vermont. *Geol. Soc. Am. Bull.*, 90: 1628-1643.
- Robert, F. and Kelly, W.C., 1987. Ore-forming fluids in Archean gold-bearing quartz veins at the Sigma mine, Abitibi greenstone belt, Quebec, Canada. *Econ. Geol.*, 82: 1464-1482.
- Roedder, E., 1971. Metastability in fluid inclusions. *Soc. Mining Geol. Japan, (Proc. IMA-IAGOD meet, '70, IAGOD Vol.)*, Spec. Issue 3: 327-334.
- Roedder, E., 1984. Fluid Inclusions. In: P.H. Ribbe (Editor), *Reviews in Mineralogy.*, 12, 646 pp.
- Sandstad, J.S., 1985. Mållejus 1833 4 geologisk berggrunnskart 1:50000. *Nor. Geol. Unders.*
- Sandstad, J.S., 1992. Kautokeinogrønnsteinsbeltet - Berggrunnskart 1:100,000. *Nor. Geol. Unders.*

Siedlecka, A., Iversen, I., Krill, A.G., Lieungh, B., Often, M., Sandstad, J.S. and Solli, A., 1985. Lithostratigraphy and correlation of the Archean and Early Proterozoic rocks of Finnmarksvidda and the Sørvaranger district. *Nor. Geol. Unders.* 403: 7-36.

Skiöld, T., 1988. Implications of new U-Pb zircon chronology to early Proterozoic crustal accretion in northern Sweden. *Precambrian Res.*, 38: 147-164.

Solli, A., 1988. Masi 1933 IV berggrunnsgeologisk kart 1:50000. *Nor. Geol. Unders.*

Sollid, K. and Torske, T., 1993. Karbonat-evaporittavsetninger i bunnen av den Proterozoiske Alta-Kautokeino riften. *Geonytt*, 20: 45.

Stevenson, F.J., 1962. Chemical state of the nitrogen in rocks. *Geochim. Cosmochim. Acta*, 26: 797-809.

Swanenberg, H.E.C., 1980. Fluid inclusions in high-grade metamorphic rocks from S.W. Norway. PhD thesis, University of Utrecht, The Netherlands. *Geol. Ultra.*, 25, 147 pp.

Tanger, J.C. IV and Pitzer, K.S., 1989. Thermodynamics of NaCl-H<sub>2</sub>O: A new equation of state for the near-critical region and comparison with other equations for adjoining regions. *Geochim. Cosmochim. Acta*, 53: 973-987.

Trommsdorff, V. and Skippen, G., 1987. Metasomatism involving fluids in CO<sub>2</sub>-H<sub>2</sub>O-NaCl. In: H.C. Helgeson (Editor), *Chemical transport in metasomatic processes*, Reidel, Dordrecht, pp. 133-152.

Trommsdorff, V. and Skippen, G., 1988. Brines and metasomatism. *Rendic.Soc.Ital. Mineral. Petrol.*, 43: 15-24.

Tuisku, P., 1983. The origin of scapolite in the Central Lapland schist area, Northern Finland; preliminary results. *Geol. Surv. Finland Bull.* 331: 159-173.

Unruh, C.H. and Katz, D.L., 1949. Gas hydrates of carbon-dioxide-methane mixture. *J. Pet. Tech.*, 1: 83-86.

Walsh, J.F., Kesler, S.E., Duff, D. and Cloke, P.L., 1988. Fluid Inclusion geochemistry of high-grade, vein-hosted gold ore at the Pamour mine, Porcupine camp, Ontario. *Econ. Geol.*, 83: 1347-1367.

Webster, J.D., 1992. Water solubility and chlorine partitioning in Cl-rich granitic systems: Effects of melt composition at 2 kbar and 800°C. *Geochim. Cosmochim. Acta*, 56: 679-687.

Wilson, J.W.J., Kesler, S.E., Cloke, P.L. and Kelly, W.C., 1980. Fluid inclusion geochemistry of the Granisle and Bell Porphyry Copper Deposit, British Columbia. *Econ. Geol.*, 75: 45-61.

#### FIGURE CAPTIONS

**Figure 1:** General geologic map of the northern portion of the Fennoscandic Shield including areas of northern Norway, Sweden and Finland with the locations of

the Bidjovagge, Pahtohavare, and Saattopora deposits. After Krill et al. (1988) and Bjørlykke et al., (1993).

**Figure 2:** Generalized geologic map of Finnmarks plateau, with the Kautokeino Greenstone belt, emphasizing metamorphic grade after Sandstad (1992) and Krill et al. (1988). Mineralized and altered areas are marked with boxes. Shear zones are marked "BBMZ" for Baltic-Bothnian megashear zone (Berthelsen and Marker, 1986) and "MSFZ" for Mierujav'ri-Sværholt Fault Zone (Olesen et al., 1991).

**Figure 3:** Stratigraphic correlation map of Kautokeino Greenstone belt after Siedlecka et al. (1985) with the approximate location of mineral deposits shown as circled letters or numbers; 43: Object 43, B: Bidjovagge Au-Cu deposit, D: Dælljadas, U: Ucca-vuovdas, and M: Masi River.

**Figure 4:** Composite photomicrographs of non-aqueous liquid-rich inclusions, photographed at room temperature and at different focal depths. Scale of all photos is similar, and bar scale in photo "a" is 0.05 mm. a.)  $\text{CO}_2 + \langle \text{N}_2 + \text{H}_2\text{O} \rangle$  inclusions from Dælljadas. b.)  $\text{CO}_2 + \langle \text{CH}_4 \rangle$  inclusions from Masi River. c.)  $\text{CO}_2 + \langle \text{N}_2 \rangle$  inclusions from Ucca-vuovdas. d.)  $\text{N}_2 + \langle \text{CH}_4 \rangle$  inclusions from Object 43.

**Figure 5:** Photomicrographs of saline aqueous fluid inclusions, photographed at room temperature. Scale of all photos is similar, and bar scale in photo "a" is 0.05 mm. a.) Salt undersaturated aqueous inclusion related to copper mineralization at the Bidjovagge deposit. b.) Salt saturated aqueous inclusions from Masi River. c.) Salt saturated aqueous inclusion from Ucca-vuovdas. d.) Salt saturated aqueous inclusions from Object 43.

**Figure 6:** Histogram showing temperatures of  $\text{CO}_2$  homogenization to liquid of fluid inclusions from Masi River, Ucca-vuovdas, and Dælljadas.

**Figure 7:** Histogram showing temperatures of H<sub>2</sub>O liquid + vapor homogenization to liquid, and salt dissolution, from Object 43, Ucca-vuovdas, Dælljadas and inclusions related to copper mineralization at the Bidjovagge Au-Cu deposit.

**Figure 8:** a.) Pressure versus temperature diagram with constructed isochores for non-aqueous liquid-rich inclusions from Masi River (MR), Dælljadas (DÆ), Ucca-vuovdas (UV), and Object 43. Pressure-temperature ranges are based on estimated molar volumes from microthermometric T<sub>h</sub> data. Isochores, showing a P-T range for inclusions related to copper mineralization at Bidjovagge (Bidj Cu), are calculated from temperatures of homogenization of aqueous inclusions, with 25 wt. % salt (NaCl equiv.). b.) P-T ranges of fluid trapping for discussed areas, based on isochores and salt melting temperatures.

**Figure 9:** Generalized diagram comparing salinity wt. % (NaCl equiv.) from Dælljadas, Bidjovagge, Masi River, Ucca-vuovdas, and Object 43. Data for salinity related to gold mineralization from the Bidjovagge Au-Cu deposit is from Ettner et al. (in prep.).

**Figure 10:** Log f<sub>O<sub>2</sub></sub> vs. pH diagram for the Fe-S-O system, showing phase relationships calculated for 350°C and 3 kbar with SUPCRT92 (Johnson et al., 1991). CH<sub>4</sub>-CO<sub>2</sub>-HCO<sub>3</sub><sup>-</sup> equilibrium shown as short dashed lines. Solubilities of AuCl<sub>2</sub><sup>-</sup> are shown as solid lines in ppm, calculated at 350°C with a log K of -2.5 (Hayashi and Ohmoto, 1991). CuCl solubilities, in ppm, shown as long dashed lines (Data from Crerar and Barnes, 1976). Fluid composition used in diagram include ΣS=0.01m, and 25 wt % NaCl (Cl<sup>-</sup>=5.7m). Arrows shows possible fluid path during gold and copper mineralization; A.) Fluids decrease in pH and f<sub>O<sub>2</sub></sub> during phase separation and buffering by the pyrite-magnetite-hematite assemblage, B.) A dramatic drop in f<sub>O<sub>2</sub></sub>

during red-ox reaction with graphitic schist results in gold precipitation together with a pyrite-pyrrhotite assemblage.

**Figure 11:** Schematic model of a shear zone with structural styles, modelled for the Abitibi greenstone belt by Colvine (1989) and adapted for the Kautokeino greenstone belt. Deposits and fluids discussed are displayed relative to the shear zone.

**Figure 12:** Interpretation of isochore data showing P-T path of fluids moving upwards along a shear zone. Within the ductile to brittle transition, fluid pressure drops dramatically. Gold and some copper mineralization occurs at higher pressures between 2 to 4 kbars, while most copper mineralization occurs at lower pressures around 1 to 2 kbars. Influx of meteoric water along some brittle structures may result in fluid mixing.

#### LIST OF TABLES

Table 1: Systematic classification of primary and pseudosecondary fluid inclusion observed from Dælljadas, Bidjovagge Au-Cu mine, Masi River, Ucca-vuovdas, and Object 43.

Table 2: Characteristic microthermometric data for selected gas-rich fluid inclusions from Dælljadas, Bidjovagge Au-Cu mine, Masi River, Ucca-vuovdas, and Object 43.

Table 3: Characteristic microthermometric data for selected H<sub>2</sub>O-rich fluid inclusions from Dælljadas, Bidjovagge Au-Cu mine, Masi River, Ucca-vuovdas, and Object 43.

Table 1: Systematic classification of primary and pseudosecondary fluid inclusions observed, at room temperature, from Dælljadas, Bidjovagge Au-Cu mine, Masi River, Ucca-vuovdas, and Object 43.

			Dælljadas	Bidjovagge*	Masi River	Ucca-vuovdas	Object 43	
Non-aqueous liquid-rich	CO <sub>2</sub> -rich	pure CO <sub>2</sub>	without H <sub>2</sub> O	X	Au			
			with H <sub>2</sub> O	X				
		CO <sub>2</sub> + CH <sub>4</sub>	without H <sub>2</sub> O		Au	X		
			with H <sub>2</sub> O					
		CO <sub>2</sub> + N <sub>2</sub>	without H <sub>2</sub> O	X			X	
			with H <sub>2</sub> O	X				
	CH <sub>4</sub> -rich	pure CH <sub>4</sub>	without H <sub>2</sub> O		Au			
			with H <sub>2</sub> O					
		CH <sub>4</sub> + CO <sub>2</sub>	without H <sub>2</sub> O		Au			
			with H <sub>2</sub> O					
N <sub>2</sub> -rich		without H <sub>2</sub> O					X	
		with H <sub>2</sub> O						
H <sub>2</sub> O-rich	pure H <sub>2</sub> O	without gas						
		with CO <sub>2</sub>						
		with CH <sub>4</sub>						
		with N <sub>2</sub>						
	H <sub>2</sub> O undersaturated with salt	H <sub>2</sub> O vapor or without vapor		X	Cu			
			with CO <sub>2</sub>	X				
			with CH <sub>4</sub>					
			with N <sub>2</sub>					
	H <sub>2</sub> O saturated with salt	H <sub>2</sub> O vapor			Au + Cu	X	X	X
			with CO <sub>2</sub>		Au			
		with CH <sub>4</sub>		Au				
		with N <sub>2</sub>						

\* Fluid inclusions from Bidjovagge are divided between Au- and Cu-related and are marked accordingly. Au-related inclusions are described by Ettner et al. (in prep.).

Table 1

Table 2: Microthermometric and Raman microprobe data for selected non-aqueous liquid-rich inclusions from Dælljadas, Masi River, Ucca-vuovdas and Object 43.

Sample Area	Inclusion No.	Microthermometric data				Raman microprobe data			
		T <sub>h</sub> N <sub>2</sub>	T <sub>m</sub> CO <sub>2</sub>	T <sub>h</sub> CO <sub>2</sub>	T <sub>m</sub> clathrate	N <sub>2</sub> peak (cm <sup>-1</sup> )	CO <sub>2</sub> peak (cm <sup>-1</sup> )	CH <sub>4</sub> peak (cm <sup>-1</sup> )	CO <sub>2</sub> mole %
Dælljadas	DÆ92-3a-3		-58.1	-7.0	8.9	2326.9	1386		
	DÆ92-3a-11		-56.8	14.4		2326.9	1386		
	DÆ92-3a-15		-57.6	-9.4	12.4				
	DÆ92-3a-17		-57.4	10.4	10.4				
	DÆ92-3a-18		-57.0	-4.7	9.4				
	DÆ92-3a-19		-56.9	-24.8	9.9				
Masi River	MB90-4b-7		-58.5	-20.8		2326.9	1386	2912.2	
	MB90-4b-8		-57.0	-32.9		2326.9	1386	2910.8	
Ucca-vuovdas	MB90-4b-14		-58.0	-36.6					
	MB90-4b-19		-62.1	-50.4					
Object 43	MB90-4b-25		-58.7						
	MB90-4b-26		-58.0						

T<sub>h</sub> N<sub>2</sub>: Temperature of homogenization of N<sub>2</sub> to liquid  
T<sub>m</sub> CO<sub>2</sub>: Temperature of final melting of solid CO<sub>2</sub>  
T<sub>h</sub> CO<sub>2</sub>: Temperature of homogenization of CO<sub>2</sub> to liquid  
T<sub>m</sub> clathrate: Temperature of final melting of gas clathrate

Table 3: Microthermometric data for selected H<sub>2</sub>O-rich inclusions from Dælljadas, Bidjovagge, Masi River, Ucca-vuovdas and Object 43.

Sample Area	Inclusion No.	T <sub>m</sub> initial ice	T <sub>m</sub> final ice	T <sub>m</sub> hydrate	T <sub>h</sub> H <sub>2</sub> O + vapor	T <sub>d</sub> salt
Dælljadas	DÆ91-6a-26	-52	-27.7			
	DÆ91-6b-8	-64.9	-15.3			
	DÆ91-6b-11	-68.3	-8.2			
	DÆ91-6c-4	-37.6	-7.0			
Bidjovagge	DÆ91-6c-9	-49.6	-1.4		135	
	BG90-23a-1	-70.0	-23.8	-5.1	104	
	BG90-23a-2	-70.9	-25.7	-0.5	159	
	BG90-23a-3	-66.0	-25.7	-5.8	118	
	BC90-156b-1	-80.9	-28.8	12.5	128	142
	BC90-156b-2	-85.9	-29	-10.3	133	
	BC90-156b-8	-85.3	-27.4	2	118	
	BC90-156b-9	-86.5	-27.3	-0.7	118	
	Masi River	MB90-6a-1	-74.8	-26.6	-6.3	128
MB90-6a-3		-71	-29.3		147	
MB90-6a-6		-69.3	-25.8			191
Ucca-vuovdas	UV90-6a-1	-82.0	-44.4			
	UV90-6a-1	-84.0	-45.0			
Object 43	SL43-239-1	-101.7	-51.9		113	250
	SL43-239-2	-87	-37.3	-1.0	128	333
	SL43-239-3	-90.6	-39.2		118	167
	SL43-258a-1	-83.3	-29.1	13.3	260	186
	SL43-258a-5	-74.6	-37.5	-3.4	153	208
	SL43-258a-7	-75.5	-34.8		118	176

T<sub>m</sub> initial ice: temperature of observed first melting  
T<sub>m</sub> final ice: temperature of final ice melting  
T<sub>m</sub> hydrate: temperature of salt hydrate final melting  
T<sub>h</sub> H<sub>2</sub>O+vapor: temperature of H<sub>2</sub>O + vapor homogenization to liquid  
T<sub>d</sub> salt: temperature of salt dissolution

Table 3

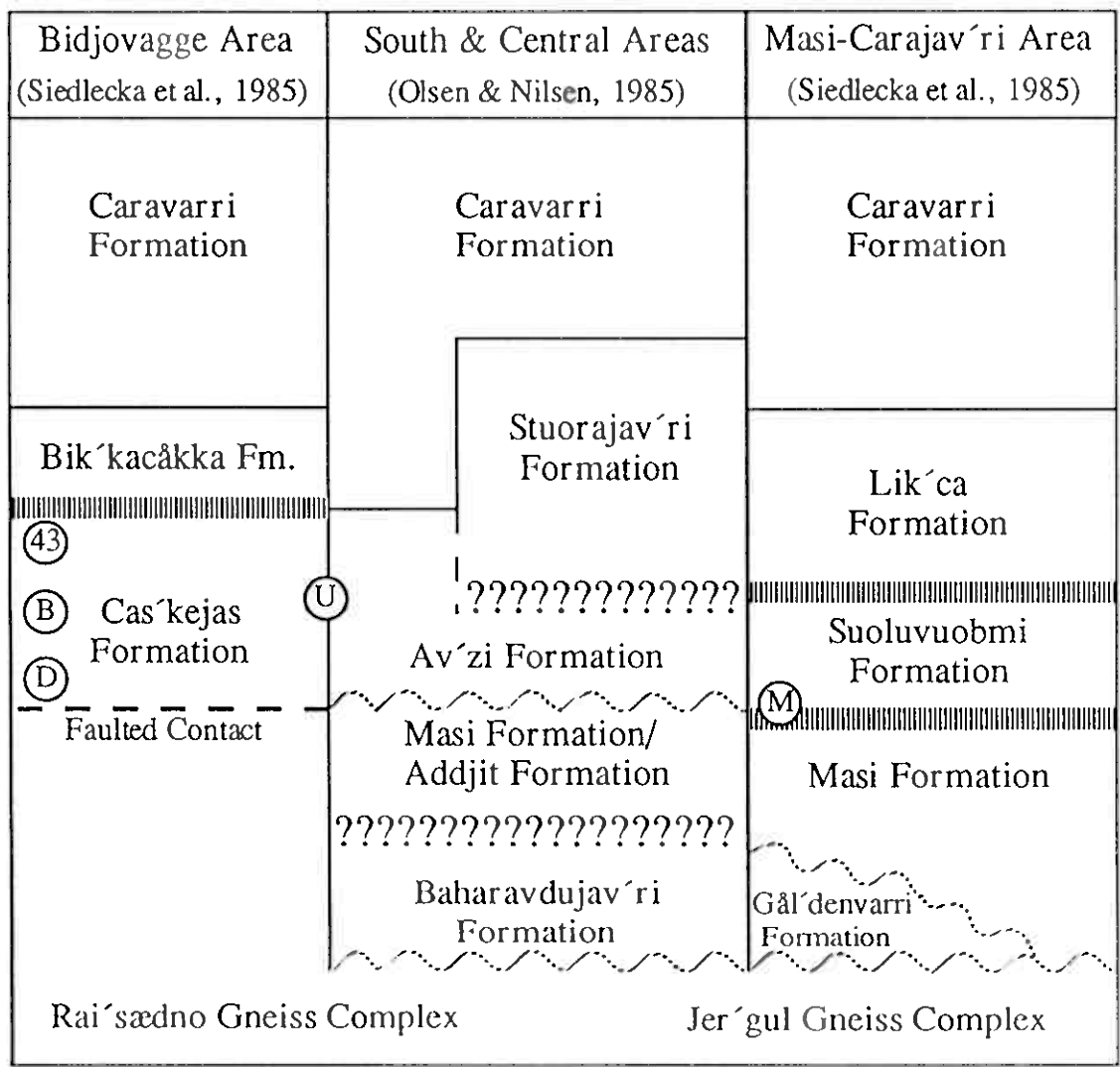
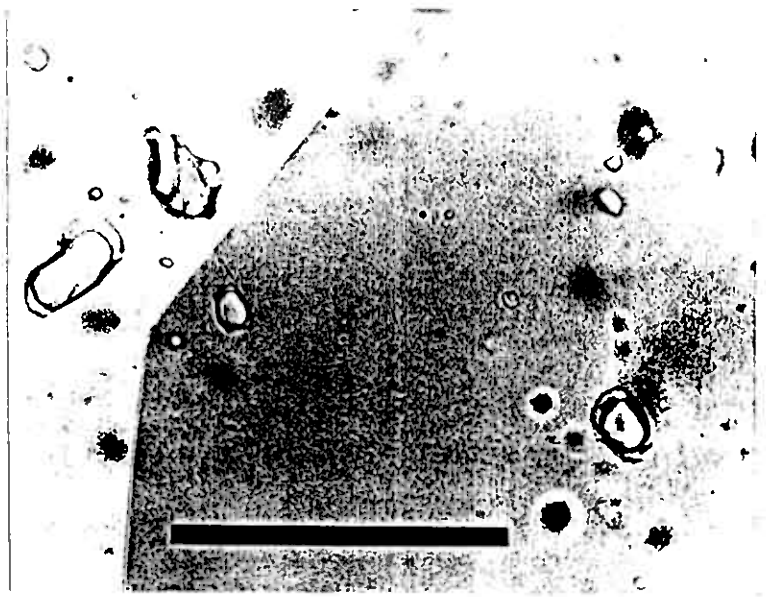


Fig. 3

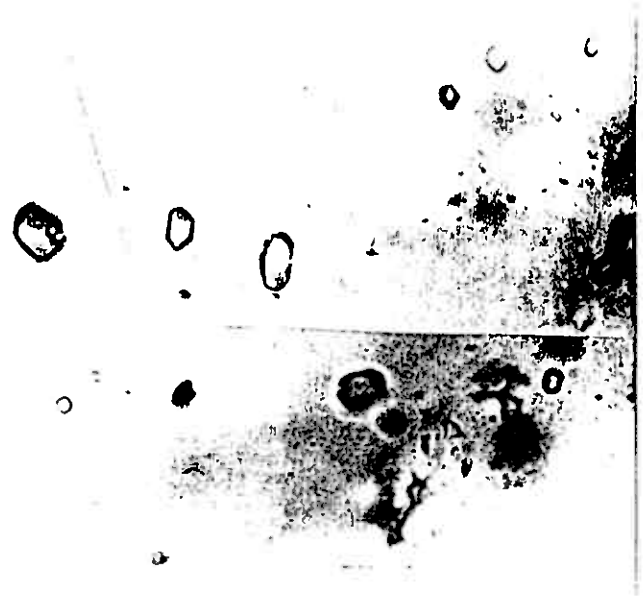
**a**



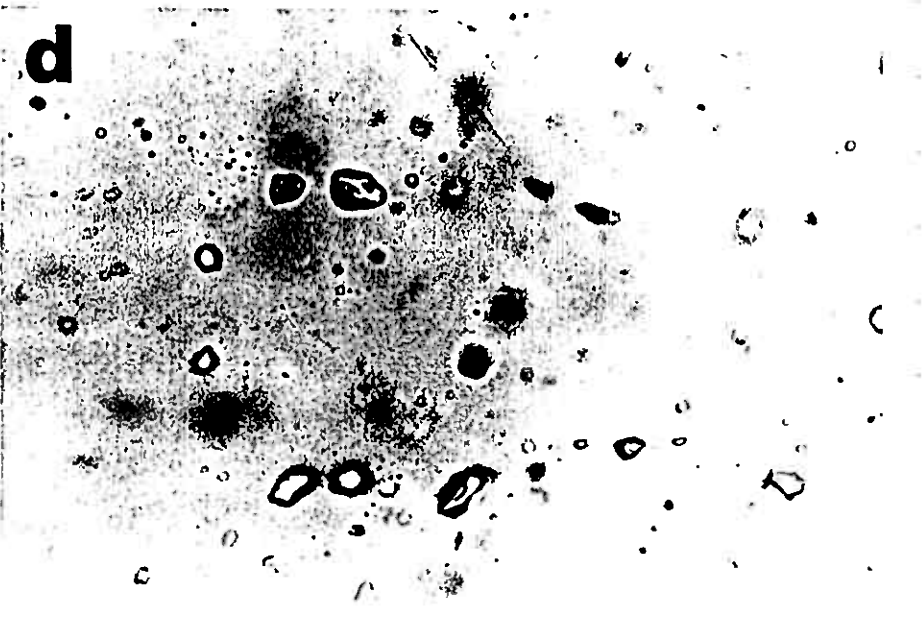
**b**

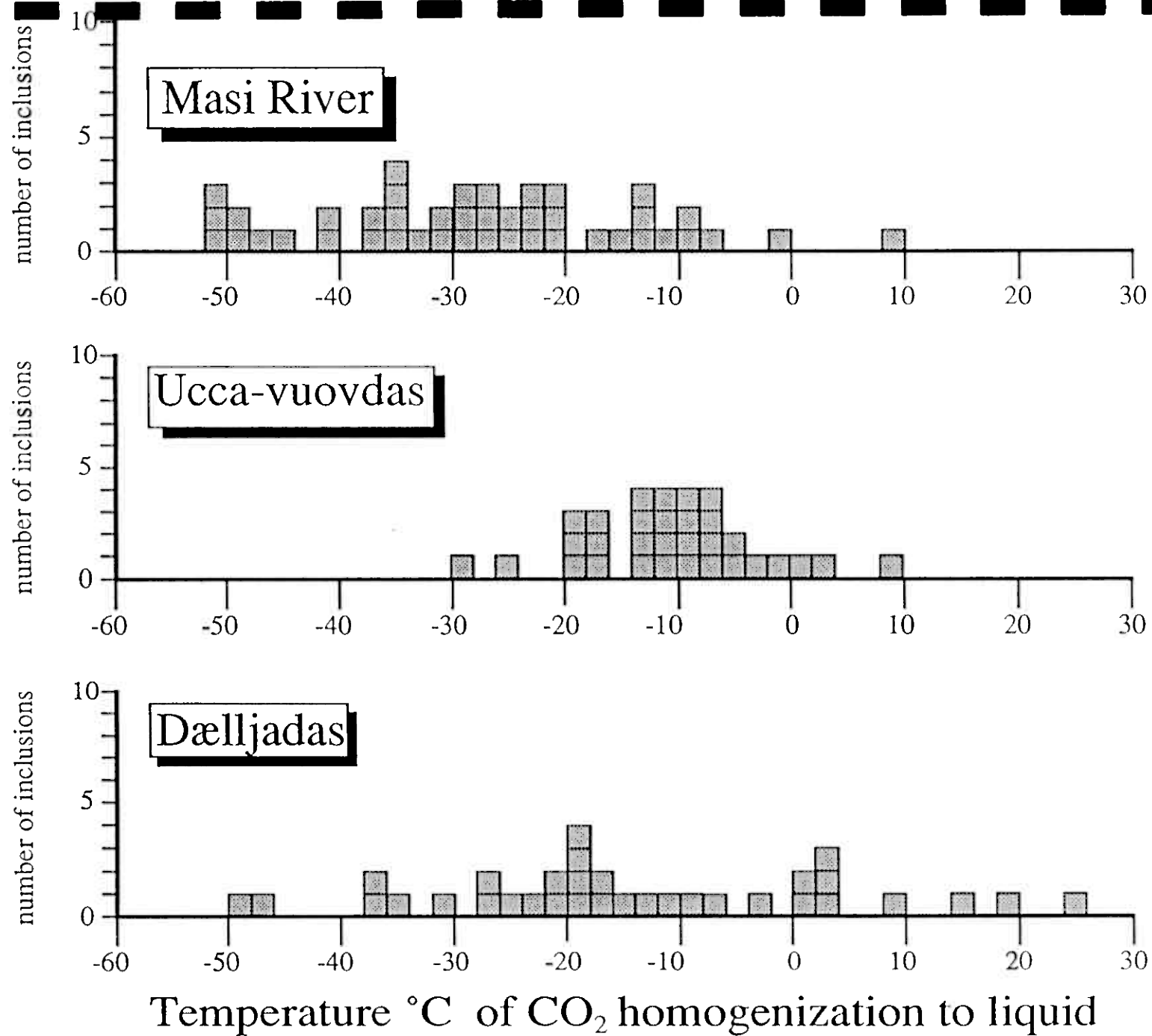


**c**



**d**





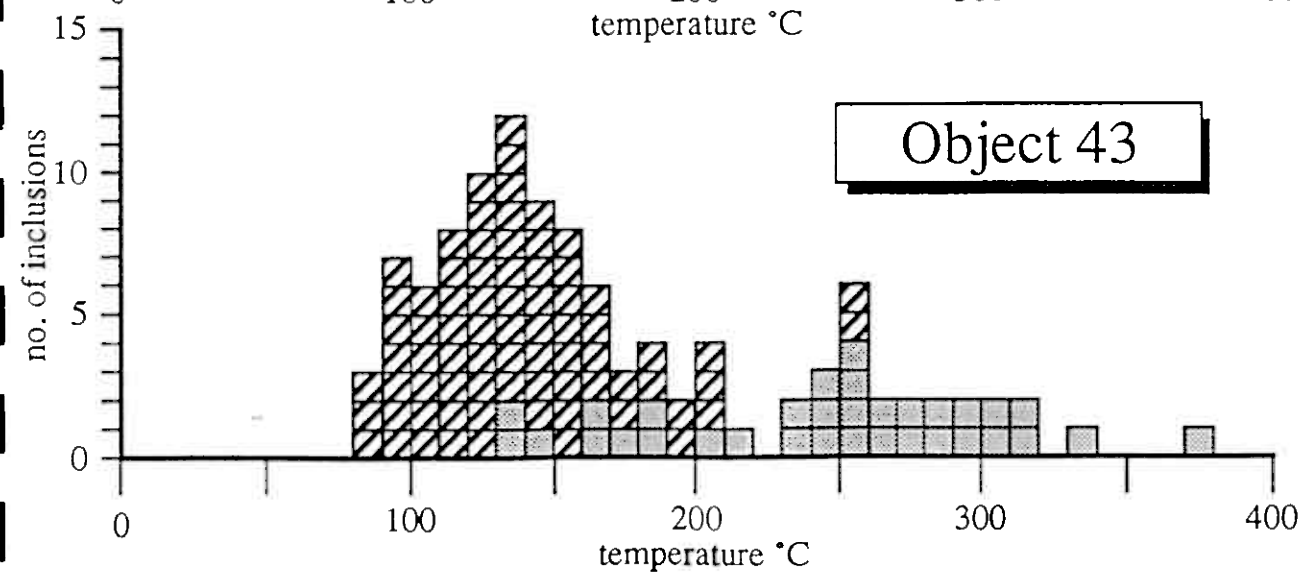
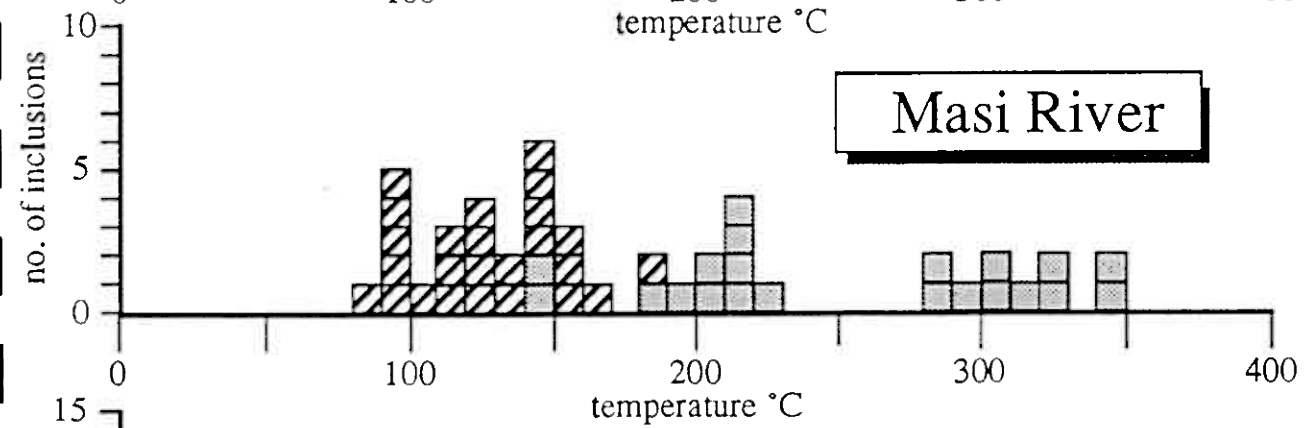
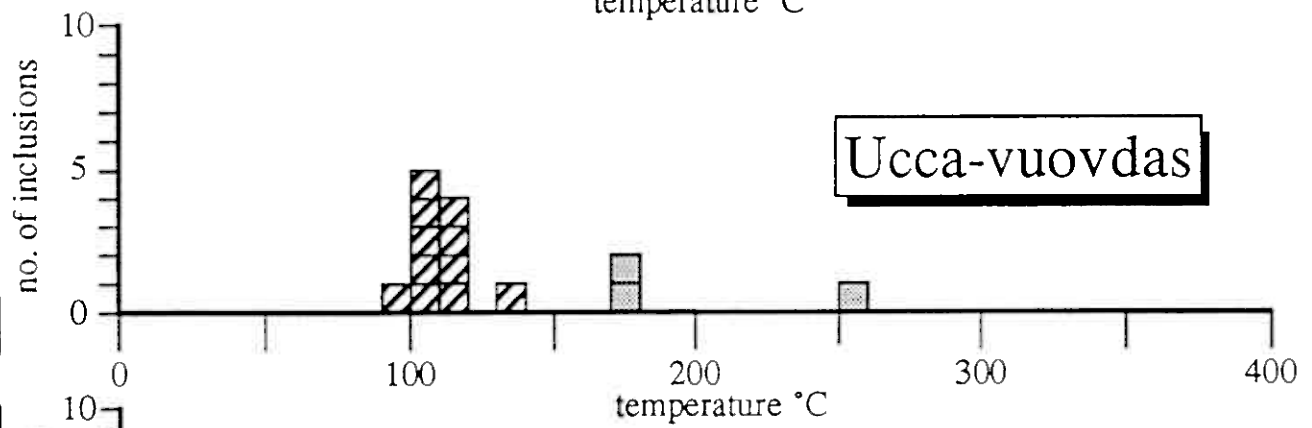
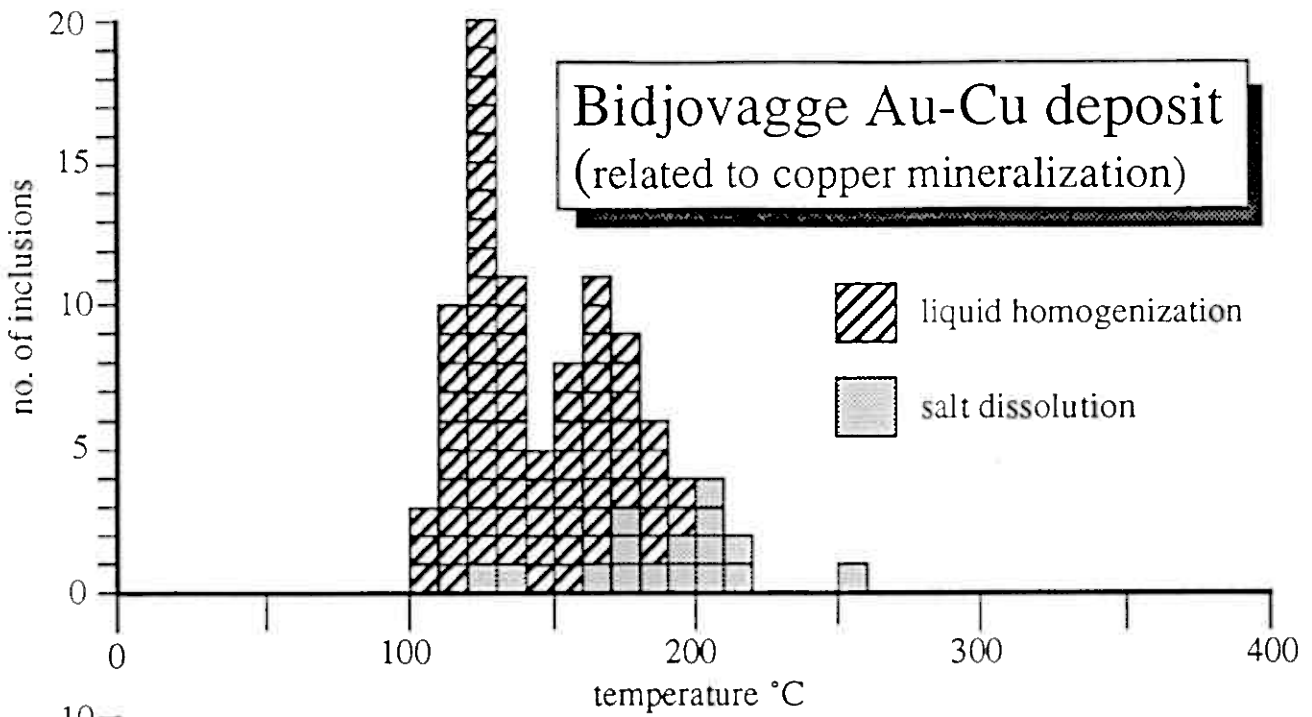
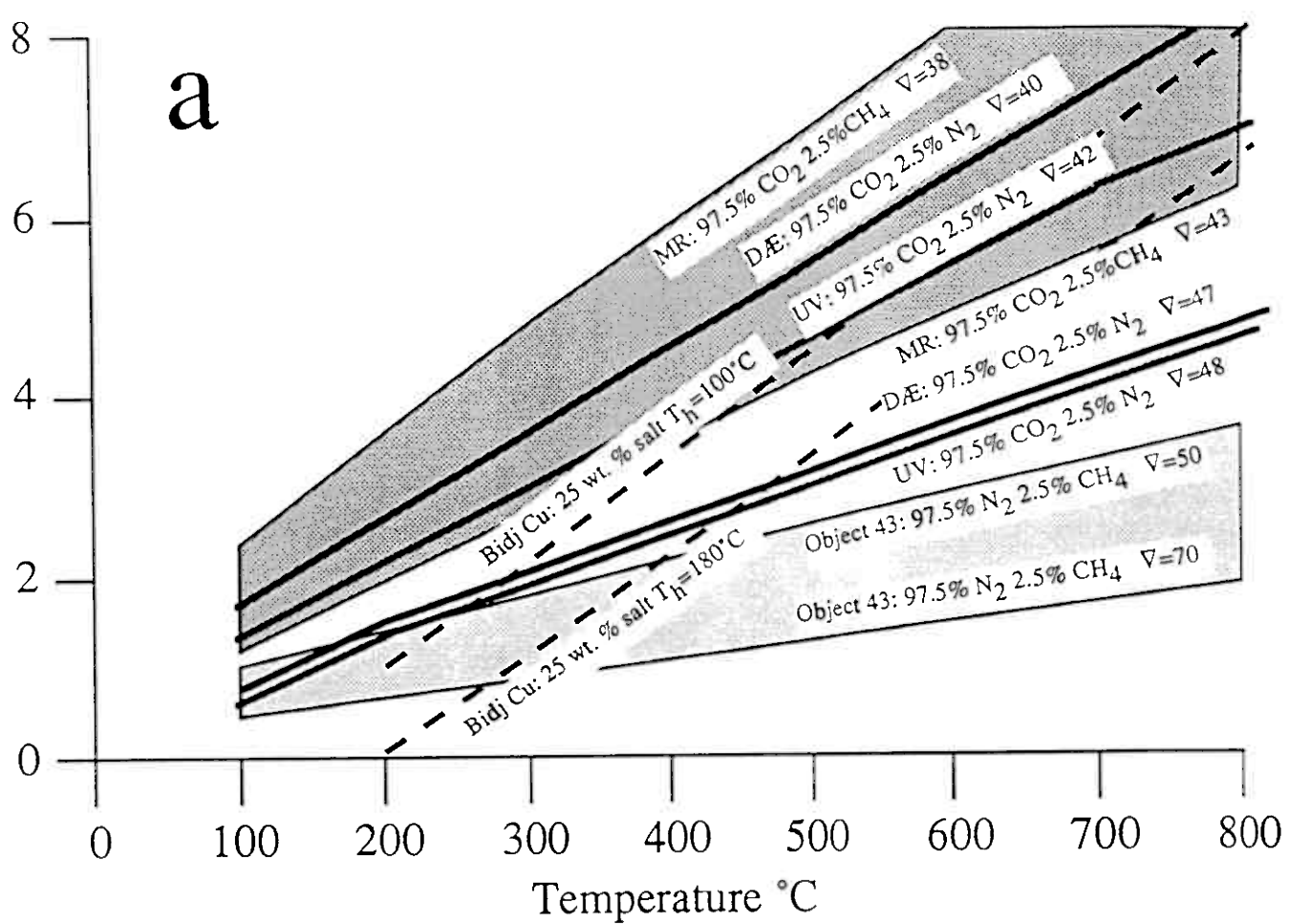
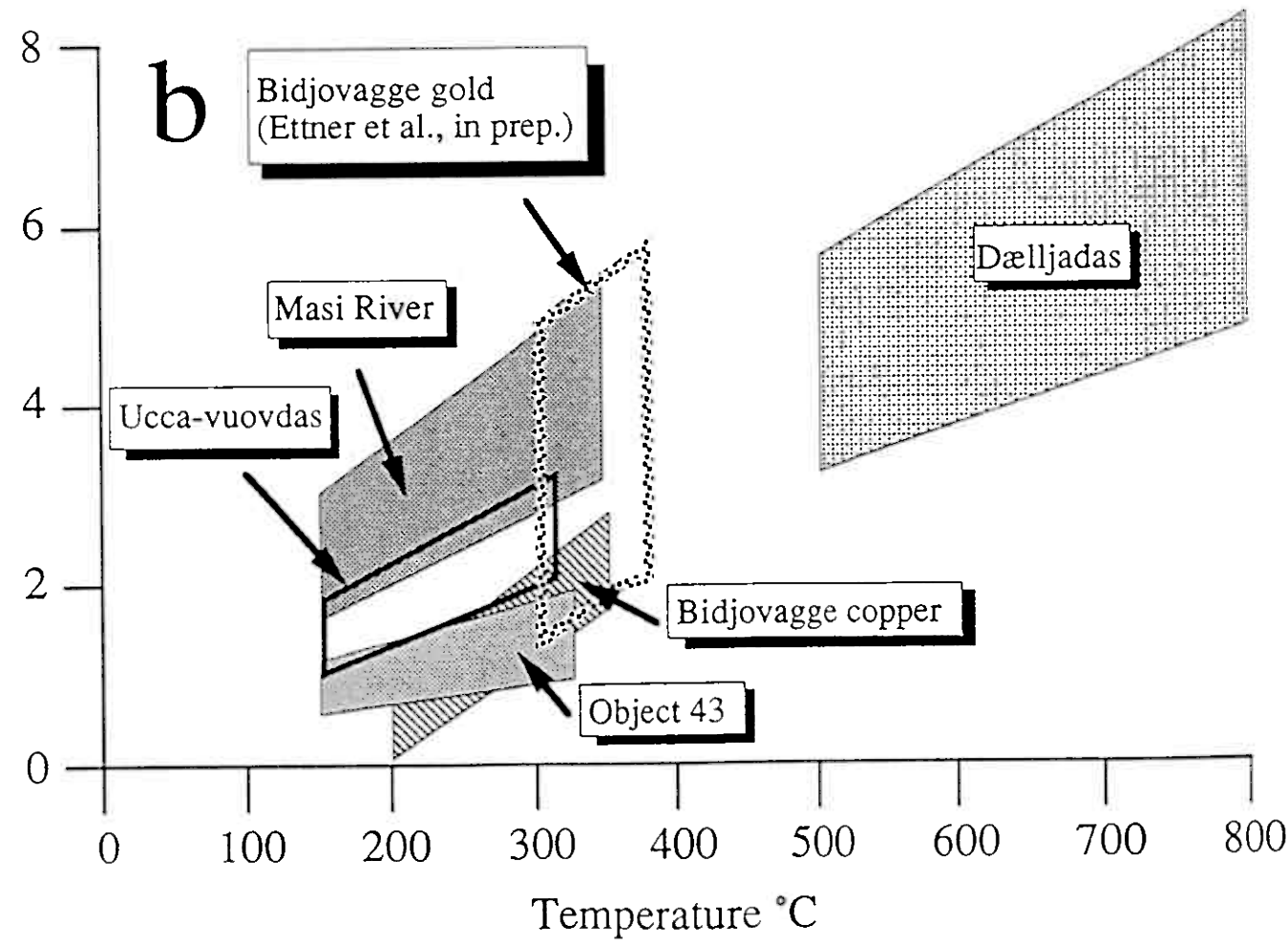


Fig. 7

kbars



kbars



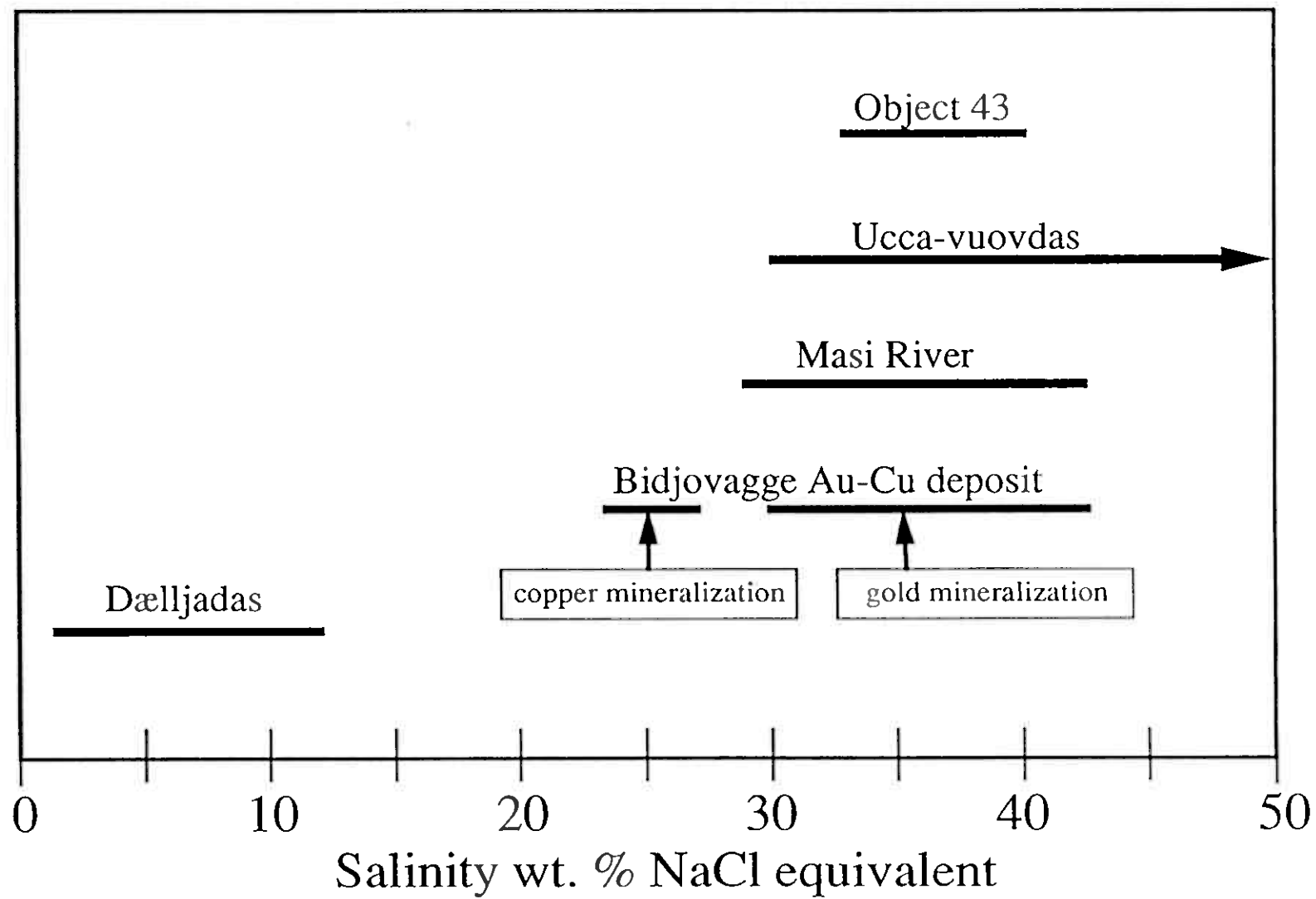


Fig. 9

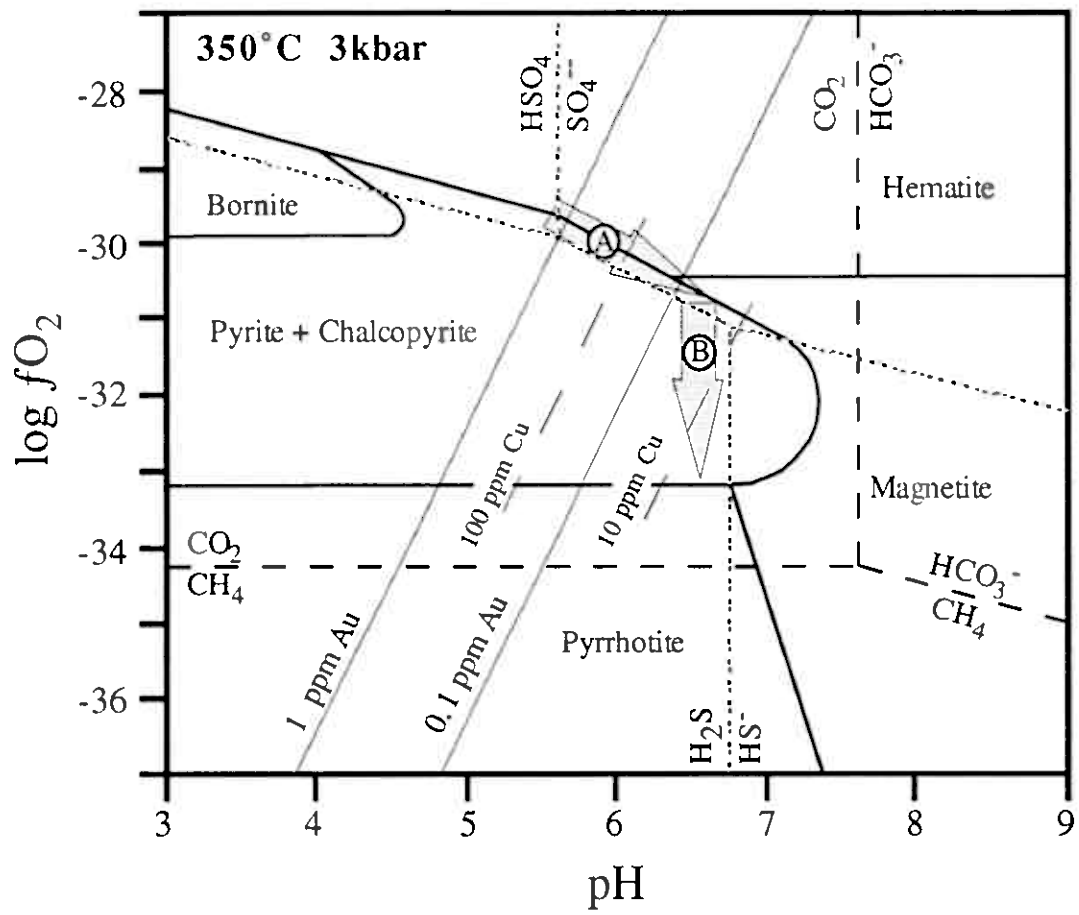
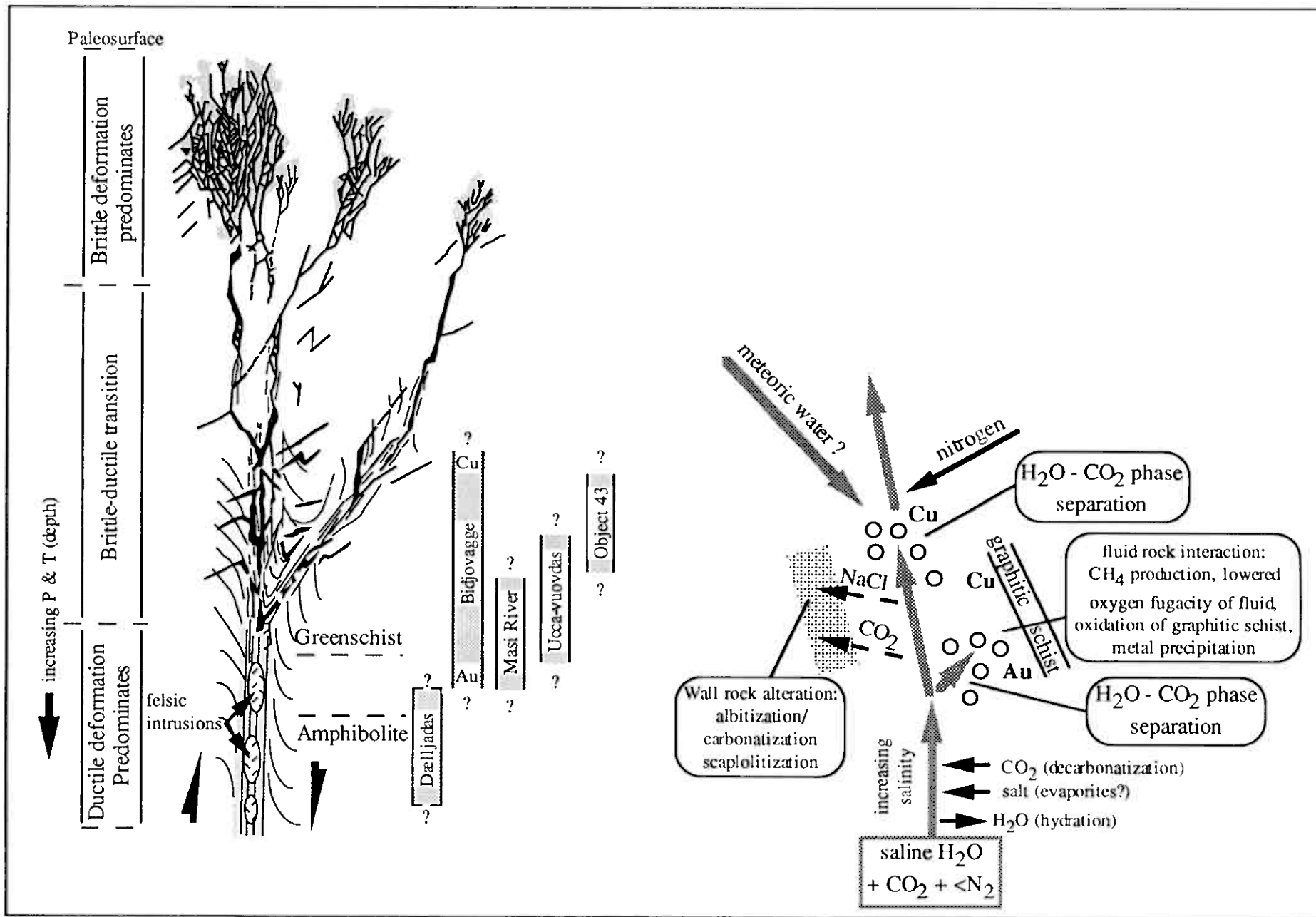
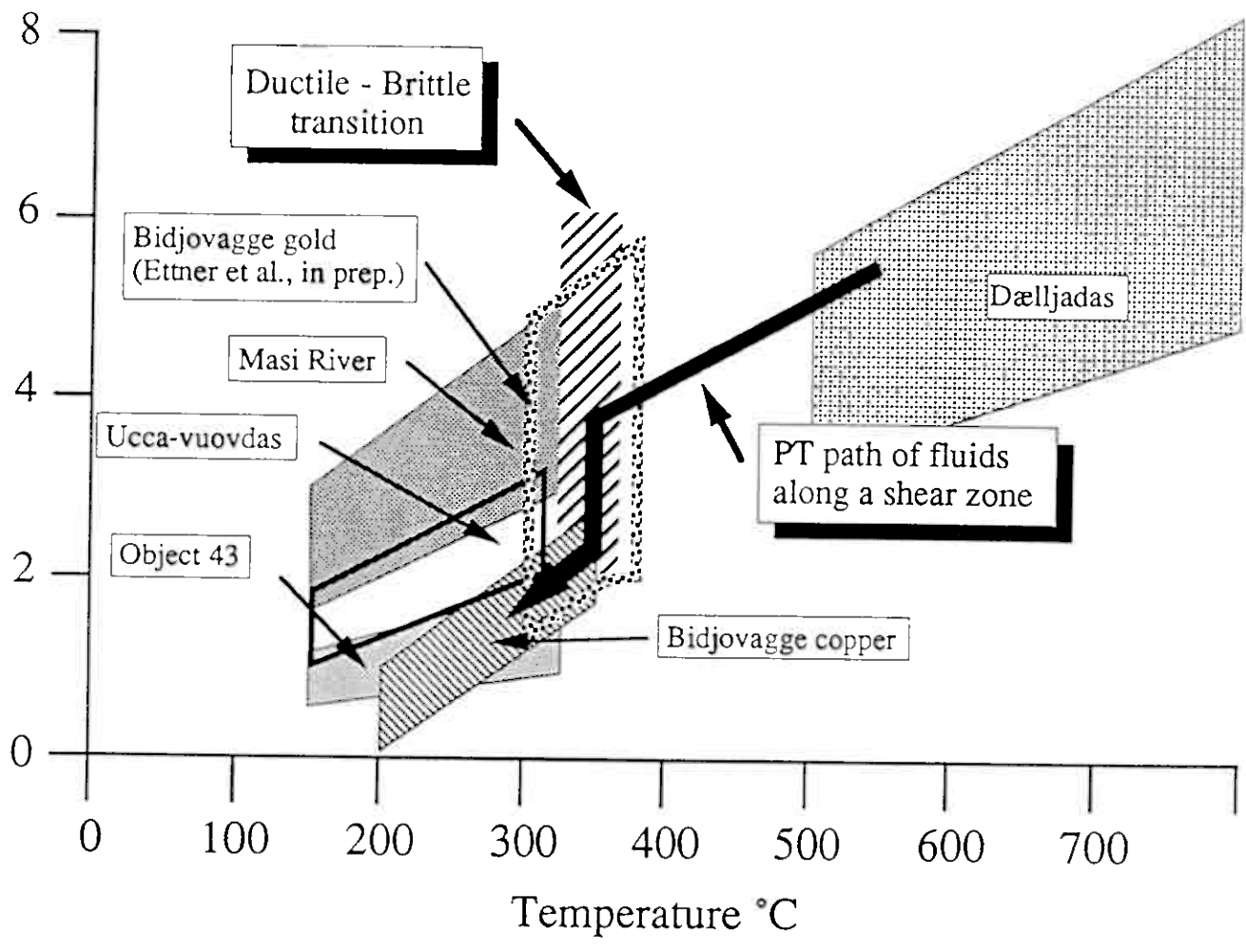


Fig 10



klaus



# PAPER III

Version of 5.6.93

## Identification and implications of light hydrocarbon fluid inclusions from the Proterozoic Bidjovagge Au-Cu deposit, Finnmark, Norway

David C. Ettner<sup>1</sup>, Sten Lindblom<sup>2</sup> & Dag Karlsen<sup>1</sup>

<sup>1</sup> Institute of Geology, University of Oslo, P.O. Box 1047, Blindern, N-0316 Oslo, Norway

<sup>2</sup> Ore Research Group, Department of Geology, University of Stockholm, S-106 91 Stockholm, Sweden

## Abstract

Carbonic fluid inclusions have been observed in quartz-bearing veins, at the Proterozoic aged Bidjovagge Au-Cu deposit within the Kautokeino greenstone belt, where mineralization occurs in an oxidation front to graphitic schist. A fluid inclusion zonation occurs, with CO<sub>2</sub>-rich fluid inclusions in the footwall of the deposit, and CH<sub>4</sub>-rich inclusions in the ore zone at the oxidation front. Fluid inclusions have been studied by microthermometric and Raman analysis, along with bulk gas analysis with gas chromatography. Microthermometry of hydrocarbon inclusions reveals 2 groups, based on homogenization temperatures, the first group which homogenize between -125°C and the critical temperature of CH<sub>4</sub> (-82.1°C), indicating pure CH<sub>4</sub>, and the second group which homogenize between the critical temperature of CH<sub>4</sub> and -42°C, indicating CH<sub>4</sub> + higher hydrocarbons (HHC). Raman microprobe analysis of the first group confirm the presence of CH<sub>4</sub>. The second inclusion group are fluorescent, but Raman spectra clearly display CH<sub>4</sub>, C<sub>2</sub>H<sub>6</sub> and occasionally C<sub>3</sub>H<sub>8</sub> peaks. A typically feature of the Raman spectra show a "mounding" below the hydrocarbon peaks. Carbon peaks are also typically detected in each inclusion by Raman analysis. Bulk gas chromatography analysis of samples containing the first group (CH<sub>4</sub>) indicates the presence of CH<sub>4</sub> and low concentrations of C<sub>2</sub>H<sub>6</sub> and C<sub>3</sub>H<sub>8</sub>. Gas chromatography analysis of samples containing the second group (CH<sub>4</sub> + HHC) confirms the presence of CH<sub>4</sub>, and higher hydrocarbons such as C<sub>2</sub>H<sub>6</sub>, C<sub>3</sub>H<sub>8</sub>, and also butanes. Zonation of hydrocarbons and the estimated PT conditions of 300 to 375°C and 2 to 4 kbars suggests a abiogenic origin of hydrocarbons. The hydrothermal fluids responsible for gold and copper mineralization is suggested to have reacted with graphitic schist and resulted in mineralization, oxidation of the graphitic rocks, and formation of light gas hydrocarbons.

## Introduction

Numerous workers have recognized CH<sub>4</sub>-rich fluid inclusions in metamorphic terrains (i.e. Hollister & Burruss, 1976; Mullis, 1979; Kreulen & Schuiling, 1982; Kerkhof, 1987; Lindblom & Burke, 1988). The presence of higher hydrocarbons have also been reported or described in metamorphic terrains (Mullis, 1987; Kerkhof, 1991; Munz et al., 1992; Ettner et al., submitted, 1993) and igneous rocks (Konnerup-Madsen et al., 1979). The origin of such higher hydrocarbon inclusions is a matter of debate. Higher hydrocarbon inclusions, described in Proterozoic metamorphic terrains, have been suggested to form from a secondary influx of Paleozoic organic fluids into Proterozoic rocks (Munz et al., 1992), *in situ* organic fluids (Kerkhof, 1991), and *in situ* reaction between hydrothermal fluids and graphitic rocks (Ettner et al., 1993).

At the Proterozoic-aged Bidjovagge Au-Cu deposit, in northern Norway, fluid inclusions containing methane and ethane were first described by Ettner et al. (submitted, 1993), based on microthermometric and Raman microprobe analysis. This initial fluid study of the Bidjovagge deposit indicated the possible presence of additional higher hydrocarbons. Identification of hydrocarbons based on results of further microthermometric and Raman microprobe analysis of the fluid inclusions and gas chromatography, are presented here accompanied by a proposed model of origin.

## Geologic Setting

The Bidjovagge gold-copper deposit is situated approximately 40 km northwest of the village of Kautokeino, on the Finnmark plateau, northern Norway (Fig. 1). The deposit occurs in Proterozoic rocks of the north-south trending Proterozoic Kautokeino greenstone belt within the Fennoscandic Shield. The Kautokeino greenstone belt is composed of a series mafic volcanic, metasedimentary, and intrusive rocks (Siedlecka et al., 1985) that are metamorphosed to amphibolite facies in the lower portions near the contact with the gneissic basement, grading to

lower greenschist in the higher tectonostratigraphic portions of the greenstone belt (Holmsen et al., 1957; Krill et al., 1988; Sandstad, 1992). Rocks are also regionally folded and cut by shear zones (Olesen et al., 1991; Sandstad, 1992).

In the vicinity of the Bidjovagge deposit the rock sequence consist of metavolcanics, sedimentary carbonates, diabase sills, albite felsites, graphitic schists, and tuffites of the Cas'kejas Formation (Hollander, 1979; Bjørlykke et al., 1987) which are metamorphosed in the upper greenschist to lower amphibolite facies (Sandstad, 1983). Albite felsite, generally composed of microcrystalline albite, occur between the diabase sills and graphitic schist, and grade to graphitic felsite and graphitic schist. These albite felsites are interpreted by Bjørlykke et al. (1987) to be the result of metasomatic alteration of black shale during the intrusion of diabase sills.

The metasedimentary rocks, albite felsites, and metavolcanics are folded in a tight antiformal structure, plunging gently northward and trending north-south for approximately 8.5 km (Fig. 2). The eastern limb of the antiform is cut by a series of shear zones which tend to be localized within the albitic felsite between the contact of metadiabase and graphitic schist.

Both metamorphism and deformation are considered to have occurred during the Svecokarelian orogeny, approximately 1,900 to 1,850 Ma, due to continent-continent and arc-continent collisions (Skiöld, 1988; Pharaoh & Brewer, 1990; Bjørlykke et al., 1993).

The Kautokeino greenstone belt is unconformably overlain by Late Precambrian sandstones of the Dividal Group, which is overlain by Caledonian thrust nappes (Ramsay et al., 1985). Both the Dividal Group and Caledonian thrust nappes outcrop within 4 km of the Bidjovagge deposits (Fig. 1) (Sandstad, 1985).

#### *Bidjovagge Au-Cu mineralization*

A series of veins occur within the shear zone, dominated by quartz, carbonates, actinolite, sulfides, and magnetite. Where the vein systems cut the graphitic schist a well developed oxidation zone in the graphitic schist is developed

(Fig. 3). A mineralogic zonation of magnetite to pyrite to pyrite + pyrrhotite occurs towards the oxidation front (Ettner et al., 1993).

Gold and copper mineralization is shear zone hosted, and occurs in a series of approximately 13 ore bodies along the shear zone (Fig. 2). Ore bodies tend to occur where graphitic schist units are truncated by the intersection of shear zones which host hydrothermal veins. Mineralization at the Bidjovagge deposit has been divided into two types, by Bjørlykke et al. (1987), the gold-ore type and copper-ore type. Typically, disseminated gold, of the gold-ore type, is hosted within sheared and microbrecciated albite felsite, within the well developed oxidation zone to the graphitic schist. Chalcopyrite also occurs related to the gold-ore type within the hydrothermal veins. Syenodiorite dikes also occur as lenses within the shear structures and are closely associated with mineralization. A later phase of copper mineralization occurs as large chalcopyrite + carbonate veins that crosscut earlier gold and copper mineralization, and is classified as the copper-ore type by Bjørlykke et al. (1987).

The occurrence of gold and copper mineralization within the oxidation zone between hydrothermal veins and the graphitic schists is interpreted, by Bjørlykke et al (1987) and Ettner et al. (1993, submitted), to be the result of ore-bearing fluid reaction with the graphitic schist.

Age determinations of the Bidjovagge Au-Cu deposit has been constrained by isotopic dating of davidite and uraninite by Bjørlykke et al. (1990) and Cumming et al. (in prep). Davidite found in association with gold gave a U/Pb date of  $1885 \pm 18$  Ma and a Sm/Nd date of  $1886 \pm 88$  Ma (Bjørlykke et al. 1990) and uraninite gives a date of  $1837 \pm 8$  Ma (Cumming et al., in prep.) which suggest that Bidjovagge mineralization occurred during the Svecokarelian orogeny.

## Methods

Doubly polished sections, 100 to 150  $\mu\text{m}$  thick, of the samples were made for microthermometric and Raman microprobe analysis. Microthermometric

measurements were conducted at the Mineralogical-Geological Museum, Oslo, Norway using a gas-cooled CHAIXMECA stage. The CHAIXMECA stage used has a consistent accuracy and precision of  $\pm 0.1^{\circ}\text{C}$  at  $-56.6^{\circ}\text{C}$  and about  $\pm 1.0^{\circ}\text{C}$  between the range  $-142$  and  $+30^{\circ}\text{C}$ , as described for the same instrument by Andersen et al. (1991). Measurements were made during heating, at a rate of approximately  $5^{\circ}$  per minute.

Laser-excited Raman microprobe analysis were conducted in the laboratory of the Geological Institute at Stockholm University, Sweden. The instrument used for analysis was a multichannel DILOR-XY, which is a successor to the MICRODIL-28 (Burke and Lustenhouwer, 1987). Measured line positions of  $\text{CH}_4$  and higher hydrocarbons were identified by listed values compiled by Dubessy et al. (1989), Kerkhof (1991) and Burke (pers. comm.).

Samples for gas chromatographic analysis were cleaned by soaking in dichloromethane for approximately 24 hours and allowed to dry for 7 days. Sample size ranged from 6.0 to 13.8 grams. Samples were powdered in a steel crushing chamber with brass cylinder equipped with a septum through which the sample was withdrawn with a gas tight syringe. For gas quantification, flushing the chamber with nitrogen was not conducted, as repeated blank runs (with mechanical agitation of the crushing chamber) showed only background methane (2ppm = 1mV). Simple subtraction of the background was sufficiently accurate.

Gas chromatography of samples were analyzed on a Varian 3500 GC-FID using a 30m DB-1 column (film thickness =  $5.0\ \mu\text{m}$ ). Between 2 to 4 ml of gas, from each sample, was injected into the gas chromatograph.

## Description of Samples

Previous fluid inclusion and stable isotope analysis of the veins and veinlets from the footwall and ore bodies at Bidjovagge have been conducted by Ettner et al. (1993). Veins studied can generally be divided into three types, footwall veins, veins

in mineralized albitic felsites within the oxidation zone, and veins cross cutting graphitic schists. Footwall veins are up to 1 m wide and are dominated by carbonate, quartz, actinolite, chalcopyrite, magnetite and pyrite. Within the mineralized zone, veins are smaller and mineralogy is dominated by carbonate, quartz, chalcopyrite, pyrite, and pyrrhotite, although actinolite may also be present. These veins and veinlets are locally folded and boudinaged (Bjørlykke et al., 1987). Veins crosscutting graphitic schist are dominantly composed of carbonate and pyrrhotite, although some contain quartz and actinolite. Oxidized haloes of are present surrounding some veins which crosscut graphitic schist (Fig. 3).

Detailed fluid inclusion work by Ettner et al. (submitted) has shown that fluid inclusions shown composition variation from the footwall veins towards the ore zone. Fluid inclusions in the footwall veins are composed of both pure liquid CO<sub>2</sub> and pure CO<sub>2</sub> + highly saline H<sub>2</sub>O. Towards the ore zone and the oxidation zone the fluid inclusions do not contain pure CO<sub>2</sub>, rather they contain CH<sub>4</sub> + highly saline H<sub>2</sub>O or a (CO<sub>2</sub> + CH<sub>4</sub>) mix + highly saline H<sub>2</sub>O (Fig. 4). Some fluid inclusions from a quartz + carbonate + pyrite + chalcopyrite vein (sample BC91-249), from the "H" ore body (Fig. 2), was found to contain CH<sub>4</sub> + C<sub>2</sub>H<sub>6</sub> (Ettner et al., 1993, submitted).

## Results of Analysis

### *Microthermometry*

Within the ore bodies and the oxidation zones, fluid inclusions are dominated by single phase fluid CH<sub>4</sub> or (CH<sub>4</sub> + CO<sub>2</sub>) mixtures, and higher hydrocarbons (Fig. 5) (Ettner et al., 1993). Based on microthermometric observation and classification of Kerkhof (1990), hydrocarbon ± CO<sub>2</sub> bearing fluid inclusions from Bidjovagge display three general phase behaviours. First, fluids in which no solid formed during supercooling, but which show liquid + vapor homogenizing to liquid between -125 and -42.1°C, classify as "H<sub>1</sub>-type inclusions" (Fig. 6). Second, hydrocarbon + CO<sub>2</sub> fluids that partially froze to solid + liquid + vapor, displayed partial homogenization

to solid + liquid during heating between -105 to -65°C, followed "sublimation" of the solid to liquid from -95 to -60°C, classify as "S<sub>2</sub>-type inclusions" (Fig. 6). Third, CO<sub>2</sub>-rich fluids which froze to solid + vapor, melt to liquid + vapor between -72 and -56.6°C, followed by homogenization to liquid from -60 to -6°C, classify as "H<sub>3</sub>-type inclusions" (Fig. 6).

Fluid inclusions of the "H<sub>1</sub>-type" that do not freeze but homogenize to liquid between -125 to -42.1°C indicate the presence of hydrocarbons. Those inclusions which homogenize to liquid between -125°C and the critical temperature of CH<sub>4</sub> (-82.1°C) fit the behaviour of CH<sub>4</sub> (Burruss, 1981; Kerkhof, 1990). Inclusions which homogenized between the critical temperature of CH<sub>4</sub> (-82.1) and -42.1°C (Fig. 5) may include CH<sub>4</sub> + higher hydrocarbons, or higher hydrocarbons such as ethane without CH<sub>4</sub> (Mullis, 1979). CH<sub>4</sub> + CO<sub>2</sub> mixes may produce similar homogenization temperatures (Burruss, 1981) but supercooling would produce solid CO<sub>2</sub> (Kerkhof, 1990) which was not observed.

Critical behaviour was observed in one fluid inclusion from the K deposit (Fig. 2) (sample BC90-51), in which the meniscus fades at -74.8°C (Fig. 5 a & b). Assuming a binary system of CH<sub>4</sub>-C<sub>2</sub>H<sub>6</sub>, this critical temperature indicates a mole fraction of approximately 0.08 C<sub>2</sub>H<sub>6</sub> and similarly, in the binary system CH<sub>4</sub>-C<sub>3</sub>H<sub>8</sub> this critical temperature indicates a C<sub>3</sub>H<sub>8</sub> mole fraction of 0.03 (Olds, 1953).

#### *Raman microprobe analysis*

Raman microprobe analysis of the "H<sub>1</sub>-type" fluid inclusions allow more precise detection of the volatile components present. Fluid inclusions homogenizing to liquid between -125 to -82.1°C show a strong CH<sub>4</sub> peak at  $\Delta\nu=2911\text{ cm}^{-1}$  which is in agreement with microthermometric data.

Fluid inclusions which homogenized above the critical temperature of CH<sub>4</sub>, between -82.1 and -42°C, fluoresce strongly, but also display a strong CH<sub>4</sub> peak around  $\Delta\nu=2911\text{ cm}^{-1}$  (Fig. 7). Background spectra around the CH<sub>4</sub> peak, in most of the inclusions analyzed is slightly anomalous, forming a "mound". On top of this

spectra mound, a peak around 2950 to 2952 $\text{cm}^{-1}$  matches the position of ethane ( $\Delta\nu=2954\text{ cm}^{-1}$ ; Kerkhof, 1991) and occasionally, a peak occurs around 2892  $\text{cm}^{-1}$  matches propane ( $\Delta\nu=2890\text{ cm}^{-1}$ ; Burke, pers. comm.) (Fig. 7). Raman microprobe analysis of these inclusions did not detect  $\text{CO}_2$ .

In the majority of  $\text{CH}_4$  bearing inclusions analyzed, characteristic carbon spectra was detected. The spectra was identified on the basis of two peaks, the strongest, but narrow and angular, peak at about  $\Delta\nu=1605$  to  $1608\text{cm}^{-1}$  and a second, wider and rounded, peak between  $\Delta\nu=1327$  to  $1340\text{cm}^{-1}$  (Fig. 8) (Lespade et al., 1982). The spectra indicates that the carbon is amorphous (Lespade et al., 1982) probably as coating on the wall of the fluid inclusions, as crystalline carbon is not visible in the inclusions.

### *Gas Chromatography*

Preliminary gas chromatography analysis of vein samples from Bidjovagge confirmed the presence of  $\text{CH}_4$  and higher hydrocarbons in veins within the mineralized zones, and indicate a lack of hydrocarbons in the footwall veins.

Separated vein quartz samples which contained "H<sub>1</sub>-type" fluid inclusions, which homogenized to liquid between  $-125$  to  $-82.1^\circ\text{C}$ , display a chromatogram showing  $\text{CH}_4$ ,  $\text{C}_2\text{H}_6$  and a trace of  $\text{C}_3\text{H}_8$  (Fig. 9 a). Separated vein quartz samples which contained "H<sub>1</sub>-type"  $\text{CH}_4$  + HHC inclusions, which homogenized to liquid between  $-82.1$  to  $-42.1^\circ\text{C}$ , give a chromatogram showing  $\text{CH}_4$ ,  $\text{C}_2\text{H}_6$ ,  $\text{C}_3\text{H}_8$  and butanes (Fig. 9 b), with a lower  $\text{CH}_4/\text{C}_2\text{H}_6$  ratio.

Ratios of  $\text{CH}_4:\text{C}_2\text{H}_6$  and  $\text{CH}_4:\text{C}_3\text{H}_8$  bulk gas chromatograph samples (Fig. 9) indicate  $\text{C}_2\text{H}_6$  to be between 2.5 and 7%, and  $\text{C}_3\text{H}_8$  between 0.5 and 2.26%, respectively. These values, although slightly lower than those indicated from the one inclusion exhibiting critical behaviour, are generally in agreement. In general, the  $\text{CH}_4/\text{C}_2\text{H}_6$  ratio tends to become smaller towards samples exhibiting higher temperatures of homogenization, and in which Raman probe analysis confirmed the presence of ethane, propane and butanes.

Analysis of a sample from a typical footwall quartz-carbonate-actinolite vein containing pure CO<sub>2</sub> inclusions detected only trace amounts of CH<sub>4</sub>, and no higher hydrocarbons. This is in agreement with the zonation of CO<sub>2</sub> inclusions in the footwall veins, and increasing hydrocarbon-bearing fluid inclusions within ore zone.

In addition, 6 graphitic schist samples have been analyzed for hydrocarbon content. In 4 of the samples only minor CH<sub>4</sub> and C<sub>2</sub>H<sub>6</sub> is detected having CH<sub>4</sub>/C<sub>2</sub>H<sub>6</sub> ratios of around 7.6 to 10. Two other samples of highly graphitized schist from shear zones contain larger amounts of CH<sub>4</sub> compared to the lower graphitized samples, together with ethane, propane and the butanes. The CH<sub>4</sub>/C<sub>2</sub>H<sub>6</sub> ratios in these samples are around 6.8 and 13.1.

## Discussion

Detection of light hydrocarbon-bearing fluid inclusions from veins within the Bidjovagge Au-Cu deposit has been accomplished by an integration of microscopic observations and microthermometry, complemented with both Raman microprobe, and gas chromatographic analysis. The recognition of light hydrocarbon-bearing fluid inclusions has obviously important genetic implications for the origin of the fluids.

The origin of higher hydrocarbon-bearing fluid inclusions, from Proterozoic metamorphic terrains, such as the Kautokeino greenstone belt, or within igneous rocks is a matter of controversy. Previous workers describing similar higher hydrocarbon bearing inclusions in metamorphic or igneous terrains have suggested that fluids resulted from *in situ* organic fluids (Kerkhof, 1990), the abiotic production of hydrocarbons (Konnerup-Madsen and Rose-Hansen, 1982), or the secondary penetration of Paleozoic organic-bearing fluids into Proterozoic rocks (Munz et al., 1992).

Light hydrocarbon zonation at Bidjovagge suggest the *in situ* production of hydrocarbons (Fig. 4) rather than a secondary penetration of organic-bearing

Paleozoic fluids. Ettner et al. (1993 & submitted) suggested that hydrocarbon-bearing fluids found at the Bidjovagge Au-Cu deposit formed during fluid reaction with graphitic schist, together with gold and copper mineralization, at about  $1885 \pm 18$  Ma. Ore-bearing fluids composed of oxidizing highly saline  $H_2O + CO_2$ , represented by saline  $H_2O + CO_2$  fluid inclusions in footwall veins (carbonate + quartz + actinolite  $\pm$  magnetite or pyrite), appear to have moved upwards along conduits in the shear zones at Bidjovagge. Temperature and pressure estimates of fluid trapping are between 300 to  $375^\circ C$  and 2 to 4 kbar (Ettner et al., submitted). Where shear zones cut graphitic schist, this fluid reacted with the graphitic schist, resulting in oxidation and albitic alteration of the schist, precipitation of metals, and the production of predominantly methane and other light hydrocarbons. Carbon isotopes analyzed from footwall and ore zone vein carbonates, and also carbonate veins crosscutting graphitic schist support a model of fluid-rock interaction. The  $\delta^{13}C$  values range from  $-0.66$  to  $-1.9\text{‰}$  in the footwall veins to between  $-1.72$  to  $-4.64\text{‰}$  in the mineralized zone to around  $-7\text{‰}$  in carbonate veins crosscutting the graphitic schist (Fig. 10) (Ettner et al., submitted). This trend of values suggest that a complex equilibrium fractionation existed between fluctuating  $CO_2$ - and  $CH_4$ -bearing fluids.

Preliminary results of gas chromatography analysis of unoxidized graphitic schists containing only  $CH_4$  and  $C_2H_6$ , although not conclusive, suggest that the schists were not a reservoir for all the light hydrocarbons found in the ore zone. Graphitic schists that have been highly graphitized along shear zones do contain similar light hydrocarbons as the mineralized zones, suggesting a secondary production of the hydrocarbons.

Hydrocarbons within hydrothermal systems may be produced *in situ* by either reaction with organic material within the wall rocks or by abiotic syntheses.

Production of hydrocarbons at submarine hydrothermal vents observed along sea floor spreading centers (i.e. Michaelis et al, 1990; Peter et al., 1990; Simoneit, 1990; Whiticar and Suess, 1990). Formation of hydrothermal petroleum at these sites occurs as hydrothermal fluids, between  $60^\circ C$  to about  $400^\circ C$  and at hydrostatic

pressure, react with organic material in the sediments (Simoneit, 1990).

Hydrothermal systems within the Guaymas Basin produce both the light hydrocarbons (C<sub>1</sub>-C<sub>12</sub>) and the C<sub>12+</sub> range (C<sub>12</sub>-C<sub>40+</sub>) which tend to migrate rapidly away from the higher temperature zones (Simoneit, 1990) but liquid light hydrocarbon are observed as inclusions within amorphous silica with trapping temperatures between 116 to 226°C (Peter et al., 1990).

Abiotic production of light hydrocarbons has been suggested for the formation of C<sub>1</sub> to C<sub>5</sub> observed in the alkaline Ilímaussaq intrusion, of South Greenland, where there is no nearby carbonaceous country rock (Konnerup-Madsen et al., 1979). Conditions for light hydrocarbons formation in the Ilímaussaq intrusion are suggested to be low fO<sub>2</sub> and a wide range of temperatures between 800 and 450°C as the magma crystallized (Konnerup-Madsen et al., 1979; Konnerup-Madsen and Rose-Hansen, 1982).

The commercial abiotic production of hydrocarbons by gasification of coal followed by the Fischer-Tropsch syntheses by catalytic hydrogenation of carbon monoxide at high temperatures and pressures (Schulz, 1980), may have significant applications to geologic problems such as Bidjovagge. Under industrial conditions, gasification of coal by reaction with steam produces CH<sub>4</sub> by the reactions



at high temperatures and elevated pressures (Goeke and Wetzel, 1980). The Fischer-Tropsch reaction CH<sub>2</sub> chain propagation occurs by the insertion of CO and H<sub>2</sub> in the presence of an active metal catalyst at temperatures up to 370°C (Schulz, 1980).

Production of hydrocarbons at Bidjovagge may have occurred either by catalyzed reaction with the graphitic schist or by reaction with organic matter in the schist, although the survival of organic material within the schist under upper greenschist facies condition would seem unlikely. Either of these processes may have resulted in the hydrocarbon zonation within the mineralized oxidation. If higher

hydrocarbons ( $C_{4+}$ ) were produced by fluid-rock interaction at Bidjovagge, preservation of only the lighter hydrocarbons was successful within the fluid inclusions. Amorphous carbon coatings on the walls of the fluid inclusions, as shown by Raman microprobe analysis, may indicate that cracking of higher hydrocarbons occurred. Carbon isotope analysis of the hydrocarbon inclusions would help to determine which process was significant.

## Conclusion

This comparison of microthermometric, Raman microprobe, and gas chromatographic analysis of fluid inclusions from the Bidjovagge Au-Cu deposit has detected the presence of methane, ethane, propane and butane within the ore zone. The recognition of higher hydrocarbons in  $CH_4$ -rich fluid inclusions by microthermometric or Raman microprobe analysis may be dependent on the types of hydrocarbons present or their ratios. Detailed microscopic and microthermometry analysis accompanied by Raman microprobe and gas chromatography is necessary for the complete identification of hydrocarbons present. The knowledge of the presence additional hydrocarbons in  $CH_4$  inclusions is important for calculation of molar volume and isochore calculations, or the validity of previous published calculations.

The origin of higher hydrocarbons in Proterozoic metamorphic terrains, such as the Kautokeino greenstone belt, is problematic. Hydrocarbon-bearing fluid inclusions from the Bidjovagge deposit appear to have been trapped at elevated temperatures and pressures of 300 to 375°C and 2 to 4 kbars within the mineralized oxidation zone to graphitic schists. Zonation of light hydrocarbons suggest that the hydrocarbons were formed at the site of mineralization rather than by infiltrating Paleozoic organic-rich fluids. Organic production of hydrocarbons fluids at these temperatures seems unlikely, as would trapping of primary organic hydrocarbons. Syntheses of light hydrocarbon by fluid interaction with organic material in the schists or an abiotic catalyzed hydrogenation reaction (Fischer-Tropsch reaction) between the fluids and the graphitic schist may have produced the light hydrocarbon

zonation observed at the Bidjovagge deposit. Evidence for fluid-rock interaction include a mineralized oxidation zone at the graphitic schist, mineralogic zonation (i.e. magnetite - pyrite - pyrrhotite zonation), together with fluid inclusion and carbon isotope zonation.

Hydrocarbon generation and the interaction with graphitic schist appears to be important for mineralization at the Bidjovagge deposit. Gold transported as chloride complexes within the fluids would become unstable by lowering the  $fO_2$  (Henley, 1973) accompanied by increased pH during phase separation of  $CO_2$  and would result in gold precipitation.

*Acknowledgements.* Thanks is given to Arne Bjørlykke and Tom Andersen for their helpful advice and help during this project. We also thank Bidjovagge Gruver A/S and Outokumpu Oy for partial support of this project, and permission to publish these results. The first author also gratefully acknowledges financial support from NTNF (Royal Norwegian Research Council for Scientific and Industrial Research), project number BF-25469. The first author is also thankful to Dr. Don Sangster from the Geological Survey of Canada, Dr. Detlef Leythaeuser at the University of Köln, and Prof. Steve Larter from University of Newcastle for their early discussions and critique.

## References Cited

- Andersen, T., Austrheim, H., and Burke, E.A.J. (1991) Mineral-fluid-melt interactions in high-pressure shear zones in the Bergen Arcs nappe complex, Caledonides of W. Norway: Implications for the fluid regime in Caledonian eclogite-facies metamorphism. *Lithos* 27: 187-204
- Bjørlykke A., Cumming, G.L., and Krstic, D. (1990) New isotopic data from davidites and sulfides in the Bidjovagge gold-copper deposit, Finnmark, northern Norway. *Mineral. Petrol.* 43: 1-12
- Bjørlykke, A., Hagen, R., and Söderholm, K. (1987) Bidjovagge Copper-Gold Deposit in Finnmark, Northern Norway. *Econ. Geol.* 82: 2059-2075

Bjørlykke, A., Nilsen, K.S., Anttonen, R., and Ekberg, M. (1993) Geological Setting of the Bidjovagge deposit and related gold-copper deposits in the northern part of the Baltic Shield.

Burke, E.A.J. & Lustenhouwer, W.J. 1987: The application of a multichannel laser Raman microprobe Microdil-28: to the analysis of fluid inclusions. *Chemical Geology* 61, 11-17.

Burruss, R.C. (1981) Analysis of phase equilibria in C-O-H-S fluid inclusions. Mineral. Assoc. Canada Short Course Handbook 6: 39-74

Cumming, G.L., Krstic, D., Bjørlykke, A. & Åsen, H. (in prep.): Further analysis of radiogenic minerals from the Bidjovagge gold-copper deposit, Finnmark, northern Norway.

Dubessy, J., Poty, B., and Ramboz, C. (1989) Advances in C-O-H-N-S fluid geochemistry based on micro-Raman spectrometric analysis of fluid inclusions. *European Jour. Mineral.* 1: 517-534

Ettner, D.C., Bjørlykke, A., & Andersen, T., submitted. Fluid composition of Proterozoic gold and copper deposits: An example from the Bidjovagge gold-copper deposit, Finnmark, northern Norway.

Ettner, D.C., Bjørlykke, A., & Andersen, T. 1993: The production of hydrocarbons and precipitation of gold during fluid-rock interaction: A fluid inclusion and stable isotope study of the Bidjovagge gold-copper deposit, Finnmark, northern Norway. *Geofluids* 1993, Torquay, England (extended abstracts) pp. 455-458.

Goeke, E.K. and Wetzell, R.E. (1980) Synthesis gas technology. In: St-Pierre, L.E. and Brown, G.R. eds. *Future sources of organic raw materials - CHEMRAWN I*. Pergamon, Oxford, pp. 155-166.

Henley, R.W. 1973: Solubility of gold in hydrothermal chloride solutions. *Chemical Geology* 11, 73-87.

Hollander, N.B. (1979) The geology of the Bidjovagge mining field, western Finnmark, Norway. *Norsk Geol. Tidsskr.* 59: 327-336

Hollister, L.S., and Burruss, R.C. (1976) Phase equilibria in fluid inclusions from the Khtada metamorphic complex. *Geochim. Cosmochim. Acta* 40: 163-175

Holmsen, P., Padget, P. & Pehkonen, E. 1957: The Precambrian geology of Vest-Finnmark, northern Norway. *Norges geologiske undersøkelse* 210, 107 pp.

Kerkhof, A.M. Van Den (1987) The fluid evolution of the Harmsarvet ore deposit, central Sweden. *Geologiska Föreningens i Stockholm Förhandlingar* 109, 1-12.

Kerkhof, A.M. Van Den 1990: Isochoric phase diagrams in the systems CO<sub>2</sub>-CH<sub>4</sub> and CO<sub>2</sub>-CH<sub>4</sub> : Application to fluid inclusions. *Geochimica et Cosmochimica Acta* 54, 621-629.

Kerkhof, A.M. Van Den (1991) Heterogeneous fluids in high-grade siliceous marbles of Pusula (SW Finland). *Geologische Rundschau* 80: 249-258

Konnerup-Madsen, J., Larsen, E. and Rose-Hansen, J., 1979. Hydrocarbon-rich fluid inclusions in minerals from the alkaline Ilímaussaq intrusion, South Greenland. *Bull. Minéral.*, 102: 642-653.

- Konnerup-Madsen, J. and Rose-Hansen, J., 1982. Volatiles associated with alkaline igneous rift activity: Fluid inclusions in the Ilímaussaq intrusion and the Gardar granitic complexes (South Greenland). *Chem. Geol.*, 37: 79-93.
- Kreulen, R., & Schuiling, R.D. 1982: N<sub>2</sub>-CH<sub>4</sub>-CO<sub>2</sub> fluids during formation of the Dôme de l'Agout, France. *Geochimica et Cosmochimica Acta* 46, 193-203.
- Krill, A.G., Kesola, R., Sjöstrand, T. & Stephens, M.B. 1988: Metamorphic, structural and isotopic age map, northern Fennoscandia 1:1,000,000. *Geological Surveys of Finland, Norway and Sweden*.
- Lespade, P., Al-Jishi, R. and Dresselhaus, M.S. 1982: Model for Raman scattering from incompletely graphitized carbons. *Carbon*, 20: 427-431.
- Lindblom, S. & Burke, E. (1988) Raman spectrometry and microthermometry data on CO<sub>2</sub>-CH<sub>4</sub> bearing fluid inclusions in late-orogenic quartz from the Saxberget Zn-Pb-Cu-Ag deposit, Central Sweden. *Geologie en Mijnbouw* 67: 471-476
- Michaelis, W., Jenisch, A. and Richnow, H.H. (1990) Hydrothermal petroleum generation in Red Sea sediments from the Kebrit and Shaban Deeps. *Appl. Geochem.* 5: 103-114.
- Mullis, J. (1979) The system methane-water as a geological thermometer and barometer from the external part of the Central Alps. *Bull. Minéral.* 102: 526-536.
- Mullis, J. (1987) Fluid inclusion studies during very low-grade metamorphism. In: Frey, M. (ed.) *Low temperature metamorphism*: Glasgow, Blackie, pp. 162-199.
- Munz, I.A., Yardley, B.W.D., Banks, D.A. & Wayne, D. (in prep.) Origin of albitite veins in basement rocks in south Norway: II. Evidence from aqueous brines and hydrocarbons in fluid inclusions
- Nilsen, K.S., & Bjørlykke, A. 1991: Geological setting of the Bidjovagge gold-copper deposit, Finnmark, northern Norway. *Geologiska Föreningens i Stockholm Förhandlingar* 113, 60-61.
- Olds, R.H. 1953: Critical behavior of hydrocarbons. In: Farkas, A. (ed.) *Physical Chemistry of the Hydrocarbons*, Acad. Press, New York, pp. 131-152.
- Olesen, O., Henkel, H. & Lile, O.B. 1991: Major fault zones within the Precambrian Kautokeino Greenstone Belt, Finnmark, Norway: combined interpretation of geophysical data. *Norges geologiske undersøkelse Unpublished Report* 90.161, 26 pp.
- Peter, J.M., Simoneit, B.R.T., Kawka, O.E., and Scott, S.D. (1990) Liquid hydrocarbon-bearing inclusions in modern hydrothermal chimneys and mounds from the southern trough of Guaymas Basin, Gulf of California. *Appl. Geochem.* 5: 51-63
- Pharaoh, T.C. & Brewer, T.S. 1990: Spatial and temporal diversity of early Proterozoic volcanic sequences - comparisons between the Baltic and Laurentian shields. *Precambrian Research* 47, 169-189.
- Ramsay, D.M., Sturt, B.A., Zwann, K.B. & Roberts, D. 1985: Caledonides of northern Norway. In Gee, D.G. & Sturt, B.A. (eds.): *The Caledonide Orogen - Scandinavia and related areas*, 163-184. John Wiley, & Sons, Chichester.
- Sandstad, J.S. (1983) Berggrunnsgeologisk kartlegging av prekambrisk grunnfjell innen kartbladet Mållejus, Kvænangen/Kautokeino, Troms/Finnmark: *Norges Geol. Unders. Unpub. report.* 84.095: 73-76

Sandstad, J.S. 1985: Mållejus 1833 4 geologisk berggrunnskart 1:50000. *Norges geologiske undersøkelse*.

Sandstad, J.S. 1992: Kautokeinogrønnsteinsbeltet - Berggrunnskart 1:100,000. *Norges geologiske undersøkelse*.

Schulz, H. 1980: Chemicals, feedstocks and fuels from Fischer-Tropsch and related syntheses. In: St-Pierre, L.E. and Brown, G.R. eds. Future sources of organic raw materials - CHEMRAWN I. Pergamon, Oxford, pp. 167-183.

Siedlecka, A., Iversen, I., Krill, A.G., Lieungh, B., Often, M., Sandstad, J.S., and Solli, A. (1985) Lithostratigraphy and correlation of the Archean and Early Proterozoic rocks of Finnmarksvidda and the Sørvaranger district. *Norges Geol. Unders.* 403: 7-36

Simoneit, B.R.T. (1990) Petroleum generation, and easy and widespread process in hydrothermal systems: an overview. *Appl. Geochem.* 5: 3-15

Skiöld, T. 1988: Implications of new U-Pb zircon chronology to early Proterozoic crustal accretion in northern Sweden. *Precambrian Research* 8, 147-164.

Whiticar, M.J. and Suess, E. (1990) Hydrothermal hydrocarbon gases in the sediments of the King George Basin, Bransfield Strait, Antarctica. *Appl. Geochem.* 5: 135-147.

#### List of Figures:

**Figure 1:** Generalized geologic map of Finnmark plateau, with the Kautokeino Greenstone belt, emphasizing metamorphic grade after Sandstad (1992) and Krill et al. (1988), showing the location of the Bidjovagge deposit.

**Figure 2:** Geologic map of the Bidjovagge antiform with location of individual ore lenses along shear zones on the eastern limb of the antiform. Modified from Nilsen and Bjørlykke (1991).

**Figure 3:** Drill core sample of graphitic schist displaying oxidation halos around veins. Scales bar: 5 cm.

**Figure 4:** Schematic geologic block diagram of a Bidjovagge deposit with the general location of CO<sub>2</sub> + H<sub>2</sub>O vs. CH<sub>4</sub> + LHC fluid inclusions. Gold mineralization is marked by "Au" where the graphitic schist is truncated by an oxidation zone.

**Figure 5:** Photomicrographs of fluid inclusions. a.) Sample BC91-249 with rectangular area marked showing location of photomicrograph b. b.) Composite photomicrograph of light hydrocarbon fluid inclusions at different focal depths, with microthermometric data for selected inclusions. c.) Sample BC91-51 with rectangular area marked showing location of photomicrograph d. d.) Composite photomicrograph of light hydrocarbon fluid inclusions at different focal depths, with microthermometric data for fluid inclusions #A20 which displays critical homogenization behaviour. Scale bar for a and c = 0.25mm; for b and d = 0.05mm.

**Figure 6:** Microthermometric melting and sublimation temperatures (below base line) and homogenization temperatures (above base line) for measured carbonic fluid inclusions. Homogenization to a carbonic liquid occurs in all inclusions.

**Figure 7:** Raman microprobe spectra of selected hydrocarbon-bearing fluid inclusions. For each fluid inclusion, the temperature of homogenization and critical homogenization is indicated.

**Figure 8:** Characteristic amorphous carbon Raman microprobe spectra from a hydrocarbon liquid inclusion at Bidjovagge.

**Figure 9:** Gas chromatographs of bulk gas analysis from separated vein quartz samples. A.) Vein quartz bearing fluid inclusions which display temperatures of homogenization between -102 and -82.1°C. A.) Vein carbonate from veins bearing fluid inclusions which display temperatures of homogenization between -61.5 and -42.1°C.

**Figure 10:** Carbon and oxygen isotope compositions of carbonates from different lithologies, ore zones and veins from the "H" deposit at Bidjovagge (from Ettner et al., submitted).

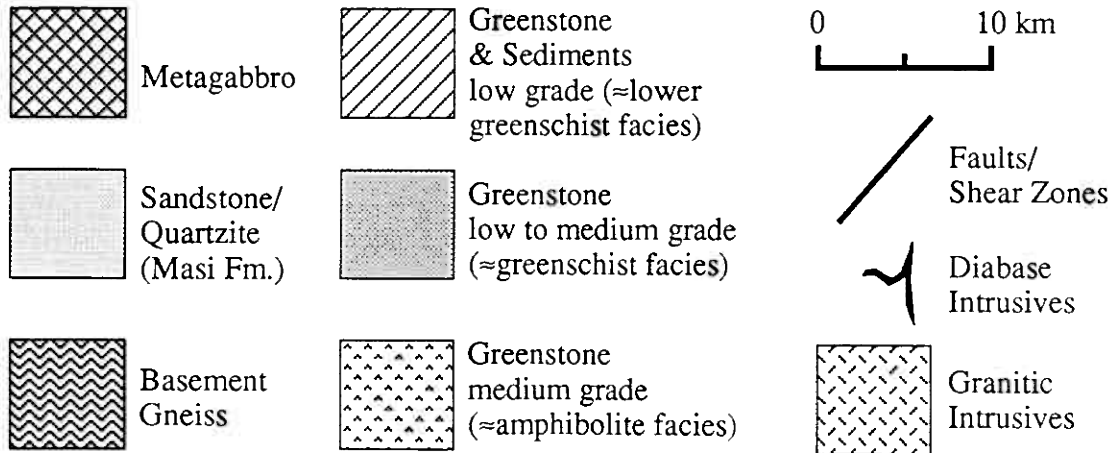
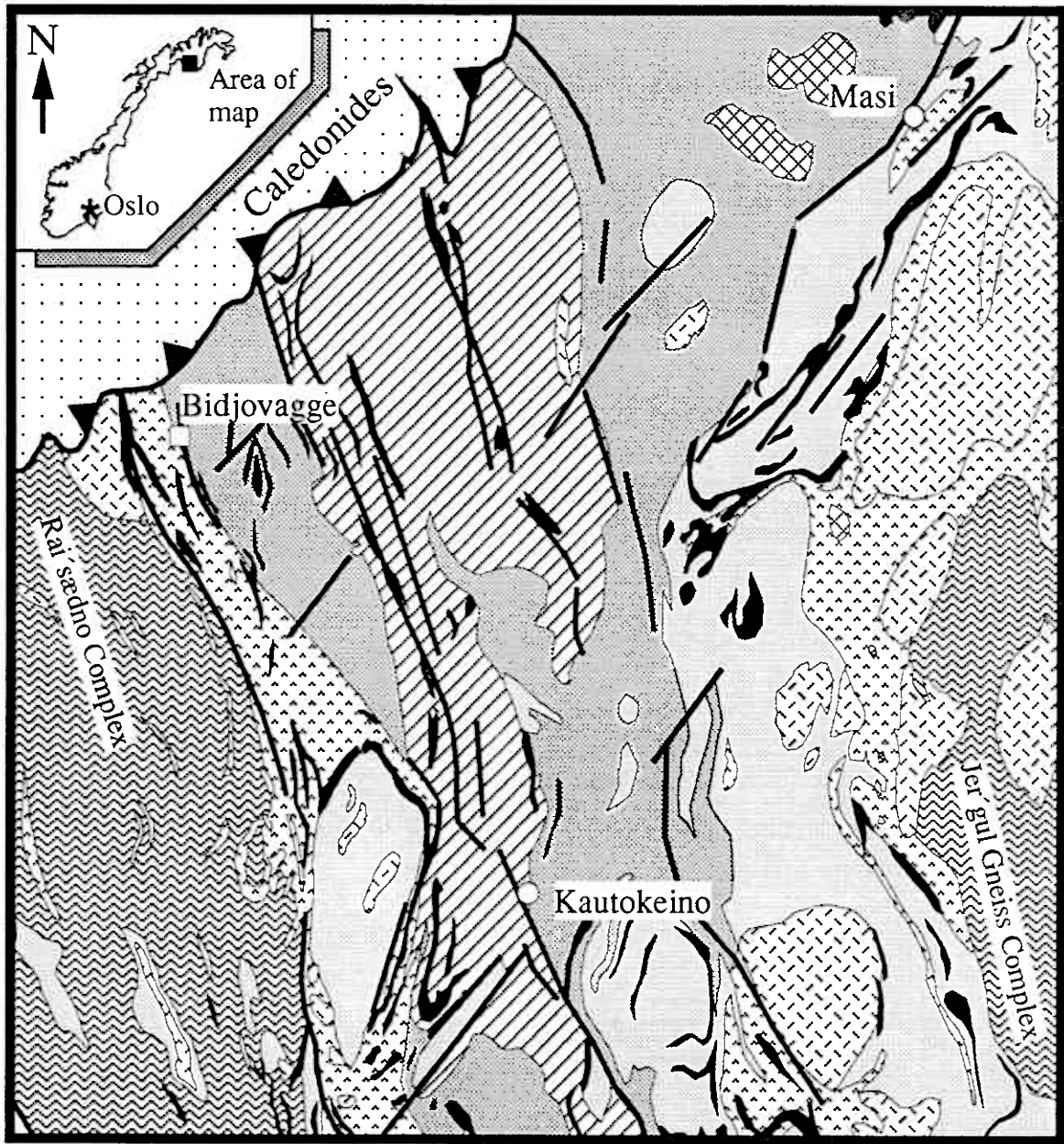


Figure 1

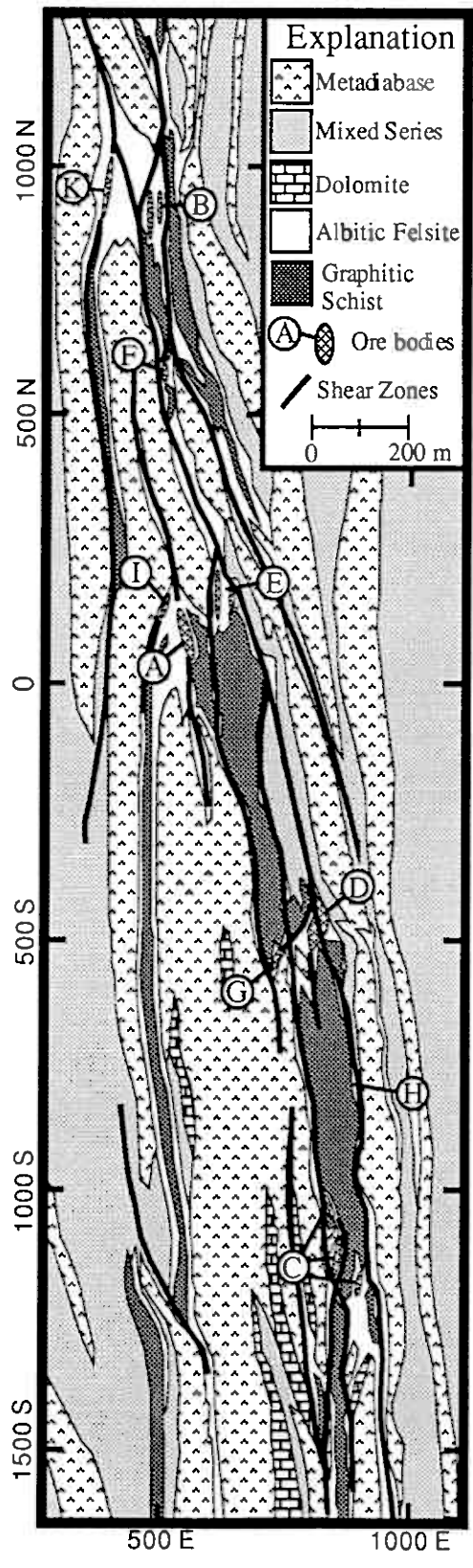


Figure 2



Figure 3

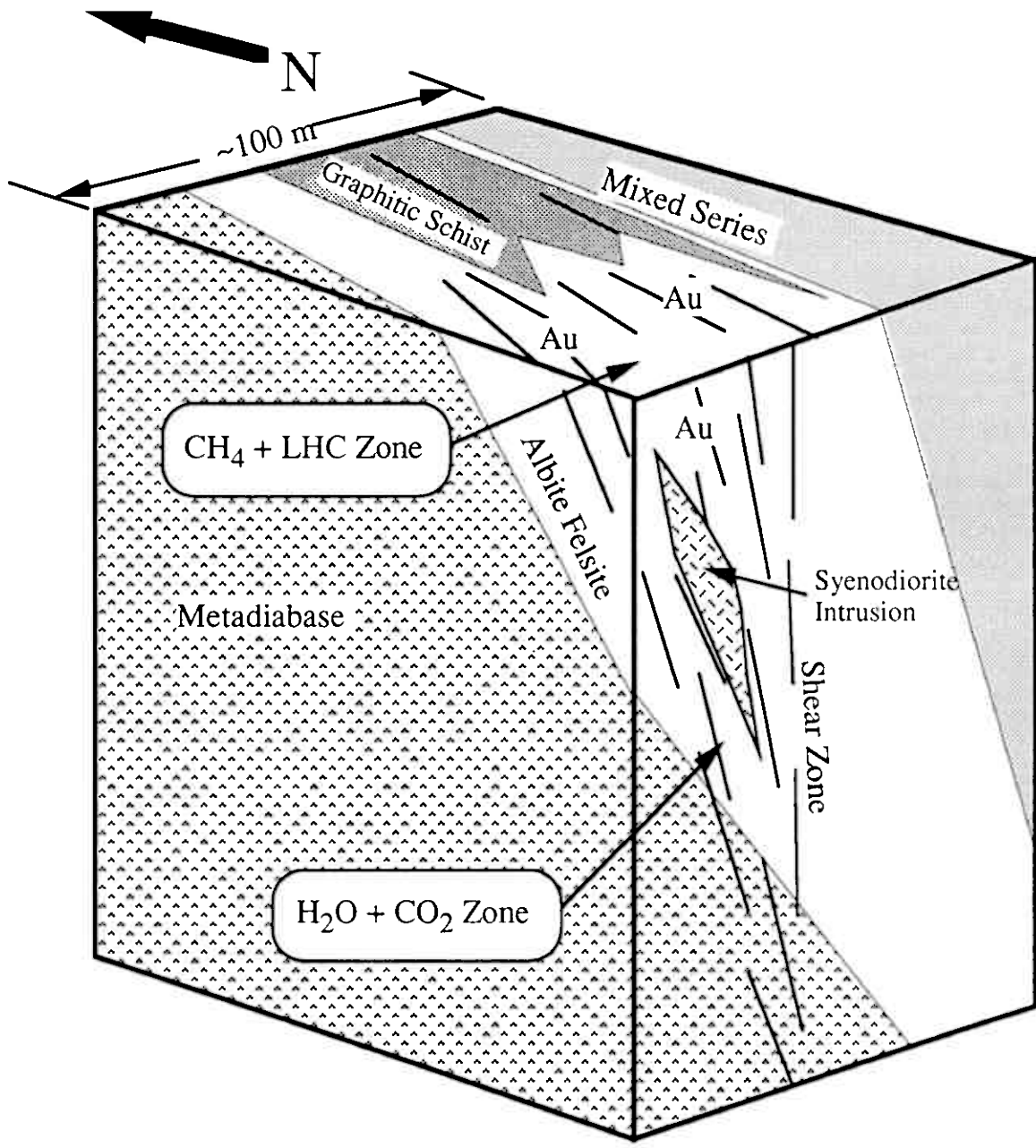
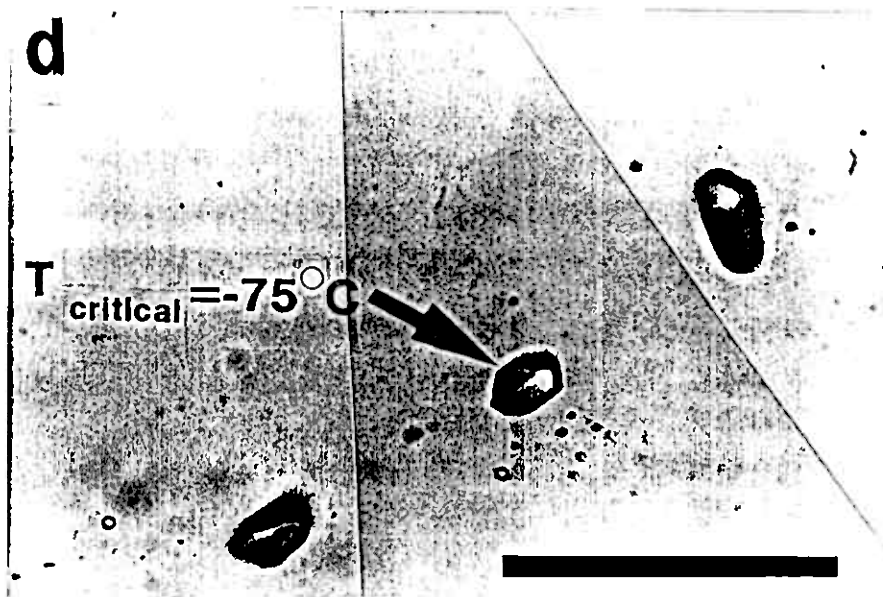
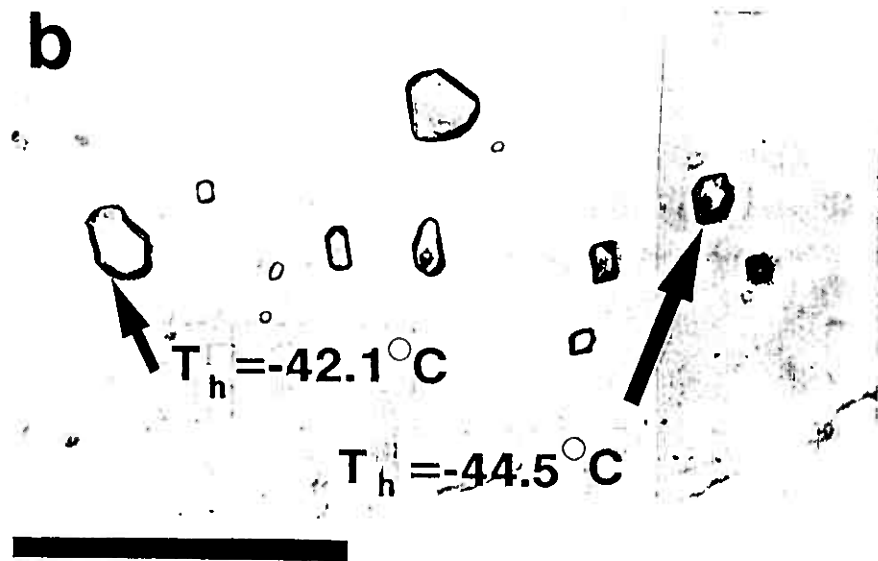
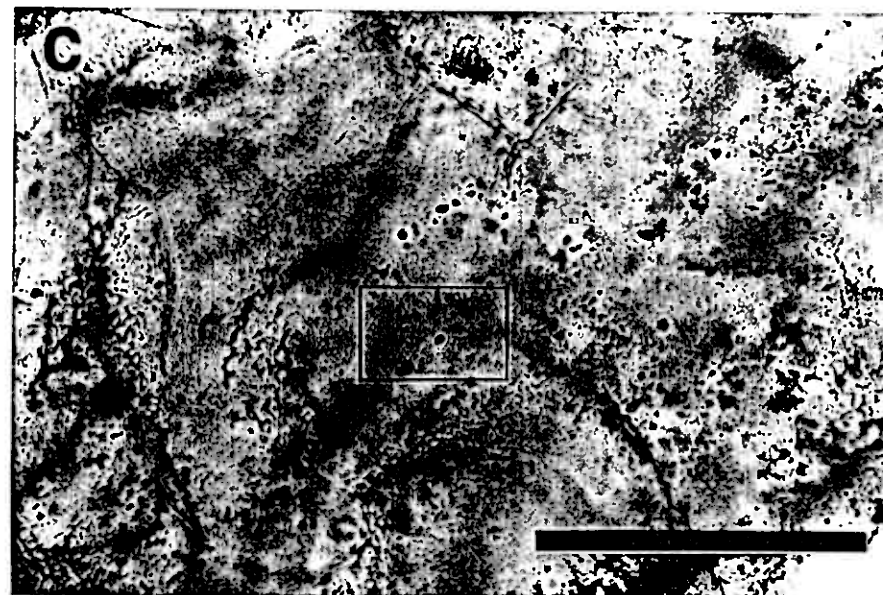
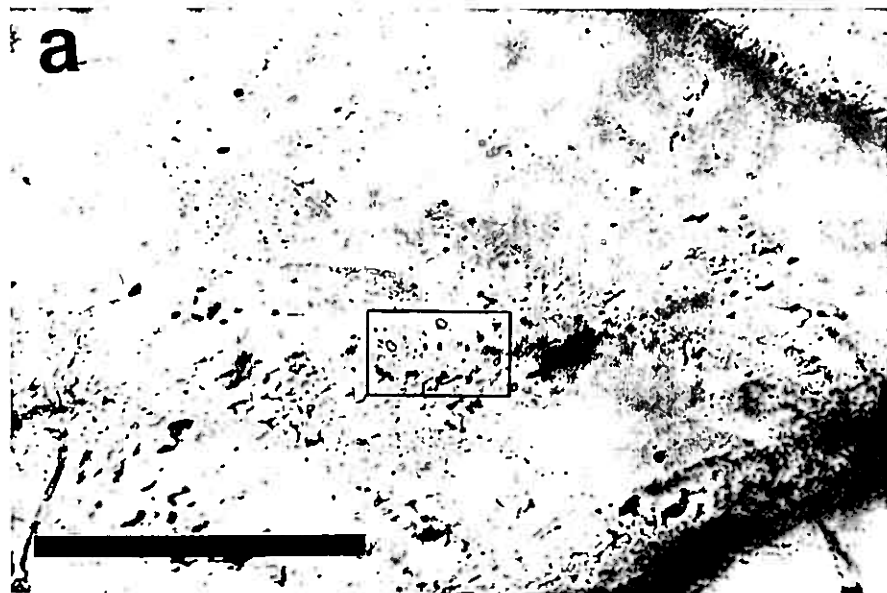


Figure 4



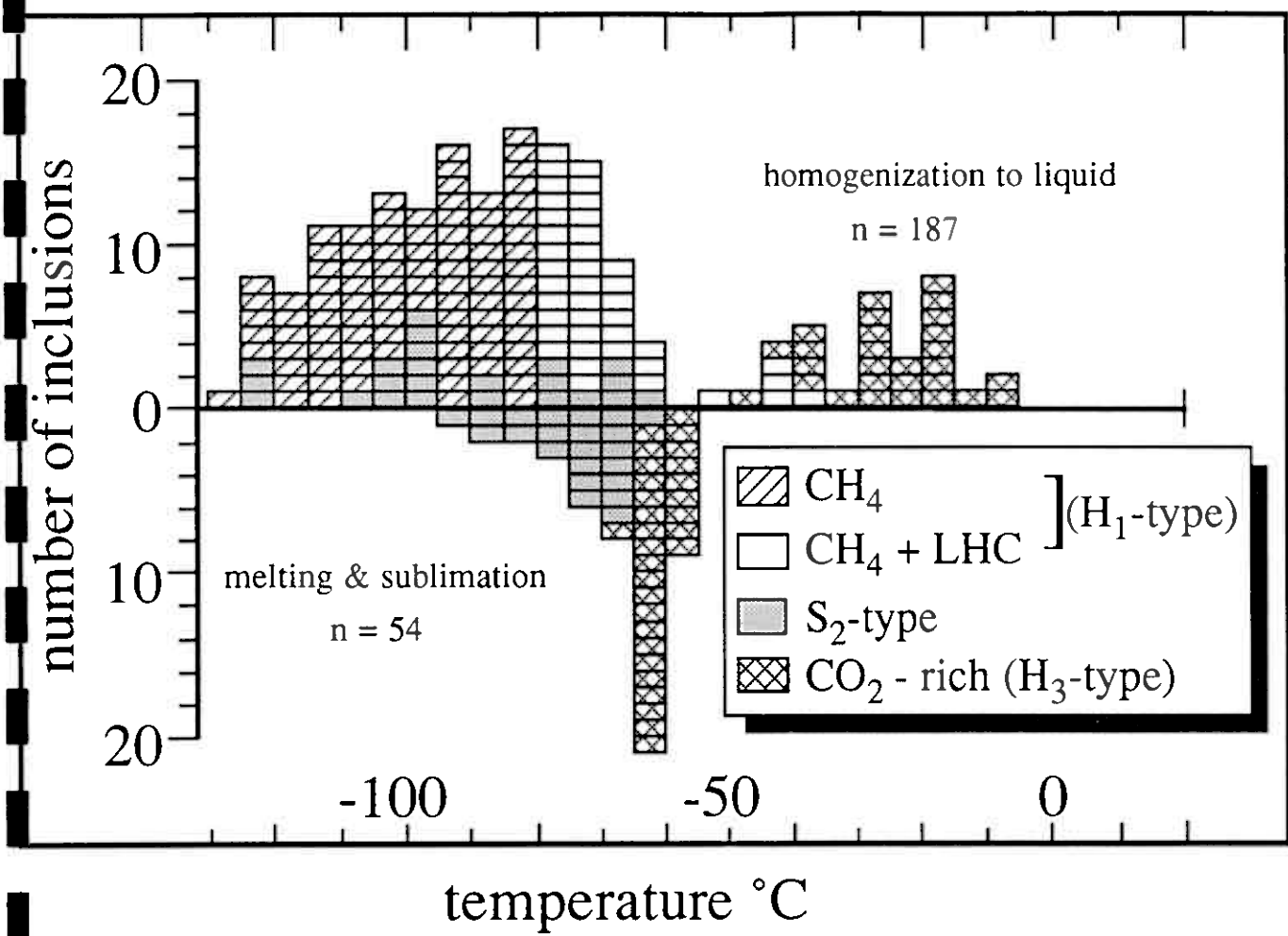


Figure 6

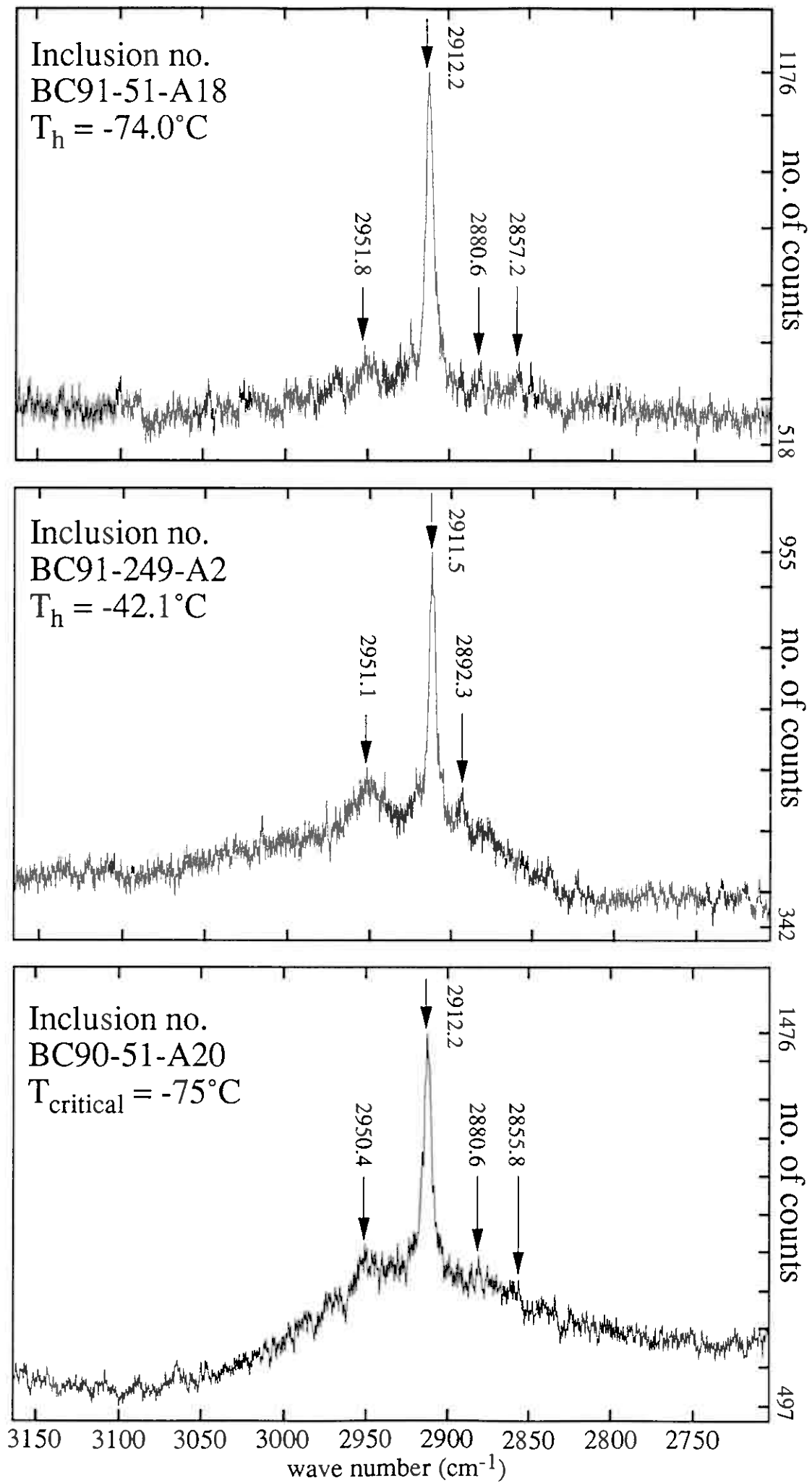


Figure 7

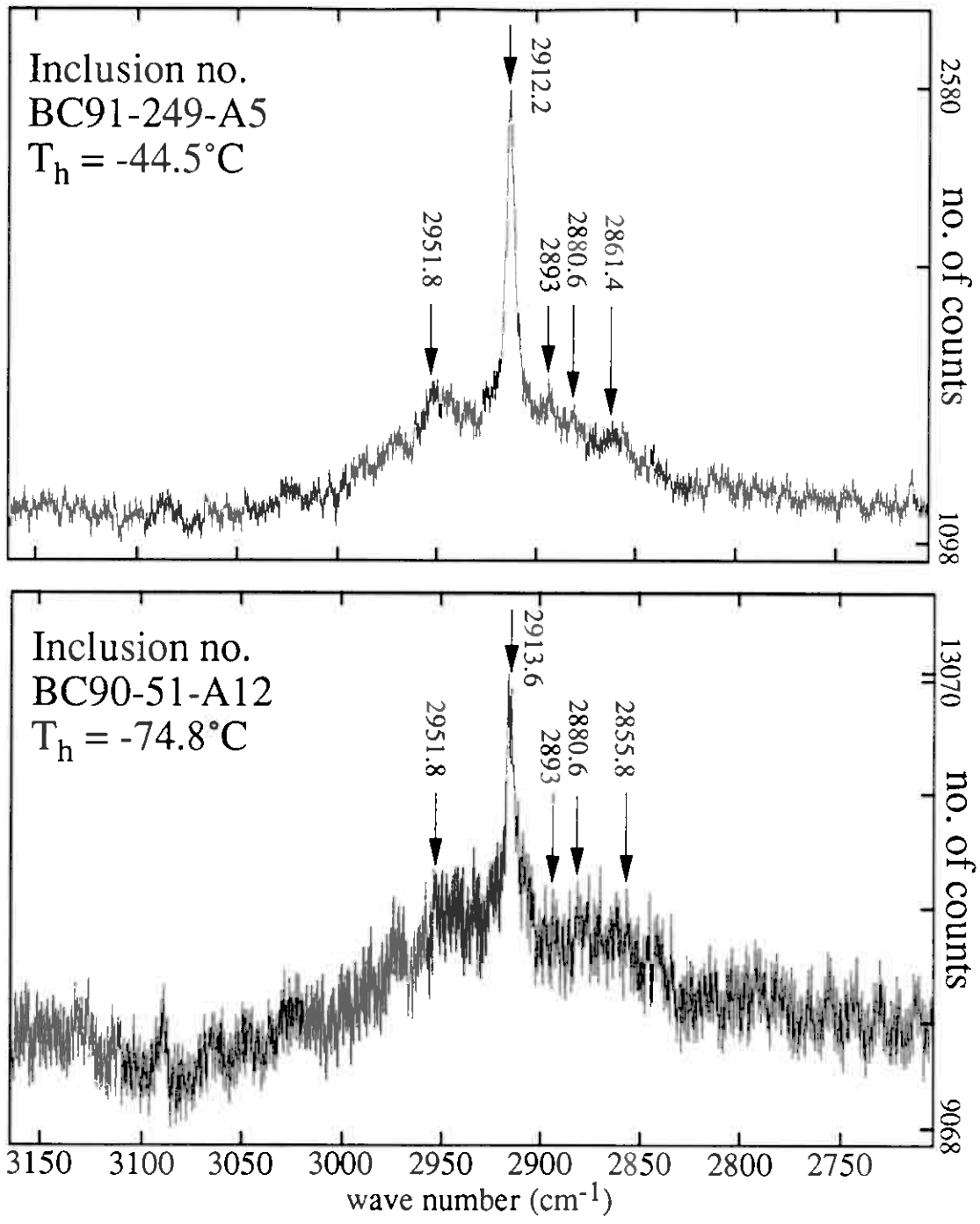


Figure 7

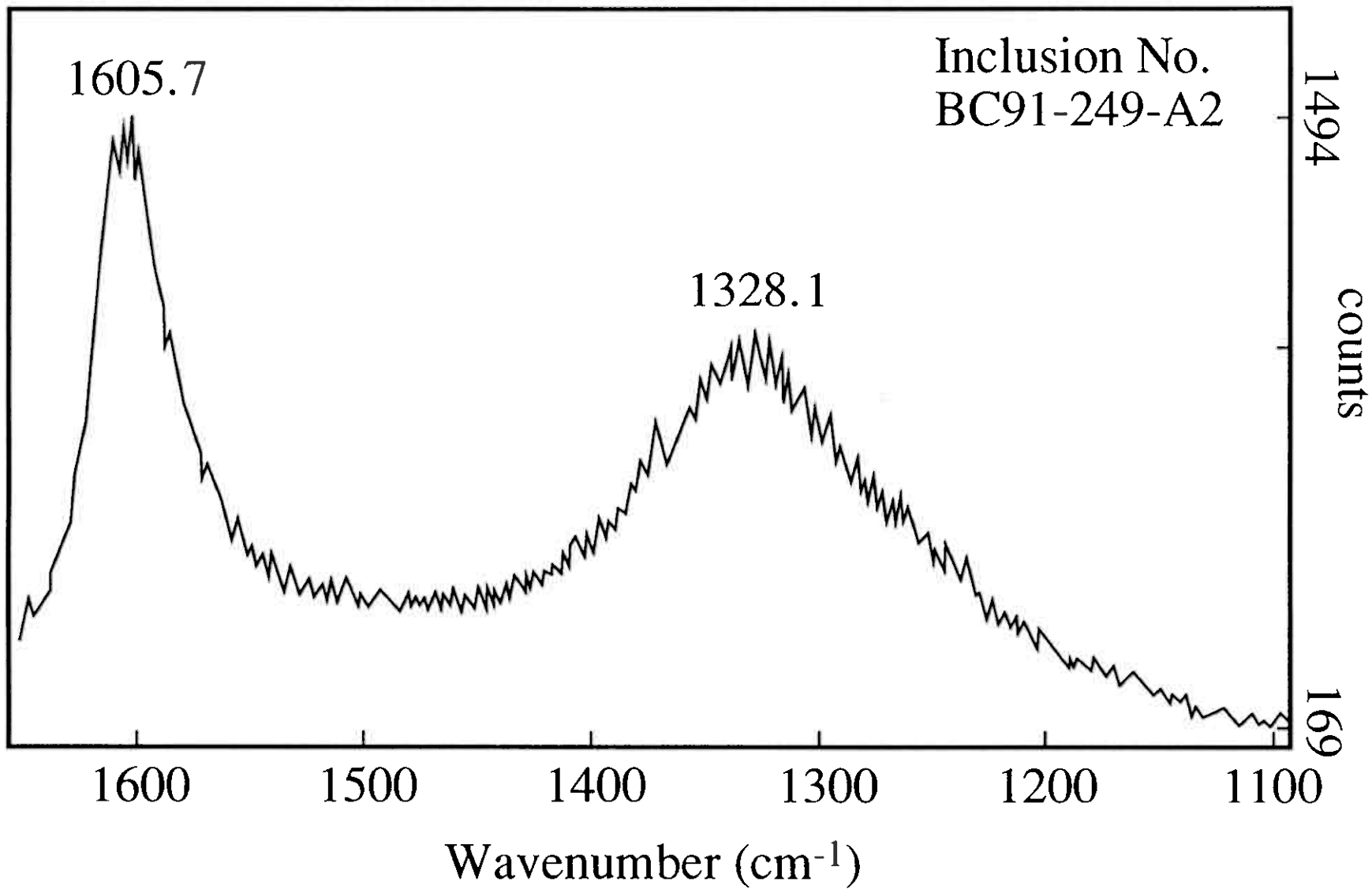


Figure 8

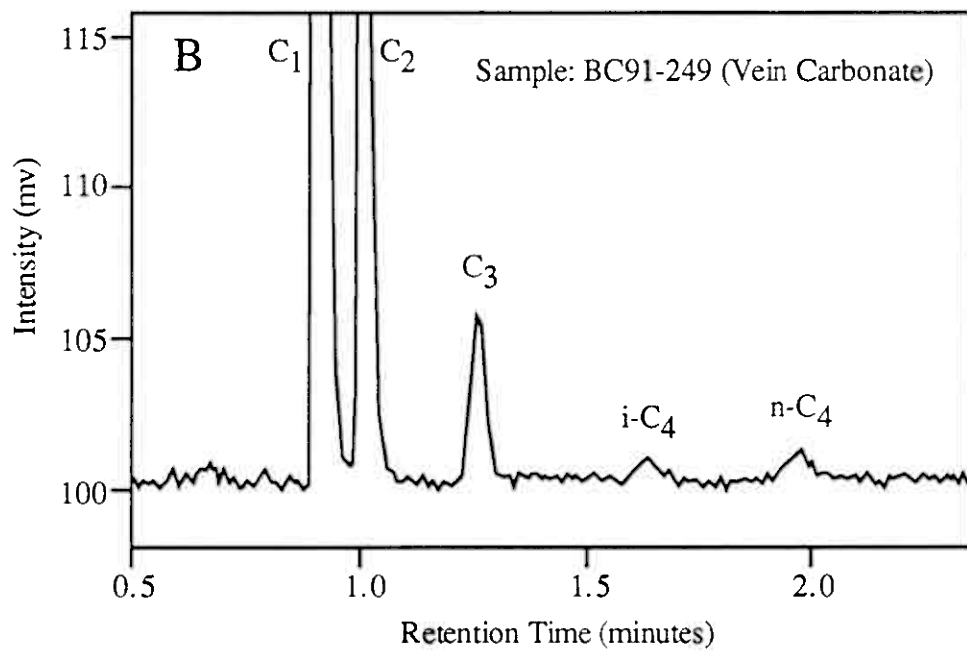
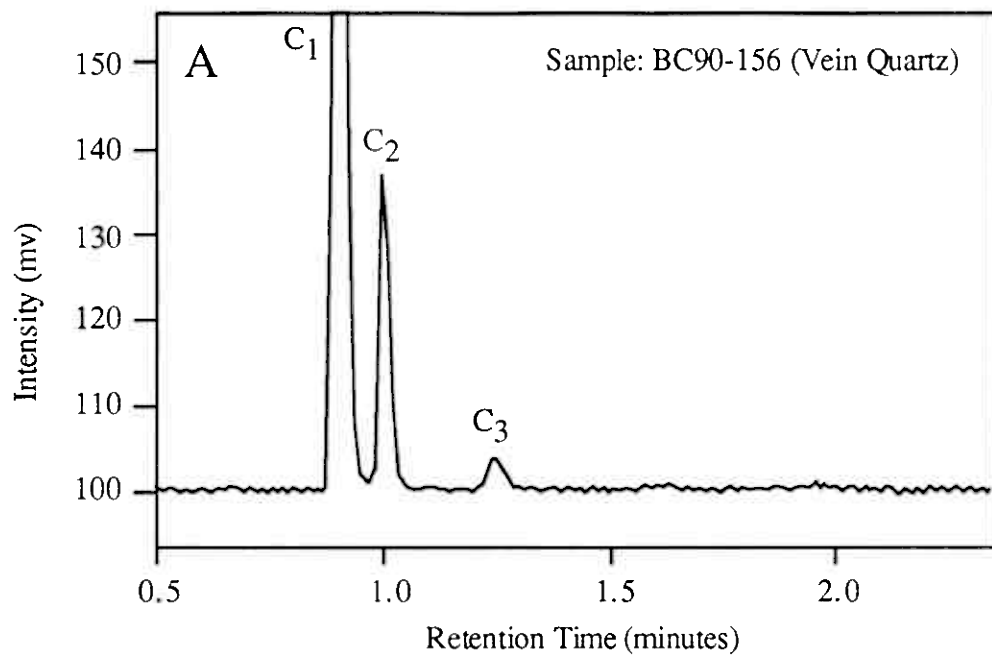


Figure 9

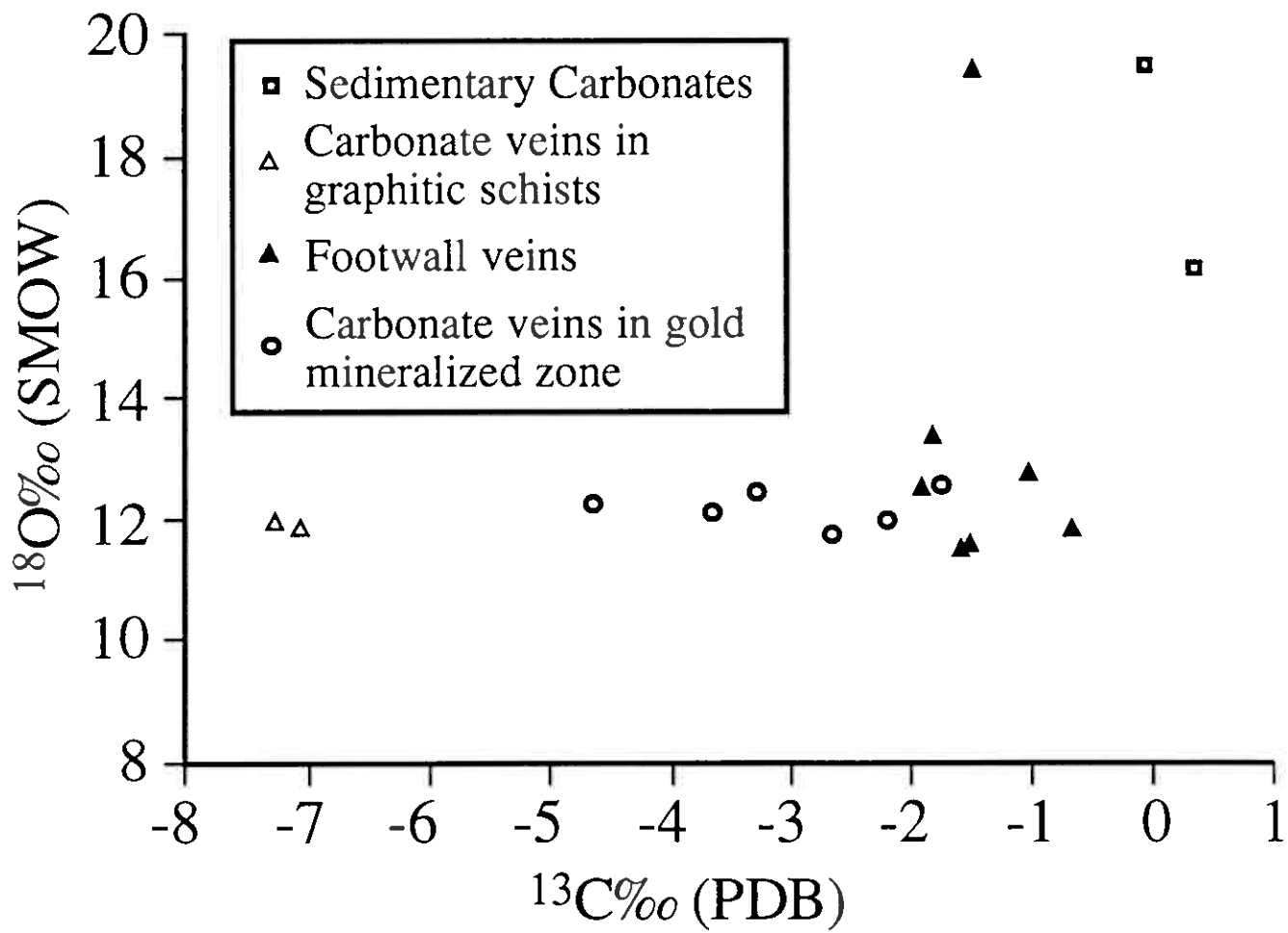


Figure 10

# PAPER IV

Version: 18.6.93

## Fluid Geochemistry of the Bidjovagge Gold-Copper Deposit, Norway: An example of a Proterozoic Greenstone belt- hosted Mesothermal Gold-Base Metal Deposit

DAVID C. ETTNER, ARNE BJØRLYKKE

*Institute for Geology, University of Oslo, N-0316 Oslo, Norway*

TOM ANDERSEN

*Mineralogical-Geological Museum, University of Oslo, N-0562 Oslo, Norway*

### **Abstract**

The Bidjovagge Au-Cu deposit in northern Norway, hosted within a shear zone in the Early Proterozoic Kautokeino greenstone belt differs from Archean mesothermal gold deposits because of high base metal to gold ratios. A study of the fluid evolution and mineralization by means of fluid inclusion microthermometry, Raman microprobe spectrometry, gas chromatography, and stable isotope geochemistry has been conducted in order to determine the mechanism of transport and precipitation of both base metals and gold in a mesothermal system.

The Bidjovagge area comprises a series of metasedimentary carbonates and tuffites, graphitic schists, metasomatic albite felsite, and diabase sills that are folded in a large upright isoclinal antiform which is cut along the eastern limb by a shear zone. Two phases of mineralization are recognized at Bidjovagge, an earlier Au-rich phase within ductile to brittle shear structures, followed by a Cu-rich phase within brittle structures. A series of syenodiorite intrusions are spatially related with mineralization and appear to crosscut structures hosting gold mineralization, but are crosscut by brittle structures related to copper mineralization.

Alteration related to the mineralization includes albitization, carbonatization, scapolitization, and minor biotitization, amphibolitization, and chloritization. Mineralization occurs within red-ox front to the graphitic schists especially where dilational structures in the shear zone have cut across the graphitic schists. From the footwall of the deposit up towards the ore zone a zonation from magnetite + pyrite, to pyrite, to pyrite + pyrrhotite is observed.

Fluid inclusion compositions show a zonation within the deposit related to Au-rich mineralization. Within the deeper parts of the footwall veins fluid inclusion are dominated by H<sub>2</sub>O + CO<sub>2</sub> + salt, having salinities between 27 and 43 wt. %, NaCl equiv., dominated by NaCl and CaCl<sub>2</sub>. Fluid inclusion assemblages within the highly sheared albite felsite closer to the ore zone comprise both single phase liquid CO<sub>2</sub> inclusions or H<sub>2</sub>O + salt inclusions. Compositions of fluid inclusions in the ore zones are dominated by liquid CH<sub>4</sub> and other light hydrocarbons.

Fluid inclusions related to Cu-rich mineralization and syenodiorite intrusions comprise lower salinity aqueous solutions, up to 25 wt. % NaCl equiv., dominated by NaCl and CaCl<sub>2</sub>. Some inclusions within veins crosscutting syenodiorite intrusions also contain CH<sub>4</sub>.

Carbon isotopic analysis of vein carbonates related to Au-rich mineralization from Bidjovagge show a zonation of  $\delta^{13}\text{C}$  values from -0.44 to -1.9‰ in footwall veins, -1.72 to -4.64‰ through the ore zone, and -7.04 to -7.25‰ in the graphitic schist. Carbonate veins related to Cu-rich mineralization also show a range in  $\delta^{13}\text{C}$  values between -2.73 to -5.5‰. A wide variation of  $\delta^{34}\text{S}$  is shown with chalcopyrite generally between 1.6 to 2.0‰, pyrite with 1.9 to -3.0‰, and pyrrhotite with values around -2.7 to -3.9‰.

The high salinity H<sub>2</sub>O + CO<sub>2</sub> fluids, as represented in the footwall, are interpreted to have transported both Au and Cu as chloride complexes at temperatures between 300 to 375°C and at pressures between 2 to 4 kbars. As the supercritical H<sub>2</sub>O + CO<sub>2</sub> + salt fluids moved upwards into the highly sheared albite felsite the drop in pressure caused phase separation resulting in an increase pH. Interaction of the fluid with graphitic schist resulted in alteration and oxidation of the graphitic schist, synthesis of light hydrocarbons, mag-py-po zonation, and trends in  $\delta^{13}\text{C}$  values. The reduced  $f\text{O}_2$  of the fluid, combined with increased pH resulted in precipitation of metals from chloride complexes.

The Bidjovagge deposit together with other Proterozoic mesothermal gold-base metal deposits display similar high salinity fluids and occur in continental rift settings associated with felsic magmatism.

## Introduction

Proterozoic mesothermal gold-base metal deposits include the Bidjovagge (Bjørlykke et al., 1987), Pahtohavare (Martinsson, 1992), and Saattopora (Nurmi et al., 1991) deposits in the Fennoscandavian Shield, and the Telfer (Goellnicht et al., 1989) and Tennant Creek (Nguyen et al., 1989; Wedekind et al., 1989) deposits in Australia. Archean mesothermal gold deposits and their Proterozoic gold-base metal equivalents occur in similar structural settings in greenstone belts within Precambrian cratonic shields but have substantial differences in the base metal to gold ratios (e.g. Card et al., 1989; Goellnicht et al., 1989; Nguyen et al., 1989; Groves and Foster, 1991; Bjørlykke et al., 1993). Numerous recent fluid studies of Archean mesothermal gold dominated deposits reveal a remarkably similar low salinity  $H_2O + CO_2$  fluid. Limited fluid inclusion studies of Proterozoic gold and copper deposits (Goellnicht et al., 1989; Nguyen et al., 1989; Lindblom and Martinsson, 1990) indicate that fluids responsible for mineralization were much more saline than for Archean gold deposits. This may be one explanation for the higher base metal ratios.

The Bidjovagge deposit, in northern Norway, contained average ore grades of 4.1 g/t Au and 1.19% Cu and operated by Outokumpu Oy between 1985 and 1991 (Ekberg and Sotka, 1991) is well described (e.g. Hollander, 1979; Bjørlykke et al., 1987; Bjørlykke et al., 1993), and was therefore chosen for a detailed fluid study. Fluid geochemistry using fluid inclusion microthermometry, Raman microspectrometry, gas chromatography together with stable isotope analysis have been combined with geological field observations to characterize the nature of the ore forming fluids at Bidjovagge. Data is presented in this paper accompanied with a comprehensive model that attempts to explain both the gold and base metal mineralization at Bidjovagge and other correlative Proterozoic mesothermal gold-base metal deposits.

## Geological Setting

Proterozoic greenstone belts occur between Archean gneiss and granulite domes in the northern part of the Fennoscandian Shield within Norway, Finland and Sweden (Fig. 1). Shear zones trending north and northeast transect the greenstone belts and appear to be the focus of gold and base metal mineralization at the Bidjovagge deposit in Norway, Saattopora deposit near Kittilä in Finland, and the Pahtohavare deposit near Kiruna in Sweden (Fig. 1).

One of the greenstone belts in Norway, the Kautokeino greenstone belt which hosts the Bidjovagge Au-Cu deposit, comprises mafic volcanic and metasedimentary rocks (Siedlecka et al., 1985). Shear structures within the Kautokeino greenstone belt trend northward and are northern extensions of the Baltic-Bothnian megashear (Berthelsen and Marker, 1986). The northern part of the Kautokeino greenstone belt is structurally overlain by Caledonian nappes, although tectonic windows near the town of Alta (Fig. 1) expose the supposed continuation of the greenstones (Olesen et al., 1990).

The Bidjovagge deposit occurs in the Cas'kejas Formation comprised of metavolcanic and metasedimentary rocks, including amphibolites, dolomites, graphitic schists, and a mixed series of metatuffites and schists (Siedlecka et al., 1985; Bjørlykke et al., 1987). Diabase sills occur within the metasedimentary sequence and are typically haloed by albite felsite, which is interpreted as the product of metasomatic alteration of the sedimentary sequence during sill intrusion (Bjørlykke et al., 1987). Contacts between diabase sills and graphitic schist display the most pronounced albitization. In the Bidjovagge area, the Cas'kejas Formation is overlain by feldspathic sandstones, shale, siltstone and limestone of the Bik'kacåkka Formation which in turn is overlain by sandstones and conglomerates of the Caravarri Formation (Siedlecka et al., 1985).

Metamorphism and structural deformation of the rocks at Bidjovagge occurred during the Svecokarelian Orogeny at 1,900 - 1,850 Ma (Skiöld, 1988; Pharaoh and Brewer, 1990; Bjørlykke et al., 1993). The metamorphic grade is upper greenschist

facies, gradually grading to amphibolite facies to the west (Sandstad, 1983). Two styles of deformation occur at Bidjovagge, ductile folding of the antiform and ductile shearing, followed by brittle shearing. Fluvial sedimentation occurred in the Baltic Shield, represented by the Caravari Formation in the Kautokeino greenstone belt, shortly after the main orogenic event, and before the intrusion of post-orogenic granites, reflecting rapid crustal uplift (Bjørlykke et al., 1993).

Lens-shaped syenodiorite intrusions occur within the shear zone, and relative timing of intrusion is constrained by structural crosscutting relationships. The syenodiorite intrusions crosscut shear texture, generally are not sheared, and are in places brittlely deformed (Fig. 3). Syenodiorite intrusions may be related to mineralization as discussed below.

### **Gold and Copper Mineralization**

Both mineralization and alteration at the Bidjovagge Au-Cu deposit are localized in the shear structures. Approximately 12 ore lenses are situated within shear zones which cut the eastern limb and nose of an upright isoclinal antiform (Fig. 2) which trends north, plunging slightly northward, and folds metasedimentary rocks and intrusive diabase sills of the Cas'kejas Formation. From figure 2, two apparent controls on the location of ore lens can be shown. First, mineralization occur at the intersection of shear structures or where dilational jogs occur along shear zones. Secondly, mineralization occurs in the albitic felsite near the contact with graphitic schist where an red-ox front has been developed (Fig. 4).

Gold and copper mineralization at Bidjovagge has been broken into two types by Bjørlykke et al. (1987) and Nilsen and Bjørlykke (1991). Ore type I is a gold-rich ore with 5 - 20 ppm Au and 0.1 - 0.5% Cu, and ore type II is copper-rich with 1 - 2 ppm Au and 2 - 5% Cu. Gold-rich mineralization occurs as finely disseminated native gold and gold telluride (calaverite) within sheared and microbrecciated albite felsite. Native gold has also been observed within uraninite crystals (Cumming et al.,

in prep.) and within actinolite (H. Åsen, pers. comm.). Minerals associated with gold-rich ore include quartz, carbonate, actinolite, pyrite, pyrrhotite, chalcopyrite, magnetite and minor amounts of apatite, Cr-rich muscovite, tellurides (altaite, melonite, and tellurobismuthite) and davidite. Davidite is a member of the crichtonite mineral series with a general formula of  $Y_6Z_{15}O_{36}$ , where Y = the larger cations dominated by REE, and Z = the smaller cations like Ti, Fe<sup>+++</sup>, V and Cr (Pabst, 1961; Gatehouse et al., 1978). A vein system related to gold-rich mineralization can be traced from the footwall metadiabase into the ore zones in the albite felsite and also the graphitic schist. Within veins cutting from the footwall upwards to the ore zone a pronounced zonation of magnetite to pyrite to pyrite + pyrrhotite occurs (Fig. 5). The pyrite + pyrrhotite assemblage occurs within the gold mineralized zone and the red-ox front. Mineralized shear planes commonly display a ductile fabric (Fig. 6) and are in places folded, boudinaged (Bjørlykke et al., 1987) or filling brittle fractures.

The copper-rich mineralization occurs predominantly as chalcopyrite and minor bornite within veins together with coarse carbonate (ankerite and calcite) and accessory amounts of albite, pyrite, pyrrhotite, quartz, actinolite, and minor amounts of telluride and native gold (Bjørlykke et al., 1987; Nilsen and Bjørlykke, 1991). Veins range in size up to 1.5 m and are lenticular in shape. Fracture filling chalcopyrite within albite felsite is also common in this ore type (Fig. 7).

#### *Timing of mineralization*

The relative timing of mineralization may be constrained by both the style of structures that are mineralized and also by crosscutting relationships displayed by the syenodiorite dikes. Gold-rich mineralization occurring in ductile to brittle structures appears to have been earlier than the copper-rich mineralization in brittle veins and fracture fills. This timing is supported by syenodiorite dikes which crosscut shear structures hosting gold mineralization (Fig. 3a), and are occasionally crosscut by brittle fractures filled with carbonate and Cu-sulfides (Fig. 3b).

The age of mineralization has been constrained by isotopic age dating of the davidite by Bjørlykke et al. (1990) and uraninite by Cumming et al. (in prep.). Ages

of davidite, found in association with the gold ore, have been estimated by U/Pb to be  $1885 \pm 18$  Ma and supported by a Sm/Nd date of  $1886 \pm 88$  Ma. Uraninite that contain gold give U/Pb dates of  $1837 \pm 8$  Ma. Based on this radiometric data, the gold-rich mineralization is considered to have occurred during or slightly after the peak of the Svecokarelian orogeny (e.g. Skiöld, 1988).

### **Wallrock Alteration**

Predominant alteration at Bidjovagge include albitization, carbonatization, and scapolitization and to a lesser extent amphibolitization, mica, and hematite alteration (Bjørlykke et al., 1987; Nilsen and Bjørlykke, 1991). The most common alteration at Bidjovagge is the albite felsite, which is host to mineralization. An early metasomatic event is evident by the albite felsite along the contact between the metadiabase sills and metasedimentary rocks. In places, this event metasomatized the graphitic schist into a hard graphitic felsite which behaved brittlely during late deformation. A second albitization occurs along shear zones within wall rocks, and is not limited to alteration of metasedimentary rocks but also occurs within metadiabase sills. Typically, the resulting albite felsite is microcrystalline, but is also coarsely crystalline especially where albite replaces plagioclase in the metadiabase (Bjørlykke et al., 1987). Rutile is ubiquitous in the albite felsite, and minor amounts of quartz, carbonate, mica and amphibole are found in occurrence.

Carbonatization is in association with the albitization, usually as carbonate replacing the amphiboles within the metadiabases (Bjørlykke et al., 1987). Scapolitization occurs extensively in the central metadiabase as poikiloblasts replacing plagioclase, and within tuffites located in the hanging wall of the deposit (Bjørlykke et al., 1987; Nilsen and Bjørlykke, 1991). Amphibolitization (actinolite) of the footwall carbonates is commonly observed especially in the southern part of the Bidjovagge trend around the "C" deposit (Fig. 2). Mica alteration occurs along structurally controlled zones, and includes the addition of biotite in the metadiabases, and sericite and fuchsite in albitized metasediments (Nilsen and Bjørlykke, 1991).

Potassic alteration tends to be in association with the Cu-rich mineralization. The hematite and chlorite alteration, associated with coarse crystalline carbonate, probably postdates the earlier gold mineralization and may be related to Cambrian supergene alteration (Bjørlykke et al., 1987).

### **Fluid Inclusion Study**

Fluid inclusions from over 40 samples from the Bidjovagge area have been analyzed during this study. Fluid inclusions analyzed are hosted within vein quartz from footwall veins and ore zones related to both gold- and copper-rich mineralization, and from apatite crystals and veinlets within syenodiorite dikes.

Doubly polished sections, 100 to 150  $\mu\text{m}$  thick, of the fluid inclusion samples were prepared, and microthermometric measurements were conducted at the fluid inclusion laboratory at the Mineralogical-Geological Museum, Oslo, Norway. All measurements were taken during heating of the sample, generally at a rate of  $5^\circ$  per minute. Measurements were mostly made using a LINKAM THM 600 heating-freezing stage, but because of temperature fluctuations, high precision low temperature measurements were made with a gas-cooled CHAIXMECA stage. Calibration of the LINKAM THM 600 stage was conducted with a series of natural and MERCK synthetic standards. Between  $-142^\circ\text{C}$  (melting point of methylcyclopentane) to  $+200^\circ\text{C}$  precision is approximately  $\pm 5^\circ\text{C}$ , and in the range of  $+200$  to  $+400^\circ\text{C}$  the instrument showed a  $+10$  to  $15^\circ\text{C}$  deviation above true temperatures. High quality low temperature measurements were made on the gas-cooled CHAIXMECA stage that has a precision of  $\pm 0.1^\circ\text{C}$  between  $-142^\circ\text{C}$  and  $+30^\circ\text{C}$ , and a deviation of  $1.0^\circ\text{C}$  which is compensated for after measurement, as described by Andersen et al. (1991).

Laser-excited Raman microprobe analysis were conducted at the Geological Institute, University of Stockholm, with the help of Dr. Sten Lindblom. The instrument used is a multichannel DILOR-XY, a successor to the MICRODIL-28

(Burke and Lustenhouwer, 1987). Measured line positions of CO<sub>2</sub>, CH<sub>4</sub> and N<sub>2</sub> were identified by comparison with listed values by Dubessy et al. (1989), Van Den Kerkhof (1991) and E.A.J. Burke (pers. comm.).

Destructive analysis of fluid inclusions from Bidjovagge samples using gas chromatography to determine hydrocarbon fluid compositions. Initial analysis with mineral separates from veins were soaked in dichloromethane for 24 hours and allowed to dry for 7 days and whole rock were not soaked in dichloromethane. Samples ranging in size from 5 to 20 grams were then crushed in a gas tight steel crushing chamber with a brass cylinder. Between 2 to 4 ml of gas were withdrawn with a gas tight syringe through a septum in the crushing chamber, and injected into a Varian 3500 GC-FID gas chromatograph with a 30m DB-1 column (film thickness = 5.0µm). For quantification, flushing the chamber with nitrogen was not conducted, as repeated blank runs with mechanical agitation of the crushing chamber showed only background CH<sub>4</sub>. Simple subtraction of the background was sufficiently accurate.

#### *Fluid inclusion description*

Fluid inclusions from Bidjovagge have been described by Ettner et al. (1992; 1993; in prep. a) related to gold mineralization and by Ettner et al. (in prep. b) related to copper mineralization. Fluid inclusions data from both gold and copper mineralization, and also from syenodiorite intrusions will be presented together here.

Fluid inclusions described include those interpreted to be primary or pseudosecondary, based on criteria presented by Roedder (1984). Secondary inclusions are omitted from this discussion. The fluid inclusions analyzed during this study contained a range of fluid types, which were composed of H<sub>2</sub>O, CO<sub>2</sub>, CH<sub>4</sub>, and light hydrocarbons (LHC) (Fig. 8), with dissolved salts, salt crystals, and other daughter crystals. A systematic division of fluid inclusion types, based on the main fluid phases present at room temperature, is presented in Table 1, together with associations of occurrence.

The first type of fluid inclusion is characterized by a dominant non-aqueous fluid (CO<sub>2</sub> or CH<sub>4</sub>) or H<sub>2</sub>O (Table 1). Non-aqueous fluid-rich inclusions are subdivided on the basis of gas impurities, and then further subdivided by the absence or presence of H<sub>2</sub>O. H<sub>2</sub>O-rich inclusions are divided on the basis of salt content; pure H<sub>2</sub>O, saline but unsaturated H<sub>2</sub>O, and saturated H<sub>2</sub>O with salt crystals at room temperature. H<sub>2</sub>O-rich inclusions are further subdivided on the presence of a second volatile component (CO<sub>2</sub> or CH<sub>4</sub>).

Fluid inclusions related to gold mineralization have been previously divided into three groups (Ettner et al., 1992; 1993; in prep. a), based on fluid composition and occurrence in the deposits. Generally, Group I include both saline aqueous solution ± CO<sub>2</sub> and CO<sub>2</sub> inclusions in footwall veins, Group II comprise both saline aqueous solution ± CH<sub>4</sub> and CH<sub>4</sub> or CH<sub>4</sub> + CO<sub>2</sub> inclusions in low grade ore zones, and Group III are dominated by CH<sub>4</sub> and LHC inclusions. This terminology of Groups I, II, and III is not used further in this discussion, although is shown in Table 1 for cross reference.

#### *Microthermometric and Raman Microprobe analysis*

*CO<sub>2</sub>-rich inclusions.* - CO<sub>2</sub>-rich inclusions occur in carbonate-quartz-actinolite veins related to gold mineralization and are subdivided into two types, pure CO<sub>2</sub> inclusions in nonmineralized footwall veins and CO<sub>2</sub> + CH<sub>4</sub> inclusions in veins within or proximal to low grade ore zones.

CO<sub>2</sub>-rich inclusions freeze to solid CO<sub>2</sub> and vapor upon supercooling to below -80°C. During heating, melting ( $T_{mCO_2}$ ) occurs either instantaneously at the CO<sub>2</sub> eutectic of -56.6°C, or display melting intervals with depressed melting temperatures between -57 and -63.5°C (Fig. 9). Eutectic melting temperatures show that inclusions contain pure CO<sub>2</sub>, whereas inclusions with melting intervals and depressed CO<sub>2</sub> final melting temperatures suggest a slight contamination of CH<sub>4</sub> (Burruss, 1981). Raman microprobe analysis of inclusions displaying eutectic melting confirmed the presence of pure CO<sub>2</sub>, with a spectra displaying two CO<sub>2</sub>

peaks, the strongest peak at  $\Delta\nu=1385\text{cm}^{-1}$  and the second peak at  $\Delta\nu=1279\text{cm}^{-1}$ . Raman spectra of inclusions having melting intervals and depressed  $\text{CO}_2$  final melting temperatures display similar  $\text{CO}_2$  spectra and also a  $\text{CH}_4$  peak between  $\Delta\nu=2910$  and  $2913\text{cm}^{-1}$  giving varying estimates of  $\text{CH}_4$  content between 8 to 22 mole %.

Further heating of the pure  $\text{CO}_2$  inclusions results in the homogenization ( $T_{\text{HCO}_2}$ ) to liquid at temperatures between  $-55$  and  $+12^\circ\text{C}$ , with a mode between  $-30$  and  $-20^\circ\text{C}$  (Fig. 9). Homogenization temperatures of the  $\text{CO}_2$  inclusions containing  $\text{CH}_4$  are similar to pure  $\text{CO}_2$ , ranging from  $-50$  to  $-10^\circ\text{C}$  (Fig. 9). No  $\text{H}_2\text{O}$  or  $\text{CO}_2$  clathrate was observed in  $\text{CO}_2$ -rich inclusions.

*CH<sub>4</sub>-rich inclusions* - Methane-rich inclusions at Bidjovagge occur predominantly in veins within the gold mineralized albite felsite which is oxidized and albitized graphitic schist. Methane-rich inclusions with  $\text{H}_2\text{O}$  have also been observed in apatite veinlets within syenodiorite dikes which are intruded in graphitic schists.  $\text{CH}_4$ -rich inclusions display varied behaviour during freezing including both homogenization type inclusions (H-type) and sublimation type inclusions (S-type) as defined by Van Den Kerkhof (1990) for  $\text{CO}_2$  -  $\text{CH}_4$  binary systems (Fig. 10). H-type inclusions observed at Bidjovagge nucleate a vapor bubble during supercooling, but no freezing to solid is observed. Homogenization to liquid occurs between  $-125$  and  $-39.6^\circ\text{C}$  (Fig. 10). Inclusions which homogenize to liquid between  $-125^\circ\text{C}$  and the critical temperature of  $\text{CH}_4$  ( $-82.1^\circ\text{C}$ ) fit the behaviour of pure  $\text{CH}_4$  (Burruss, 1981; Kerkhof, 1990). Inclusions which homogenize to liquid between the critical temperature of  $\text{CH}_4$  ( $-82.1$ ) and  $-39.6^\circ\text{C}$ , in the absence of solid melting, include  $\text{CH}_4$  + higher hydrocarbons, or higher hydrocarbons such as ethane without  $\text{CH}_4$  (critical temp. =  $+32.2^\circ\text{C}$ ; Weast et al., 1988). The absence of solid melting indicates that  $\text{CO}_2$  is not present. Some of these inclusion fluoresce with light golden colors under the UV microscope.

Raman microprobe analysis of  $\text{CH}_4$ -rich inclusions from Bidjovagge displaying H-type behaviour are discussed by Ettner et al. (in prep. c). Raman spectra

of CH<sub>4</sub> inclusions which homogenize below -82.1°C show a strong CH<sub>4</sub> peak at  $\Delta\nu=2911\text{cm}^{-1}$ . Fluid inclusions which homogenize between -82.1 and -42°C analyzed with Raman microprobe fluoresce strongly but also display a strong CH<sub>4</sub> peak around  $\Delta\nu=2911\text{cm}^{-1}$  (Fig. 11). The Raman spectra of these inclusion also display a "mound" surrounding the CH<sub>4</sub> peak along with an ethane peak around  $\Delta\nu=2950$  to  $2952\text{cm}^{-1}$  and rarely a propane peak at  $\Delta\nu=2892\text{cm}^{-1}$  (Fig. 11). Carbon spectra is found in nearly all CH<sub>4</sub>-rich inclusion analyzed, showing a strong narrow peak between  $\Delta\nu=1605$  to  $1608\text{cm}^{-1}$  and a second wider and rounded peak between  $\Delta\nu=1327$  to  $1340\text{cm}^{-1}$ . Carbon is considered to be present in the inclusions at a thin amorphous coating on the walls of inclusions (Ettner et al., in prep. c).

Critical behaviour was observed in one fluid inclusion from the K deposit at Bidjovagge (Fig. 2) in which the meniscus fades at -74.8°C. Assuming a binary system of CH<sub>4</sub>-C<sub>2</sub>H<sub>6</sub>, this critical temperature indicates a mole fraction of approximately 0.08 C<sub>2</sub>H<sub>6</sub> (Olds, 1953). Similarly, this critical temperature in the binary system CH<sub>4</sub>-C<sub>3</sub>H<sub>8</sub> indicates a C<sub>3</sub>H<sub>8</sub> mole fraction of 0.03 (Olds, 1953).

S-type inclusions are characterized by partial freezing during super cooling to about -180°C and during heating, homogenization to liquid occurred before final melting of the solid phase. Partial homogenization to liquid ( $T_{\text{h}}\text{CH}_4+\text{CO}_2$ ), in the presence of a CO<sub>2</sub>-rich solid, usually occurs between -105 to -65°C, and sublimation of the solid ( $T_{\text{s}}\text{CO}_2+\text{CH}_4$ ), the final melting in a S2-type inclusion, occurs between -95 and -60°C (Fig. 10). This behaviour is found in the CO<sub>2</sub> - CH<sub>4</sub> binary system with fluids of lower molar volume, dominated by CH<sub>4</sub> (Van Den Kerkhof, 1990). No H<sub>2</sub>O or gas clathrate was observed in these inclusions. Raman microprobe analysis of these S-type inclusions show spectra with both a CH<sub>4</sub> peak around  $\Delta\nu=2911\text{cm}^{-1}$  and two CO<sub>2</sub> peaks, the largest at  $\Delta\nu=1294\text{cm}^{-1}$  and the second peak at  $\Delta\nu=1383\text{cm}^{-1}$ . Estimations of CO<sub>2</sub> content range between 1.5 and 15 mole %, based on Raman analysis. Carbon spectra is found in S-type inclusions, similar to that described from H-type inclusions above.

$\text{CH}_4 + \text{H}_2\text{O}$  inclusions are observed in albite crystals within albite - chalcopyrite veinlets in a syenodiorite which intrude graphitic schist. Upon supercooling the  $\text{H}_2\text{O}$  freezes to ice and a vapor bubble nucleates. Generally homogenization to liquid, in the presence of ice, occurs between  $-89$  to  $-82^\circ\text{C}$ , indicating  $\text{CH}_4$  (Burruss, 1981). First ice melting ( $T_{\text{m initial ice}}$ ) is generally observed around  $-20^\circ\text{C}$ , followed by final ice melting ( $T_{\text{m final ice}}$ ) between  $-7.5$  and  $-10.5^\circ\text{C}$ .  $\text{CH}_4$  clathrate melting is observed between  $-1.8$  and  $0^\circ\text{C}$ . No salt hydrate melting was observed. Ice melting behaviour indicates the presence of NaCl in the aqueous solutions (Crawford, 1981). The salinity of the aqueous solution may not be accurately estimated based on gas clathrate melting, but the maximum salinity may be estimated by the final melting of  $\text{H}_2\text{O}$  ( $<14.5\text{wt. \% NaCl equiv.}$ ; Potter et al., 1978). Raman microprobe spectra of these inclusions confirm the presence of pure  $\text{CH}_4$ .

*Salt saturated  $\text{H}_2\text{O}$  inclusions* - Aqueous solutions saturated with salt at room temperature are common in veins related gold mineralization in the footwall and lower grade ore zones but are rare in the high grade ore zones. These inclusions contain aqueous solution, one to two salt crystal, bubbles of either  $\text{H}_2\text{O}$  vapor,  $\text{CO}_2$  or  $\text{CH}_4$ , and sometimes daughter crystals. At room temperature the degree of  $\text{H}_2\text{O}$  fill of inclusions is generally about 95 volume %. Daughter crystals present include carbonate, actinolite and small opaque crystals.

Fluid inclusions of this type freeze to ice plus salt, hydrates, and vapor while supercooling. During heating the ice appears to melt ( $T_{\text{m initial ice}}$ ) in the range of  $-90$  to  $-30^\circ\text{C}$ , but with two distinct groups with modes around  $-78^\circ\text{C}$  and  $-40^\circ\text{C}$  (Fig. 12). Final ice melting temperatures ( $T_{\text{m final ice}}$ ) are generally between  $-33$  and  $-16^\circ\text{C}$  with a mode between  $-28$  and  $-20^\circ\text{C}$  (Fig. 12). Hydrohalite melting was difficult to observe because of the high wt. % of salt but were observed between  $-16$  and  $+6^\circ\text{C}$  (Fig. 12). The low  $T_{\text{m initial ice}}$  melting behaviour of the saline brine indicates that both NaCl and  $\text{CaCl}_2$  are present in the inclusions (Crawford, 1981). The unusual initial melt temperatures observed below  $-50^\circ\text{C}$  may be due to metastable melting of the saline brine (Roedder, 1971) or the presence of LiCl (Borisenko, 1977).

Salt saturated aqueous inclusions with CO<sub>2</sub> bubbles exhibit eutectic melting of the CO<sub>2</sub> followed by clathrate melting between -13 and -3°C, then homogenization to liquid between -2 and +26°C, with a mode around 25°C. Inclusions bearing CH<sub>4</sub> bubbles exhibit CH<sub>4</sub> homogenization to liquid between -102 and -81°C followed by clathrate melting between -2.4 and -3.0°C.

Further heating of the inclusions first result in the partial homogenization of the water and gas or vapor bubble range between 90 and 365°C with a mode between 100 to 200°C, usually followed by salt dissolution ( $T_{d_{salt}}$ ) in a wide range between 90 to 370°C with a mode around 250°C (Fig. 13). Salt contents are calculated from Haas (1976) and Tanger and Pitzer (1989), based on the salt dissolution temperatures ( $T_{d_{salt}}$ ), to be between 28 to 43 wt. %, NaCl equivalent. Decrepitation before the final dissolution of the salt is common, with average decrepitation temperatures between 200 and 250°C.

*Salt undersaturated H<sub>2</sub>O inclusions* - Fluid inclusions containing only an aqueous solution and a vapor bubble at room temperature are observed in quartz related to copper-rich mineralization and in apatite crystals in syenodiorite intrusions. At room temperature, the degree of H<sub>2</sub>O fill is greater than 95 volume % of the fluid. During supercooling these fluid inclusions freeze to ice. First melting is observed between -90 and -50°C, with a mode around -80°C and final melting generally occurs between -30 and -20°C with a mode around -26°C (Fig. 14). Inclusions within apatite crystals in the syenodiorite have similar  $T_{m_{ice}}$  between -72 and -76°C and  $T_{m_{final\ ice}}$  between -30 and -20°C (Fig. 14). Salt hydrates were observed in some inclusions within quartz related to copper mineralization, melting between -15 and +6°C (Fig. 14), but were not observed in fluid inclusions within apatite crystals. The very low first ice melting temperatures are similar to those observed in salt saturated inclusions related to the gold-rich mineralization. The final ice melting temperatures and observed salt hydrate melting temperatures correspond to a solution dominated by approximately a 25 wt. % salt mixture of NaCl + CaCl<sub>2</sub> (Crawford, 1981b). Inclusions related to copper mineralization homogenize to liquid between 100 to 200°C, and display a

mode between 105 to 140°C (Fig. 15). Inclusions from apatite crystals within syenodiorite homogenize between 95 and 130°C (Fig. 15).

### *Gas Chromatography*

Based on the detection of methane, ethane, and propane within fluid inclusions in the ore zone using microthermometry and Raman microprobe, further gas chromatography analysis of the fluid has been conducted on volatiles released from crushed samples. In a preliminary study of the hydrocarbon gases, Ettner et al. (in prep. c) separated quartz and carbonate from both veins in the footwall containing CO<sub>2</sub>-rich inclusions and veins in the mineralized zones bearing CH<sub>4</sub>-rich inclusions were analyzed for hydrocarbons. Analysis of samples bearing H-type CH<sub>4</sub>-rich confirmed the presence of methane, ethane, and propane, as was indicated by microthermometric and Raman microprobe, and also the presence of butane was detected in some samples. Samples bearing CH<sub>4</sub>-rich inclusions, where higher hydrocarbons were not detected by microthermometry and Raman microprobe, showed gas chromatograms revealing methane, ethane and minor propane. Analysis of quartz within footwall veins bearing pure CO<sub>2</sub> inclusions detected only trace CH<sub>4</sub> and no higher hydrocarbons.

Continued work using whole rock samples from 3 drill cores through a ore lens at the Bidjovagge deposit has been conducted to delineate the hydrocarbon zonation. Samples were collected every 5 to 10 meter through the hanging wall, ore zone and footwall (Fig. 16). Generally, gas chromatograms show methane, ethane, propane, butane and pentane (Fig. 17) within the ore zone. Outward of the ore zone, butane and pentane is not detected, but methane, ethane, and propane is detected usually within albite metasomatized zones and veins. CH<sub>4</sub> has the largest zone of occurrence of the light hydrocarbons. This zonation of light hydrocarbons agrees with the fluid inclusion study which shows CO<sub>2</sub>-rich fluids occurring in the footwall and hydrocarbon fluids occurring within the mineralized zones.

### *Pressure - Temperature Estimation*

No independent potential geothermometric or geobarometric mineral assemblages have been found at Bidjovagge, although temperatures and depths of burial during metamorphism have been estimated. The metamorphic grade is approximately upper greenschist facies (chlorite + biotite + actinolite + hornblende + plagioclase) grading to amphibolite facies (garnet + hornblende + cummingtonite + plagioclase) towards the basement gneisses to the west (Sandstad, 1983). The stratotectonic depth of burial is estimated as 10 to 15 km.

An attempt has been made to calculate isochores from the fluid inclusion data from Bidjovagge. Isochores for different compositions of fluid inclusions have been calculated by the MRK equation of state (Holloway, 1981; Nicholls and Crawford, 1985). Molar volumes of CO<sub>2</sub> + CH<sub>4</sub> inclusions were estimated from application of Raman microprobe data, described below, and microthermometric data to TX diagrams of the system CO<sub>2</sub> + CH<sub>4</sub> by Van Den Kerkhof (1990). Fluid inclusions composed of CH<sub>4</sub> + light hydrocarbons (LHC) or H<sub>2</sub>O + CH<sub>4</sub> ± CO<sub>2</sub> + salt were not used for calculation of isochores. Combined data for the mode and maximum temperature of salt dissolution are as 250°C and 370°C, respectively.

For fluid inclusions related to gold-rich mineralization, isochores constructed for CO<sub>2</sub> and H<sub>2</sub>O + CO<sub>2</sub> + salt inclusions within the footwall generally plot at higher pressures and temperatures than H<sub>2</sub>O + salt and CH<sub>4</sub>-bearing inclusions within the ore zone (Fig. 18a). At fixed temperatures, isochore calculated from fluid inclusions related to copper-rich mineralization plot at lower pressures than inclusions related to gold-rich mineralization (Fig. 18a).

Considering that gold mineralization occurred contemporaneously with deformation and upper greenschist metamorphism we may loosely constrain the PT conditions of mineralization to be around 2 to 4 kbars, lithostatic, and less than 450°C. Salt dissolution temperatures indicate minimum trapping temperatures, as there is no indication of salt saturation during trapping. For fluid inclusions related to gold mineralization, most isochores cross the 2 to 4 kbar range between 300 to 375°C

resulting in a "polygon" of possible trapping conditions. By correlating the isochores, salt dissolution temperatures, and the regional geology we suggest that fluids related to the gold-rich phase of mineralization at Bidjovagge to have been trapped at pressures of 2 to 4 kbars and at temperatures of 300 to 375°C (Fig. 18b). Fluid inclusions related to the copper-rich phase of mineralization are interpreted to have been trapped at around 2 kbars and at temperatures between 200 to 350° (Fig. 18b).

## **Stable Isotope Geochemistry**

### *Carbon and Oxygen Isotopes*

At Bidjovagge, copper and gold mineralization at the oxidation front to graphitic schist indicates that fluid-rock interaction was involved in mineralization. Carbon and oxygen isotope analysis of 59 samples of vein carbonate, related to both gold-rich and copper-rich mineralization have been made to characterize the carbon sources. Preliminary results of Ettner et al. (1993; in prep. a) along with further analysis show that carbonate related to gold mineralization from a single profile across the "H" ore lens at Bidjovagge (Fig. 2) display fairly consistent  $\delta^{18}\text{O}$  values, but variable  $\delta^{13}\text{C}$  values (Fig. 19). Carbonate samples analyzed were selected from footwall veins associated with  $\text{CO}_2$ -rich inclusions, veins within the mineralized zone associated with  $\text{CH}_4$ -rich inclusions, carbonate veins crosscutting graphitic schist, and also from carbonate altered syenodiorite dikes. Sedimentary carbonate from the core of the Bidjovagge anticline was also analyzed for carbon and oxygen isotopes along with graphitic schist for carbon isotopes.

Analysis of 6 carbonate samples from the footwall veins show  $\delta^{13}\text{C}$  values of -0.66 to -1.9‰, relative to PDB. Six carbonate samples separated from veinlets within the higher grade gold zones have  $\delta^{13}\text{C}$  values ranging from -1.72 and -4.64‰. Carbonate separated from mineralized carbonate veins from within the graphitic schist have  $\delta^{13}\text{C}$  values of -7.04 and -7.25‰. Carbon analysis from two carbonate altered syenodiorite dikes have  $\delta^{13}\text{C}$  values of -1.22 to -1.55‰. Carbon isotope

values around 0‰ PDB are displayed by both the sedimentary carbonate and the skarn altered sedimentary carbonate, with  $\delta^{13}\text{C}$  values of +0.36 and -0.05 ‰, respectively. Graphite from 4 graphitic schist samples have  $\delta^{13}\text{C}$  values which group around -20‰. Analysis of  $\delta^{18}\text{O}$ , from the carbonates, typically have values between +10.92 and +13.43‰, relative to SMOW (Fig. 19). The sedimentary carbonate and the skarn altered sedimentary carbonate display higher  $\delta^{18}\text{O}$  values of +16.11 and +19.42‰, respectively.

Carbonate veins related to copper-rich mineralization generally have  $\delta^{13}\text{C}$  values of between -3.71 and -2.76‰ and  $\delta^{18}\text{O}$  values between 10.9 and 12.9‰ (Fig. 19). These  $\delta^{13}\text{C}$  and  $\delta^{18}\text{O}$  values lie along the same trend defined by  $\delta^{13}\text{C}$  and  $\delta^{18}\text{O}$  values from carbonates related to gold-rich mineralization.

### *Sulfur Isotopes*

A total of 15 pyrrhotite, pyrite, and chalcopyrite samples veins and ore zones from Bidjovagge show a range of  $\delta^{34}\text{S}$  values between -3.9 and +2.0‰ (Fig. 20). These  $\delta^{34}\text{S}$  values show a change between the sulfide species with pyrrhotite having the lightest values around -3‰, chalcopyrite the heaviest values, generally around 1.6 to 2.0‰ but with one sample at -2.5‰, and pyrite showing values in between pyrrhotite and chalcopyrite. This wide range in  $\delta^{34}\text{S}$  values may be explained by either rapid changes in  $f\text{O}_2$  causing depletion of  $^{34}\text{S}$  by the reduction of  $\text{SO}_4^{2-}$  to  $\text{H}_2\text{S}$  or mixing of two sulfur sources. Sulfur sources may include the heavier  $^{34}\text{S}$  in the hydrothermal fluids and lighter sulfur from sulfide bands within the graphitic schists.

## **Discussion and Interpretation**

### *Fluid Zonation*

Microthermometric, Raman microprobe, and gas chromatography analysis of fluid inclusions, combined with stable isotope data has helped to understand the processes involved in copper and gold mineralization at the Bidjovagge deposit. The

model proposed for the genesis of the Bidjovagge deposit may be compared with other Proterozoic mesothermal gold-base metal deposits.

Fluid inclusions related to gold mineralization display a well defined zonation from the footwall to the ore zone. Fluids in the footwall veins within the metadiabase, fluids are dominated by highly saline aqueous solutions (30- 43 wt. %, NaCl equiv.), dominated by NaCl and CaCl<sub>2</sub>, with liquid CO<sub>2</sub> that appears to have been miscible during trapping. Sources for fluids in greenstone mesothermal gold deposits, whether metamorphic or magmatic, are a matter of debate (e.g. Cameron, 1989; Kerrich, 1989; Newton, 1990). The highly saline CO<sub>2</sub> + H<sub>2</sub>O fluids at Bidjovagge and also observed regionally in shear zone-hosted copper mineralization (Ettner et al., in prep. b), may have originated from either a metamorphic or igneous source. If a syenodiorite magma was the source for the saline solutions at Bidjovagge then early exhalations of fluids must have been either highly saline or the salinity increased during migration by either hydration reactions with the wall rocks (Trommsdorff and Skippen, 1987) or addition of salts from the metasedimentary rocks sequence. Although the existence of evaporites in the Kautokeino greenstone belt is plausible and has been suggested by Solli and Torske (1993), no occurrences have been described. Albite metasomatism of wet sediments, as suggested for the early albitization at Bidjovagge (Bjørlykke et al., 1987), would indicate that a highly saline seawater was present during sedimentation and during the intrusion of the diabase sills. Amphibolitization observed in the footwall carbonates at Bidjovagge indicate that hydration of the wall rocks during fluid ascent may also be a potential explanation for an increase in fluid salinity and also a source for CO<sub>2</sub>. The alteration assemblage at Bidjovagge of albitization, carbonatization, and scapolitization concurs with the a highly saline H<sub>2</sub>O + CO<sub>2</sub> fluid described.

Further up in the shear zone, within the highly sheared albite felsite, and towards the ore zone, highly saline aqueous solutions and pure liquid CO<sub>2</sub> occur as separate primary fluid inclusions. The coeval nature of these two inclusion types considered together with the occurrence of miscible saline aqueous solutions deeper

within the same veins indicates that phase separation occurred (Ramboz et al., 1982). Trommsdorff and Skippen (1988) show that supercritical fluid composed of  $H_2O + CO_2 +$  salt may unmix to a  $CO_2$ -rich phase and a saline  $H_2O$  phase during a drop in P-T conditions or during fluid-rock reaction. In the samples from Bidjovagge, phase separation of a supercritical fluid moving upwards along the shear zones is easily explained by a drop in pressure as the fluid encountered the highly deformed albite felsite. Because of the occurrence of pure single phase  $CO_2$  inclusions, the addition of  $CH_4$  resulting in phase separation of the supercritical fluid as suggested by Walsh et al. (1988) at Pamour Mine in Canada, does not appear to be the mechanism for phase separation at Bidjovagge.

Fluids occurring within the gold-rich mineralization in albite felsite are dominated by the same saline aqueous solutions as found in the footwall, and by  $CH_4$  and other light hydrocarbons (LHC). Rarely, saline aqueous solutions occur together with  $CH_4$  or  $CH_4 + CO_2$  in samples from veins in less deformed and albite altered zones, but proximal to graphitic schist. Fluid inclusions of this type are similar to the highly saline aqueous +  $CO_2$  inclusions found in the footwall diabases as they indicate miscibility in less deformed host rocks.

Light hydrocarbon fluids dominated by  $CH_4$ , but also including ethane, propane, butanes, and pentanes are zoned around the ore deposit and around minor oxidized and altered graphitic schist zones (Fig. 16). Interaction between the saline aqueous solutions, which moved upwards along the shear zone, and the graphitic schist is supported by the red-ox front, albitization, and carbon isotopes from vein carbonates. This hydrocarbon zonation is not expected by the migration of hydrocarbons into the ore zone, but would be produced by the *in situ* synthesis of light hydrocarbons during this fluid-rock interaction.

Fluid inclusions found in one vein crosscutting syenodiorite dikes in the "K" deposit at the northern end of the Bidjovagge area (Fig. 2) comprise high salinity aqueous solutions dominated by  $NaCl$  and  $CaCl_2$  and immiscible liquid  $CH_4$  similar to fluid inclusions related to gold-rich mineralization. Fluid inclusions within apatite

crystals and chalcopyrite-albite veinlets from another syenodiorite dikes in the "B" deposit at Bidjovagge (Fig. 2) contain salt undersaturated aqueous solutions similar to fluids related to the copper-rich mineralization. The fluids related to copper mineralization are moderately saline aqueous solutions, dominated by NaCl and CaCl<sub>2</sub>; approximately 25 wt. %, NaCl equivalent. The decrease in salinity from Au- to Cu-rich phases of mineralization is interpreted to be a result of either the introduction of a second fluid, the decrease in available salts from the source or metasedimentary rock sequence, or the diminishing effect of hydration reactions with the wall rocks. CO<sub>2</sub> or CH<sub>4</sub> do not appear to have been significant components during the copper-rich phase of mineralization, but large copper-carbonate veins produced during this event show that HCO<sub>3</sub><sup>-</sup> was present in the fluid. Minor CH<sub>4</sub>-bearing fluid inclusions within a albite-chalcopyrite veinlet a syenodiorite dike indicates that minor CH<sub>4</sub> may have been produced during the copper-rich phase of mineralization.

#### *Role of Syenodiorite Intrusions*

The syenodiorite intrusions at Bidjovagge have a complex relationship with mineralization at Bidjovagge. As discussed above, the dikes crosscut ductile shear that hosts gold-rich mineralization and are in places crosscut veins carbonate ± sulfides that fill brittle fractures (Fig. 3). Both fluid inclusions related to gold- and copper-rich mineralization are found in veins and veinlets crosscutting syenodiorite intrusions, although primary igneous inclusions within apatite crystals are similar to fluids related to copper-rich mineralization.

The relationship between the structural fabric and syenodiorite intrusions suggests that the syenodiorite began to be intruded after ductile deformation had ceded and brittle deformation had provided weakness that promoted the intrusion of dikes. Some syenodiorite dikes appear to have been intruded during the gold-rich phase of mineralization as they are crosscut by veins bearing high salinity aqueous solutions ± CH<sub>4</sub>. Saline solutions observed within syenodiorite intrusions are similar

to fluid inclusions related to Cu-rich mineralization suggesting that the intrusives were also involved with the Cu-rich phase of mineralization. Potassic alteration related to Cu-rich mineralization may be the result of fluids related to the aqueous fluids exsolved from the K-rich syenodiorite dikes, although the presence of KCl in the fluid inclusions can not be confirmed by microthermometric phase behaviour. The syenodiorite dikes are therefore interpreted to have intruded during a prolonged period spanning both Au- and Cu-rich phases of mineralization, but the most profound influence of the syenodiorite intrusions occurred during Cu-mineralization.

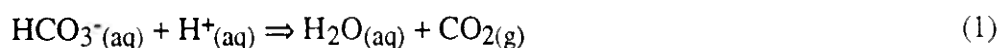
#### *Metal Transport and Precipitation*

As discussed above, mineralization at Bidjovagge occurred in two phases, a gold-rich phase which also includes the introduction of copper and uranium (Fig. 21a), and a copper-rich phase which also introduced minor amounts of gold (Fig. 21b). Fluids related to these two phases of mineralization observed at Bidjovagge are somewhat similar, but differ in the concentration of dissolved salts and non-aqueous liquids (e.g. CO<sub>2</sub> or CH<sub>4</sub>) present, and indicate different P-T conditions.

The H<sub>2</sub>O + CO<sub>2</sub> + salt fluid described from footwall veins related to gold mineralization is interpreted to resemble the fluids which transported Au, Cu, and U during the first phase of mineralization. Temperatures and pressures during transport in the footwall are estimated by fluid inclusion microthermometry to be in the order of 300 to 375°C and between 2 to 4 kbars. Initially, the fluids were relatively oxidizing as shown by the oxidation of the graphitic schists (Fig. 4) and also by the magnetite to pyrite to pyrite + pyrrhotite zonation found in the veins (Fig. 5). Transport of Au as chloride complexes is favored under these higher temperature, oxygen fugacity conditions around the magnetite stability field, and high saline conditions (Henley, 1973; Barnes, 1979), as opposed to sulfide complexes which favor temperatures <300°C and oxygen fugacity conditions near the pyrite-pyrrhotite boundary (Hayashi and Ohmoto, 1991; Seward, 1991) (Fig. 22). Similarly, copper transported as chloride complexes is favored by temperatures >250°C, slightly acidic

conditions, and increased oxygen fugacity (Crerar and Barnes, 1976). Uranium can be transported in a relatively oxidizing fluid in the uranyl state, possibly complexed with CO<sub>2</sub> as an uranyl dicarbonate complex (Rich et al., 1977; Kimberley, 1978).

Deposition of metals at Bidjovagge during the gold-rich phase of mineralization is interpreted to be due to a combination of effects as the fluids entered the highly sheared albite felsites and reacted with graphitic schists (Fig. 21a). Phase separation of the supercritical H<sub>2</sub>O + CO<sub>2</sub> + salt fluid transported metals is interpreted to have occurred as the fluid move upward into the highly sheared albite felsite, possibly due to a drop in pressure. Phase separation by the reaction...



would result in the increase of pH (Reed and Spycher, 1985). The increase in pH apparently not large enough to result in a major drop in gold solubility as chloride complexes, shown by the lack of gold mineralization in samples indicating phase separation of the fluid.

Interaction of the fluids transporting metals with the graphitic schist appears to have resulted in gold precipitation from the fluids. The  $f\text{O}_2$  of the fluid was dramatically lowered by the fluid-rock interaction and formation of hydrocarbons, evidenced by the zonation of magnetite to pyrite to pyrrhotite + pyrite in the veins (Fig. 5). The precipitation of gold from chloride complexes occurred at the pyrite - pyrrhotite boundary due to reduction of  $f\text{O}_2$  coupled with the increase of pH due to phase separation (Fig. 22). It is apparent that precipitation of gold from sulfide complexes at the stability pyrite - pyrrhotite boundary due to a reduction of  $f\text{O}_2$  would be unlikely.

Copper chloride complexes carried in the same solutions the as gold chloride complexes during the gold-rich mineralization phase would be similarly effected by lowered  $f\text{O}_2$  and pH increase. Chalcopyrite zonation is wider and more sporadic than gold mineralization suggesting that increasing  $\Sigma\text{S}$  of the solution was also important in mineralization. Uraninite found together with gold at Bidjovagge (Bjørlykke et al.,

1987; Cumming et al. in prep.) would precipitate by the reduction of a fluid carrying U in the uranyl state of  $U^{6+}$  (Rich et al., 1977; Kimberley, 1978).

The role of fluid interaction with the graphitic schist during the copper-rich phase of mineralization is not obvious because of the earlier alteration and oxidation during the gold-rich phase. The effect of  $fO_2$  on the zonation of magnetite, pyrite, and pyrrhotite is not clearly observed, although pyrrhotite is observed together with fracture fill chalcopyrite in high grade copper ore. Indication that interaction between the fluid and graphitic schist is evident through carbon isotopes of carbonates from the large chalcopyrite-carbonate which have  $\delta^{13}C$  values that lie along the fluid-rock  $\delta^{13}C$  trend displayed by carbonates related to the gold-rich phase.

Transport of copper and minor amounts of gold as chloride complexes during the copper phase of mineralization, but reduced gold precipitation during this phase may be due to decreasing solubilities because of reduced fluid temperatures or salinities. Mineralization during this phase occurs in large brittle structures and within breccia fill indicating decreased pressures relative to the gold phase mineralization (Fig. 21b). Phase separation of  $CO_2$  from the saline aqueous solutions due to this drop in pressure may have driven the remaining fluids to higher pH and produced the carbonate fill of the veins. Similar effects of increased pH coupled with reduced  $fO_2$  could have resulted in the precipitation of copper and minor gold.

#### *Correlation with other Precambrian mesothermal gold deposits*

The fluids observed at the Bidjovagge Au-Cu deposit are similar to other Proterozoic mesothermal gold-base metal deposits, but strikingly different than fluids described from Archean greenstone belt mesothermal gold deposits. Fluids described from Proterozoic mesothermal gold-base metal deposits tend to be higher saline solutions (Table 2) than Archean mesothermal gold deposits which typically are  $CO_2$ -rich low salinity aqueous solutions (e.g. Wood et al., 1986; Robert and Kelly, 1987; Walsh et al., 1988; Burrow and Spooner, 1990; VAN Hees and Kesler, 1990; Phillips, 1990).

A comparison of some Proterozoic mesothermal gold-base metal deposits from Fennoscandia and Australia (Table 2) show that fluid inclusions observed from these deposits are generally composed of  $H_2O + salt \pm CO_2$ , with high salinities between 22 and 54 wt. %, NaCl equivalent. Host rocks comprise metasedimentary and metavolcanic rocks, and granite breccia at the Olympic Dam deposit. Alteration assemblages are not consistent between the deposits, although albitization is common in deposits within Fennoscandia.

A general comparison between Proterozoic mesothermal gold-base metal deposits and Archean mesothermal gold deposits show that, aside from base metal contents, these deposits tend to be hosted in different lithologic assemblages and tectonic settings. While Archean mesothermal gold deposits are typically hosted in tholeiitic volcanic rocks interpreted to have formed along convergent plate margins (e.g. Groves and Foster, 1991; Card et al., 1989; Groves et al., 1989), while most Proterozoic mesothermal gold-base metal deposits generally occur within continental rifts with more sedimentary-rich or felsic-rich rocks. Within Fennoscandia, the Bidjovagge, Pahtohavare, and Saattopora deposits are also associated with tholeiitic volcanic rocks but are interpreted to lie within intracratonic rifts with felsic basements (Bjørlykke et al., 1993). The Olympic Dam deposit in Australia displays some mineralogical and fluid geochemical similarities to the mesothermal gold-base metal deposits (Table 2) but the genetic correlation is not clear.

The origin of highly saline fluids and the source of gold and base metals for these deposits is not known for certain. It is evident that the high salinities of the fluids are probably controlled by the lithologic assemblages, such as the felsic intrusions or the metasedimentary rocks. Fluid inclusion data at Bidjovagge suggest that the saline aqueous fluids were derived from syenodiorite intrusions, and similar magmatic sources for fluids have been suggested for Telfer (Goellnicht et al., 1989), the White Devil deposit (Nguyen et al., 1989) and the Pahtohavare deposit (Martinsson, 1992).

Transport of gold and base metals both as chloride complexes in the saline fluids would be favoured by high  $fO_2$ , high temperature, low pH and high chlorinity (Henley, 1973; Hayashi and Ohmoto, 1991). Precipitation of the metals from chloride complexes in these deposits may result by a combination of factors such as increasing pH and decreasing  $fO_2$  as suggested at Bidjovagge, or decreased chlorinity or temperature. The importance of the ductile-brittle transition for the precipitation of gold, as shown for the Archean mesothermal gold deposits (Cameron, 1989; Colvine, 1989; Kerrich and Feng, 1992) appears to be important for Proterozoic mesothermal gold-base metal deposits as well. Mineralization close to the ductile-brittle transition is shown at the Bidjovagge deposit, and for the White devil deposit (Nguyen et al., 1989), where mineralization is associated with ductile or semiductile to brittle deformation. The drop in pressure, such as at the ductile to brittle transition, would result in fluid unmixing of a supercritical  $H_2O + CO_2 +$  salt fluid (Bowers and Helgeson, 1983; Trommsdorff and Skippen, 1988). The most significant effect upon chloride complexes by the separation of a  $CO_2$ -rich phase from a  $H_2O +$  salt-rich phase would be the increase of pH.

### **Acknowledgements**

We wish to thank Bidjovagge Gruver A/S and Outokumpu Oy for partial financial support of this research, and permission to publish these results. We also gratefully acknowledge financial support from NTNF (Royal Norwegian Research Council for Scientific and Industrial Research), project number BF-25469. We are grateful to Sten Lindblom from the Institute of Geology, University of Stockholm, for his generous help with Raman microprobe analysis and also, Dag Karlsen, Institute for Geology, University of Oslo, for his assistance with the gas chromatography analysis.

## References

- Andersen, T., Austrheim, H., and Burke, E.A.J., 1991, Mineral-fluid-melt interactions in high-pressure shear zones in the Bergen Arcs nappe complex, Caledonides of W. Norway: Implications for the fluid regime in Caledonian eclogite-facies metamorphism: *Lithos*, v. 27, p. 187-204.
- Barnes, H.L., 1979, Solubilities of ore minerals: In: Barnes, H.L., (ed.) *Geochemistry of Hydrothermal Ore Deposits*. Wiley, New York, p. 404-460.
- Berthelsen, A., and Marker, M., 1986, 1.9-1.8 Ga old strike-slip megashears in the Baltic Shield, and their plate tectonic implications: *Tectonophysics*, v. 128, p. 163-181.
- Bjørlykke A., Cumming, G.L., and Krstic, D., 1990, New isotopic data from davidites and sulfides in the Bidjovagge gold-copper deposit, Finnmark, northern Norway: *Mineral. Petrol.*, v. 43, p. 1-12.
- Bjørlykke, A., Hagen, R., and Söderholm, K., 1987, Bidjovagge Copper-Gold Deposit in Finnmark, Northern Norway: *ECON. GEOL.*, v. 82, p. 2059-2075.
- Bjørlykke, A., Nilsen, K.S., Anttonen, R., and Ekberg, M., 1993, Geological setting of the Bidjovagge deposit and related gold-copper deposits in the northern part of the Baltic Shield: In: Y.T. Maurice (Editor), *Proc. 8th Quadrenn. IAGOD Symp.*, Ottawa, Can. 1990, Schweizerbart'sche, Stuttgart, p. 667-680.
- Borisenko, A.S., 1977, Study of the salt composition of solutions of gas-liquid inclusions in minerals by the cryometric method: *Geol. Geofizika* v. 18, p. 16-27. (English translation).
- Bowers, T.S., and Helgeson, H.C., 1983, Calculation of the thermodynamic and geochemical consequences of nonideal mixing in the system H<sub>2</sub>O-CO<sub>2</sub>-NaCl on phase relations in geologic systems: Equation of state for H<sub>2</sub>O-CO<sub>2</sub>-NaCl fluids at high pressures and temperatures: *Geochim. Cosmochim. Acta*, v. 47, p. 1247-1275.
- Burke, E.A.J., and Lustenhouwer, W.J., 1987, The application of a multichannel laser Raman microprobe Microdil-28: to the analysis of fluid inclusions, *Chem. Geol.*, v. 61, p. 11-17.
- Burrows, D.R., and Spooner, E.T.C., 1990, Archaean intrusion-hosted, stockwork Au-quartz vein mineralization, Lamaque mine, Val d'Or, Quebec: Part I. Geological and fluid characteristics: In: Robert, F., Sheahan, P.A., and Green, S.B., eds., *Greenstone Gold and Crustal Evolution: NUNA Conference Vol.*, Geol. Assoc. Canada, pp. 139-141.
- Burruss, R.C., 1981, Analysis of phase equilibria in C-O-H-S fluid inclusions. *Mineral. Assoc. Canada Short Course Handbook* 6, p. 39-74.
- Cameron, E.M., 1989, Derivation of gold by oxidative metamorphism of a deep ductile shear zone: Part 1. Conceptual model: *J. Geochem. Expl.*, v. 31, p. 135-147.
- Card, K.D., Poulsen, K.H., and Robert, F., 1989, The Archean Superior province of the Canadian Shield and its lode gold deposits: *ECON. GEOL.*, Mon. 6, p. 19-36.

Colvine, A.C., 1989, An empirical model for the formation of Archean gold deposits: Products of final cratonization of the Superior Province, Canada: *ECON. GEOL.*, Mon. 6, p. 37-53.

Crawford, M.L., 1981, Phase equilibria in aqueous fluid inclusions: Mineralogical Association of Canada Short Course Handbook 6, p. 75-100.

Crerar, D.A., and Barnes, H.L., 1976, Ore solution chemistry V. Solubilities of chalcopyrite and chalcocite assemblages in hydrothermal solution at 200° to 350°C: *ECON. GEOL.*, v. 71, p. 772-794.

Cumming, G.L., Krstic, D., Bjørlykke, A., and Åsen, H., (in prep.) Further analysis of radiogenic minerals from the Bidjovagge gold-copper deposit, Finnmark, northern Norway.

Dubessy, J., Poty, B., and Ramboz, C., 1989, Advances in C-O-H-N-S fluid geochemistry based on micro-Raman spectrometric analysis of fluid inclusions: *European Jour. Mineral.*, v. 1, p. 517-534.

Ekberg, M., and Sotka, P., 1991, Production mineralogy and selective mining at Bidjovagge mine, northern Norway: *Int. Con. Appl. Mineral.*, Pretoria, Aust.

Ettner, D.C., Bjørlykke, A., and Andersen, T., 1992, Fluid inclusion study and model of gold transport and deposition from the Bidjovagge Au-Cu mine in Finnmark, Norway: 20th Nordic Geological Winter Meeting, Reykjavík, Iceland Abstracts, p. 38.

Ettner, D.C., Bjørlykke, A., and Andersen, T., 1993, The production of hydrocarbons and precipitation of gold during fluid-rock interaction: A fluid inclusion and stable isotope study of the Bidjovagge gold-copper deposit, Finnmark, northern Norway: *Geofluids 1993*, Torquay, England (extended abstract) p. 455-458.

Ettner, D.C., Bjørlykke, A., and Andersen, T., (in prep. a) Fluid composition of Proterozoic gold and copper deposits: An example from the Bidjovagge gold-copper deposit, Finnmark, northern Norway.

Ettner, D.C., Bjørlykke, A., and Andersen, T., (in prep. b) Fluid evolution and Au-Cu genesis along a shear zone: A regional fluid inclusion study of shear zone-hosted gold and copper mineralization, and alteration, in the Kautokeino greenstone belt, Finnmark, Norway.

Ettner, D.C., Lindblom, S., and Karlsen, D. (in prep. c) High density hydrocarbon fluid inclusions: A comparison of microthermometric, Raman microprobe, and gas chromatographic analysis of fluid inclusions from the Bidjovagge Au-Cu deposit, Finnmark, Norway.

Gatehouse, B.M., Greay, I.E., Campbell, I.H., and Kelly, P., 1978, The crystal structure of loveringite-a new member of the crichtonite group. *Amer. Mineral.* v. 63, p. 28-36.

Goellnicht, N.M., Groves, D.I., McNaughton, N.J., and Dimo, G., 1989, An epigenetic origin for the Telfer gold deposit, Western Australia. *ECON. GEOL.*, Mon. 6, p. 151-167.

Groves, D.I., Barley, M.E., and Ho, S.E., 1989, Nature, genesis, and tectonic setting of mesothermal gold mineralization in the Yilgarn Block, Western Australia: *ECON. GEOL.*, Mon. 6, p. 71-85.

- Groves, D.I., and Foster, R.P., 1991, Archaean lode gold deposits: In: Foster, R.P. (ed.) Gold metallogeny and exploration. London, Blackie, p. 63-103.
- Haas, J.L., 1976, Physical properties of the coexisting phases and thermochemical properties of the H<sub>2</sub>O component in boiling NaCl solutions: U.S. Geol. Surv. Bull., 1421-A, 73 p.
- Hayashi, K., and Ohmoto, H., 1991, Solubility of gold in NaCl- and H<sub>2</sub>S-bearing aqueous solutions at 250-350°C: Geochim. Cosmochim. Acta, v. 55, p. 2111-2126.
- Hees, E.H.P.VAN, and Kesler, S.E., 1990, Geochemistry of fluid inclusions in gold, Porcupine camp, Ontario: In: Robert, F., Sheahan, P.A., and Green, S.B. (eds.) Greenstone Gold and Crustal Evolution: NUNA Conference Vol., Geol. Assoc. Canada, p. 222.
- Henley, R.W., 1973, Solubility of gold in hydrothermal chloride solutions: Chem. Geol., v. 11, p. 73-87.
- Hollander, N.B., 1979, The geology of the Bidjovagge mining field, western Finnmark, Norway: Norsk Geologisk Tidsskrift, v. 59, p. 327-336.
- Holloway, J.R., 1981, Compositions and volumes of supercritical fluids in the earth's crust: Mineralog. Assoc. Canada Short Course Handbook, v. 6, p. 13-38.
- Johnson, J.W., Oelkers, E.H., and Helgeson, H.C., 1991, SUPCRT92: A software package for calculating the standard molal thermodynamic properties of minerals, gases, aqueous species, and reactions from 1 to 5000 bars and 0° to 1000°C: Univ. of California, Berkeley, 101 p.
- Kerkhof, A.M. Van Den, 1990, Isochoric phase diagrams in the systems CO<sub>2</sub>-CH<sub>4</sub> and CO<sub>2</sub>-CH<sub>4</sub> : Application to fluid inclusions: Geochim. Cosmochim. Acta, v. 54, p. 621-629.
- Kerkhof, A.M. Van Den, 1991, Heterogeneous fluids in high-grade siliceous marbles of Pusula (SW Finland): Geologische Rundschau, v. 80, p. 249-258
- Kerrick, R., 1989, Archean gold: Relation to granulite formation or felsic intrusions? Geology, v. 17, p. 1011-1015.
- Kerrick, R. and Feng, R., 1992, Archean geodynamics and the Abitibi-Pontiac collision: implications for advection of fluids at transpressive collisional boundaries and the origin of giant quartz vein systems: Earth Sci. Rev., v. 32, p. 33-60.
- Kimberley, M.M., 1978, High-temperature uranium geochemistry: Mineralog. Assoc. Canada Short Course Handbook, v. 3, p. 101-104.
- Krill, A.G., Kesola, R., Sjöstrand, T., and Stephens, M.B., 1988, Metamorphic, structural and isotopic age map, northern Fennoscandia 1:1,000,000: Geological Surveys of Finland, Norway and Sweden.
- Lindblom, S., 1993, Carbonic fluids and gold mineralization in Precambrian greenstone-hosted gold deposits: Evidence from Kiruna, northern Sweden. Terra Abstracts, v. \_\_, p. 438.
- Lindblom, S., and Martinsson, O., 1990, Fluids associated with Au-Au mineralization in the Kiruna greenstone belt at Viscaria and Pahtohavare, northern Sweden: In: Robert, F., Sheahan, P.A., and Green, S.B., eds., Greenstone Gold and Crustal Evolution: NUNA Conference Vol., Geol. Assoc. Canada, p. 185.

- Martinsson, O., 1992, Greenstone hosted Cu-Au ores, the Viscaria and Pahtohavare sulfide deposits and the stratigraphy of the Kiruna greenstone: Unpub. M.S. thesis, Luleå, Sweden, Luleå Univ. Tech., 79 p.
- Newton, R.C., 1990, Fluids and shear zones in the deep crust: *Tectonophysics*, v. 182, p. 21-37.
- Nguyen, P.T., Booth, S.A., Both, R.A., and James, P.R., 1989, The White Devil gold deposit, Tennant Creek, Northern Territory, Australia: *ECON. GEOL.*, Mon. 6, p. 180-192.
- Nicholls, J., and Crawford, M.L., 1985, FORTRAN programs for calculation of fluid properties from microthermometric data on fluid inclusions: *Computers Geosci.*, v. 11, p. 619-645.
- Nilsen, K.S., and Bjørlykke, A., 1991, Geological setting of the Bidjovagge gold-copper deposit, Finnmark, northern Norway: *Geologiska Föreningens i Stockholm Förhandlingar*, v. 113, p. 60-61.
- Nurmi, P.A., Lestinen, P., and Niskavaara, H., 1991, Geochemical characteristics of mesothermal gold deposits in the Fennoscandian Shield, and a comparison with selected Canadian and Australian deposits: *Geol. Surv. Finland, Bull.* 351, 83 p.
- Olds, R.H., 1953, Critical behavior of hydrocarbons. In: Farkas, A. (ed.) *Physical Chemistry of the Hydrocarbons*, Acad. Press, New York, p. 131-152.
- Olesen, O., Henkel, H., and Lile, O.B., 1991, Major fault zones within the Precambrian Kautokeino Greenstone Belt, Finnmark, Norway: combined interpretation of geophysical data: *Norges geologiske undersøkelse Unpublished Report 90.161*, 26 p.
- Olesen, O., Roberts, D., Henkel, H., Lile, O.B., and Torsvik, T.H., 1990, Aeromagnetic and gravimetric interpretation of regional structural features in the Caledonides of West Finnmark and North Troms, northern Norway. *Norges geologiske undersøkelse* 419, p. 1-24.
- Oreskes, N., and Einaudi, M.T., 1992, Origin of hydrothermal fluids at Olympic Dam: Preliminary results from fluid inclusions and stable isotopes: *ECON. GEOL.*, v. 87, p. 64-90.
- Papst, A., 1961, X-ray crystallography of davidite: *Amer. Mineral.*, v. 46, p. 700-718.
- Pharaoh, T.C., and Brewer, T.S., 1990, Spatial and temporal diversity of early Proterozoic volcanic sequences - comparisons between the Baltic and Laurentian shields: *Precambrian Research*, v. 47, p. 169-189.
- Phillips, G.N., 1990, Nature of Archean gold-bearing fluids in Australian greenstone terrains: In Robert, F., Sheahan, P.A. & Green, S.B. (eds.): *Greenstone Gold and Crustal Evolution: NUNA Conference Volume*, Geological Association of Canada, 192a-192b.
- Potter, R.W. II, Clynne, M.A., and Brown, D.L., 1978, Freezing point depression of aqueous sodium chloride solutions: *ECON. GEOL.*, v. 73, p. 284-285.
- Ramboz, C., Pichavant, M., and Weisbrod, A., 1982, Fluid immiscibility in natural processes: Use and misuse of fluid inclusion data, II. Interpretation of fluid inclusion data in terms of immiscibility: *Chem. Geol.*, v. 37, p. 29-48.

Reed, M.H., and Spycher, N., 1985, Boiling, cooling, and oxidation in epithermal systems: A numerical modeling approach: In Berger, B.R. & Bethke, P.M. (eds.): *Geology and geochemistry of epithermal systems, Reviews in ECON. GEOL.*, v. 2, p. 249-272.

Rich, R.A., Holland, H.D., and Petersen, U., 1977, *Hydrothermal uranium deposits: Amsterdam, Elsevier*, 264 p.

Robert, F., and Kelly, W.C., 1987, Ore-forming fluids in Archean gold-bearing quartz veins at the Sigma mine, Abitibi greenstone belt, Quebec, Canada. *ECON. GEOL.*, v. 82, p. 1464-1482.

Roberts, D.E., and Hudson, G.R.T., 1983, The Olympic Dam copper-uranium-gold deposit: Roxby Downs, South Australia: *ECON. GEOL.*, v. 78, p. 799-822.

Roedder, E., 1971, Metastability in fluid inclusions: Society of Mining Geology Japan, (Proceedings IMA-IAGOD meetings '70, IAGOD Volume) Special Issue 3, p. 327-334.

Roedder, E., 1984, Fluid Inclusions: In: Ribbe, P.H. (ed.) *Reviews in Mineralogy*, v. 12, 646 p.

Sandstad, J.S., 1983, Berggrunnsgeologisk kartlegging av prekambrisk grunnfjell innen kartbladet Mållejus, Kvænangen/Kautokeino, Troms/Finnmark: Norges geologiske undersøkelse report 84.095, p. 73-76.

Sandstad, J.S., 1992, Kautokeinogrønnsteinsbeltet - Berggrunnskart 1:100,000: Norges geologiske undersøkelse.

Seward, T.M., 1991, The hydrothermal geochemistry of gold: In: Foster, R.P. (ed.) *Gold metallogeny and exploration*. London, Blackie, p. 37-62.

Siedlecka, A., Iversen, I., Krill, A.G., Lieungh, B., Often, M., Sandstad, J.S., and Solli, A., 1985, Lithostratigraphy and correlation of the Archean and Early Proterozoic rocks of Finnmarksvidda and the Sørvaranger district. *Norges geologiske undersøkelse* 403, p. 7-36.

Skiöld, T., 1988, Implications of new U-Pb zircon chronology to early Proterozoic crustal accretion in northern Sweden: *Precambrian Research*, v. 8, p. 147-164.

Sollid, K., and Torske, T., 1993, Karbonat-evaporittavsetninger i bunnen av den Proterozoiske Alta-Kautokeino riften., *Geonytt*, v. 20, p. 45.

Tanger, J.C. IV, and Pitzer, K.S., 1989, Thermodynamics of NaCl-H<sub>2</sub>O: A new equation of state for the near-critical region and comparison with other equations for adjoining regions: *Geochim. Cosmochim. Acta*, v. 53, p. 973-987.

Trommsdorff, V., and Skippen, G., 1988, Brines and metasomatism. *Rendiconti della Società Italiana di Mineralogia e Petrologia*, v. 43, p. 15-24.

Walsh, J.F., Kesler, S.E., Duff, D., and Cloke, P.L., 1988, Fluid Inclusion geochemistry of high-grade, vein-hosted gold ore at the Pamour mine, Porcupine camp, Ontario: *ECON. GEOL.*, v. 83, p. 1347-1367.

Weast, R.C., Astle, M.J., and Beyer, W.H. (eds.), 1988, *Handbook of chemistry and physics*, 6th ed. CRC Press, Boca Raton, Florida.

Wedekind, M.R., Large, R.R., and Williams, B.T., 1989, Controls on high-grade mineralization at Tennant Creek, Northern Territory, Australia: *ECON. GEOL.*, Mon. 6, p. 168-179.

Wood, P.C., Burrows, D.R., Thomas, A.V., and Spooner, E.T.C., 1986, The Hollinger-McIntyre Au-quartz vein system, Timmons, Ontario, Canada; Geological characteristics, fluid properties and light stable isotope geochemistry. In: Macdonald, A.J. (ed.) *Proceedings of Gold '86, an International Symposium on the Geology of Gold*: Toronto, 1986, pp. 56-80.

### Figure Captions

**Figure 1:** Generalized geologic map of the northwest portion of the Baltic Shield including areas of northern Norway, Sweden and Finland. After Krill et al. (1988), Olesen et al., (1991) and Bjørlykke et al. (1992).

**Figure 2:** Geologic map of the Bidjovagge antiform with location of individual ore lenses along shear zones on the eastern limb of the antiform. Modified from Nilsen and Bjørlykke (1991).

**Figure 3:** Syenodiorite dikes. A.) Sharp contact between syenodiorite and albite felsite. Note that syenodiorite does not display shear texture, but crosscuts shear texture in albite felsite. B.) Syenodiorite lens with open spaced fractures filled with carbonate-sulfide gangue.

**Figure 4:** Oxidation front to graphitic schist. A.) Outcrop scale oxidation front within a open pit at Bidjovagge. B.) Small scale oxidation fronts along veinlets within drill core. Scale bar = 5 cm.

**Figure 5:** Profiles through gold mineralized areas at Bidjovagge showing zonation of magnetite + pyrite, to pyrite, to pyrite + pyrrhotite, and also chalcopyrite mineralization along 5 drill holes. Note that pyrite + pyrrhotite zone occurs along the

boundaries to the graphitic schist and the magnetite + pyrite occurs within the footwall of the mineralized zone. Grid is in meters.

**Figure 6:** Gold-rich mineralization-related oxidized albite felsite with pyrite + quartz gangue displaying ductile shear fabric. Scales = 5 cm.

**Figure 7:** Copper-rich mineralization with chalcopyrite filling brecciated albite felsite. Scales = 5 cm.

**Figure 8:** Composite photos of the main fluid inclusion types found at Bidjovagge, photographed at room temperature and different focal levels. Scale bars: 0.05 mm.

**Figure 9:** Microthermometric data for CO<sub>2</sub>-rich inclusions. A.) Homogenization to liquid of pure CO<sub>2</sub> inclusions. B.) Final melting and homogenization to liquid of CO<sub>2</sub> + CH<sub>4</sub> inclusions.

**Figure 10:** Microthermometric data of CH<sub>4</sub>-rich inclusions, with homogenization to liquid temperatures above the baseline and gas melting, and sublimation to liquid temperatures for "S" type inclusions (VAN DEN Kerkhof, 1990) below the baseline.

**Figure 11:** Typical Raman microprobe spectra for CH<sub>4</sub> + LHC inclusions from the gold-rich ore zone at Bidjovagge. The CH<sub>4</sub> peak occurs between  $\Delta\nu=2911.5$  to  $2912.2\text{cm}^{-1}$ , ethane around  $\Delta\nu=2951\text{cm}^{-1}$ , and a possible propane peak around  $\Delta\nu=2892.3$  to  $2893\text{cm}^{-1}$ . Typically a "mound" occurs around the hydrocarbon peaks.

**Figure 12:** Low temperature microthermometric data for ice and salt hydrate melting of salt saturated aqueous solutions related to gold-rich mineralization.

**Figure 13:** High temperature microthermometric data for salt saturated aqueous solutions related to gold-rich mineralization. A.) salt dissolution temperature. B.) homogenization of the aqueous solution + vapor to liquid usually in the presence of a salt crystal.

**Figure 14:** Low temperature microthermometric data for ice and salt hydrate melting of saline aqueous solutions related to copper-rich mineralization. "S" denotes inclusions measured from apatite crystals within syenodiorite dikes.

**Figure 15:** High temperature microthermometric data for saline aqueous solutions related to copper-rich mineralization. A.) Temperatures of homogenization of saline aqueous solution + vapor to liquid and rare salt dissolution measurements in vein-hosted fluid inclusions. B.) Temperatures of homogenization of saline aqueous solution + vapor to liquid of fluid inclusions in apatite crystal within syenodiorite intrusion.

**Figure 16:** Profile of the "D" ore body at Bidjovagge showing detection of light hydrocarbons within samples collected along 3 drill cores. Grid is in meters.

**Figure 17:** Gas chromatograms of three samples analysed for light hydrocarbons from Bidjovagge. A.) Separated vein carbonate. B.) Separated vein quartz. C.) Whole rock analysis of albite felsite from the ore zone.

**Figure 18:** a.) Pressure vs. temperature diagram with constructed isochores for different  $H_2O + salt$ ,  $H_2O + CO_2 + salt$ ,  $CO_2$ ,  $CH_4$ , and  $CO_2 + CH_4$  inclusions at Bidjovagge. b.) Interpretation of isochore data showing trapping conditions for fluids related to both Au- and Cu-rich mineralization, and a possible fluid path as fluids moved through the ductile-brittle transition.

**Figure 19:** Carbon and oxygen isotope compositions of carbonates from different lithologies, ore zones and veins at Bidjovagge. Carbon isotopes are standardized to PDB and oxygen isotopes are standardized to SMOW.

**Figure 20:** Sulfur isotope compositions of pyrrhotite, pyrite and chalcopyrite from different ore zones and veins at Bidjovagge.

**Figure 21:** Schematic model of fluid evolution and mineralization at Bidjovagge. An oxidizing CO<sub>2</sub> and saline brine carrying Au as chloride complexes moves up along shear zone and oxidizes the graphitic schists producing CH<sub>4</sub> and resulting in gold precipitation.

**Figure 22:** Log  $f_{O_2}$  vs. pH diagram for the Fe-S-O system, showing phase relationships calculated for 350°C and 3 kbar with SUPCRT92 (Johnson et al., 1991). CH<sub>4</sub>-CO<sub>2</sub>-HCO<sub>3</sub><sup>-</sup> equilibrium shown as short dashed lines. Solubilities of AuCl<sub>2</sub><sup>-</sup> are shown as solid lines in ppm, calculated at 350°C with a log K of -2.5 (Hayashi and Ohmoto, 1991). CuCl solubilities, in ppm, shown as long dashed lines (Data from Crerar and Barnes, 1976). Fluid composition used in diagram include  $\Sigma S=0.01m$ , and 25 wt % NaCl (Cl<sup>-</sup>=5.7m). Arrows shows possible fluid path during gold and copper mineralization; A.) Fluids decrease in pH and  $f_{O_2}$  during phase separation and buffering by the pyrite-magnetite-hematite assemblage, B.) A dramatic drop in  $f_{O_2}$  during red-ox reaction with graphitic schist results in gold precipitation together with a pyrite-pyrrhotite assemblage.

Table 1: Systematic classification of primary and pseudosecondary fluid inclusions observed, at room temperature, from the Bidjovagge deposit.

Non-aqueous liquid-rich	CO <sub>2</sub> -rich	pure CO <sub>2</sub>	without H <sub>2</sub> O	Au <sup>I</sup>
			with H <sub>2</sub> O	
		CO <sub>2</sub> + CH <sub>4</sub>	without H <sub>2</sub> O	Au <sup>II</sup>
			with H <sub>2</sub> O	
	CH <sub>4</sub> -rich	pure CH <sub>4</sub>	without H <sub>2</sub> O	Au <sup>III</sup>
			with H <sub>2</sub> O	S
		CH <sub>4</sub> + CO <sub>2</sub>	without H <sub>2</sub> O	Au <sup>III</sup>
			with H <sub>2</sub> O	
	CH <sub>4</sub> + LHC	without H <sub>2</sub> O	Au <sup>III</sup>	
		with H <sub>2</sub> O		
H <sub>2</sub> O-rich	pure H <sub>2</sub> O	without gas		
		with CO <sub>2</sub>		
		with CH <sub>4</sub>		
	H <sub>2</sub> O undersaturated with salt	H <sub>2</sub> O vapor or without vapor		Cu + S
			with CO <sub>2</sub>	
			with CH <sub>4</sub>	
	H <sub>2</sub> O saturated with salt	H <sub>2</sub> O vapor		Au <sup>I</sup> & II
		with CO <sub>2</sub>	Cu	
		with CH <sub>4</sub>	Au <sup>I</sup> Au <sup>II</sup>	

Au = fluid inclusions related to gold-rich mineralization, I, II, & III refer to three groups discussed by Ettner et al. (in prep. a) (see text), Cu = fluid inclusions related to copper-rich mineralization, S = fluid inclusions related to syenodiorites, LHC = light hydrocarbons.

Table 2

Deposit	Mineralization	Fluid Inclusion Type	Salinity wt. %, NaCl eq.	Host Rocks	Alteration
Bidjovagge, Norway <sup>1</sup>	4.1 g/t Au, 1.19% Cu (U-Th) (mag, py, po, chalc)	H <sub>2</sub> O + CO <sub>2</sub> + salt + CH <sub>4</sub> /LHC	25 - 43	Albitized graphitic schist	Albitization, carbonatization, & scapolitization
Pahtohavare, Sweden <sup>2,3,4</sup>	1.3 ppm Au, 2% Cu (mag, py, po, chalc <sphal)	H <sub>2</sub> O + CO <sub>2</sub> + salt + <N <sub>2</sub>	<40	tholeiitic basalt, tuffites, & black schists	Albitization, scapolitization & biotitization
Saattopora, Finland	3.0 g/t Au, 0.7% Cu (U-Th) (py, po, chalc)			metavolcanic & metasedimentary rocks	Albitization, carbonatization, sulfidization, & hydration
Telfer, Australia <sup>5</sup>	<28.7 ppm Au, <1% Cu (py, po, chalc)	H <sub>2</sub> O + CO <sub>2</sub> + salt	21 - 54	sandstones, siltstones, & carbonaceous sediments	silicification, sericitization, & tourmalinization
White Devil-Tennant Ck. <sup>6</sup> Australia	< 1000 g/t Au, 17.6 g/t Cu (Bi) (mag, py, chalc, marcasite, bismuthite, molybdenite)	H <sub>2</sub> O + salt	5 - 22	siliciclastic sedimentary rocks	chloritization & magnetite
Olympic Dam, Australia <sup>7,8</sup>	0.6 g/t Au, 1.6% Cu (Ag + U) (mag, py, hematite)	H <sub>2</sub> O + CO <sub>2</sub> + salt	7.3 - 42	granite breccia	sericitization & hematitic

References: <sup>1</sup>Ekberg and Sotka (1991) <sup>2</sup>: Lindblom and Martinsson (1990), <sup>3</sup>: Martinsson, 1992, <sup>4</sup>Lindblom (1993), <sup>5</sup>Goellnicht et al. (1989), <sup>6</sup>Nguyen et al. (1989), <sup>7</sup>Roberts and Hudson (1983), <sup>8</sup>Oreskes and Einaudi (1992).

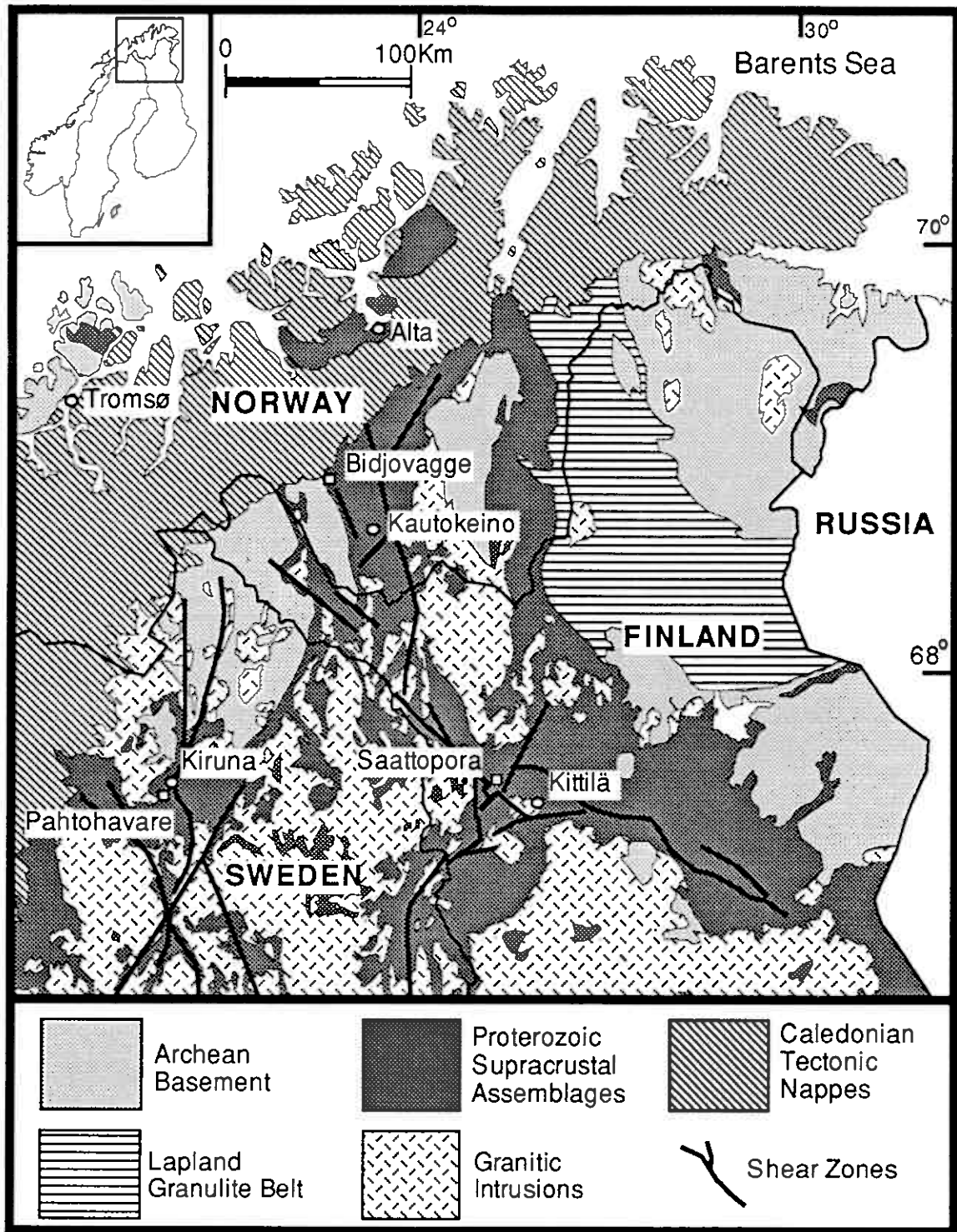


Fig. 1

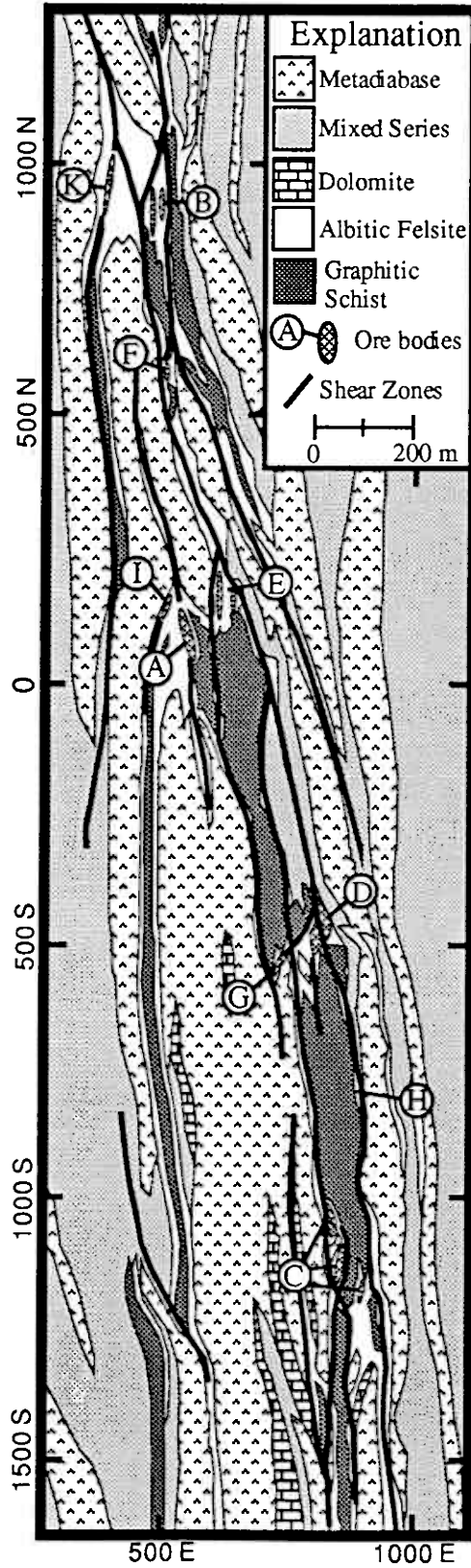
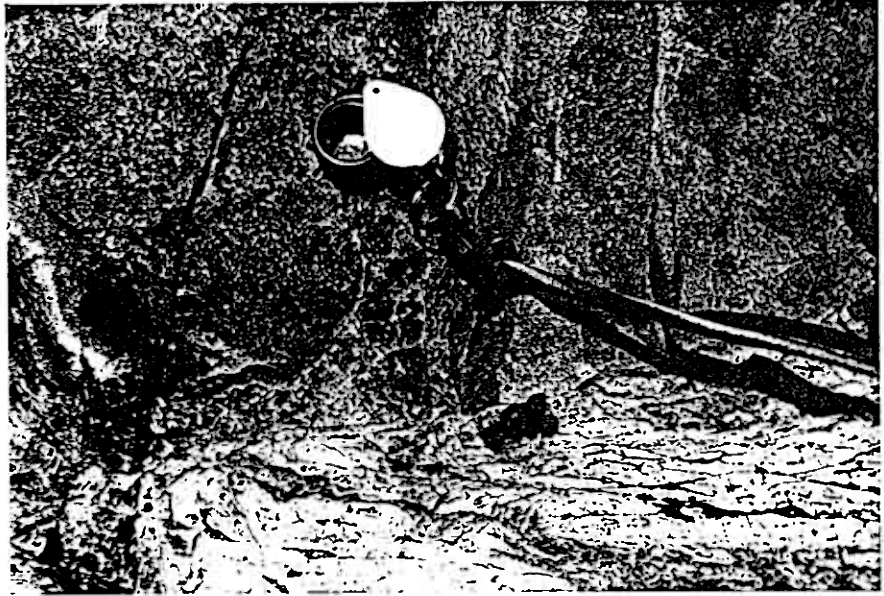


Fig. 2

A



B

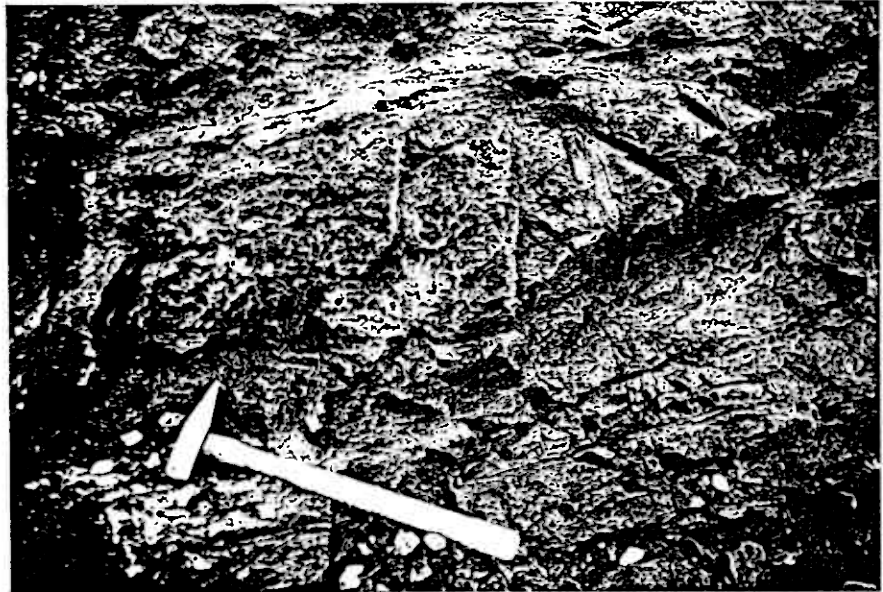
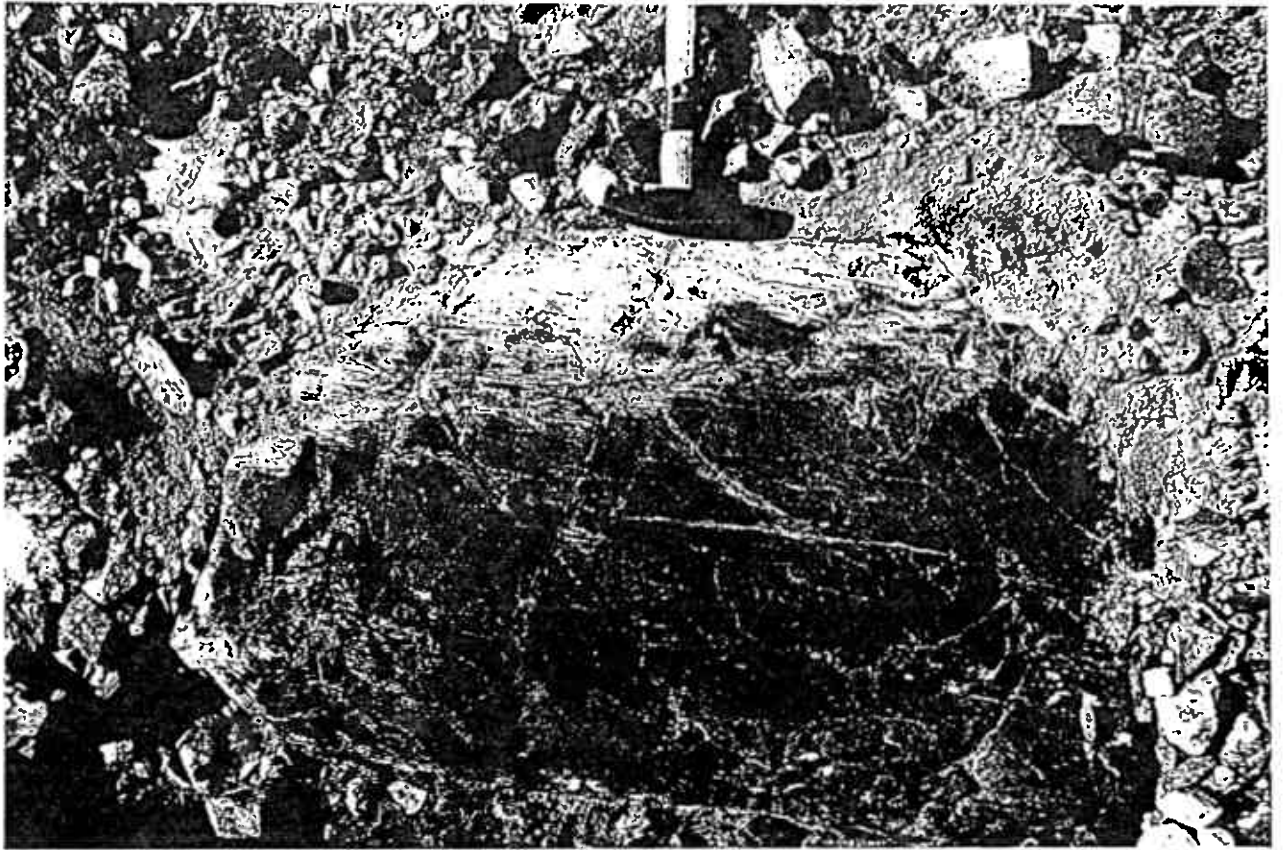


Fig. 3

A



B



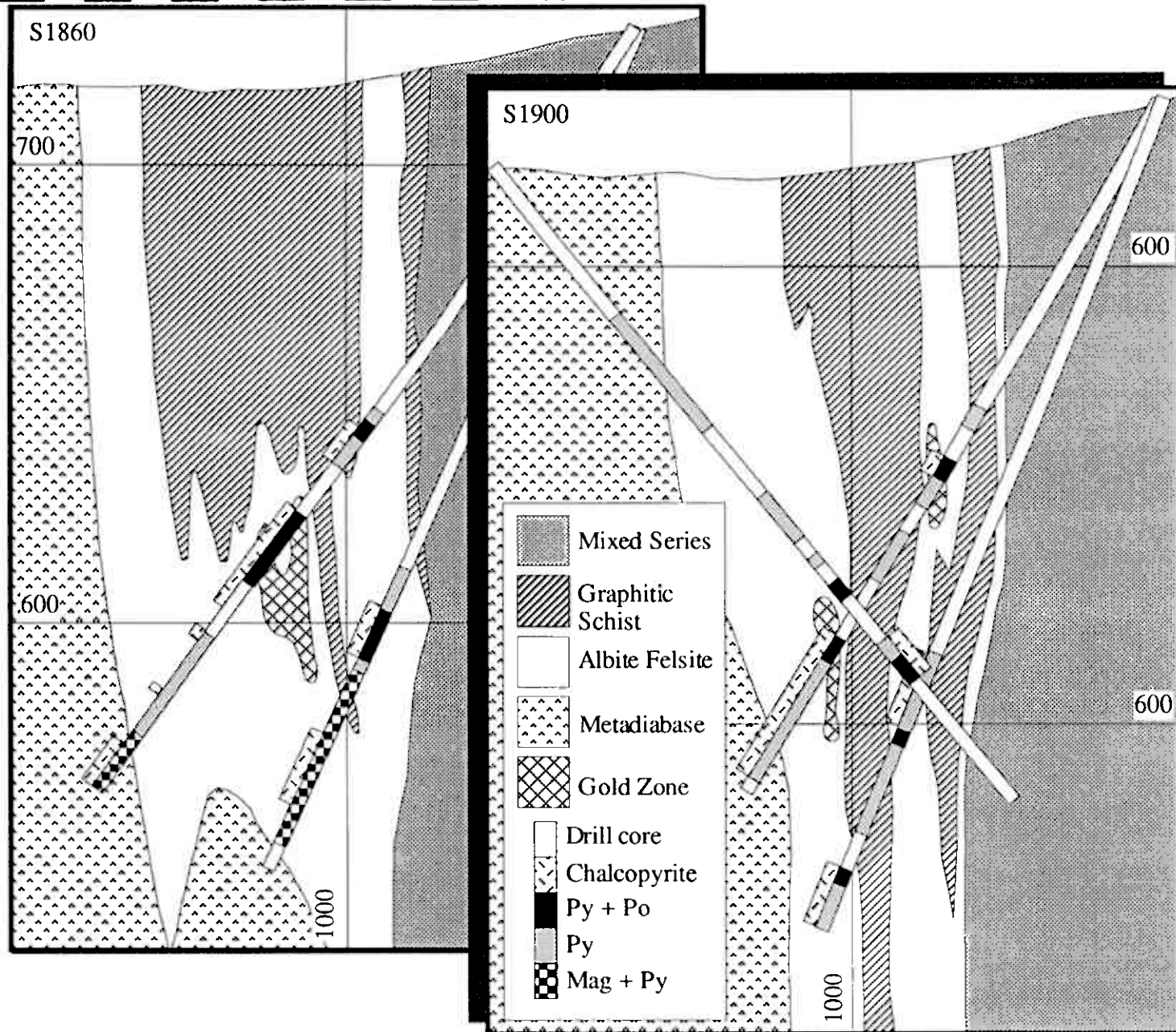


Fig. 5

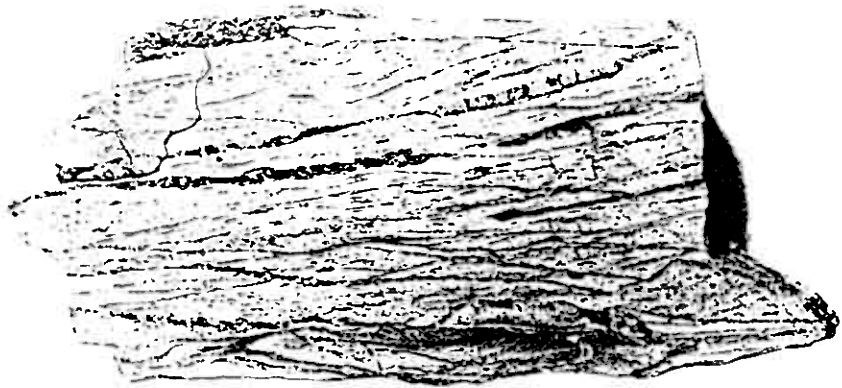


Fig. 6

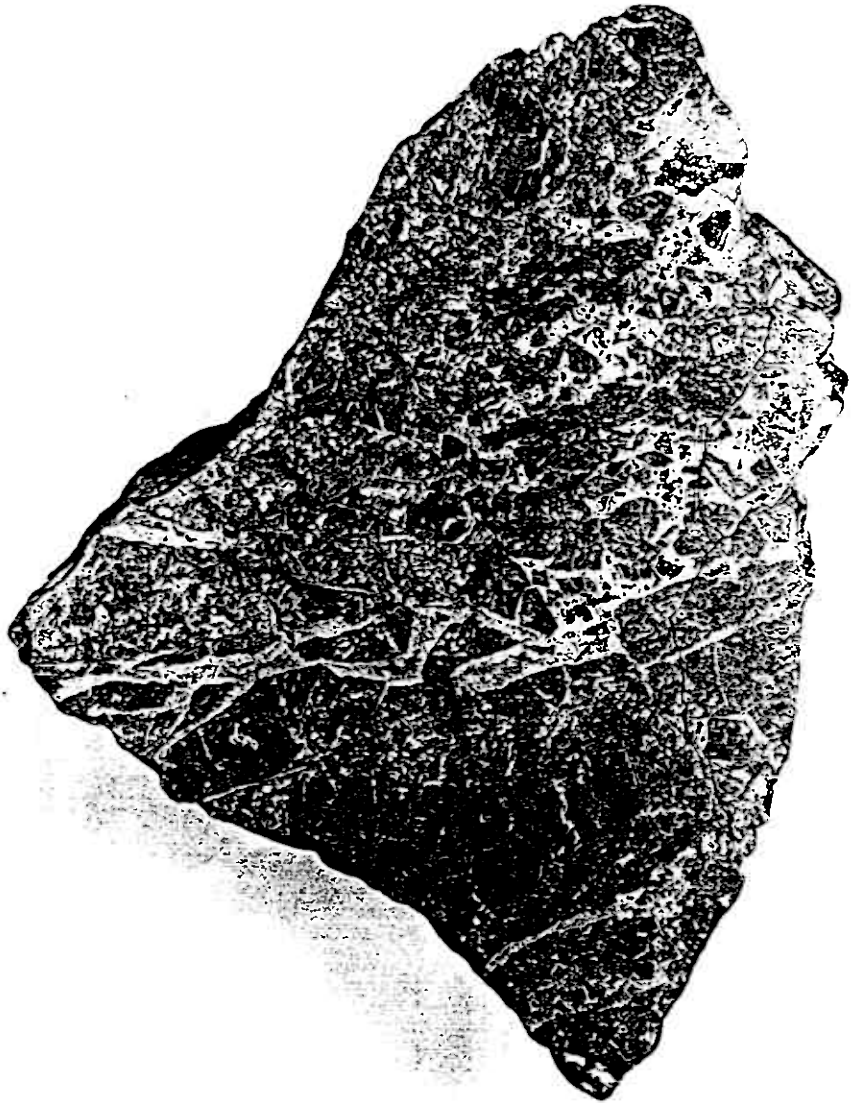
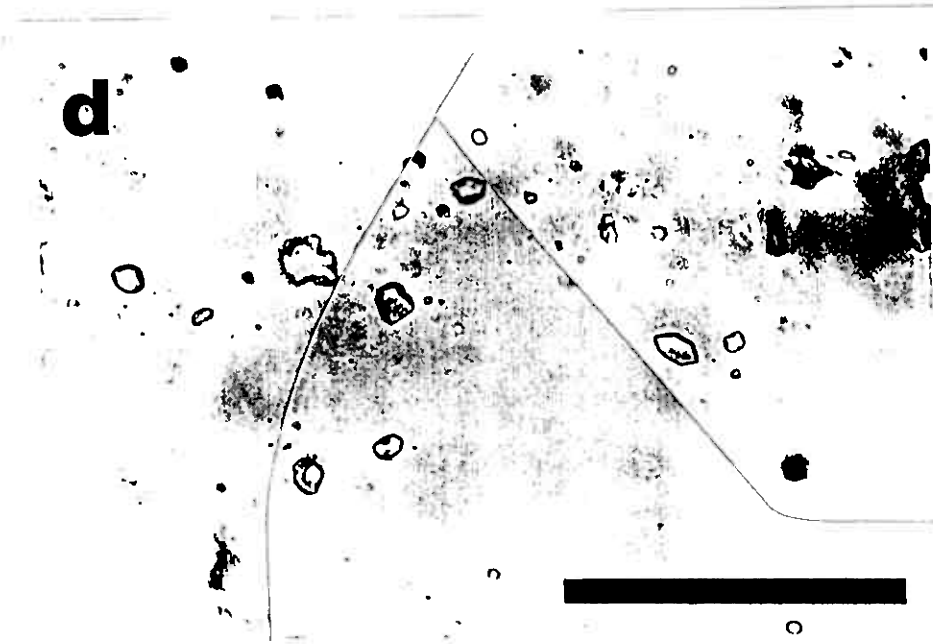
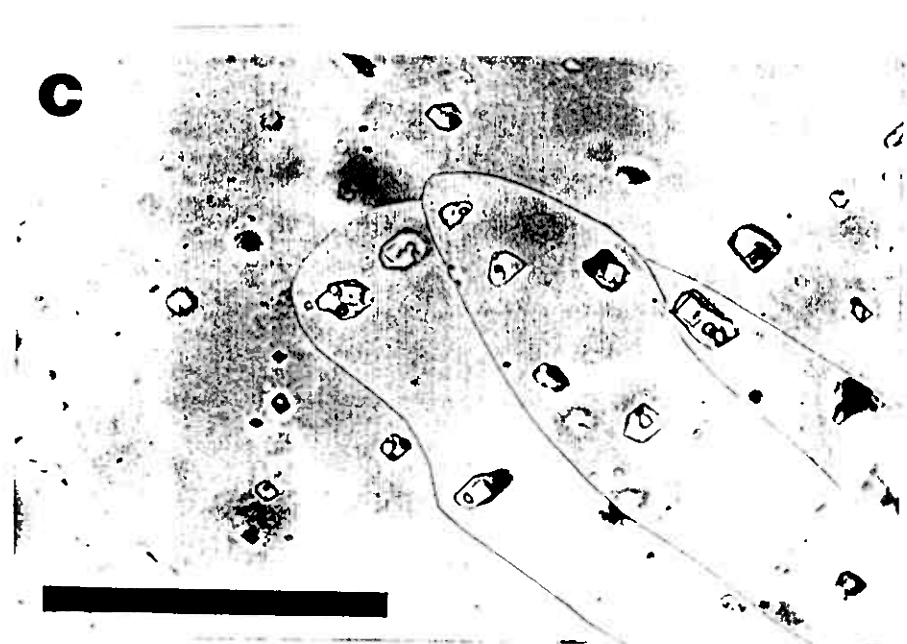
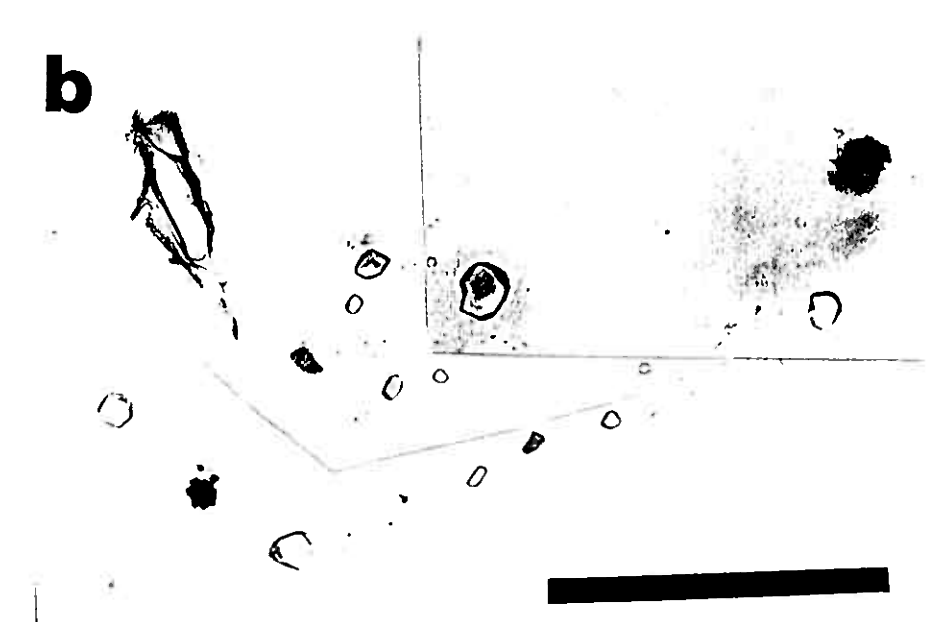
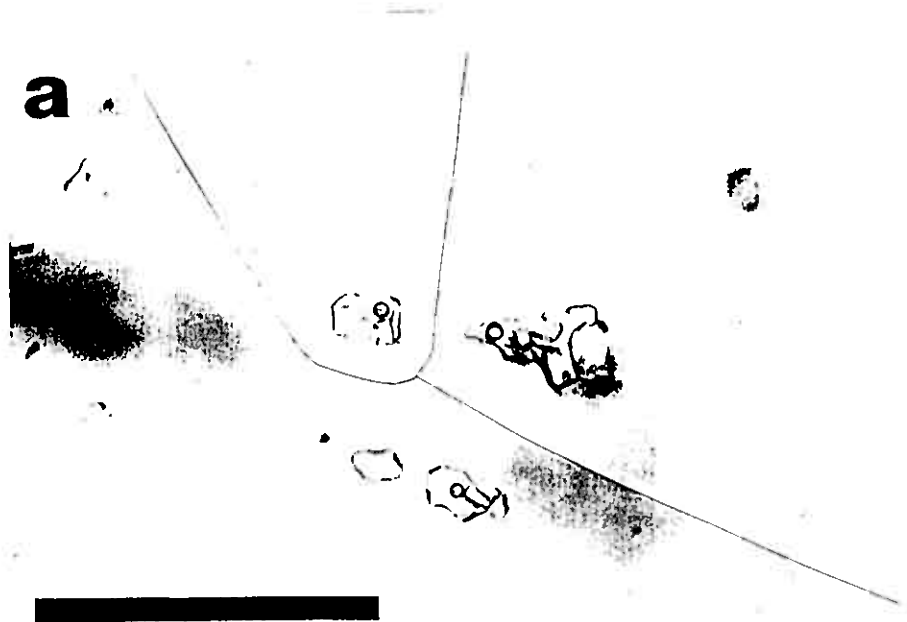
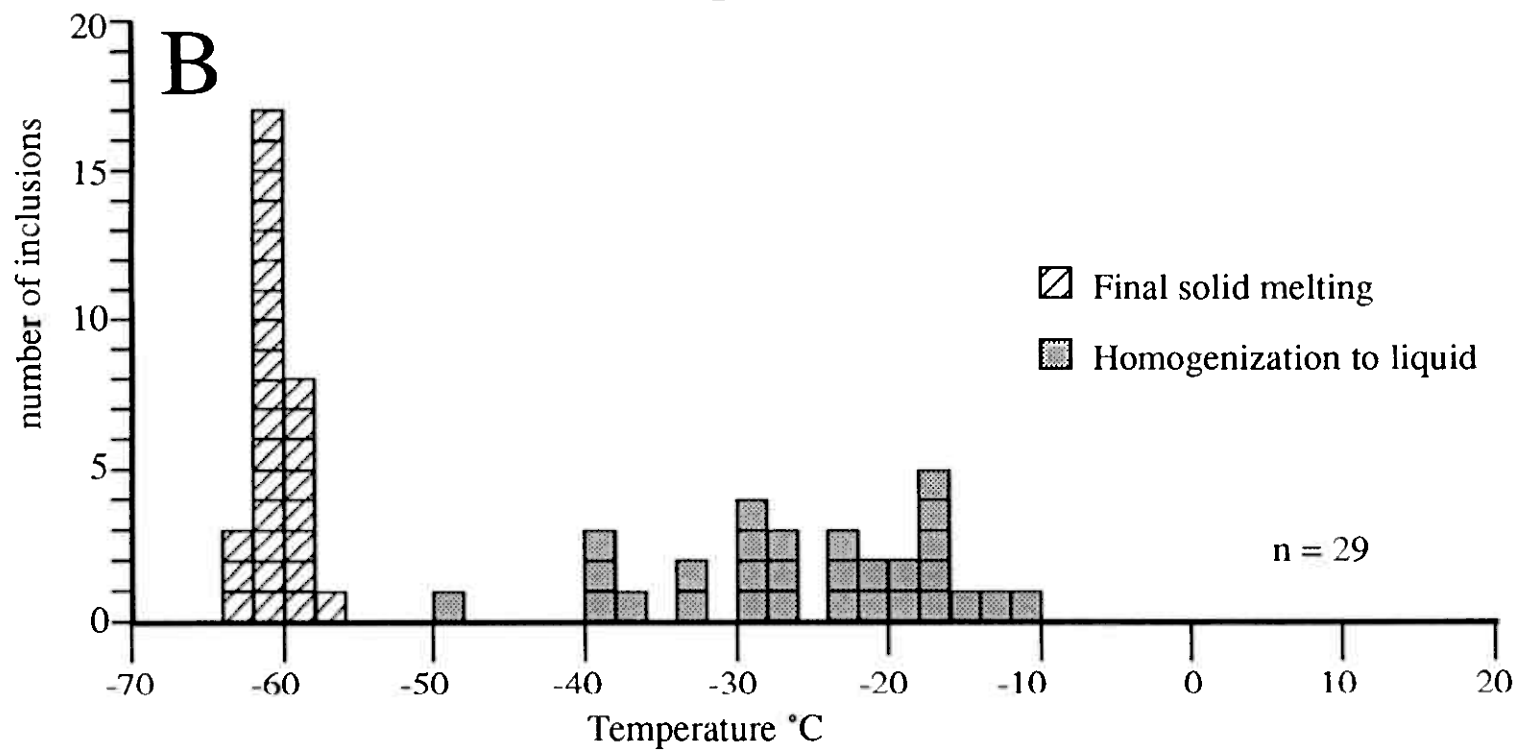
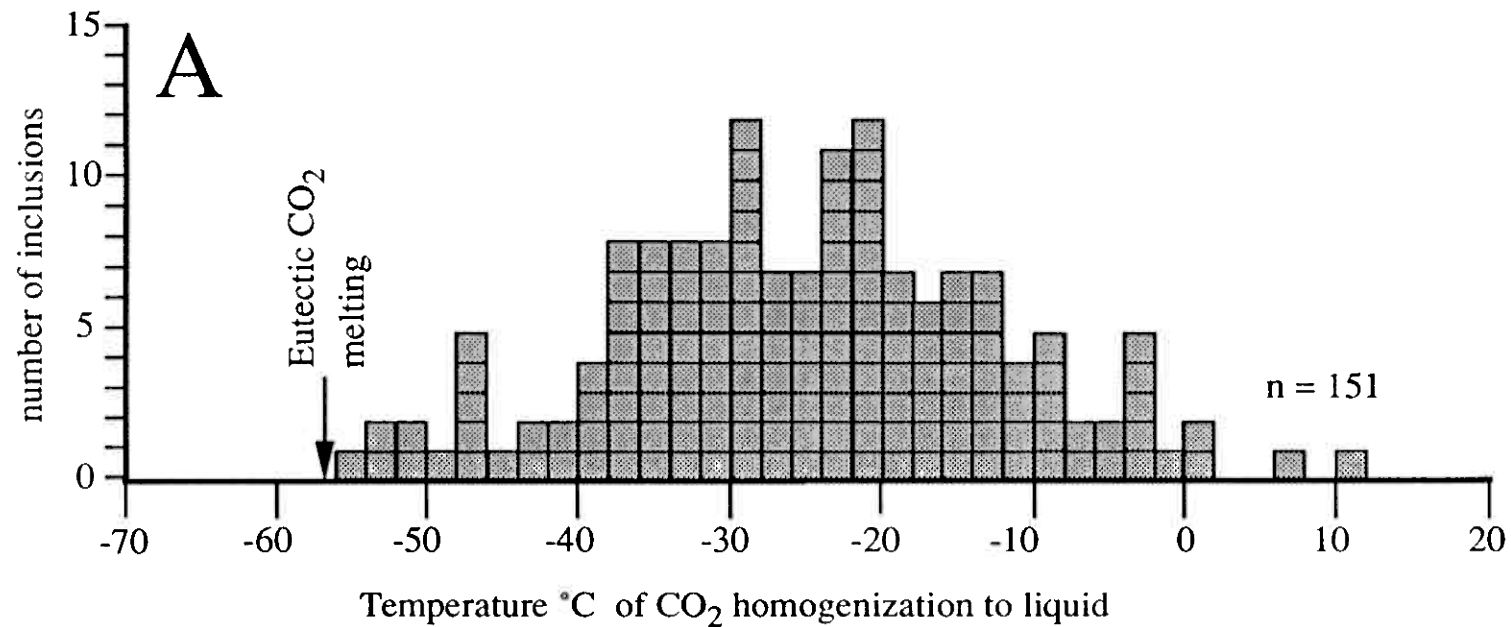
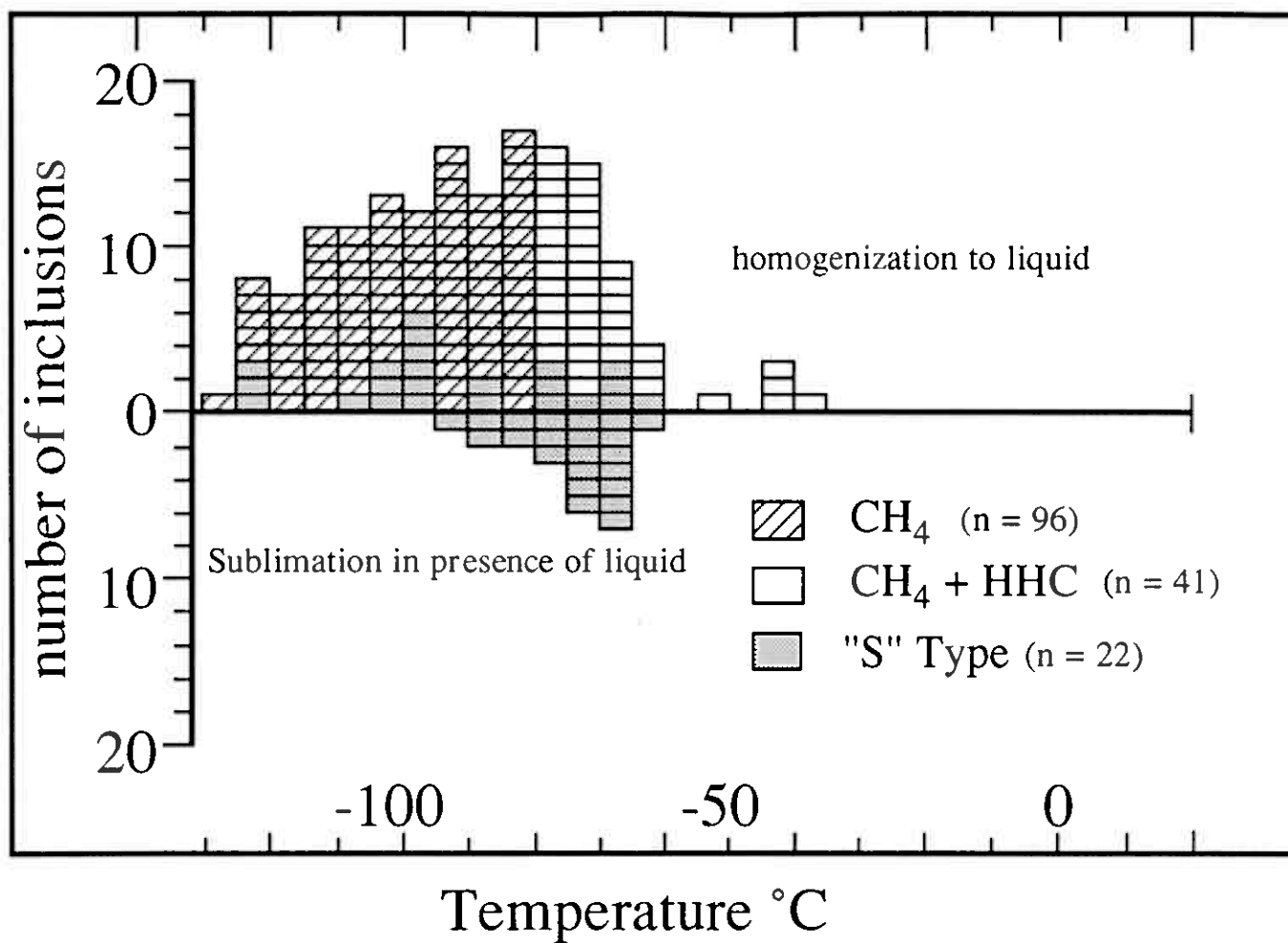


Fig. 7







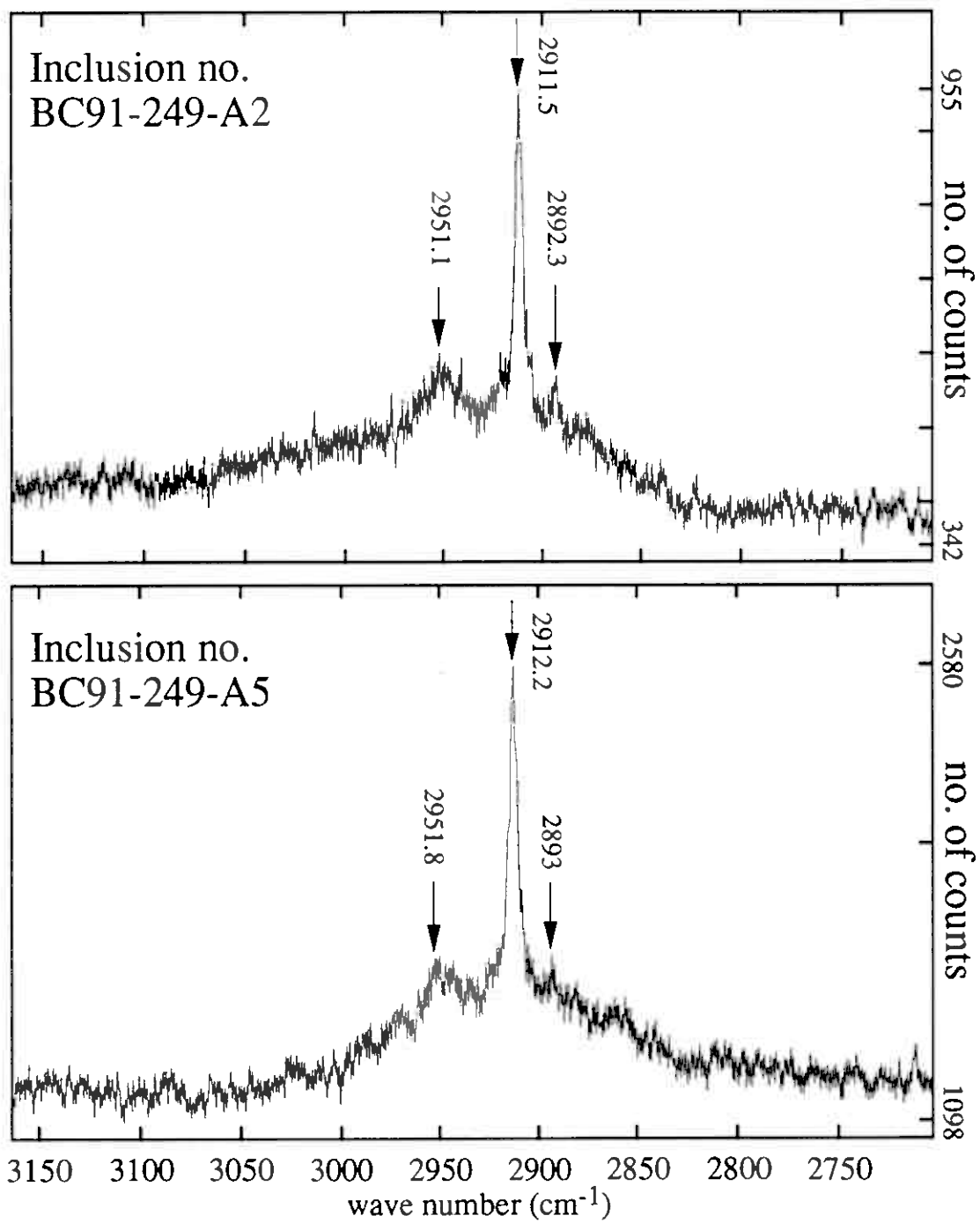


Fig. 11

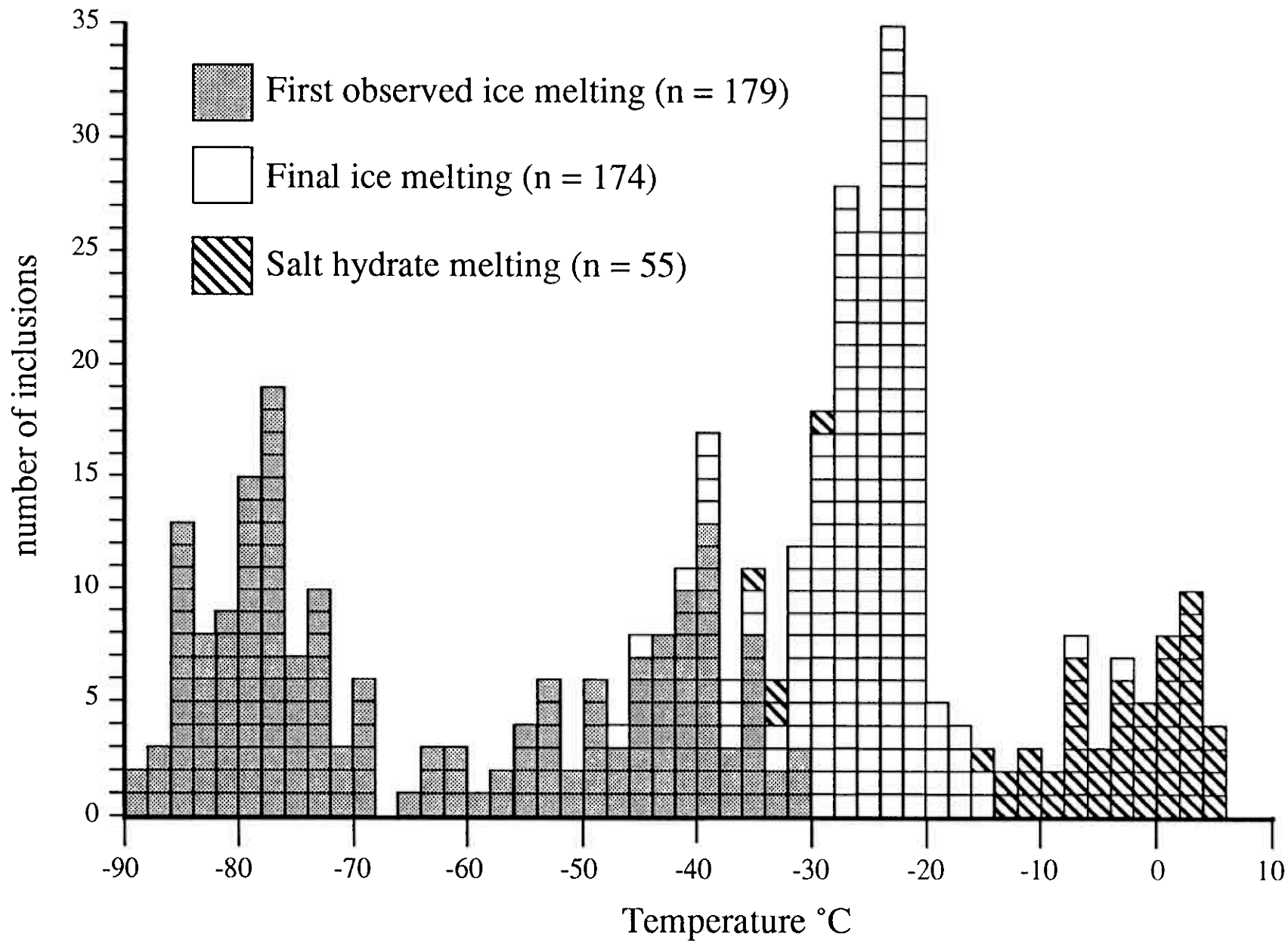
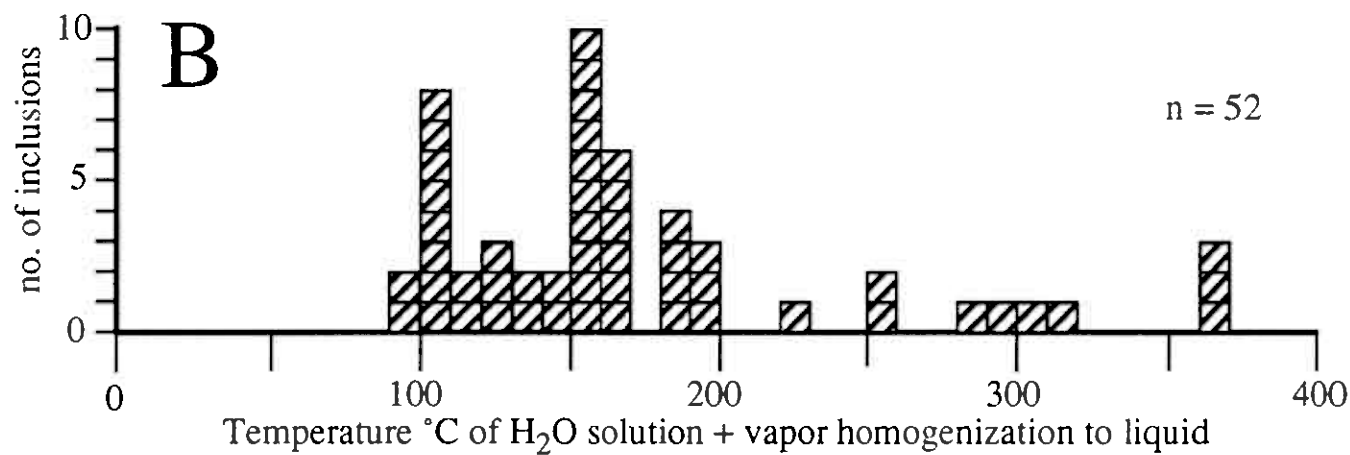
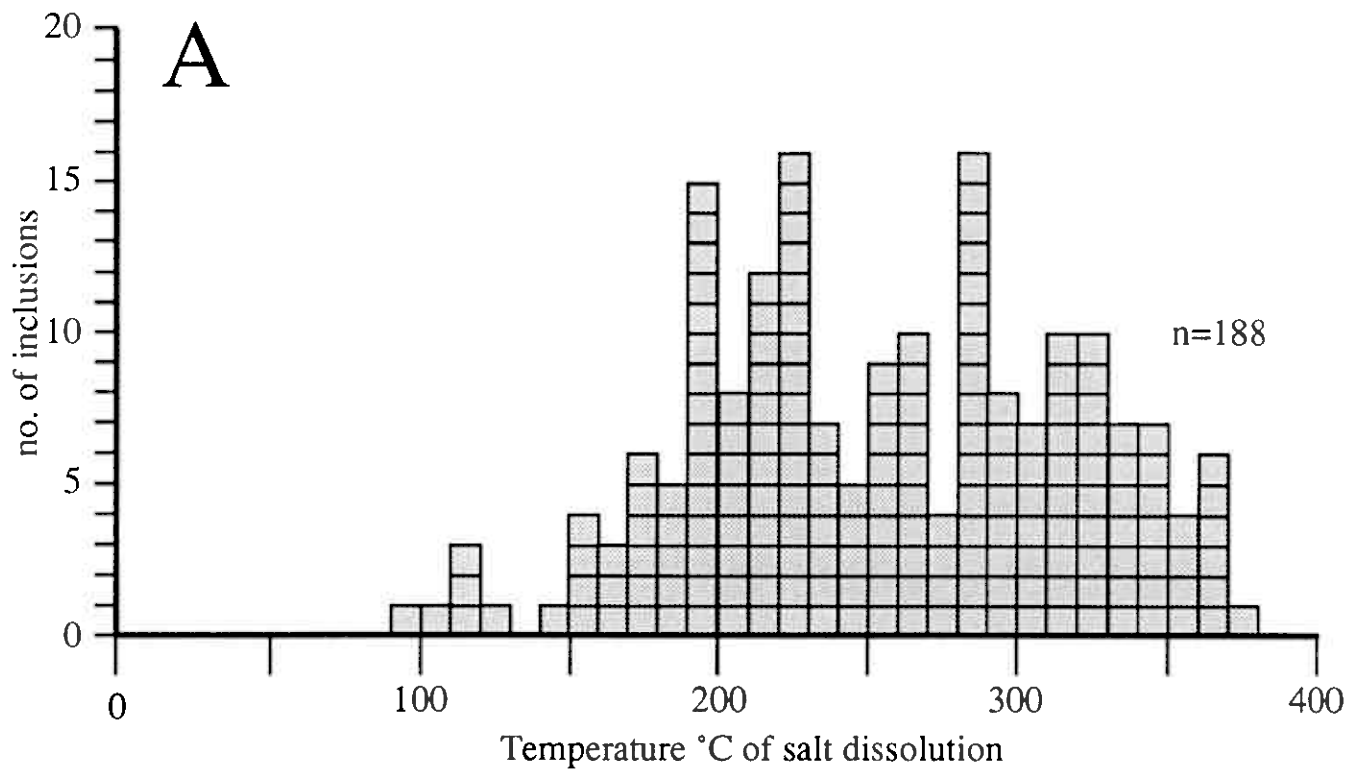


Fig. 12



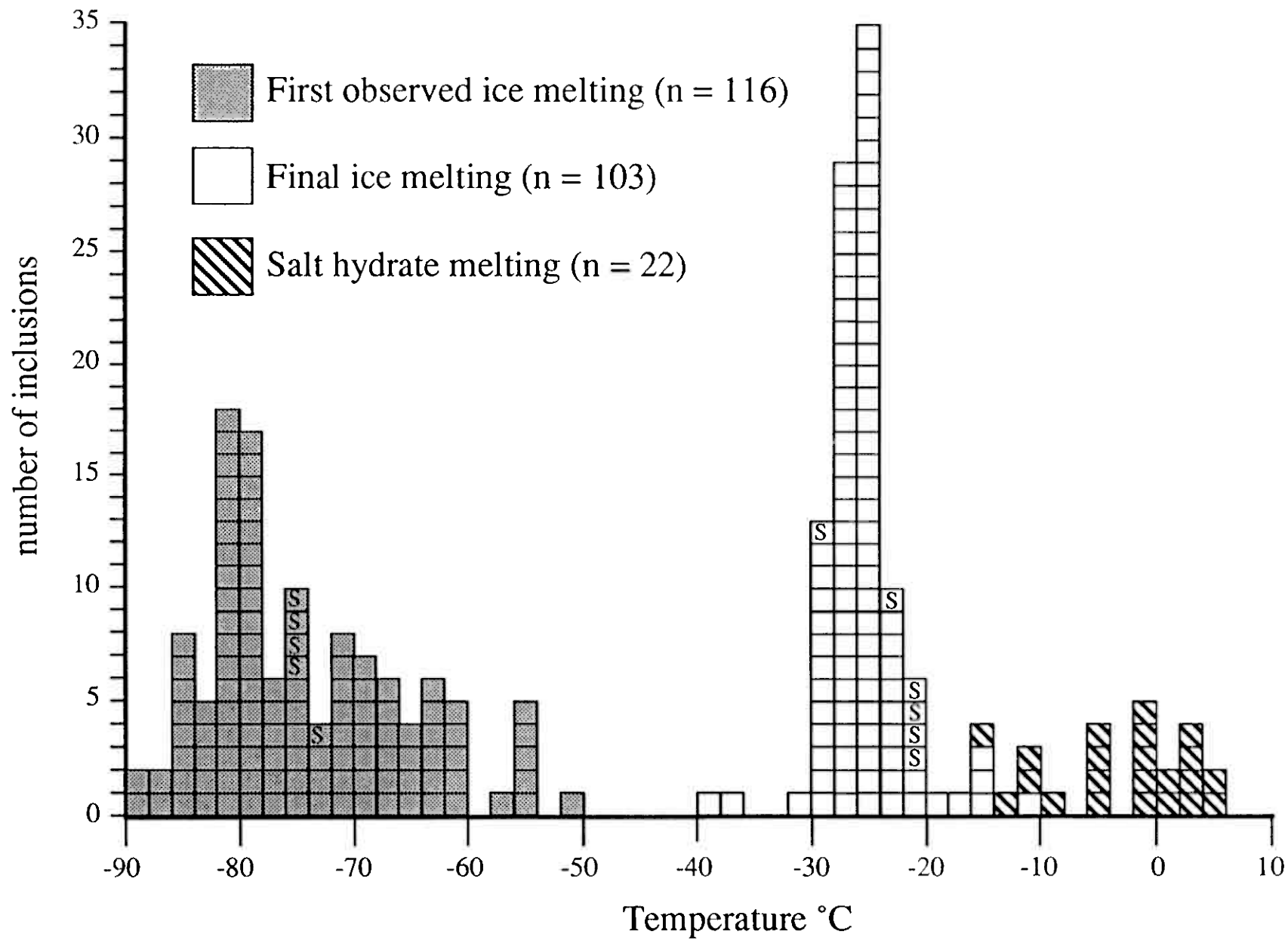
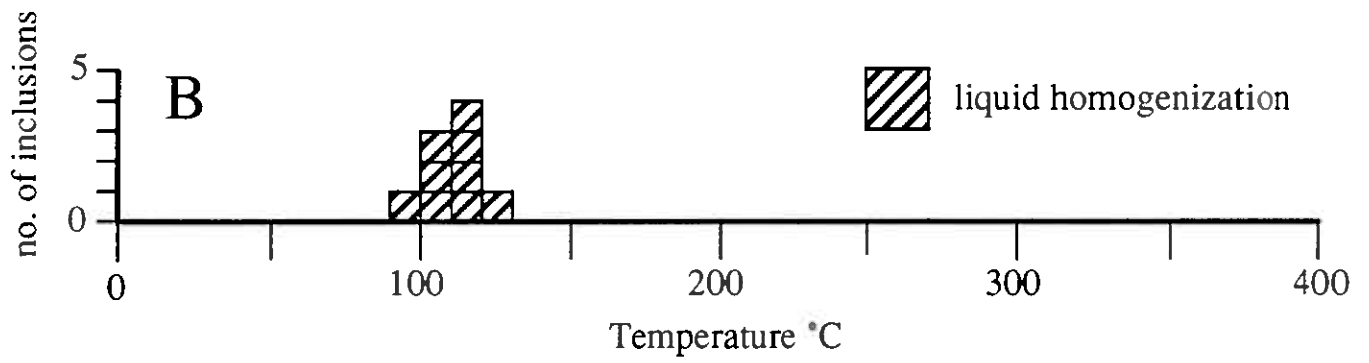
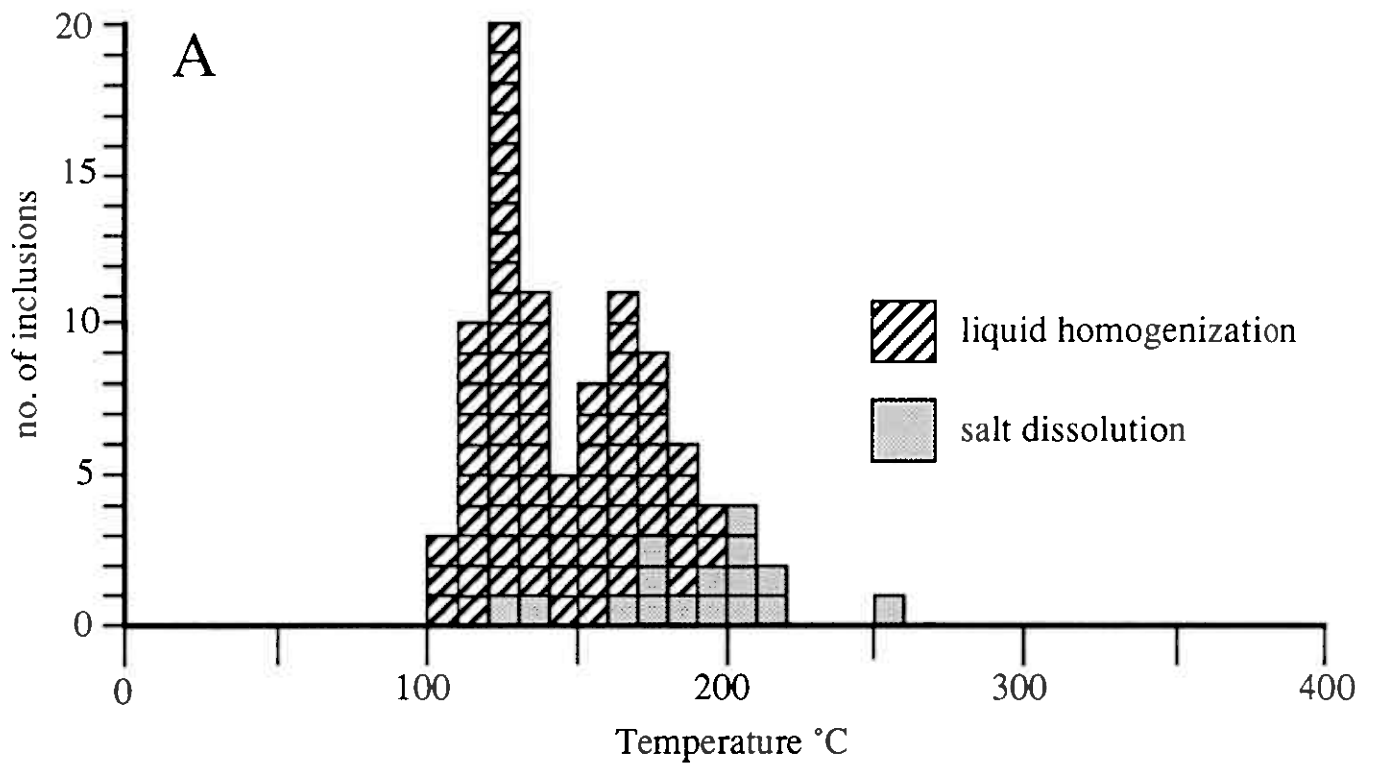


Fig. 14



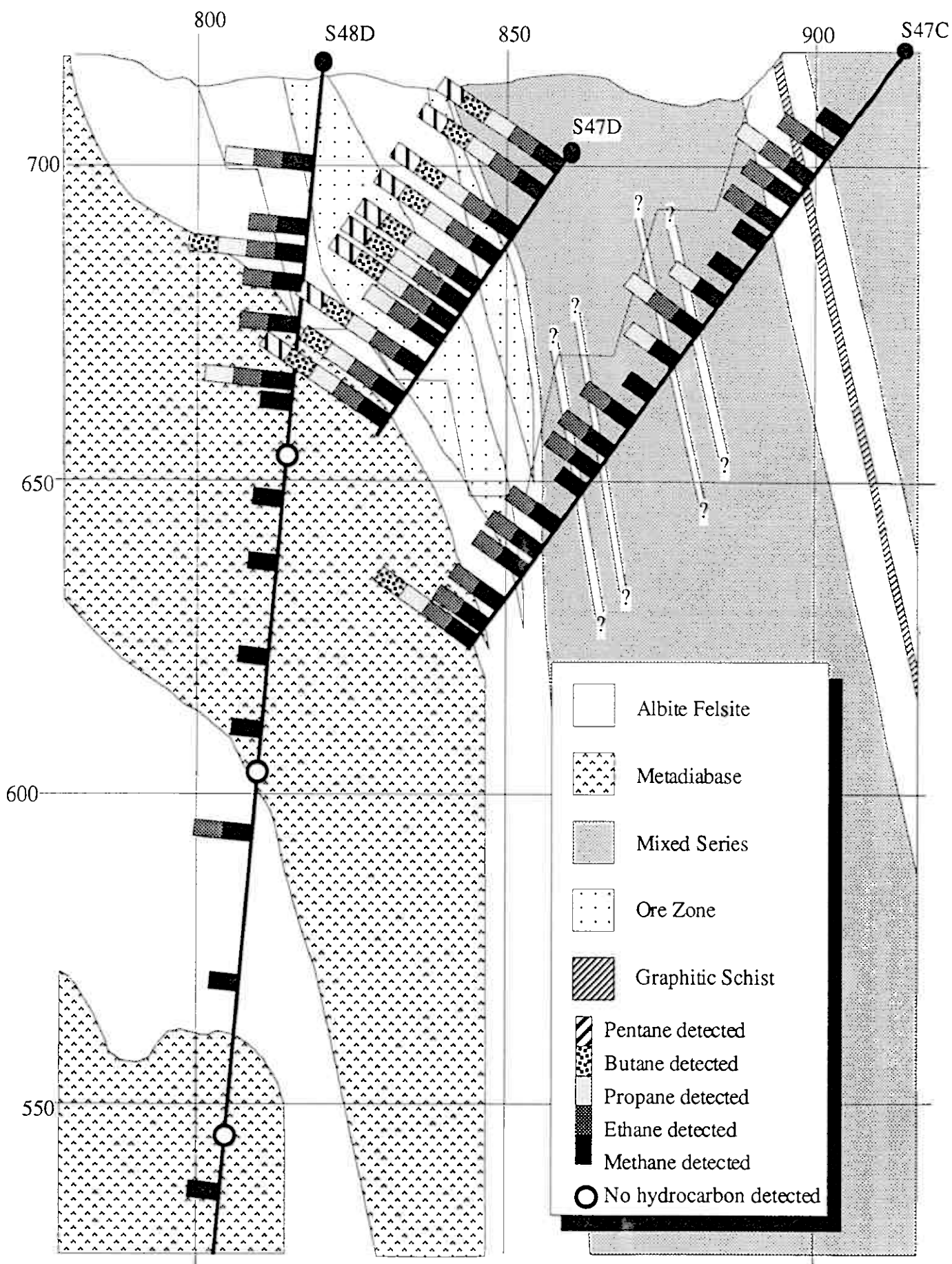
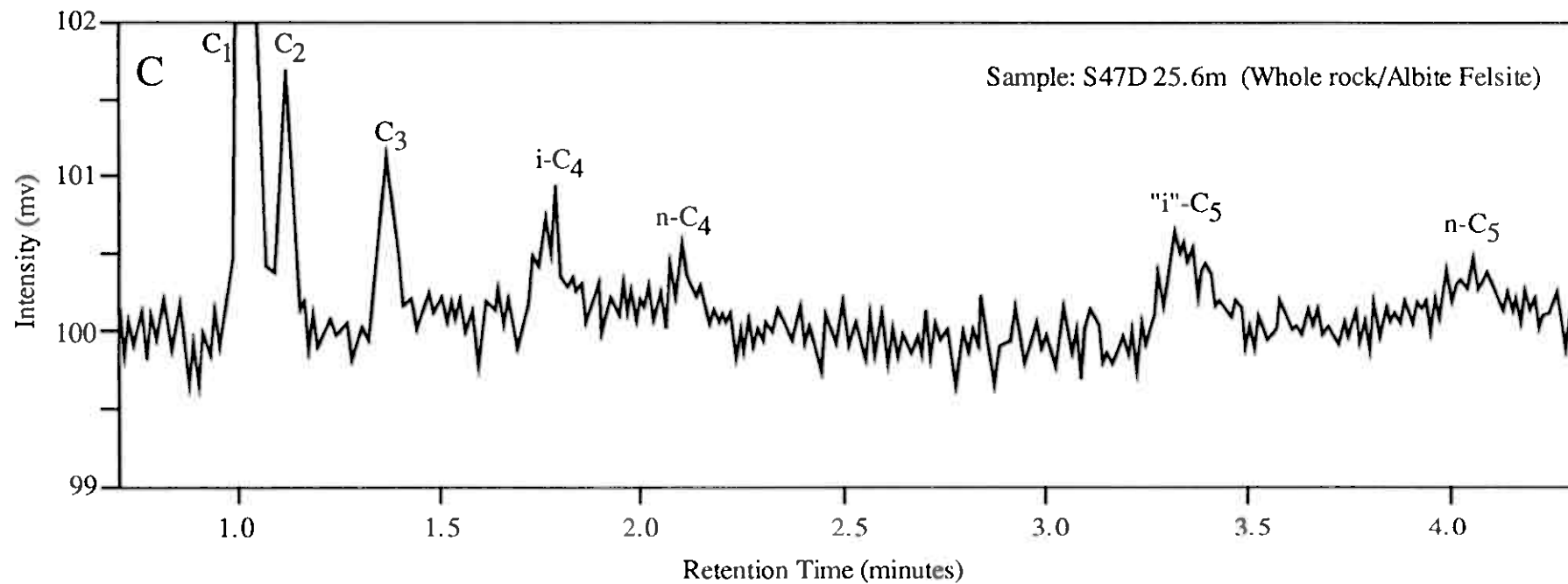
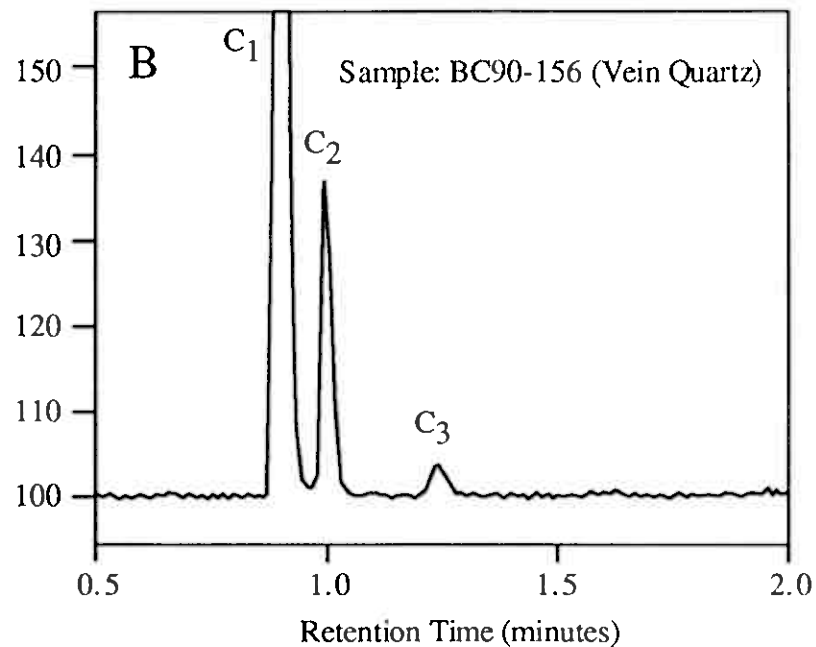
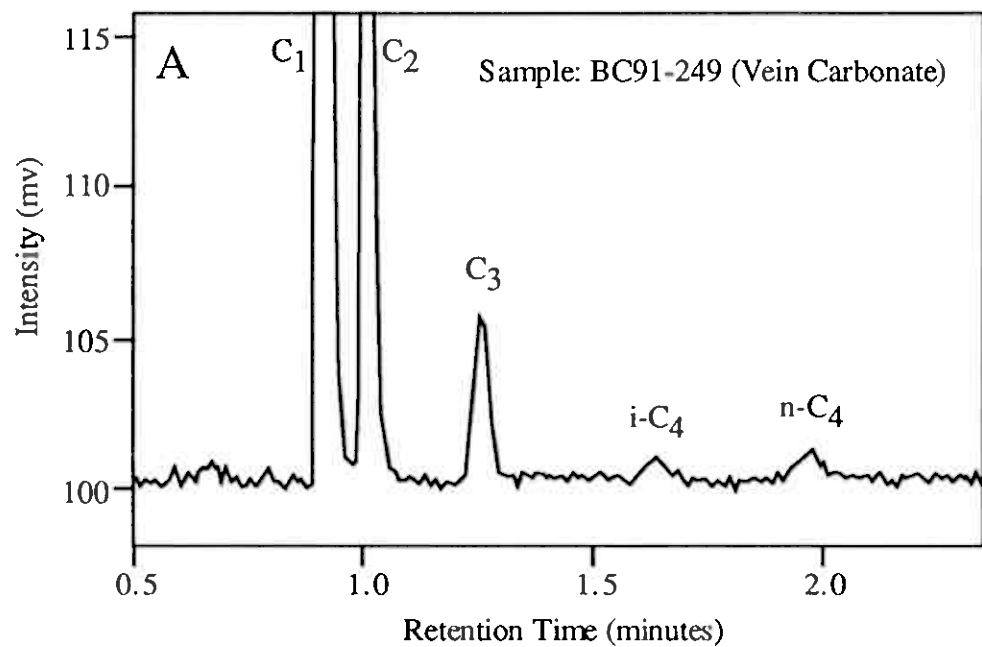


Fig. 16



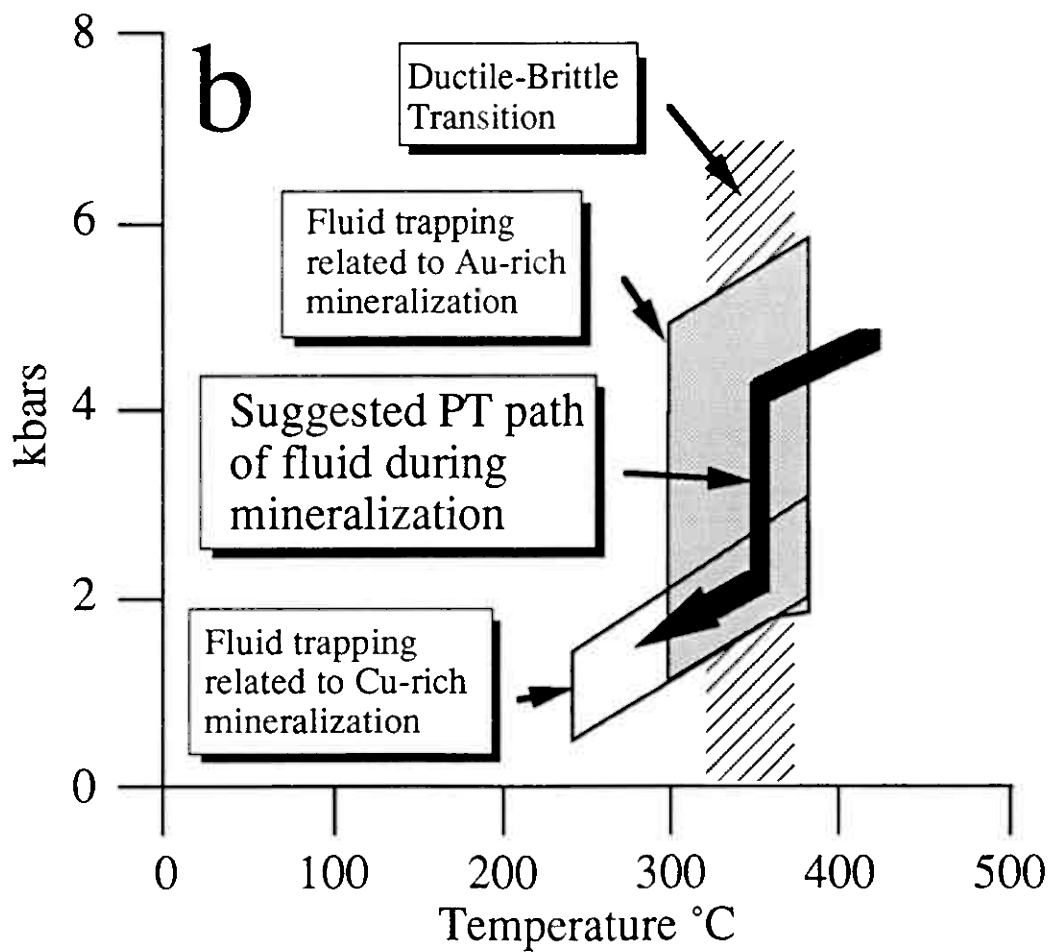
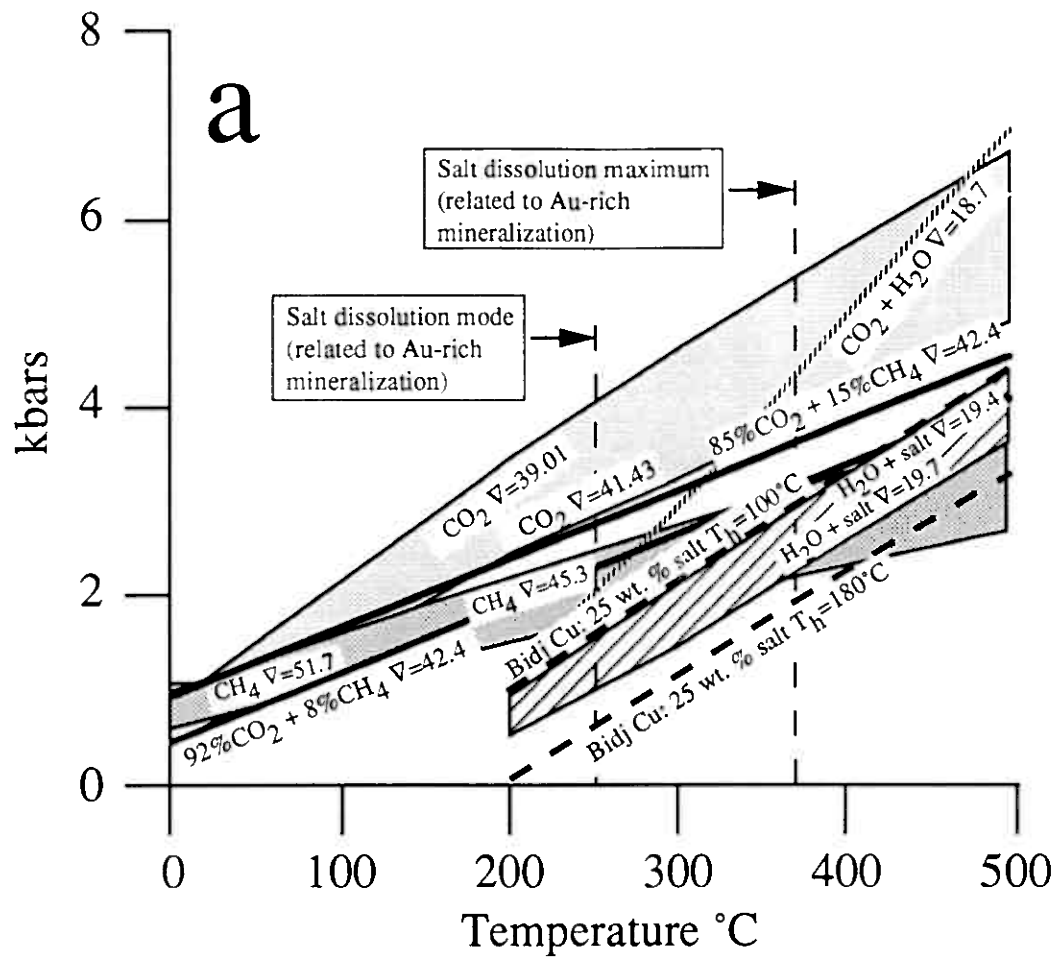


Fig. 18



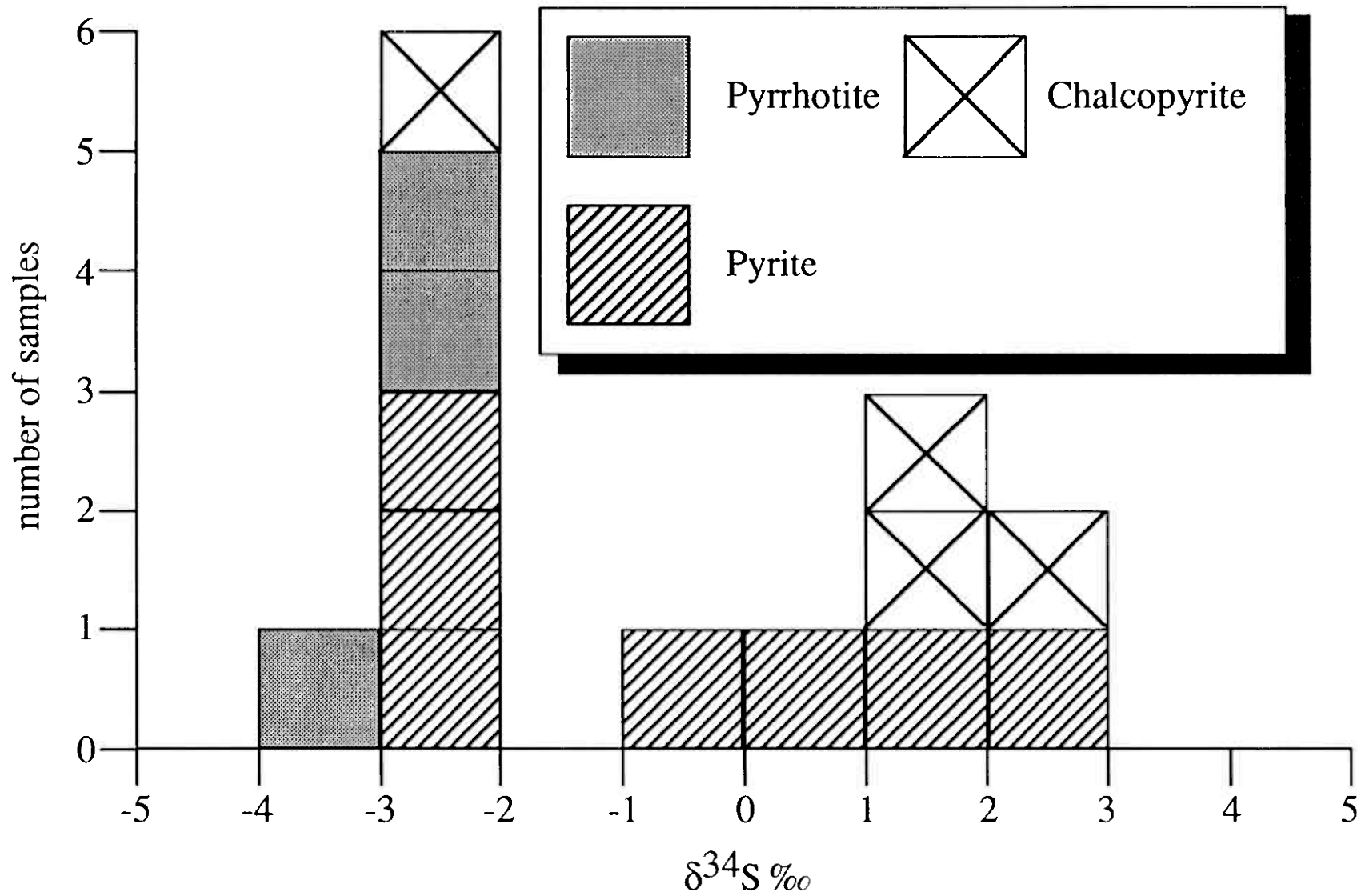
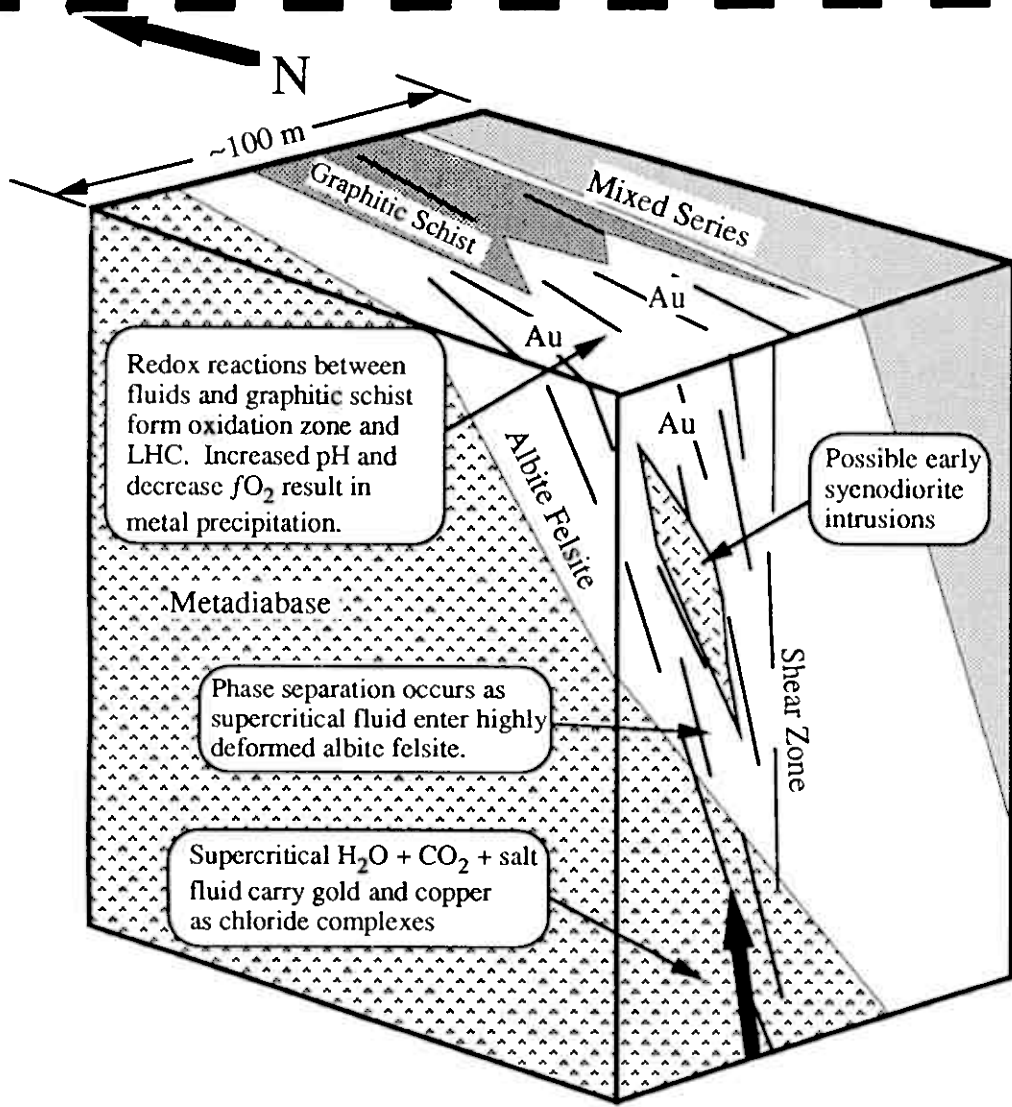
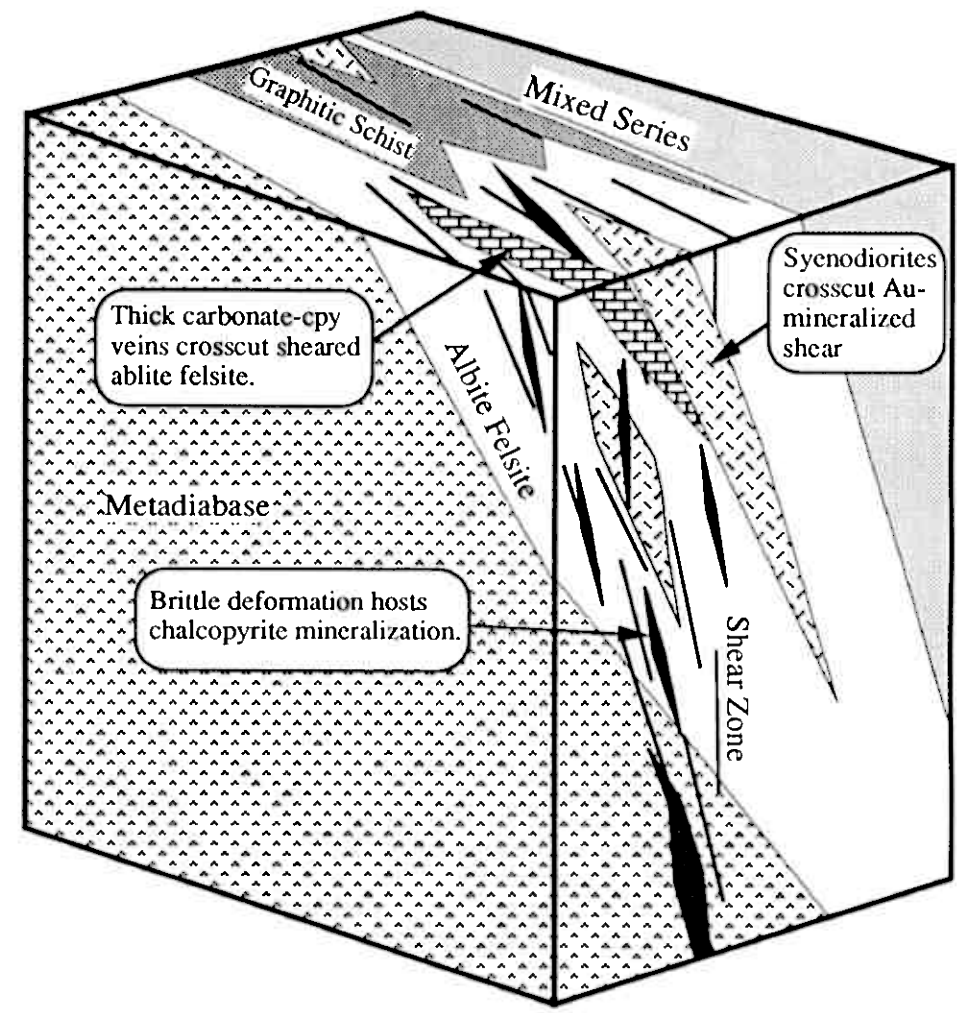


Fig. 20



a.) Early Au-rich phase



b.) Later Cu-rich phase

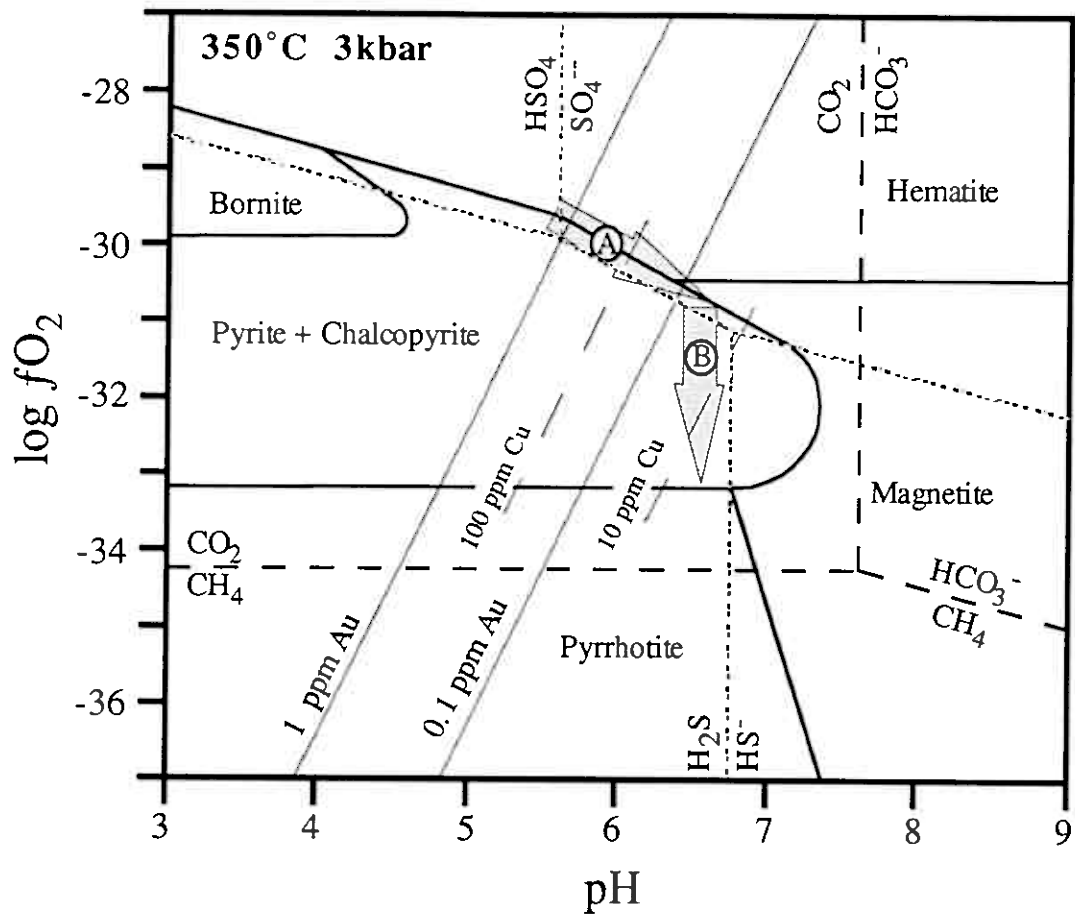


Fig. 22